A Study of Performance on Compression Ignition Engine Fueled by Biodiesel-Diesel Blends with the inclusion of Al_20_3 Nanoparticles

Hadish Teklehaimanot Gebru

A Dissertation Submitted to the Department of Mechanical Engineering, College of Mechanical, Chemical and Materials Engineering

Presented in Fulfillment of the Requirement for the Degree of Doctor of Philosophy in Automotive Engineering

Office of Graduate Studies

Adama Science and Technology University

July, 2025

Adama, Ethiopia

A Study of Performance on Compression Ignition Engine Fuelled by Biodiesel-Diesel Blends with the inclusion of Al_20_3 Nanoparticles

Hadish Teklehaimanot Gebru

Supervisor: Dr. Neeraj Gupta

Co Supervisor: Dr. Ramesh Babu

A Dissertation Submitted to the Department of Mechanical Engineering, College of Mechanical, Chemical and Materials Engineering

Presented in Fulfillment of the Requirement for the Degree of Doctor of Philosophy in Automotive Engineering

Office of Graduate Studies

Adama Science and Technology University

July, 2025

Adama, Ethiopia

DECLARATION

I hereby declare that this dissertation is my original work and has not been presented for a degree in any other university, and all sources of material used for this dissertation have been duly acknowledged through appropriate citations.

Name of student	Signature:	Date
Hadish Teklehaimanot Gebru	_____	_____

RECOMMENDATION

We, the supervisors of this dissertation, hereby certify that we have read and revised the dissertation entitled "A Study of Performance on Compression Ignition Engine Fueled by Biodiesel-Diesel Blends with the inclusion of Al_20_3 Nanoparticles" prepared under our guidance by Hadish Teklehaimanot Gebru submitted for fulfillment of the requirements for the degree of Doctor of Philosophy in Automotive Engineering. Therefore, we recommend the submission of the dissertation to the department for further review and defense.

Major Supervisor	Signature	Date
Dr. Neeraj Gupta (prof.)	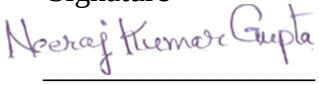	10/28/2025
Co-supervisor	Signature	Date
Dr. Ramesh Babu (Assoc prof.)		10/21/2025

ORIGINALITY'S DECLARATION

Name of Student	Hadish Teklehaimanot Gebru
ID.NO.	Pgr/18473/11
Department	Automotive Engineering
college	CoMCME
Course Title	A study of Performance on compression Ignition Engine fueled by Biodiesel-diesel blends with the inclusion of Al_2O_3 Nanoparticles
Title of Work	
Date o Submission	

1. I understand what plagiarism is and I am aware of the university's policy in this regard.
2. I declare that this dissertation Titled '**A study of Performance on compression Ignition Engine fueled by Biodiesel-diesel blends with the inclusion of Al_2O_3 Nanoparticles'** is my original work and has not been submitted elsewhere for examination or award of degree or publication. Where ever others' work or my own work has been utilized, it has been duly acknowledged and referenced in compliance with the University's requirements.
3. I have not sought or used services of any professional agencies to produce this work
4. I have not permitted, nor will I permit, any one to plagiarize my work with the intension of presenting it as their own.
5. I am aware that making any false claims regarding this work will lead to disciplinary action in accordance with the University's Anti-plagiarism Guide lines.

Signature _____

Date: - _____

APPROVAL OF PhD DISSERTATION

We hereby certify the recommendations and suggestions made by the board of examiners are appropriately incorporated into the final version of the dissertation entitled '**A study of Performance on compression Ignition Engine fueled by Biodiesel-diesel blends with the inclusion ofAl_2O_3 Nanoparticles'** by Mr. Hadish Teklehaimanot Gebru

Prof. Neeraj Kumar Gupta	Neeraj Kumar Gupta	10/28/2025
Major supervisor	Signature	Date
Dr. Ramesh Babu Nallamothu		10/21/2025
Co-Advisor	Signature	Date

We, the undersigned, members of the Board of Examiners of the final open defense by Hadish Teklehaimanot Gebru have read and evaluated his dissertation entitled " A Study of Performance on Compression Ignition Engine Fueled by Biodiesel-Diesel Blends with the inclusion of Al_20_3 Nanoparticles" and examined the candidate. This is, therefore, to certify that the dissertation has been accepted for the fulfillment of the requirement of the degree of doctor of philosophy (PhD) in Automotive Engineering

Dr. Derse Firew		
Chairperson	Signature	Date
Dr. Dawit Gudeta		
Internal Examiner	Signature	Date
Dr. Joshua Isaas (Prof.)		28/10/2025
External Examiner 1	Signature	Date
Samson Mekbib Atnaw (PhD)		28/10/2025
External Examiner 2	Signature	Date

Finally, approval and acceptance of the dissertation is contingent upon submission of its final copy to the office of Postgraduate Studies (OPGS) through the candidates Graduate Council (DGC) and school Graduate Committee (SGC)

Department Head	Signature	Date
School dean	Signature	Date
Office of Postgraduate Studies Dean	Signature	Date

ACKNOWLEDGEMENTS

I would like to express my sincere gratitude to my advisors, Professor Neeraj Gupta and Dr. Ramesh Babu of Adama Science and Technology University, for their invaluable expertise, unwavering encouragement, and continuous guidance, all of which were instrumental in the successful completion of this dissertation.

My heartfelt appreciation also goes to Adama Science and Technology University, my employer, for granting me the opportunity to pursue my studies. I am especially grateful to Dr. Lemi Guta, President of the university, for his motivation and financial support throughout my academic journey.

I would like to express my sincere gratitude to Miss Tsehaynesh Mekonnen for her generous support and for allowing me access to the mechanical screw press in her workshop, which was crucial for the extraction of oil from Jatropha curcas seeds.

I would also like to acknowledge Dr. Shimelis Lemma, Dean of the School of Mechanical, Dr. Tesfay GebremichaelChemical, and Materials Engineering, for his continued encouragement, and Dr. Alemayehu Wakejira for his valuable encouragement and financial support.

I am deeply thankful to my friends, Dr. Habtamu Deresso, Dr. Amanuel Gabissa, and Ato Addis Alemayehu, for their sincere support and assistance throughout the course of my studies. I would also like to express my gratitude to my former advisor, Dr. Daniel Biserat, whose mentorship significantly contributed to shaping my expertise in biodiesel production.

A special word of thanks goes to Jimma University, especially Professor Venkata, the founder of the Jimma University Technology Campus, for his guidance and support during the execution of my experiments. I am also grateful to Ato Balewgize Amare for his dedicated support throughout the engine performance experimental work.

TABLE OF CONTENTS

DECLARATION ii
RECOMMENDATION iii
ORIGINALITY'S DECLARATION iv
APPROVAL OF BOARD OF EXAMINERS v
ACKNOWLEDGEMENTS vi
TABLE OF CONTENTS vii
LIST OF FIGURES xiii
LIST OF ACRONYMS AND ABBREVIATIONS xix
ABSTRACT xxii
CHAPTER ONE 1
INTRODUCTION 1
1.1. Background of the Study 1
1.2. Statement of the Problem 2
1.3. Objectives of the Study 3
1.3.1. General Objective 3
1.3.2. Specific Objectives 3
1.4. Significance of the Study 4
1.5. Beneficiaries 4
1.6. Scope of the Study 4
1.7. Limitation 5
CHAPTER TWO 6
LITERATURE REVIEW 6
2.1. Transportation and Energy 6
2.2. The Role of Petroleum Fuels in Ethiopia. 8
2.3. Transportation and Emission 10
2.4. Global Biofuel Scenario 12
2.6. Advantages and disadvantages of biodiesel 15
2.6.1. Advantages of biodiesel 16
2.6.2. Disadvantages of biodiesel 16
2.7. Biofuel Feed Stocks 17
2.7.1. Non-edible vegetable oil resources 22
2.7.2. Fatty Acid Composition Profile of Various Feedstock 33

2.8. Classification of Biofuels 34
2.8.1. First-Generation Biofuels 34
2.8.2. Second-Generation Biofuels 34
2.8.3. Third-Generation Biofuels 35
2.8.4. Fourth-Generation Biofuels 35
2.9. Ethiopia and Biofuel 35
2.10. Oil Extraction Method 36
2.10.1. Mechanical extraction 37
2.10.2. Solvent extraction (chemical extraction) 37
2.10.3. Enzymatic oil extraction 38
2.11. Vegetable oil Processing and refining 38
2.12. Direct use of vegetable oils in diesel propulsion 39
2.13. Challenges and potential solutions of using plant oils 40
2.14. Biodiesel production technologies 41
2.14.1. Pyrolysis (thermal cracking) 41
2.14.2. Dilution 42
2.14.3. Micro-emulsion. 42
2.14.4. Transesterification Process 43
2.14.5. The mechanism and kinetics 43
2.14.6. The effects of moisture and free fatty acids 44
2.14.7. The effect of molar ratio 44
2.14.8. The effect of catalyst 45
2.14.8. The effect of reaction temperature 45
2.15. Biodiesel Standard Requirement 45
2.16. Engine Performance 46
2.16.1. Engine Design Parameters 47
2.16.2. Engine operating parameters 47
2.16.2.1. Fuel quality 47
2.17. Variables that influence combustion and emission 48
2.17.1. Compression Ratio 48
2.17.2. Direct Injection versus Indirect Injection Engines 49
2.17.3. Fuel Injection Timing and Injection Pressure 49
2.18. Metal Based Nano Particles Additives in Diesel-Biodiesel Blends 49
2.19. Basic Engine lubricating oil parameters 49
2.20. Engine Friction Wear and Lubricity 52

2.20.1. Engine friction 52
2.19.2. Engine wear 53
2.19.3. Engine lubrication 53
2.20. Contamination of lubricant 55
2.20.1. Engine Oil Dilution When Using Biodiesel 57
2.20.2. Problems Associated with Engine oil Dilution by Diesel Engine Fuel 58
2.20.3. Reduced Oil Viscosity and Lubrication Efficiency 58
2.20.4. Increased Engine Wear and Component Damage 58
2.20.5. Decreased Oil Pressure 58
2.20.6. Increased Sludge and Deposit Formation 59
2.20.7. Higher Oil Consumption and Blow-by Gases 59
2.20.8. Poor Engine Performance and Reduced Efficiency 59
2.20.9. Potential for Engine Overheating 59
2.21. Engine endurance test 60
2.21.1. Federal Aviation Administration (Rosli et al.) Regulations 60
2.21.2. Environmental Protection Agency (EPA) Regulations 60
2.21.3. Industry Standards: 60
2.21.4. The ISO Engine Endurance Test Standard 60
2.22. Engine vibration 64
2.22.1. Primary vibration 65
2.22.2. Secondary Vibration 66
2.23. Summary and Research Gap 67
Effect of Al_2O_3 nano-additives on the performance and 73
emission characteristics of jatropha and pongamia methyl esters in compression ignition engine 73
CHAPTER THREE 75
MATERIALS AND METHODS 75
3.1. Materials and reagents 75
3.1.1. Screw Oil Pressing Machine 76
3.1.2. Soxhlet Apparatus 76
3.1.3. Sodium Hydroxide 77
3.1.4. Aluminum Oxide Nanoparticles 78
3.1.5. Surfactant 79
3.1.6. Bath Ultra-sonicator 79
3.1.7. Zeta potential meter 80

3.1.8. Engine Test Stand 80
3.1.9. Exhaust Gas Analyzer 82
3.1.10. Soot Tester 82
3.1.11. Robin DY-23 -2D Diesel Engines 83
3.1.12. Vibration tester 84
3.1.13. Engine disassembly and measuring devices 85
3.2. Methodology 85
3.2.1 Preparation for Biodiesel Production 88
3.2.2. Transesterification of Oil 91
3.3. Fourier Transform Infrared Spectroscopy 96
3.4. Engine Performance Test 96
3.4.1. Experimental Setup 98
3.4.2. Method of Performance Test 98
3.5. Emission Test 103
3.6. Uncertainty Analysis 103
3.7. Endurance Test 103
3.8. Vibration Measurement 104
3.9. Engine Disassembly and Measurement of Carbon Deposited 106
3.9.1. Physical Wear Measurements 107
3.9.2. Measurement of the Cylinder Bore 107
3.9.3. Measurement of Connecting Rod Bearing Bore 108
3.9.4. Measurement of the Gudgeon Pin, Pin Bore, and Small End Bushing 109
3.9.5. Measurement of Piston Wear 110
3.9.6. Measurement of Piston Ring Wear 110
3.9.7. Measurement of Inlet and Exhaust Valve 111
3.9.8. Measurement of the Rocker Arm 112
CHAPTER FOUR 113
RESULT AND DISCUSSION 113
4.1. Introduction 113
4.2. Oil Extraction from Jatropha Carcus Seeds 113
4.3. Determination of percentage of free fatty acid 114
4.4. Transesterification and optimization of biodiesel yield 114
4.5. Fatty Acid Profile Jatropha Carcus Biodiesel 117
4.6. Characterization of fuel samples 117
4.7. Optimization of Nanoparticle Dose for Engine Performance (pilot test) 118

4.7.1. Two-way ANOVA analysis 120
4.7.2. Response optimization of CO, UHC and NOx 121
4.8. Inclusion of Aluminum oxide nanoparticles (Al_2O_3) 123
4.9. Combustion analysis 123
4.9.1. Engine cylinder pressure 123
4.9.2. Heat release rate 125
4.9.3. Ignition delay 126
4.9.4. Combustion duration 127
4.10. Emission analysis 128
4.10.1. Carbon monoxide (CO) 128
4.10.2. Unburned hydrocarbons (UHC) 129
4.10.3. Nitrogen oxide emission (NO_X) 130
4.10.4. Soot opacity 131
4.11. Evaluation of engine performance 132
4.11.1. Brake power 132
4.11.2. Brake torque 133
4.11.3. Brake-specific fuel consumption 134
4.11.4. Equivalence ratio 134
4.11.5. Brake thermal efficiency (BTE) 135
4.11.6. Mechanical efficiency 136
4.12. Engine endurance Test 136
4.12.1. Steady state Vibration analysis the two test fuels 137
4.12.2. Dynamic Vibrational acceleration of engine operated by B0 137
4.12.3. Dynamic Vibrational acceleration of engine operated by B20 with 100ppm 138
4.13. Soot particle size (TEM) 139
4.14. Lubricant properties 140
4.14.1. Kinematic viscosity 142
4.14.2. Viscosity Index 143
4.14.3. Density 144
4.14.4. Flash Point 146
4.14.5. Carbon Residue 146
4.14.6. Water and Sediment 147
4.14.7. Ash Content 148
4.14.8. Total Acid number 149
4.15. Metallic traces in lubricants 150

4.16. Engine disassembly and quantifying carbon deposited 153
4.17. Carbon deposit formed on engine components 153
4.18. Engine Parts Wear Measurements after Endurance Test 155
4.18.1. Measurement of wear on vital engine parts 155
4.18.2. Piston rings 155
4.18.3. Cylinder bore 156
4.18.4. Piston skirt 157
4.18.5. Valve train 157
4.18.6. Connecting rod big end bore 158
CHAPTER FIVE 160
CONCLUSIONS AND RECOMENDATION 160
5.1. Conclusion Based on the production method 160
5.2. Based on the physio-chemical properties 160
5.3. Based on emission and combustion 162
5.4. Based performance characteristics 163
5.5. Based on the endurance characteristics 163
5.6. Based on the tribological properties 163
5.7. Recommendation 164
5.8. Future work 164
REFERENCES 165
Appendix 198

LIST OF FIGURES

Figure 2. 1 Projected oil consumption of 2007 to 2035 6

Figure 2. 2Total oil proved reserves between2015 to 2023 7

Figure 2. 3 Total oil production and consumption (2015 and 2023) 7

Figure 2. 4 Breakdown of world energy consumption in 2007 and 2035 8

Figure 2. 5 Trends in the volume of petroleum imported from 2016 to 2021 9

Figure 2. 6 Trends in the value of imported petroleum from 2015 to 2021 10

Figure 2. 7 Total world biodiesel productions since 2019 to 2023 15

Figure 2. 8 Biodiesel production cost (Gebremariam & Marchetti, 2018) 19

Figure 2. 9 Edible oil feed stocks (Compiled by the author from Atabani et al. (2012) and Demirbas (2009). 20

Figure 2. 10 Non-edible oil feedstock (Compiled by the author from Atabani et al. (2012) and Demirbas (2009). 20

Figure 2. 11 The transesterification of triglycerides with alcohol 44

Figure 2. 12 Lubrication Circuit and Flow Path of Oil in Engine 55

Figure 2. 13 The two typical lubricating condition of oil film formation 55

Figure 2. 14 Basic path of the blow by of partially burn fuel 56

Figure 3. 1 Screw oil pressing machine 76

Figure 3. 2 Soxhlet apparatus 77

Figure 3.3 Sodium hydroxide Pilates 77

Figure 3. 4 Scheme of the transesterification reaction 78

Figure 3. 5 Scheme of the transesterification reaction 78

Figure 3. 6 Cetyl-trimethyl-ammonium bromide 79

Figure 3. 7 Bath ultra-Sonicator 79

Figure 3. 8 Zeta potential meter 80

Figure 3. 9 Engine test stand 81

Figure 3. 10 Exhaust gas analyzer 82

Figure 3. 11 Soot tester 83

Figure 3. 12 Robin DY-23 -2D Diesel Engines and Tacho-meter 83

Figure 3. 13 Vibration tester 84
Figure 3. 14Assembly and measuring tools 85
Figure 3. 15 Graphical abstract 86
Figure 3. 16 Conceptual framework 87
Figure 3. 17 Dried Jatropha Seeds and weighed 88
Figure 3. 18 Mechanically crushed and soaked Jatropha seeds with hexane 89
Figure 3. 19 Filtered solution of crude oil and hexane 89
Figure 3. 20 Filtration of crude oil by using Whatman paper Grade 41 90
Figure 3. 21 Hexane recovery 90
Figure 3. 22 Water removal by addition of sodium sulfate 91
Figure 3. 23 Water-free crude Jatropha oil 91
Figure 3. 24 Samples of biodiesel 93
Figure 3. 25 Temperature control 93
Figure 3. 26 Separation of glycerin 94
Figure 3. 27 Waste oil recovery 94
Figure 3. 28 Pure biodiesel 95
Figure 3. 29 Preparing the biodiesel for washing Figure 95
Figure 3. 30 Washing the biodiesel by spray method 95
Figure 3. 31 Separation of soap and the biodiesel 96
Figure 3. 32 Biodiesel, glycerin, and soap 96
Figure 3. 33 Engine geometry 97
Figure 3. 34 Points of vibration measurement 105
Figure 3. 35 a) diesel b) B20+Al_20_3 100ppm fueled 106
Figure 3. 36 Measurement of cylinder bore (IS standard) 108
Figure 3. 37 Measurement of connecting rod bearing (IS standard) 109
Figure 3.38 Connecting rod Gudgeon pin, pin bore, and small end bush (IS standard) . 109
Figure 3. 39 Measurement of piston (IS standard) 110
Figure 3. 40 Measurement of piston rings (IS standard) 111
Figure 3. 41 Measurement of piston rings (IS standard) 111
Figure 3. 42 Measurement of rocker arm (IS standard) 112

Figure 4. 1 Oil samples 114
Figure 4. 2 Maximum biodiesel yield based on temperature and time 116
Figure 4. 3 Multiple interaction plot of the input parameters 116
Figure 4. 4 Fourier Transform infrared test (FTIR) 117
Figure 4. 5 Interaction plot for CO, UHC, and NOx 121
Figure 4. 6 Desirability plots for CO,UHC and NOx 122
Figure 4. 7 Surface plots of emission versus Dose of NPs 123
Figure 4. 8 Cylinder pressure vs. CA with and without Al_2O_3 Nps 124
Figure 4. 9 HRR vs. with and without Al_2O_3 Nps 126
Figure 4. 10 Ignition delay 127
Figure 4. 11 Combustion Duration (^{0}CA) of all blends 128
Figure 4. 12 CO a) without Al_2O_3, b) with Al_2O_3 Nps 129
Figure 4. 13 UHC a) without Al_2O_3, b) with Al_2O_3 Nps 130
Figure 4. 14 NO_x a) without Al_2O_3, b) with Al_2O_3 Nps 131
Figure 4. 15 Soot opacity a) without Al_2O_3, b) with Al_2O_3 Nps 132
Figure 4. 16 Brake power vs. engine speed and blend ratio 133
Figure 4. 17 Brake torque vs. engine speed and blend ratio 133
Figure 4. 18 BSFC vs. engine speed and blend ratio 134
Figure 4. 19 Equivalence ratio vs. engine speed and blend ratio 135
Figure 4. 20 Thermal efficiency vs. engine speed and blend ratio 135
Figure 4. 21 Mechanical efficiency vs. engine speed and blend ratio 136
Figure 4. 22 Vibration acceleration 137
Figure 4. 23 Dynamic vibration acceleration for B0 138
Figure 4. 24 Dynamic vibration acceleration for (B20+100ppm), ... 139
Figure 4. 25 Soot particle size (TEM) 140
*F*igure 4. 26 Variation of Kinematic viscosity @ 40°C 142
Figure 4. 27 Variation of Kinematic viscosity @ 100°C 142
Figure 4. 28 Variation of viscosity index of lubricating oil 144
Figure 4. 29 Variation of density of lube oil @ 15°C 145

Figure 4. 30 Variation of density of lube oil @ 20°C 145
Figure 4. 31 Variation of Flash point of lube oil 146
Figure 4. 32 Variation of Carbon residue lube oil 147
Figure 4. 33 Variation of Water and sediment lube oil 148
Figure 4. 34 Variation of Ash Content 149
Figure 4. 35 Variation of Total acid number 149
Figure 4. 36 Metallic traces in lubricants 152
Figure 4. 37 Engine disassembly and quantifying carbon deposited 153
Figure 4. 38 Carbon deposits (B20) with 100-ppm Al_2O_3 and diesel 155

LIST OF TABLES

Table 2. 1 Top 10 countries in terms of biodiesel potential 15

Table 2. 2 Current potential feed stocks for biodiesel worldwide 18

Table 2. 3 Biodiesel feed stocks (Eriksson & Sivertsson, 2015) 19

Table 2. 4 Estimated oil content and yields of different biodiesel feed stocks 21

Table 2. 5 The chemical structures of common fatty acids 34

Table 2. 6 Calculated oil yields (% of contained oil) of mechanical extraction methods Keneni, Y.G., & Marchetti, J.M. (2017). 37

Table 2. 7 Reported oil yields for different chemical and enzymatic extraction methods of Jatropha Carcus,Castor and Rapeseed 38

Table 2. 8 Problems, cause and potential solutions for using straight vegetable oil 40

Table 2. 9 Comparison of main biodiesel production technologies (L. Lin et al., 2011) 41

Table 2. 10 The range of the main operating parameters for pyrolysis processes 42

Table 2. 11 Biodiesel standard requirements(Bringas, 2004; Carrero & Pérez, 2012). 46

Table 2. 12 Comparison of total glycerol removal and transesterification method 68

Table 2. 13 Summary review of literature 72

Table 2. 14 Sumary of esterification 74

Table 3. 1 Specification of equipment, laboratory ware, and chemicals 75

Table 3. 2 Stability of Nano fluids (Verma et al., 2017) 80

Table 3. 3 Specification of CT 100.22 engine 82

Table 3. 4 Robin DY23-2D diesel engine specification 84

Table 3. 5 Design of experiment for transesterification 92

Table 3. 6 Accuracy and uncertainties 103

Table4. 1 Optimization of the esterification reaction 115

Table4. 2 Fatty acid profile of Jatropha Carcus 117

Table4. 3 Physiochemical properties of biodiesel blends 118

Table4. 4 Experimental design 119

Table4. 5 Pilot test emission results of measurement 119

Table4. 6 Two-way ANOVA analysis 120

Table4. 7 Emission influencing factors 120
Table4. 8 Physio-chemical property of diesel operated used oil 141
Table4. 9 Physio-chemical property of B20+Al_2O_3 operated engine used oil 141
Table4. 10 Metallic contents of lubricating oil [ppm] and the standard limit 152
Table4. 11 Comparison of Carbon deposit 154
Table4. 12 Comparison of wear of piston ring 156
Table4. 13 Comparison of wear of cylinder between B_{20} biodiesel-diesel and diesel 156
Table4. 14 Comparison of wear on Piston skirt 157
Table4. 15 Wear on valve 158
Table4. 16 Wear on rocker arm 158
Table4. 17 Wear on connecting rod big end bore 158
Table4. 18 Wear on Gudgeon pin bore 159

LIST OF ACRONYMS AND ABBREVIATIONS

AAS	Atomic absorption spectroscopy
AEOE	Aqueous enzymatic oil extraction
AgO	Silver oxide
Al_2O_3	Aluminium oxide
AOE	Aqueous oil extraction
ASTM	American Standards of Testing Materials
a_w	Weighted acceleration
B0	Diesel fuel
B5	5% biodiesel with 95% diesel
B10	10% biodiesel with 90% diesel
B20	20% biodiesel with 80% diesel
B40	40% biodiesel with 60% diesel
BN	Base number
BSFC	Brake specific fuel consumption
BuOH	Barium hydroxide
CA	Crank angle
CI	Compression ignition
CO	Carbon mono-oxide
CO_2	Carbon dioxide
Cr	Chromium
CR	Compression ratio
cSt	Cent-stoke
CTAB	Cetyl-trimethyl Ammonium Bromide
D2	Diesel no-2
DI	Direct injection
DPF	Diesel particulate filter
EGR	Exhaust gas recirculation
EIA	International Energy Agency
EN	European
EU	European Union
FDI	Foreign direct investment
Fe	Iron

FP	Flash point
ft	feet
g	Gram
GEE	Green Energy Ethiopia
GHG	Greenhouse gas
GJ	Giga joule
HC	Hydrocarbon
HFCs	Hydrofluorocarbons
HSDI	High-speed direct injection
IDI	Indirect Injection
IDP	Ignition delay period
ILC	International land coalition
IP	Injection pressure
IT	Injection timing
in	inch
IS	Indian Standard
ISO	International standard organization
K_2CO_3	Potassium Carbonate
Kg	Kilogram
KHz	Kilo Hertz
KOH	Potassium hydroxide
LOME	Linseed oil methyl ester
m	Meter
mm	Millimeter
MoME	Ministry of Mines and Energy
Na_2SO_4	Sodium sulphate
NaOH	Sodium hydroxide
NaOH	Sodium hydroxide
nm	Nanometer
NO	Nitrogen monoxide
NOx	Nitrogen oxides
NPs	Nanoparticles
P_b	Brake power
P_f	Friction power

PMCC	Pensky Martin's close cup
PM	particulate matter
Pm	Mean effective pressure
P_{red}	Reduce power
PRG	Piston ring groove
R_R	Kinematic Rod Ratio
SAE	Society of American Engineers
SNNPRS	South Nations Nationalities and Peoples' Regional State
SO_2	Sulphur dioxide
TAN	Total acid number
T_b	Brake torque
TBN	Total base no
TEM	Transmission electron microscope
T_f	Friction torque
TFC	Total fuel consumption
UHC	Unburned hydrocarbon
ULSD	Ultra-low sulphur diesel
$\bar{U}_{max}$	Maximum uncertainty
USA	United States of America
V/W	Volume to weight ratio
V_h	Swept volume
VI	Viscosity Index
VOC	Volatile organic compound
Wt	Weight
Zn	Zinc

ABSTRACT

In the current energy scenario, biodiesel serves as an alternative to diesel engine propulsion, addressing concerns over limited fossil fuel reserves and the impacts of global warming. Researchers focus on investigating the combustion, emission, performance, and tribological effects of various biofuel feedstocks, necessitating further exploration. Feedstock selection for biodiesel production considers availability, location, and environmental conditions, which in turn influence both the quality and quantity of the product. This study utilized Jatropha curcas as feedstock, which was mechanically extracted and then trans-esterified with alkaline catalysts. The research evaluated the impact of aluminum oxide (Al_2O_3) nanoparticles on combustion, emission, and performance on four fuel mixtures (diesel (B0), B5, B10, B20, and B40) both with and without a 100ppm dose of Al_2O_3 nanoparticle additive in a Gunt diesel engine test stand (Gunt C110). Finally, from the samples, B20 with 100 ppm dose nano additive was selected. The tribological behaviour and endurance of two identical Robin DY23-2D diesel engines were studied, one using baseline diesel fuel and the other using B20 with 100 ppm Al2O3 N. Emission characteristics (HC, CO, NOx, and soot opacity) were also examined. Combustion components, including cylinder pressure and heat release rate (HRR), were studied. Blends with 100-ppm Al_2O_3 nano additives exhibited average reductions of 10.1% (UHC), 29.4% (CO), 13.9% (NOx), and 8.4% (smoke) compared to the fuel without the additive. Cylinder pressure increased with Al_2O_3 nanoparticles, rising by 0.44, 1.16, 2.85, 5.06, and 5.63 bar for B0, B5, B10, B20, and B40. The net heat release rate rose by 6%, 2.8%, 12.6%, 8.4%, and 9.6% for B0, B5, B10, B20, and B40. The higher surface area-to-volume ratio of Al_2O_3 nanoparticles reduces ignition delay, thereby enhancing combustion. The reference diesel had a shorter combustion duration, whereas B40 exhibited an increased combustion duration, both with and without additives. Adding 100 ppm of Al_2O_3 additive improved combustion while reducing exhaust emissions in all blends. The brake power output results, incorporating Al_2O_3, demonstrated increases of 3.06%, 8.02%, 0.79%, 5.46%, and 4.55% for B0, B5, B10, B20, and B40, respectively. Al_2O_3 inclusion notably increased engine torque for B20 between 2500 and 2800 rpm. Across all blends, with or without Al_2O_3, brake-specific fuel consumption (BSFC) was at its lowest between 2100 and 2800 rpm. Biodiesel-diesel blends with Al_2O_3 exhibited a BSFC reduction of 0.20%, 0.20%, 0.51%, 0.52%, 0.70%, and 0.90% for B0, B5, B10, B20, and B40, respectively. Both with and without Al_2O_3 nano-additives, the equivalence ratio decreased compared to the reference diesel fuel.

Keywords: Aluminum oxide nanoparticles, biodiesel, Engine endurance, Engine performance, Jatropha carcus

CHAPTER ONE

INTRODUCTION

1.1. Background of the Study

The rise of industrial development and the expanding transport sector worldwide are encountering significant challenges related to energy demand and heightened environmental concerns (Hussain & Zhou, 2022). The increasing demand for fuel, coupled with the limited availability of mineral oil, creates a strong incentive to develop alternative fuels from renewable sources that have a lower environmental impact. One promising alternative to petroleum-based fuels is the use of fuels derived from plant sources. (Malla et al., 2023). Using biodiesel as a renewable resource offers the benefits of nearly unlimited availability and ecological advantages, including an integrated closed carbon cycle(El-Araby, 2024). In the early 1980s, vegetable oil was used as a fuel. However, the widespread availability of conventional diesel fuel made the development of alternative fuels from renewable sources seem less important (Atabani et al., 2012).The first report of using vegetable oil-based fuel, specifically the ethyl esters of palm oil, as a substitute for diesel was in a Belgian patent in 1973.(Knothe, 2005). Research on vegetable oil development became increasingly important in the 1990s. Key oil seed crops identified for bio fuel production include sunflower, soybean, rapeseed, linseed, cottonseed, peanut, and canola (Waseem et al., 2017).

Using edible oil for biofuel appears to be of limited significance for developing countries, which mainly rely on imports of edible oils. Instead, non-edible tree-borne oils, such as Jatropha curcas and castor oil, are considered promising feed stocks for the production of biodiesel.

The oils produced from this non-edible are toxic(Gui et al., 2008). In this research work, oils derived from Jatropha curcas are chosen for the development of an alternative vegetable oil for diesel fuel.

Petroleum reserves are limited in a few countries worldwide. Additionally, most of the world imports petroleum fuel to meet its energy needs. The demand and price of petroleum fuel is increasing at an alarming rate from time to time(Bhandari, 2018). Moreover, most oil-importing countries do not utilize alternative energy sources to substitute fossil fuels (Marques et al., 2018). To ensure sustainable development, clean energy is also crucial. In this regard, it is important to find alternative sources, such as vegetable oil, which have become increasingly attractive recently due to their environmental benefits and renewable nature.

Diesel engines have a major role in the transportation sector, agricultural industry, and in industrial power generation (Marques et al., 2018). In the early stages, vegetable fuel was not competitive with petroleum because it was more expensive than fossil fuels. The current rise in prices and the uncertainties surrounding fossil fuel availability, there is growing interest in and a shift toward using vegetable oil in diesel engines. (Joshi et al., 2017). Hence, there is a need to find ways of utilizing renewable alternative fuels that emit low levels of emission species from IC engines. For agricultural applications, decentralized fuel production near consumption points is preferred. Farmers can produce straight vegetable oil for their needs. Additionally, using vegetable oil is more economical and time-saving due to the energy and material savings it provides (Rodionova et al., 2017). Using vegetable oil as a substitute for fossil fuel offers several advantages: it is portable, has a high heating content about 88% that of diesel No. 2, contains low levels of sulfur and aromatics, and is biodegradable. (S.-Y. No, 2011).

The problems of using plant oil as a substitute for diesel fuel are - high viscosity, lower volatility, and reactivity of unsaturated hydrocarbon chains (Negm et al., 2017). Therefore, problems appear after engines operate on straight vegetable oils for more extended periods, which leads to injector coking, oil ring sticking, carbon deposits, gelling, and thickening of lubricants because of contamination of vegetable oil (Panchal et al., 2017). The major problem of vegetable oil is its higher viscosity; hence, it needs engine modification (S.-Y. No, 2011).

This research proposed and conducted studies on the use of Jatropha biodiesel as a diesel substitute, with minimal fuel processing and without requiring engine modification, by enhancing the property of the biodiesel to facilitate proper combustion reactions. It is intended to minimize the viscosity of the parent oil through transesterification using an alkaline catalyst before it is admitted to the combustion chamber. Moreover, the performance and emission characteristics of the fuel was executed in CT110 test engine for different blends. In addition, the optimum blend with the best emission and performance profile, was selected, and engine tribology and endurance tests were performed on two Robin DY23-2D direct injection diesel engines: one for the base reference fossil fuel and the second for the diesel-biodiesel blend with nanoparticles.

1.2. Statement of the Problem

Securing consistent access to transportation fuels is a challenge for all countries, but emerging countries that import fossil fuels, such as Ethiopia, are particularly impacted because it significantly impedes their development (Benti et al., 2021; Yacob Gebreyohannes Hiben, 2013). Ethiopia should explore all possible alternatives to reduce its dependency on petroleum imports. Diesel fuel is the main transportation fuel in the country, as nearly all public transportation relies

on it. Therefore, partially or completely substituting petroleum fuel will enhance access and security (Kebede et al., 2022). The need for fuel and changes in people's lifestyles around the world are making the demand for oil rise quickly. This will lead to an increase in the import bill due to rising petroleum prices(Armaroli & Balzani, 2007). The government will be able to use its foreign cash for other purposes if petroleum import expenses are reduced by the practical replacement of petroleum diesel with biodiesel.

Therefore, this research work tried to address the following research questions.

- Whether diesel-biodiesel blend with alumina nanoparticle operates the diesel engines as to the rated power and torque of the test engine.
- Whether it satisfies the emission standard requirements and possibilities to reduce emission output.
- Whether the fuel blends with its additives are compatible with the engine hardware.
- Whether the application of bio-diesel diesel blend with alumina nanoparticles is compatible with the life of lubricating oil and lubricating system.

1.3. Objectives of the Study

1.3.1. General Objective

The general objective of the research was to study the performance of a compression ignition engine fuelled by biodiesel-diesel blends with the inclusion of Al_2O_3 nanoparticles.

1.3.2. Specific Objectives

The specific objectives of the research were:

- To optimize the trans-esterification reaction parameters which are the reaction temperature, catalyst concentration, reaction time and stirring speed using Response Surface Method (RSM) and measure the physio-chemical properties.
- To investigate the performance of the diesel-biodiesel blends with alumina nanoparticles and select the best blend.
- To investigate a short-term endurance characteristic of two identical test engines (Robin DY23-2D diesel engines) with the best-chosen blend in comparison to the base line diesel fuel.
- To assess the tribological effects of the diesel and the optimum blend with the inclusion of Al_2O_3NPs by comparing the wear of vital engine components and the lubricant property.
- To investigate the effect of Al_2O_3 NPs on soot opacity in comparison to the base line diesel fuel.

1.4. Significance of the Study

- Producing biodiesel from Jatropha curcas seeds can help reduce the trade gap by replacing imported petroleum.
- To fuel the diesel engine, by biodiesel derived from Jatropha, either as a complete replacement or blended at an appropriate mixing ratio.
- To reduce emissions, including greenhouse gases, while also generating environmental benefits.
- The pressed residue can be used for agriculture as fertilizer
- The pressed cake or residue can be used as a source of heat energy for industries.
- To secure oil fuel supply.
- Ample residue can be supplied as a feedstock for biogas producers.
- The by-product glycerine can be supplied for the cosmetic industry and generate revenue.

Therefore, this laboratory-scale investigation demonstrates the potential of utilizing locally available renewable energy sources, particularly the extraction of biodiesel from *Jatropha curcas*, as a sustainable alternative to petroleum-based fuels. This approach serves as a strategic response to the escalating global oil prices that adversely impact Ethiopia's economy (Tamrat et al., 2023; Ganapathy et al., 2011). Expanding *Jatropha* biodiesel production at a national scale could offer multiple benefits, including conservation of foreign exchange, job creation, promotion of local industrial capacity, economic stimulation, and a reduction in environmental pollution (Bibin et al., 2019; Bibin et al., 2020).

1.5. Beneficiaries

- It helps to create opportunities and awareness to create jobs for farmers who can produce vegetable oil seeds.
- Governments can save foreign currency for the purchase of fossil fuels.
- It helps carbon sequestration or carbon dioxide removal (CDR) from the atmosphere and mitigates global warming.

1.6. Scope of the Study

The scope was to produce biodiesel from Jatropha curcas seeds, characterized the parent oil and the blends with nanoparticles by the ASTM standard test methods, executed emission and performance tests by an engine test rig, execute short-term endurance tests, investigated the tribological effect on engine lubricants and evaluating the wear effects of the vital parts of the test engines.

1.7. Limitation

The engine performance test using alumina nano additives faced experimental limitations, including engine stalling during endurance testing, which resulted in variations in performance and emissions. Fluctuations in blend ratios, time intervals, and air psychometric conditions further affected combustion consistency. Additionally, measurement reliability was impacted by prolonged engine operation, leading to inconsistent emission readings due to residual deposits, fuel degradation, increased thermal load, lubricant changes, and exhaust build up. These factors contributed to data variability, making it challenging to ensure accurate performance assessment.

CHAPTER TWO

LITERATURE REVIEW

2.1. Transportation and Energy

Since the Industrial Revolution, energy has played a crucial role in driving the economic growth of societies. (Barca, 2011). In the past thirty years, the transportation sector has significantly expanded, driven by the rising number of vehicles worldwide. (Newman et al., 2013). This sector represents 30% of the world's total energy consumption, with road transport accounting for 80% of that portion (A. Atabani et al., 2011). According to (Yin et al., 2015), the energy for transportation is estimated to grow at an average annual rate of 1.8% from 2005 to 2035.

Transportation is the second energy-consumer next to industry, responsible for about 60% of global oil demand. It is projected to experience the fastest growth in energy consumption in the coming years. Approximately 97.6% of the sector's fossil fuel energy is derived from oil, with natural gas contributing only a small portion (Hao et al., 2015). It is also projected that nearly 75% of the increase in oil demand between 2006 and 2030 will be driven by the transportation sector (ArifSyed et al., 2010). Figure 2.1 illustrates the forecasted oil consumption trends for the transportation and other sectors globally from 2007 to 2035 (A. E. Atabani et al., 2011; Silitonga et al., 2011; U.S Energy Information Administration, 2010)

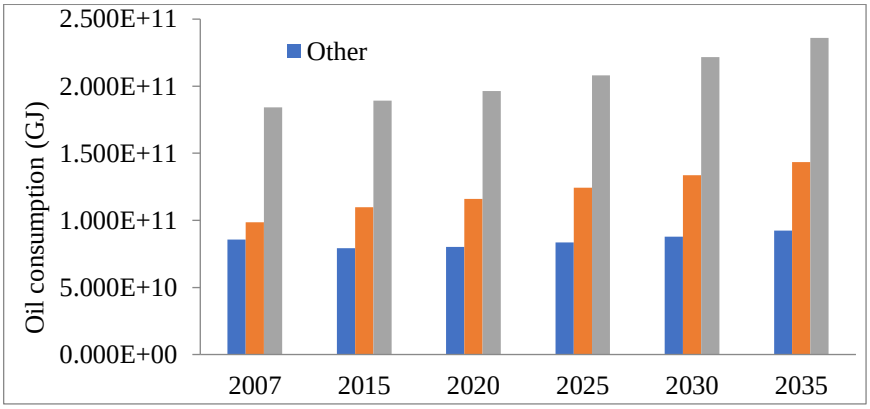

Figure 2. 1 Projected oil consumption of 2007 to 2035

Figures 2.2 and 2.3 illustrate the history of oil-proved reserves, production, and consumption between 2015 and 2023, respectively. Alternative energy sources, including natural gas, renewables, and nuclear power, continue to grow. Advances in technology, policy shifts toward cleaner energy, and increasing electrification in transportation and industry are driving this trend. While oil will remain a crucial component of the global energy mix, its relative share is expected to decrease by 14.29% from 2015 to 2035 as economies transition toward more sustainable and

diversified energy sources, as shown in Figure 2.4 (U.S Energy Information Administration, 2010). However, global oil production is expected to grow until the early 2030s before entering a long-term decline influenced by economic, technological, and environmental factors (Aleklett et al., 2010). Peak production is projected between 2025 and 2045, depending on demand trends and energy transitions. The rate of decline will be shaped by energy policies, advancements in technology, and investments in renewables, with net-zero scenarios predicting a sharp drop in oil use from 2050 to 2070 (Norouzi et al., 2020).

The World Energy Forum predicts that reserves will be depleted in less than 100 years. However, some experts believe that if consumption increases by 3% annually, they could be exhausted in under 45 years.(Ahmad et al., 2011; British petroleum (BP), 2010; Sharma, 2009)

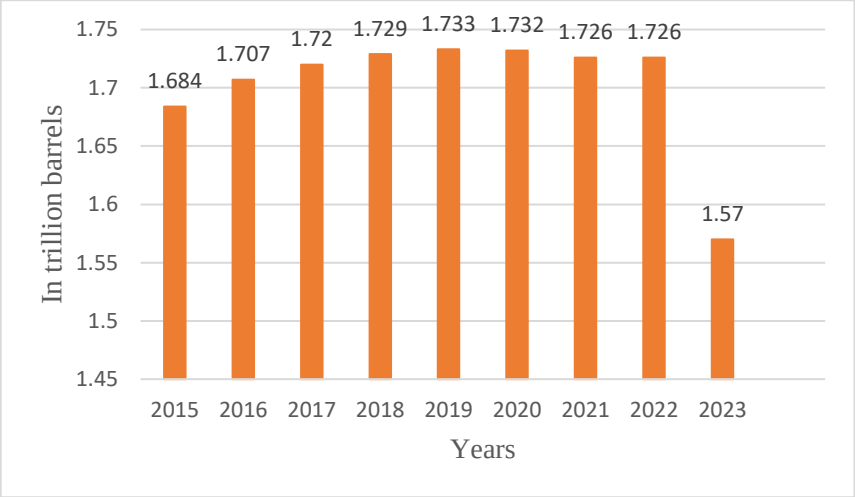

Figure 2. 2Total oil proved reserves between2015 to 2023

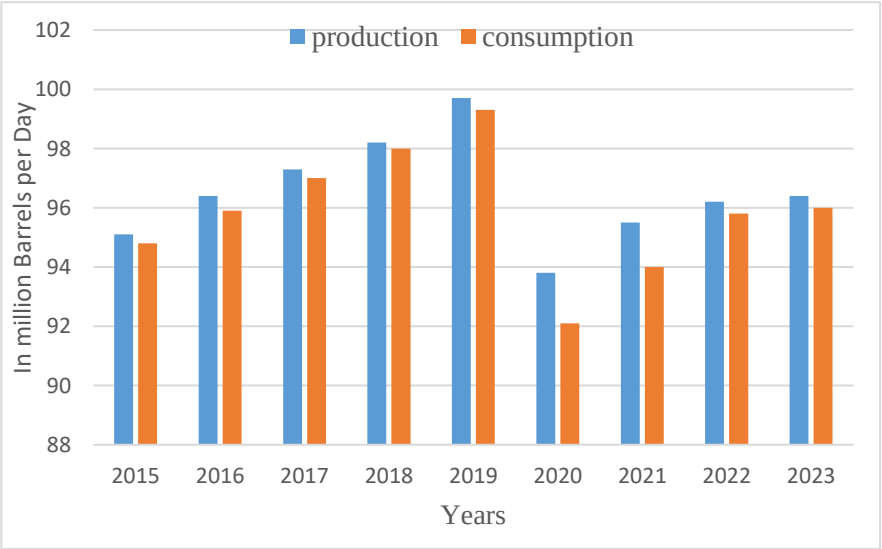

Figure 2. 3 Total oil production and consumption (2015 and 2023)

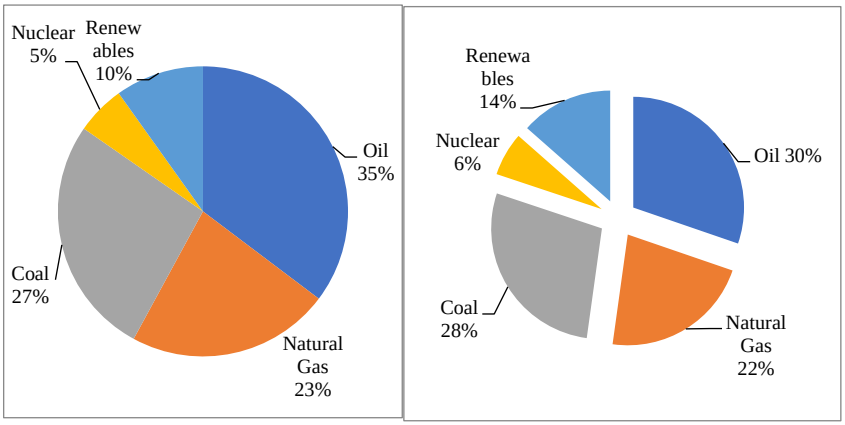

(a) 2015 (b) 2035

Figure 2. 4 Breakdown of world energy consumption in 2007 and 2035

2.2. The Role of Petroleum Fuels in Ethiopia.

In Ethiopia, biomass is the primary energy source, accounting for more than 85% of the nation's total energy consumption. Its main components, firewood, charcoal, agricultural waste, and animal dung, are utilized extensively for small-scale businesses, cooking, and heating (Benti et al., 2021). Due to limited access to electricity and other modern energy sources, rural households rely heavily on biomass. Inefficient use of biomass, however, increases indoor air pollution, deforestation, and health hazards, especially for women and children (Amare et al., 2015).Ethiopia is promoting improved cook stoves, afforestation initiatives, and alternative energy sources, such as ethanol and biogas, to address these issues. Although biomass remains necessary, the nation is increasing its investments in hydroelectricity, wind, and solar energy to create a more efficient and sustainable energy mix (Boke et al., 2022). Petroleum fuels are the primary energy source for industry, transportation, and power generation. Due to the lack of substantial crude oil reserves, the nation is dependent on imports to satisfy its rising demand (Benti et al., 2021). The transportation industry is dominated by gasoline and diesel, which underpin trade, logistics, and agriculture. Petroleum fuels power building, manufacturing, and machinery in the industrial sector. Furthermore, home energy still depends heavily on kerosene, especially in rural areas with consistent access to power. To minimize its dependence on petroleum and enhance its energy security, Ethiopia is vigorously working to diversify its energy sources and is investing in renewables, including solar, wind, and hydroelectric power (Sawo, 2024).Data from the Ethiopian Petroleum Enterprise indicate that since 2015, Ethiopia's petroleum imports have fluctuated significantly due to changes in policy, economic growth, and the volatility of the global oil price. About $2.1 billion worth of mineral

fuels and oils were imported by the nation in 2016, but that amount dropped to about $1.5 billion in 2018 (Asfaw, 2017). There have also been noticeable shifts in the proportion of fuel imports to Ethiopia's overall merchandise imports. Petroleum and bituminous mineral oils made up 14.2% of the nation's total imports in 2022, up from 5.38% in 2021. Ethiopia imported fuel at a cost of about €6 billion in 2023 (Yalew et al., 2023).Ethiopia became the first nation to impose a ban on the importing of gasoline and diesel automobiles in January 2024 to alleviate the economic burden of fuel imports and deal with the shortage of foreign currency (Mitiku, 2020). This program aims to reduce dependency on foreign fuels and promote using electric vehicles (Matveevsky & Buyanovsky). However, this shift is hampered by issues such as a lack of maintenance facilities, inconsistent electrical supply, and inadequate EV infrastructure (Adhikari et al., 2020).All things considered, Ethiopia's petroleum import patterns since 2015 reveal a dynamic interplay between legislative measures, economic demands, and efforts to transition to more sustainable energy sources. As shown in Figure 2.5, Ethiopia has been importing petroleum products in metric tons since 2016.

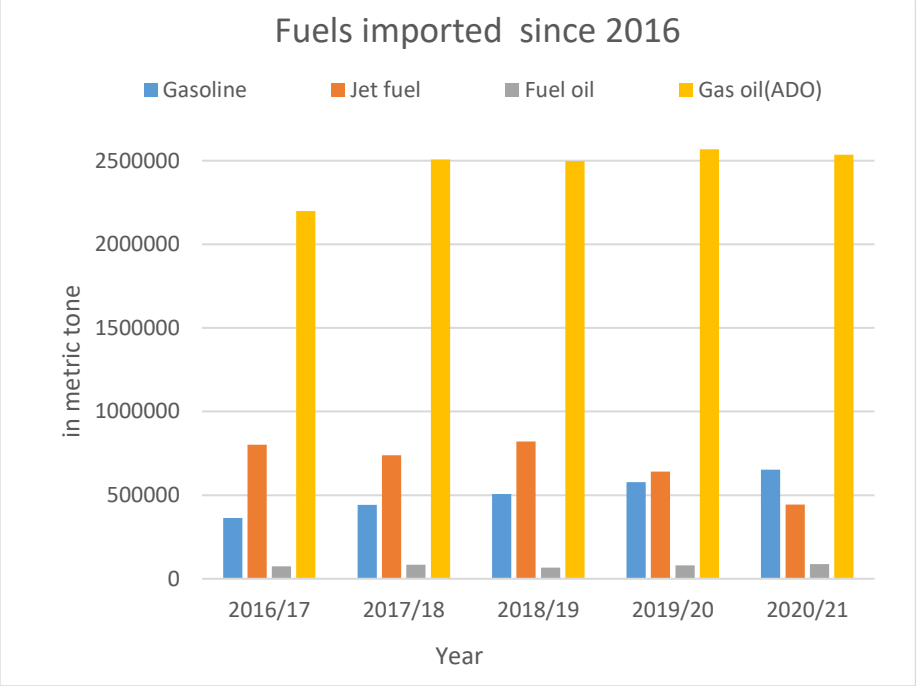

Figure 2. 5 Trends in the volume of petroleum imported from 2016 to 2021

Moreover oil import bill since 2016 to 2021 has shown a significant value for all sorts of fuel imported as shown in Figure 2.6 below.

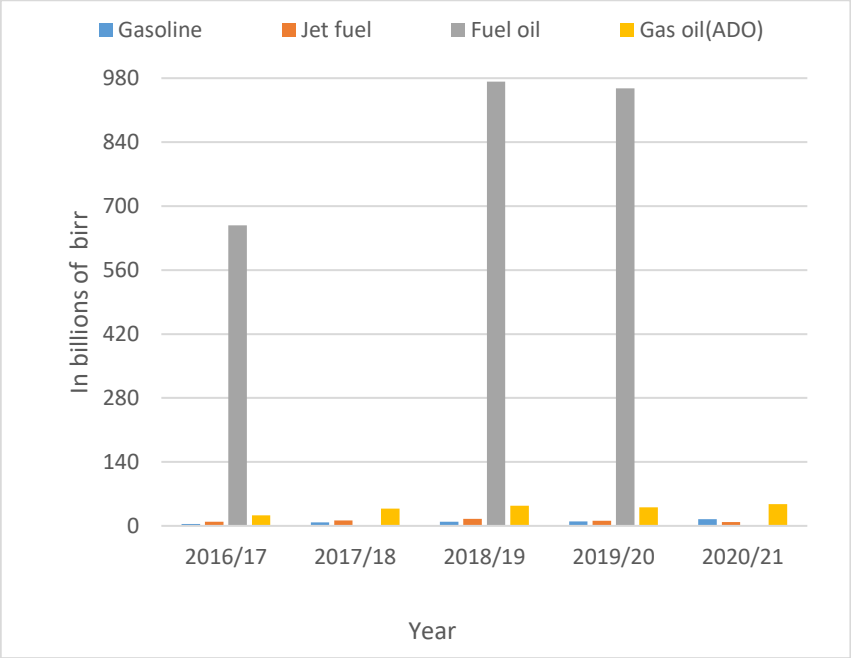

Figure 2. 6 Trends in the value of imported petroleum from 2015 to 2021

2.3. Transportation and Emission

Transportation contributes significantly to global greenhouse gas emissions, accounting for between 14% and 16% of total emissions (Azhar et al., 2024). The combustion of gasoline and diesel for air travel, ships, railroads, and road transportation is the primary source of CO_2 emissions from fossil fuels worldwide (Aminzadegan et al., 2022). The most pressing global environmental issue at present is climate change. A rise of more than 2 °C in the average global temperature might lead to the extinction of up to one million species and the deaths of hundreds of millions of people (Hoegh-Guldberg et al., 2019). Most emissions associated with transportation are generated by cars, trucks, and buses. High-income nations' transportation sectors are the largest emitters, with road transport in the US and Europe producing the most emissions (Li & Tang, 2017). One of the primary reasons for road transport's substantial contribution to global emissions is its reliance on fossil fuels for personal and commercial vehicles. Approximately 12% of the worldwide transportation emissions are attributed to aviation (Graver et al., 2019).Air travel emissions are growing in other transport sectors due to an increasing flight demand, particularly in emerging economies. As the global middle class expands, air travel has become increasingly accessible, contributing to increased aviation emissions. International shipping contributes approximately 10% of global transportation emissions (Graver et al., 2019). The shipping industry relies heavily on bunker fuel, a carbon-intensive fuel derived from crude oil. As global trade continues to expand, emissions from shipping are expected to rise unless cleaner technologies are adopted within the sector. Although rail transport generally has lower emissions than road and air travel, it still

accounts for a significant share of global transportation emissions, especially in regions with extensive freight networks. The high dependence on diesel-powered locomotives in many countries means that rail transport remains a significant source of emissions despite its relatively efficient operation. Global transportation emissions have increased steadily, with developing economies contributing more due to urbanization, rising incomes, and higher vehicle ownership. The growth in emissions from emerging economies like China, India, and Brazil, combined with increased demand for aviation and shipping, has offset reductions seen in developed nations (Wang & Jiang, 2020).

Most transportation-related greenhouse gas (GHG) emissions consist of carbon dioxide (CO2), which accounts for 95%. Methane (CH4) and nitrous oxides (NOx) contribute an additional 1%, while leakage of hydrofluorocarbons (HFCs) from vehicle air conditioning systems is responsible for the remaining 3% (Bleviss, 2021).

Transportation sources also emit ozone, carbon monoxide (CO), and aerosols. Although these substances are not classified as greenhouse gases, they are believed to indirectly affect global warming. However, their precise impact remains unmeasured (A. E. Atabani et al., 2011). Transportation is central to global emissions, and addressing its environmental impact is crucial for achieving international climate goals. Different technological innovations, policies, and awareness will be necessary to minimize emissions in this sector. Continued progress in electrifying transportation, improving fuel efficiency, and transitioning to sustainable practices will shape the future of global transportation emissions.

Transportation plays a major role in global greenhouse gas emissions, accounting for approximately 14 to 16 percent of the total emissions (Azhar et al., 2024). The primary contributor to the largest source of CO_2 emissions from fossil fuels worldwide is the burning of gasoline and diesel for air travel, shipping, rail, and road transport (Aminzadegan et al., 2022). Climate change is currently viewed as the most urgent environmental challenge facing the world.An increase of over 2°C in the global average temperature could result in the extinction of up to one million species and the loss of hundreds of millions of lives (Hoegh-Guldberg et al., 2019).

Thus, transportation plays a key role in global emissions, and addressing its environmental impact is essential for meeting international climate targets. Achieving significant emission reductions in this sector will require a mix of technological innovations, policy measures, and behavioral shifts. Continued progress in the electrification of transport, boosting fuel efficiency, and adopting sustainable practices will be pivotal in shaping the future of global transportation emissions.

2.4. Global Biofuel Scenario

Global energy demand is expected to rise due to rapid population growth, increasing urbanization, and improved living standards (khan et al., 2014). Though it is non-renewable and has a negative impact on global climate (Selvakumar & Alexis, 2016),until this time, fossil fuels continue to be the primary source of energy.(Outlook, 2016). Due to concerns about energy security and the need for environmental sustainability regarding greenhouse gas (GHG) emissions (Kirschstein & Meisel, 2015; O'Driscoll et al., 2018) associated with fossil fuels, which are projected to reach approximately 37 giga tones (Gt) by 2035 (Akbar et al., 2009; Change, 2013; Ho et al., 2014), the production of biofuel was introduced. Renewable energy sources are more evenly distributed across the globe compared to fossil fuels and nuclear resources. Additionally, the energy they produce exceeds the current world energy consumption by more than three orders of magnitude(Lakshmi & Lakshmi, 2020). Renewable energy makes up 13% of total global energy consumption, with bioenergy contributing 10% of that share.(Change, 2013). The growing demand for energy, the depletion of fossil fuels, and rising GHG emissions are driving up petroleum prices and significantly impacting global economic activity(A. Atabani et al., 2013). Therefore, biofuels are candidates to replace fossil fuels. Moreover, they are biodegradable, renewable, and with acceptable-quality of exhaust gases (Kannahi & Arulmozhi, 2013). In the transport sector, diesel engines are widely used on cars, buses, and heavy-duty vehicles, and they are mainly used in agricultural equipment, on-road engineering machinery, and ships due to their higher efficiency, power outputs, and low CO and UHC emissions (Chen et al., 2019). However, diesel engines are the major contributors of particulate matter (Ramegouda & Joseph) and nitrogen oxides emission (Chen et al., 2017). For this reason, searching for an appropriate partial or complete substitute for fossil fuel is the best choice to overcome scarcity and reduce the environmental impact. The global trend to substitute fossil fuel for the application of internal combustion engines (ICE) is biofuel. The choice of biofuel feed stocks is based on the availability and difficulty of growing a specific crop for biofuel, where they can be cultivated geographically, and whether they are set aside for other purposes like livestock feed or human nitration (Bergmann et al., 2013; Sarwer et al., 2022). Regarding biofuel generation, the second generation is the most suitable choice for producing biofuel. Because it can be made from different feedstock of various types of non-food biomass that can grow either on arable land or on marginal lands (Chen et al., 2017). The processes of producing and burning biodiesel are essential in minimizing these emissions. Biodiesel production and combustion can reduce greenhouse gas emissions (Hanaki & Portugal-Pereira, 2018). Compared to fossil fuels, biodiesel has been associated with a 41% reduction in greenhouse gas

emissions (Nordin et al., 2024). Moreover, biodiesel tends to burn cleaner than traditional diesel, resulting in reduced emissions of carbon monoxide (CO), particulate matter (Ramegouda & Joseph), and unburned volatile organic compounds (VOCs) (Chen et al., 2018). This cleaner combustion is due to the higher oxygen content which promotes more complete combustion (Ghadikolaei et al., 2018). Based on economic and sustainability considerations of energy balance, biodiesel yields more energy than is invested in production. Studies indicate that biodiesel produces 93% more energy than the energy invested in its production. It presents economic advantages, but first-generation technology's sustainability and cost competitiveness remain a concern. Further generations of biodiesel production are not yet price-competitive due to the technology's immaturity and high production costs (Singh et al., 2020).

However, the challenges of biodiesel utilization are the availability of feedstock and the production process. (Singh et al., 2020). Utilizing food crops can lead to competition with food production, raising concerns about food security and the sustainable use of land. Alternative feedstock, such as algae and nonedible oil feed stocks, offer promising solutions due to their high oil yields and non-competition with food resources (Pydimalla et al., 2023). The other aspect is the production process, where advancements in production processes are essential to enhance the stability and efficiency of biodiesel. Recent progress includes improvements in the stability of biodiesel fuels, addressing issues such as oxidation and microbial contamination (Lin & Lu, 2021). Hence, biodiesel presents a promising alternative energy source with notable environmental and economic benefits. However, addressing challenges related to feedstock selection, production processes, and financial viability is crucial for this technology's sustainable and widespread adoption.

Biodiesel has significant potential to be part of a sustainable energy mix in the future (Perona, 2017). Between 2019 and 2023, global biodiesel production experienced notable changes. In 2019, production was approximately 0.93 million barrels per day. This figure increased to nearly1.06 million barrels per day in 2022, as shown in Figure 2.7. The European Union, excluding the United Kingdom, was the most significant contributor, accounting for approximately 101.38 barrels per day in 2022. 85% of biodiesel production is believed to originate from the European Union (Raboni et al., 2015). To meet consumer demand, many European countries are heavily reliant on imports. The import value of biodiesel in Europe rose particularly sharply in 2022 when the Russia-Ukraine war affected purchases of feedstock (Balat, 2007; Charles et al., 2013).2.5. Biodiesel as a Potential Energy.

The global dependence on fossil fuels has raised critical concerns regarding energy security, climate change, and environmental degradation(Holechek et al., 2022). In response, biodiesel has

gained significant attention as a renewable and sustainable energy source capable of reducing greenhouse gas (GHG) emissions and decreasing reliance on petroleum-based fuels (Bessou et al., 2011). One of the most important factors influencing the efficiency, cost-effectiveness, and sustainability of biodiesel is the choice of feedstock(Ziolkowska, 2013). In developed countries such as the United States and those in Europe, edible oils like soybean, rapeseed, and sunflower have traditionally been used. However, the growing food-versus-fuel debate has prompted a shift toward non-edible oils such as *Jatropha curcas*, *Pongamia pinnata(Khurana & Bhatnagar, 2024)*, and castor oil particularly suitable for developing nations like Ethiopia and India. Additionally, alternative feedstock such as waste cooking oil and microalgae have emerged due to their availability and minimal impact on food supply chains. Algae, in particular, offer high lipid productivity and carbon sequestration capabilities, making them attractive for next-generation biodiesel production.

Biodiesel can be used in conventional diesel engines, often with minimal or no modifications especially in blends like B20 (20% biodiesel, 80% diesel). Its use generally results in improved lubricity, lower emissions of unburned hydrocarbons, carbon monoxide, and particulate matter, and biodegradability that reduces environmental risk in the event of spills. However, biodiesel typically delivers slightly lower engine power and higher brake-specific fuel consumption due to its lower calorific value(Oliveira & Da Silva, 2013). One notable drawback is the increase in nitrogen oxide (NOx) emissions, which may require mitigation through engine calibration or additives.

From an environmental and energy efficiency standpoint, biodiesel is promising, offering up to a 78% reduction in lifecycle GHG emissions and generating about 93% more energy than what is consumed during its production(El-Araby, 2024). Nonetheless, the sustainability and economic viability of first-generation biodiesel mainly derived from food crops remain under scrutiny. While later-generation technologies, including those based on algae and other non-edible feedstock, show better sustainability potential, they are not yet commercially competitive due to high production costs and technological limitations(Luque et al., 2008).

Key challenges facing biodiesel include feedstock availability, production efficiency, fuel stability, and cost(Anuar & Abdullah, 2016). Reliance on food crops raises concerns about land use and food security(Koizumi, 2015). To address these issues, recent advancements have focused on improving biodiesel production processes to enhance fuel quality and long-term stability by mitigating problems like oxidation and microbial contamination.

Globally, biodiesel is becoming an integral part of the future sustainable energy mix(Suardi et al., 2023). Between 2019 and 2023, global production increased from approximately 0.93 million

barrels per day to around 1.06 million barrels per day(Santos et al., 2025). The European Union excluding the United Kingdom has led this growth, accounting for about 85% of global production in 2022. However, to meet rising demand, many European countries have become increasingly reliant on imports particularly in 2022, when the Russia-Ukraine conflict disrupted feedstock supply chains. Countries such as Brazil, France, Germany, Indonesia, Italy, and Malaysia are also prominent producers(Bajan et al., 2021). According to global assessments, Malaysia holds one of the highest potentials for biodiesel production as indicated in the Table 2.1.

Table 2. 1 Top 10 countries in terms of biodiesel potential

Country	Biodiesel potential (Laurens et al.)	Production($/L)	Rank
Malaysia	14,540	0.53	1
Indonesia	7,595	0.49	2
Argentina	5,255	0.62	3
USA	3,212	0.70	4
Brazil	2,567	0.62	5
Netherlands	2,496	0.75	6
Germany	2,024	0.79	7
Philippines	1,234	0.53	8
Belgium	1,213	0.78	9
Spain	1,073	1.71	10

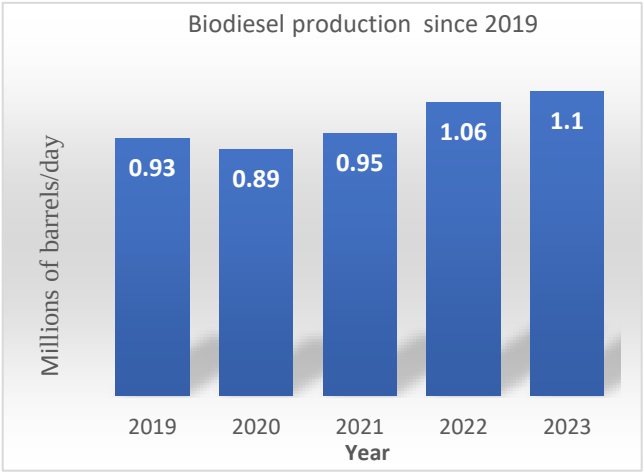

Figure 2. 7 Total world biodiesel productions since 2019 to 2023

2.6. Advantages and disadvantages of biodiesel

The advantages and disadvantages of biodiesel are summarized and indicated in sections 2.6.1 and 2.6.2, respectively

2.6.1. Advantages of biodiesel

The following points are the advantages of biodiesel according to (Firoz, 2017; Torkashvand et al., 2022).

- Biodiesel's 10–11% oxygen content improves its combustion efficiency.
- Biodiesel cuts lifecycle of CO_2 emissions by 78% and reduces smoke by limiting free soot relative to diesel fuel.
- Biodiesel supports rural development, aids in land restoration over time, and offers strong potential for job creation in rural areas.
- Biodiesel is climate-neutral and plays a vital role in sustainable energy use and development.
- Biodiesel has a higher cetane number (60–65) than petroleum diesel (around 53), resulting in shorter ignition delay
- Production is easy to increase and requires less time.
- Biodiesel production requires no drilling, transportation, or refining like petroleum diesel, allowing countries to produce it locally. This also eliminates tariffs and taxes paid on imported oil and diesel
- Biodiesel offers superior lubricity, enhancing fuel pump and injector lubrication, which reduces engine wear and boosts efficiency.
- Biodiesel is safer to transport, handle, distribute, use, and store because its flash point (100–170 °C) is higher than petroleum diesel's (60–80 °C).
- Biodiesel reduces environmental impact by recycling waste products like used cooking oils and animal fats
- Biodiesel blends up to B20 usually do not need engine modifications, but higher blends might require minor changes.

2.6.2. Disadvantages of biodiesel

The following points are the advantages of biodiesel according to (Firoz, 2017; Torkashvand et al., 2022)

- Biodiesel contains about 12% less energy than diesel, causing a 2–10% increase in fuel consumption. It also has higher cloud and pour points, emits more nitrogen oxides, and lower volatility, which can lead to engine deposits from incomplete combustion.
- Biodiesel can cause excessive carbon deposits and gum formation in engines, leading to oil contamination and flow issues. Its viscosity is 11–18 times higher than diesel, and with lower volatility, it requires higher injector pressure.

- Biodiesel has lower oxidation stability than diesel and can oxidize into fatty acids when exposed to air, leading to corrosion in fuel tanks, pipes, and injectors.
- Due to its high oxygen content, advanced fuel injection timing, and earlier combustion onset, biodiesel generates approximately 10–14% more NOx emissions than diesel during combustion
- Biodiesel can corrode materials like copper and brass, leading to fuel system blockages, seal failures, filter clogging, and deposits in injection pumps.
- Using biodiesel in internal combustion engines may cause durability issues such as injector clogging, filter blockage, and piston ring sticking.
- Over 95% of biodiesel is made from edible oils, raising concerns about diverting food to fuel and disrupting global food supply and economics
- Transesterification is costly due to expensive fatty acid, which raises fuel prices.
- Transesterification poses environmental challenges, such as waste disposal, high water use for washing, and soap formation.

2.7. Biofuel Feed Stocks

There are over 350 oil-bearing crops worldwide recognized as potential sources for biodiesel production. (Eryilmaz et al., 2016). Tables 2.2 and 2.3 present the primary feed stocks used in biodiesel production. The diverse array of feed stocks available for biodiesel production is a key factor in the successful production of biodiesel. (Ambat et al., 2018). The feedstock should ideally meet two key requirements: low production costs and a large production scale. (You et al., 2008). The availability of feed stock for biodiesel production is influenced by regional climate, geographical location, soil conditions, and agricultural practices in each country(Amigun & Musango, 2011). Literature indicates that feed stock alone contributes to 75% of the total biodiesel production cost, as shown in Figure 2.8. Consequently, choosing the most cost-effective feed stock is essential for minimizing production costs. Figures 2.9 and 2.10 display images of various edible and non-edible biodiesel feed stocks, respectively. Generally, biodiesel feed stock can be classified into four main categories, as outlined in Table 2.3 below. (Roick et al., 2021; Shaah et al., 2021): Table 2.2 shows primary biodiesel feedstock for some selected countries around the world (Ahmad et al., 2011; Karmakar et al., 2010)

Table 2. 2 Current potential feed stocks for biodiesel worldwide

Country	**Feedstock**
USA	Soybeans, waste oil, Peanut
Canada	Rapeseed, Animal fat, Soybeans, Tallow, Mustard, Flax
Mexico	Animal fat, Waste oil
Germany	Rapeseed
Italy	Rapeseed, Sunflower
France	Rapeseed, Sunflower
Spain	Linseed oil, Sunflower
Greece	Cottonseed
UK	Rape seed, Waste cooking oil
Sweden	Rapeseed
Ireland	frying oil, animal fats
India	Jatropha,karanja, Soybean, Rapeseed, Sunflower, Peanut
Malaysia	Palm oil
Indonesia	Palm oil, Jatropha, Coconut
Singapore	Palm oil
Philippines	Coconut, Jatropha
Thailand	Palm, Jatropha, Coconut
China	Jatropha, Waste cooking oil, Rapeseed
Brazil	Soybeans, Palm oil, Castor, Cotton oil
Argentina	Soybeans
Japan	Waste cooking oil
New Zealand	Waste cooking oil,Tallow

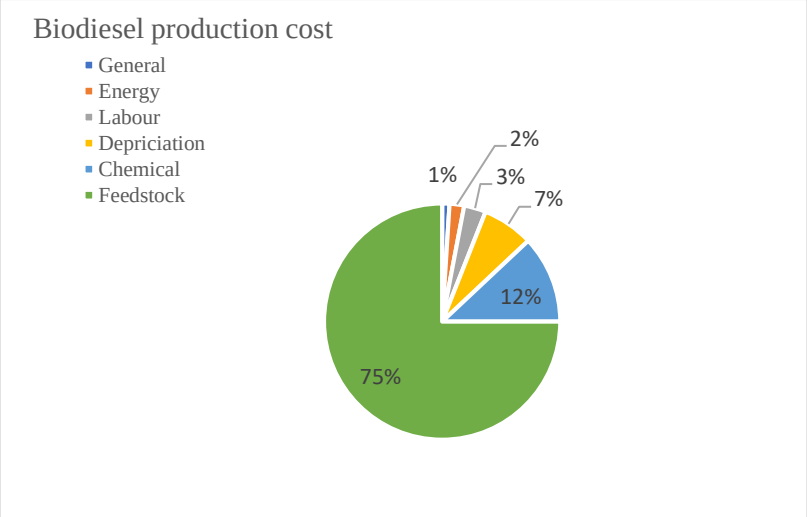

Figure 2. 8 Biodiesel production cost (Gebremariam & Marchetti, 2018)

Table 2. 3 Biodiesel feed stocks (Eriksson & Sivertsson, 2015)

None edible oil	**Edible oil**	**Animal fats**	**Other sources**
Abutilon muticum	Barley	Beef tallow	Algae
Aleurites moluccana	Canola	Chicken fat	Bacteria
Camelina (Camelina Sativa)	Coconut	Fish oil	Fungi
Coffee ground (Coffea arabica)	Corn	Pork lard	Latexes
Cotton seed (Gossypium hirsutum)	Groundnut	Poultry Fat	Microalgae
Croton megalocarpus	Palm		Miscanthus
Cumaru	Peanut		Poplar
Cynara cardunculus	Rapeseed		Switchgrass
Jatropha curcas	Rice bran oil		Tarpenes
Jojoba (Simmondsia chinensis)	Safflower		
Mahua (Madhuca indica)	Sesame		
Moringa (Moringa oleifera)	Sorghum		
Nagchampa(Calophyllum inophyllum)	Soybeans		
Neem (Azadirachta indica)	Sunflower		
Pachira glabra	Wheat		
Passion seed (Passiflora edulis)			
Pongamia (Pongamia pinnata)			
Rubber seed tree			
Salmon oil			
Tall (Carnegiea gigantean)			
Terminalia belerica			
Tobacco seed			

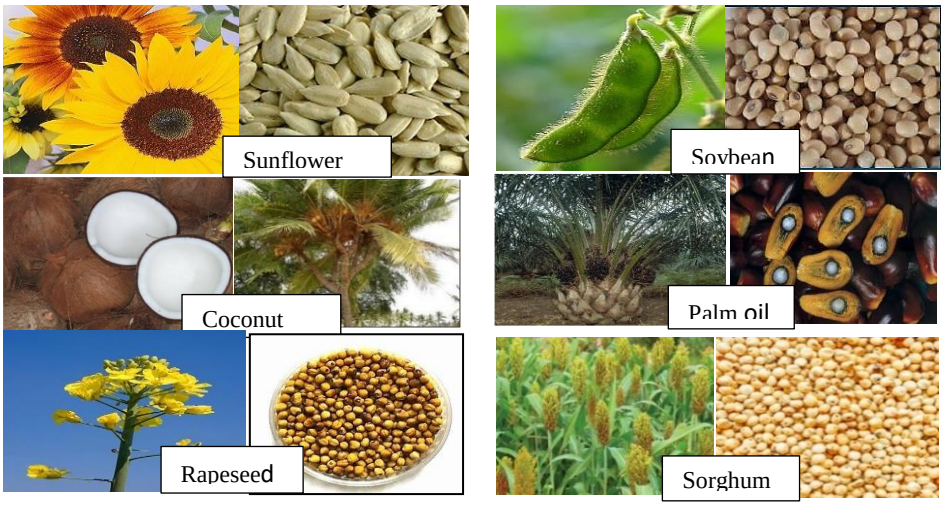

Figure 2. 9 Edible oil feed stocks (Compiled by the author from Atabani et al. (2012) and Demirbas (2009).

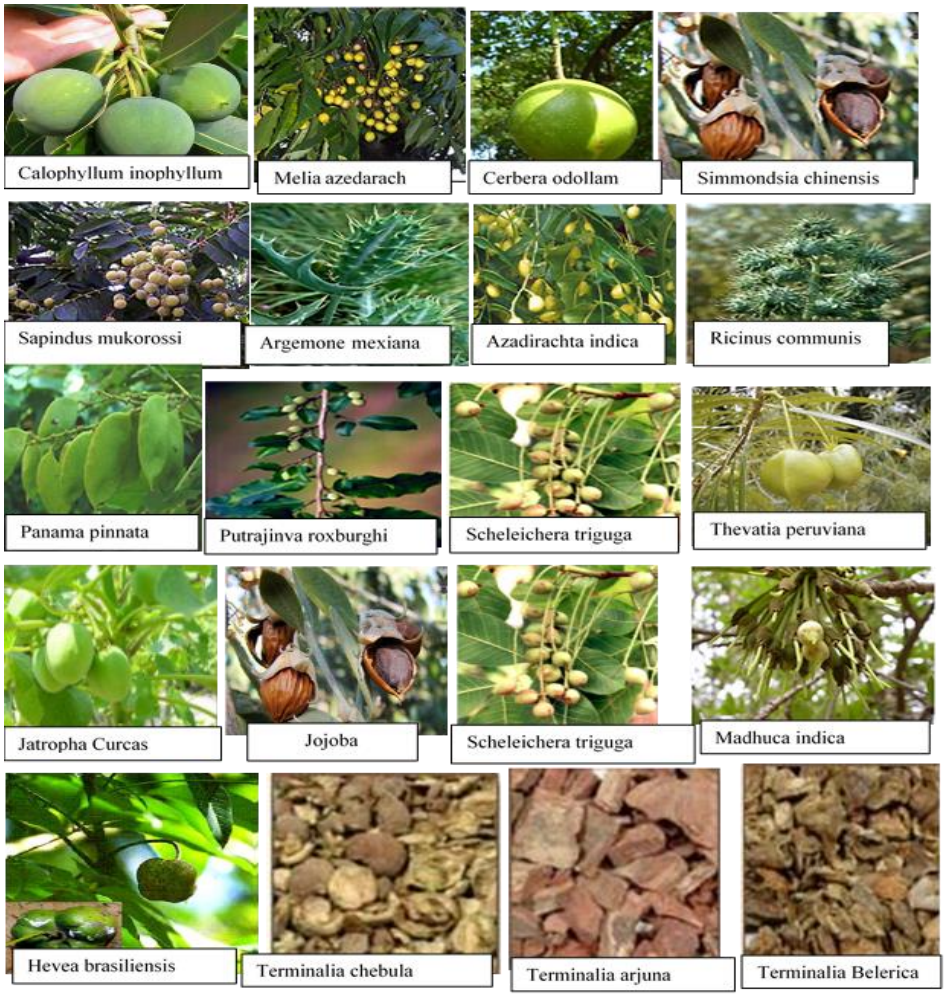

Figure 2. 10 Non-edible oil feedstock (Compiled by the author from Atabani et al. (2012) and Demirbas (2009).

When comparing different feed stocks, it is essential to consider several factors, with a full life-cycle analysis being key for each option (Wang et al., 2019). This involves assessing land availability, cultivation practices, energy supply, greenhouse gas emissions, pesticide usage, soil fertility, water requirements, air quality effects, logistics, and economic value of co-products, employment opportunities, and impacts on biodiversity.(Ahmad et al., 2011; Balat, 2011; Chisti, 2007). Additionally, when evaluating feedstock as a source for biodiesel, the oil percentage and yield per hectare are crucial parameters, as indicated in Table 2.4. *(Mijić et al., 2009)*

Table 2. 4 Estimated oil content and yields of different biodiesel feed stocks

* (kg oil/ha)

Feedstocks	**Oil content (%)**	**Oil yield (L/ha/year)**
Calophyllum inophyllum L.	65	4680
Castor	45-50	1413
Coconut	63-65	2689
Corn (Diaz et al.)	48	172
Cottonseed	18-25	325
Euphorbia lathyris L.	48	1500-2500*
Jatropha	50-60	1892
Jojoba	45-50	1818
Linseed	35-45	-
Microalgae (high oil content)	70	136,900
Microalgae (low oil content)	30	58,700
Microalgae (medium oil content)	50	97,800
Moringa oleifera	40	-
Neem	20-30	-
Olive oil	45-70	1212
Pachira Glabra	40-50	-
Palm oil	30-60	5950
Peanut oil	45-55	1059
Pongamia pinnata (Karanja)	30-40	225-2250*
Rapeseed	38-46	1190
Rice bran	15-23	828
Rubber seed	40-50	80-120*
Sapium sebiferum L.	Kernel 12-29	-
Sea mango	54	-
Sesame	-	696
Soybean	15-20	446
Sunflower	25–35	952
Tung	16-18	940

Edible oil resources, including soybeans, palm oil, sunflower oil, rapeseed oil, coconut oil, and peanuts, are classified as first-generation biodiesel feed stocks because they were among the earliest crops used for biodiesel production.(Mijić et al., 2009). Their plantations are well-established in various countries, including Malaysia, the United States, and Germany(Abdul-Manan et al., 2014). Currently, over 95% of the world's biodiesel is produced from edible oils,

with rapeseed accounting for 84%, sunflower oil for 13%, palm oil for 1%, and soybean oil and other oils making up the remaining 2%(Gunstone, 2011). However, their use raises several concerns, including the food versus fuel crisis and significant environmental issues, such as the degradation of essential soil resources, deforestation, and the use of a large portion of available arable land (Gunstone, 2011). Additionally, the prices of vegetable oil plants have risen dramatically, impacting the economic viability of the biodiesel industry(Gebremariam & Marchetti, 2018). Furthermore, using edible oils for biodiesel production is not a sustainable long-term solution due to the widening gap between demand and supply. In many countries, the availability of these oils is limited. For example, if all soybeans in the United States were allocated to biodiesel production, it would only satisfy 6% of the nation's diesel demand (Chapagain et al., 2009)(Chapagain et al., 2009). One potential solution to decrease the use of edible oils in biodiesel production is to utilize non-edible oils(Gashaw & Teshita, 2014).

2.7.1. Non-edible vegetable oil resources

Non-edible vegetable oils are unsuitable for human consumption because they contain toxic components(Ahmad et al., 2011). Selecting non-edible vegetable oils as feed stocks for biodiesel production necessitates a review of existing literature. Recent comprehensive reviews highlight the benefits of using non-edible oils compared to edible oils in biodiesel production. Utilizing non-edible oil feed stocks can mitigate the food versus fuel controversy and address the environmental and economic challenges associated with edible vegetable oils(Gui et al., 2008). Non-edible biodiesel crops are expected to be grown on largely unproductive lands, in impoverished areas, and on degraded forests. Additionally, they can be planted along the boundaries of cultivators' fields, on shallow lands, and in public spaces such as railways, roads, and irrigation canals.(A. E. Atabani et al., 2013). The development of non-edible biodiesel could serve as a significant poverty alleviation program for the rural poor, enhancing energy security, particularly in rural areas, and strengthening the rural non-farm sector. These factors greatly influence the sustainability of biodiesel production. Many researchers agree that non-edible feed stocks for biodiesel should be recognized as sustainable alternative fuels.(Ahmad et al., 2011; Ravi & Sastry, 2009; Syers et al., 2007). Non-edible oil plants are well adapted to arid and semi-arid conditions, thriving with low fertility and minimal moisture requirements(Yang et al., 2014).

They are typically propagated through seeds or cuttings. Additionally, because these plants do not compete with food crops, the seed cake produced after oil extraction can be used as fertilizer to enrich the soil(Azam et al., 2005). Several potential tree-borne oilseeds (TBOs) and non-edible crop sources have been identified as suitable feedstock for biodiesel, as shown in Figure 2.11

(Razon, 2009; Syers et al., 2007). The following section provides a brief overview of different types of non-edible plant oils.

2.7.1.1. Jatropha curcas

Jatropha curcas L. is a small tree or large shrub, reaching heights of 5 to 7 meters, and it belongs to the Euphorbiaceae (Balat, 2011; Kibazohi & Sangwan, 2011; Misra & Murthy, 2011). It is a drought-resistant plant that can thrive in abandoned and fallow agricultural lands.(Kibazohi & Sangwan, 2011; Kumar & Sharma, 2011; Pinzi et al., 2009). This tropical plant flourishes in diverse climatic zones, thriving in areas with rainfall between 250 and 1,200 mm. It is native to Mexico, Central America, Africa, India, Brazil, Bolivia, Peru, Argentina, and Paraguay.(Azam et al., 2005; Kibazohi & Sangwan, 2011; Kumar & Sharma, 2011). This plant is highly suited to arid and semi-arid environments, where soil fertility and moisture are low. It can also thrive in moderately sodic, saline, degraded, and eroded soils. The optimal planting density is 2,500 plants per hectare. It begins producing seeds after 12 months, achieves maximum productivity by the fifth year, and has a lifespan of 30 to 50 years. Seed production varies significantly, ranging from 0.1 to over 8 tons per hectare annually, depending on soil conditions.(Azam et al., 2005; Kibazohi & Sangwan, 2011). Depending on the variety, the seed of Jatropha contains 43-59% oil.(S. Y. No, 2011).

2.7.1.2. Pongamia pinnata L.

Pongamia pinnata (L.) Pierre, also known as Karanja or Honge, is a medium-sized evergreen leguminous tree from the Millettieae tribe of the Papilionaceae (Leguminosae) family(Ramanjaneyulu et al., 2025). Native to the Indian subcontinent and Southeast Asia, it has also been successfully introduced to humid tropical areas and parts of Australia, New Zealand, China, and the USA(Karmee & Chadha, 2005). Traditionally, it has been used for medicinal purposes, animal fodder, green manure, timber, natural pesticides, fish poison, and as a binder and fuel. More recently, it has emerged as a potential feedstock for the biofuel industry. Recommended planting spacing is 3^2 meters (Sharma & Kumar, 2011).

Its seeds contain 30–40% oil by weight (Balat, 2010). The oil is reddish-brown and high in oleic acid and unsaponifiable matter(Sanford & Kelly, 2011).

2.7.1.3. Croton megalocarpus

Croton *megalocarpus*, a tree native to Eastern and Central Africa, has been increasingly recognized as a promising non-edible biodiesel feedstock(Resta, 2024) . Commonly found in countries such as Kenya, Uganda, Tanzania, and Ethiopia, this species belongs to the Euphorbiaceae

family(Osawa, 2016). It is a fast-growing, drought-resistant tree that can reach heights between 15 and 40 meters and thrives at altitudes ranging from 1200 to 2450 meters above sea level(Kibazohi & Sangwan, 2011). A tree of Croton megalocarpus produces up to 50 kg of seeds, and a hectare produces 5 to 10 t of seeds per year (Kibazohi & Sangwan, 2011) Its adaptability to a range of ecological zones, along with its low maintenance requirements, makes it particularly suitable for biodiesel production in tropical and subtropical climates.

The seeds of *Croton megalocarpus* contain a high oil content, typically ranging from 30% to 45% by weigh(Aliyu et al., 2010). This oil has favorable physicochemical properties, including moderate acid value and acceptable viscosity, which make it suitable for transesterification. The fatty acid composition includes a significant proportion of unsaturated fatty acids such as linoleic acid (C18:2) and oleic acid (C18:1), along with saturated fatty acids like palmitic acid (C16:0), contributing to a cetane number and iodine value that are within desirable ranges for biodiesel (Wu et al., 2012).

2.7.1.4. Moringa oleifera

Moringa oleifera, commonly referred to as the "miracle tree," is a fast-growing, drought-resistant plant native to the Indian subcontinent and widely cultivated in tropical and subtropical regions across Africa, Asia, and Latin America(Bania et al., 2023). Traditionally valued for its nutritional and medicinal properties, *Moringa* has also attracted attention in recent years as a potential non-edible feedstock for biodiesel production due to the high oil content of its seeds and the favorable properties of the derived oil(Ebert et al., 2019)

The seeds of *Moringa oleifera* contain approximately 30–40% oil by weight(Kibazohi & Sangwan, 2011), with oil yields estimated at around 250–500 liters per hectare under normal cultivation conditions. The extracted oil has a high monounsaturated fatty acid content, particularly oleic acid (C18:1), which constitutes about 70–78% of the total fatty acids(Rashid et al., 2008). This composition contributes to superior oxidative stability, a high cetane number, and excellent cold flow properties which are key characteristics that make *Moringa* oil an attractive feedstock for biodiesel(Rashid et al., 2008).

2.7.1.4. Aleurites moluccana

Aleurites moluccana, commonly known as candlenut or kukui nut, is a tropical tree from the Euphorbiaceae family, native to Southeast Asia and the Pacific Islands(Elevitch & Manner, 2006). It grows well between the altitudes of 0-1200 m, a temperature of 18-28 $^{\circ}$C, a rainfall of 650-4300 mm, and a soil pH of 5-8 in marginal soils with minimal input, making it a potential non-edible

biodiesel feedstock for tropical and subtropical regions. The seeds contain 50–60% oil by weight, which is relatively high compared to other oil crops(Abd & Mohamad, 2010).

The oil is rich in unsaturated fatty acids, particularly linoleic and oleic acids that contributes to good flow and ignition properties(Kibazohi & Sangwan, 2011). However, the high degree of unsaturation also results in lower oxidative stability, potentially affecting long-term storage.

Fuel properties of *A. moluccana* biodiesel include acceptable viscosity, density, flash point, and a high cetane number (Setyadi et al., 2020). However, the iodine value tends to be high, indicating susceptibility to oxidation. Engine tests have shown that candlenut biodiesel reduces carbon monoxide, hydrocarbons, and particulate emissions, though nitrogen oxides (NOx) may increase slightly, a common trend with biodiesel(Md Ruhul, 2017).

The plant's non-edible nature ensures it does not compete with food crops, and its seedcake can be used as fertilizer, though toxicity (e.g., phorbol esters) limits use in animal feed. Despite promising fuel characteristics and environmental benefits, commercial adoption is hindered by limited seed supply, lack of processing infrastructure, and the need for further research on storage stability and large-scale feasibility(Ubeda et al., 2017).

2.7.1.5. Pachira glabra

Pachira glabra, a member of the Malvaceae family, is a fast-growing tropical tree native to Central and South America and also cultivated in parts of Asia and Africa(Castellanos & Stevenson, 2011). It is often planted for ornamental and agroforestry purposes. The tree produces large, nut-like seeds that contain significant oil content, positioning it as a potential non-edible feedstock for biodiesel production (Kibazohi & Sangwan, 2011).Its seeds of contain approximately 40–50% oil, making them a viable candidate for biofuel applications(Tebe et al., 2024). The extracted oil exhibits a favorable fatty acid composition, with high levels of oleic and linoleic acids. These contribute to good fuel properties, such as low viscosity, high cetane number, and acceptable cold flow characteristics. Studies have shown that the oil can be efficiently converted into biodiesel via base-catalyzed transesterification, yielding over 90% under optimal conditions (A. E. Atabani et al., 2013).

2.7.1.6. Ricinus communis (Castor)

Ricinus communis, commonly known as castor, is a hardy, fast-growing shrub or small tree from the Euphorbiaceae family, widely cultivated in tropical and subtropical regions(Chakrabarty, 2021). It is well-adapted to arid and semi-arid climates and thrives on marginal land with minimal agricultural input (Gui et al., 2008; Lopez & Neto, 2011; Sanford et al., 2009). Castor is

traditionally grown for its oil-rich seeds, and in recent years, it has gained attention as a promising non-edible biodiesel feedstock due to its high oil content and ease of cultivation.

Castor seeds contain approximately 40–55% oil, which is unusually rich in ricinoleic acid (over 85%). This unique fatty acid, characterized by a hydroxyl group, imparts distinct physical and chemical properties to castor oil such as high viscosity, polarity, and lubricity which differentiate it from conventional vegetable oils. These properties are advantageous in certain industrial applications but pose challenges in direct biodiesel use, particularly regarding fuel flow and atomization in diesel engines (A. E. Atabani et al., 2013).

2.7.1.7. Calophyllum inophyllum L. (Polanga)

Calophyllum inophyllum L., commonly known as Polanga, Tamanu, or Alexandrian laurel, is a tropical tree native to coastal regions of South and Southeast Asia, the Pacific Islands, and East Africa(Azam et al., 2005; Sahoo et al., 2007; Venkanna & Venkataramana, 2009) . It belongs to the Clusiaceae (formerly Guttiferae) family and thrives in sandy, saline, and degraded soils, often along shorelines. Traditionally valued for its medicinal, timber, and oil-producing properties, the tree has emerged as a promising non-edible biodiesel feedstock due to its high oil content and ability to grow in marginal lands(Susanto et al., 2017).

The seeds of *C. inophyllum* contain 40–73% oil by weight, depending on location, tree maturity, and processing method and has a tinted green, thick, and has a woodsy or nutty smell (Hathurusingha et al., 2011; Sahoo et al., 2007; Venkanna & Venkataramana, 2009). The oil is rich in oleic acid (C18:1), linoleic acid (C18:2), stearic acid (C18:0), and palmitic acid (C16:0), giving it a balanced saturation profile suitable for biodiesel. Its high oil yield per hectare and non-edibility make it an attractive feedstock, especially in regions where land use competition with food crops is a concern (A. E. Atabani et al., 2013)

2.1.7.8. Sterculia foetida L.

Sterculia foetida L., commonly known as the wild almond, Java olive, or hazel sterculia, is a deciduous tree species native to tropical Asia and parts of Africa(Vélez-Gavilán, 2023). It belongs to the family Malvaceae and grows well in arid and semi-arid regions, making it a potential candidate for sustainable biodiesel production on marginal lands. The tree produces oil-rich seeds with an average oil content of 30–45%, depending on geographic and environmental factors(Patil-Gadhe & Pokharkar, 2014)

The seed oil of *S. foetida* is non-edible due to the presence of cyclopropene fatty acids (CPFAs), mainly sterculic and malvalic acids, which are known to be toxic and potentially

carcinogenic(Bose, 2022). However, these properties do not impede its suitability as a feedstock for biodiesel, since the toxic components are not carried over in the transesterified methyl esters (biodiesel) in significant amounts.

Environmentally and socio-economically, *S. foetida* offers advantages due to its drought tolerance, ability to grow on degraded soils, and potential for afforestation(Sarangthem et al., 2023). However, due to the presence of CPFAs, care must be taken in handling and processing the seeds and oil. The species also has multiple uses: its wood is used locally for carpentry, and the seed cake (after oil extraction) is being studied for its use as fertilizer or industrial feedstock(Sen, 2020).

2.1,7,9, Madhuca indica

Madhuca indica, commonly known as Mahua, is a deciduous tree indigenous to the Indian subcontinent and belongs to the Sapotaceae family. It is widely distributed in central and northern India, particularly in tribal and forested regions (Balat & Balat, 2010; A. Demirbas, 2009; Jena et al., 2010). It quickly to approximately 20 m in height, possesses evergreen or semi-evergreen foliage, and is adapted to arid environments (Kumar & Sharma, 2011; Pinzi et al., 2009)The tree is valued for its oil-rich seeds, which contain approximately 30–40% oil by weight, making it a viable non-edible feedstock for biodiesel production. Mahua oil is traditionally used for soap making, lighting, and even cooking in rural areas, but its high free fatty acid (FFA) content initially limited its suitability for direct transesterification(Pradhan et al., 2016).

Recent studies also explore blends of Mahua biodiesel with diesel and additives to improve engine performance and emission profiles. Experimental investigations report that B20 blends (20% Mahua biodiesel with 80% diesel) generally show a slight reduction in brake thermal efficiency but notable decreases in CO, HC, and particulate matter emissions, although NOx emissions may increase slightly(Chatterjee et al., 2021).

2.1.7.10. Sapium sebiferum (Linn.) Roxb (Chinese tallow)

Sapium sebiferum (Linn.) Roxb, widely known as the Chinese tallow tree**,** is a fast-growing deciduous tree native to eastern Asia, especially China and Japan. Belonging to the Euphorbiaceae family, this species has attracted considerable interest as a biodiesel feedstock due to its high oil yield and adaptability to a range of soil types and climates, including degraded or marginal lands(Yang et al., 2015).

The seeds of *S. sebiferum* are covered with a waxy, tallow-like aril and contain up to 45–60% oil by weight(Ma et al., 2023)**.** This oil is non-edible and comprises long-chain fatty acids such as palmitic, stearic, oleic, and linoleic acids, which are favorable for biodiesel conversion. The

presence of high free fatty acids (FFA) in crude oil, however, requires a two-step transesterification process (acid esterification followed by alkaline transesterification) for efficient biodiesel production (Tang et al., 2015).

Sapium sebiferum is a promising biodiesel feedstock due to its high oil content, favorable fatty acid profile, and suitability for cultivation on non-arable lands. However, its potential invasiveness must be considered in land management and sustainability assessments. Future research is needed to optimize its agronomy, oil extraction, and transesterification techniques to facilitate commercial-scale biodiesel production(Zhao et al., 2019).

2.1.7.11. Aleutites fordii (Tung)

Aleurites fordii, commonly referred to as the Tung tree**,** is a fast-growing deciduous tree belonging to the family Euphorbiaceae. Native to southern China, Burma, and Vietnam, it has been cultivated in various subtropical and tropical regions for its high-value oil, historically used in paints, varnishes, and wood finishes (PENFOLD & SMITH-WHITE, 1941). The seeds of the Tung tree contain 50–60% oil by weight, making it one of the highest-yielding non-edible oilseed sources(Park et al., 2015).

Tung oil is composed primarily of α-eleostearic acid, a conjugated triene fatty acid that constitutes up to 80% of its total fatty acid profile (Murawski, 2017). This high degree of unsaturation provides the oil with excellent drying and polymerizing properties but also presents challenges for biodiesel production. The presence of conjugated double bonds can lead to poor oxidative stability, high viscosity, and potential polymerization at elevated temperatures (Lacerda & Gandini, 2020). Despite these drawbacks, several studies have demonstrated the feasibility of converting Tung oil into biodiesel via two-step transesterification using modified catalysts like acid-base or enzymatic catalysts (Kaur et al., 2017). The resulting methyl esters have acceptable fuel properties in terms of calorific value, flash point, and density but require oxidative stabilizers to meet long-term storage and engine performance standards. Cold flow properties may be acceptable in warmer climates but can be limiting in temperate zones(Kaur et al., 2017).

2.1.7.12. Azadirachta indica (Neem)

Azadirachta indica, commonly known as Neem, is a fast-growing, evergreen tree native to the Indian subcontinent and widely cultivated in arid and semi-arid regions of Africa and Asia. Belonging to the Meliaceae family, Neem is renowned for its medicinal, pesticidal, and environmental benefits(Kaur et al., 2017). In recent decades, Neem has gained attention as a non-

edible oilseed feedstock for biodiesel production, due to its abundance, drought tolerance, and high oil yield potential (Kaur et al., 2017).

Neem seeds contain approximately 30–45% oil, depending on the region and seed quality (Azam et al., 2005; S. Y. No, 2011; Ragit et al., 2011). The oil is highly bitter and non-edible due to the presence of bioactive compounds like Azadirachtin, making it ideal for non-food biofuel applications. The fatty acid profile of Neem oil typically includes palmitic (C16:0), stearic (C18:0), oleic (C18:1), and linoleic (C18:2) acids, which provide a good balance of saturation and unsaturation for biodiesel production (Kaur et al., 2017).

2.1.7.13. Nicotiana tabacum (Tobacco)

Nicotiana tabacum, commonly known as tobacco**,** is a widely cultivated plant of the Solanaceae family, traditionally grown for its leaves used in cigarette and cigar production (Kaur et al., 2017). However, due to declining global tobacco consumption and the plant's rich lipid content in its seeds, researchers have explored its potential as a non-edible biodiesel feedstock (Kaur et al., 2017)**.**

Tobacco seeds contain approximately 30–40% oil by weight, which is non-edible and toxic due to alkaloids such as nicotine. This toxicity prevents it from entering the food chain, making it suitable for bioenergy application**s** without raising food-versus-fuel concerns (Kaur et al., 2017). The fatty acid composition of tobacco seed oil includes linoleic (C18:2), oleic (C18:1), palmitic (C16:0), and stearic acids (C18:0), a profile that supports good biodiesel conversion and combustion characteristics (Kaur et al., 2017).

Tobacco offers an interesting advantage: it can be grown on marginal lands and does not compete with food crops. Moreover, genetically modified tobacco is being researched not only for higher oil yield but also for bioengineering traits such as lower nicotine content and altered oil profiles for better fuel quality. The leftover biomass after seed oil extraction can be used for biogas, biochemicals**,** or even cellulosic ethanol production, enhancing the plant's bioenergy potential (Kaur et al., 2017).

2.1.7.14. Hevea brasiliensis (Rubber seed)

Hevea brasiliensis, commonly known as the rubber tree is primarily cultivated for natural latex, but its rubber seeds, typically considered an agricultural byproduct, have gained attention as a non-edible and sustainable feedstock for biodiesel production(Kaur et al., 2017). Native to the Amazon Basin and widely cultivated in tropical regions like Southeast Asia and West Africa, the tree

produces large quantities of seeds approximately 800–1,200 kg/hectare/year, making them a valuable secondary product(Kaur et al., 2017).

Rubber seeds contain 35–45% oil by weight, and the oil has a favorable fatty acid profile for biodiesel conversion, dominated by oleic acid (~24–40%), linoleic acid (~20–36%), linolenic acid, and some saturated fatty acids like palmitic and stearic acids(Kaur et al., 2017). However, rubber seed oil (Zhao et al.) has a high free fatty acid (FFA**)** content (often >10%), necessitating a two-step transesterification process (acid esterification followed by base catalysis) for efficient biodiesel production (Kaur et al., 2017).

Studies have shown that biodiesel produced from RSO meets ASTM D6751 and EN 14214 fuel standards when properly processed. Its viscosity, flash point, density, and calorific value are within acceptable ranges. However, oxidative stability may be a concern due to high polyunsaturated fatty acid content, and may require antioxidant additives for long-term storage and use (Kaur et al., 2017).

Engine tests using rubber seed biodiesel blends ranging from B10–B40 report performance characteristics comparable to diesel, with slight reductions in brake thermal efficiency and power output. Emissions testing generally shows reduced CO, HC, and smoke, but a modest increase in NOx emissions, a common trade off in biodiesel fuels(Kaur et al., 2017).

2.1.7.15. Rice bran

Rice bran oil, extracted from the outer layer of rice grains during milling, is an abundant byproduct of rice production(Kaur et al., 2017). Given that rice is a staple crop in many parts of Asia and Africa, rice bran presents a readily available and underutilized resource for biofuel production. The oil content of rice bran typically ranges from 15–22%, and crude rice bran oil (CRBO) often contains high levels of free fatty acids (FFA), especially if not processed immediately after milling due to rapid hydrolysis (Dunford, 2019).

Crude rice bran oil contains a balanced fatty acid profile including oleic (C18:1, ~40–45%), linoleic (C18:2, 30–40%), and palmitic acid (C16:0, 15–20%), which are favorable for biodiesel production (Mas'ud et al., 2017). However, the high FFA content (>5%) necessitates a two-step transesterification process: an initial acid esterification to lower FFAs followed by base-catalyzed transesterification. With proper pretreatment, rice bran biodiesel has been shown to meet international standards such as ASTM D6751 and EN 14214 (Sutanto et al., 2020).

Fuel properties of rice bran biodiesel include good viscosity, moderate cetane number (48–52), and acceptable calorific value (39–41 MJ/kg). Cold flow properties are somewhat inferior due to the high unsaturation level but can be improved with additives or blending. The oxidative stability

of rice bran biodiesel is relatively low, again due to its polyunsaturated fatty acids, and may require antioxidants during storage(Sutanto et al., 2020).

Engine performance studies using rice bran biodiesel blends (B10–B30) have shown comparable results to conventional diesel in terms of brake thermal efficiency and fuel consumption, with significantly reduced emissions of CO, HC, and particulate matter. However, a slight increase in NOx emissions has been observed, consistent with biodiesel fuels (Dharmaraja et al., 2019).

2.1.7.16. Crambe abyssinica (Hochst)

Crambe abyssinica, a member of the Brassicaceae family, is a fast-growing, oilseed crop native to the Ethiopian highlands. It has gained attention as a non-edible industrial oilseed due to its high oil content and adaptability to temperate and semi-arid climates. Unlike many food crops, *C. abyssinica* does not compete with food systems, making it a sustainable biodiesel feedstock option (Dharmaraja et al., 2019).

The seeds contain 30–40% oil, with a unique fatty acid composition(Dharmaraja et al., 2019). The oil is especially rich in erucic acid (C22:1) often comprising 50–60% of total fatty acids alongside oleic (C18:1) and linoleic acids (C18:2). While the high erucic acid content renders the oil unsuitable for human consumption, it makes the oil valuable for lubricants, coatings, and biofuels. Its long-chain fatty acids enhance lubricity, but pose some challenges for cold flow and oxidation stability when used as biodiesel (Dharmaraja et al., 2019).

Crambe abyssinica oil has been successfully converted to biodiesel through base-catalyzed transesterification, often requiring pretreatment if the free fatty acid (FFA) content is high(Dharmaraja et al., 2019). The resulting biodiesel meets major fuel standards (ASTM D6751 and EN 14214) in terms of viscosity, density, and cetane number, though oxidative stability and cold flow properties may require improvement via antioxidants or blending with methyl esters from more saturated oils (Dharmaraja et al., 2019).

Engine performance trials using *Crambe*-based biodiesel and blends B20, B50 show comparable unburned hydrocarbons (HC), and smoke opacity. NOx emissions may slightly increase, a typical biodiesel trait, but can be managed through exhaust after-treatment technologies or combustion optimization. (Dharmaraja et al., 2019).

2.1.7.17. Thevetia peruviana (yellow oleander)

Thevetia peruviana, commonly known as yellow oleander, belongs to the Apocynaceae family and is a fast-growing, drought-tolerant evergreen shrub or small tree native to Central and South America(Dharmaraja et al., 2019). It is widely found in tropical and subtropical regions as an

ornamental plant. The seeds of T. peruviana are highly toxic to humans and animals due to the presence of cardiac glycosides, making the oil non-edible and safe for biofuel application (Ramos-Silva et al., 2017).

The seeds contain around 60–65% oil by weight, making it one of the richest oil-bearing non-edible feedstocks. The oil is composed mainly of oleic (30–50%), linoleic (20–40%), and palmitic acid (15–25%), which contribute to favorable fuel properties.(Ramos-Silva et al., 2017) Due to moderate free fatty acid (FFA) content, the oil typically requires acid esterification followed by base-catalyzed transesterification to produce high-quality biodiesel(Ramos-Silva et al., 2017).

Studies (Ramos-Silva et al., 2017) have confirmed that Thevetia biodiesel meets key specifications under ASTM D6751 and EN 14214 standards, with acceptable kinematic viscosity, cetane number, flash point, and calorific value. However, due to its high degree of unsaturation, oxidative stability may be relatively low, and cold flow properties may require improvement depending on the region of use.

Engine performance tests using yellow oleander biodiesel blends (especially B20 and B40) demonstrate comparable brake thermal efficiency and reduced emissions of carbon monoxide (CO), hydrocarbons (HC), and smoke compared to diesel fuel(Ramos-Silva et al., 2017). As with most biodiesels, a modest increase in NOx emissions has been observed, which may be addressed with EGR or additives.

2.1.7.18. Sapindus mukorossi (Soapnut)

Apindus mukorossi, commonly known as soapnut or reetha, is a deciduous tree belonging to the family Sapindaceae (Ramos-Silva et al., 2017). It is native to the Indian subcontinent and widely distributed in the Himalayan foothills, northeastern India, and parts of Southeast Asia. Traditionally valued for its natural saponins used in soaps and detergents, S. mukorossi has recently attracted attention as a non-edible biodiesel feedstock due to its oil-rich seeds, drought tolerance, and ecological adaptability(Singh & Sharma, 2019).

The seeds of S. mukorossi contain 30–40% non-edible oil by weight. The oil is characterized by a favorable fatty acid profile, rich in oleic acid (40–50%), linoleic acid (30–40%), and palmitic acid (10–15%), which make it suitable for biodiesel production(Chang-Chih et al., 2019). The oil has a moderate free fatty acid (FFA) content, and biodiesel can be produced either through single-step alkaline transesterification (when FFAs are below 2%) or two-step transesterification for higher FFA levels (Singh & Sharma, 2019).

Experimental studies (Chang-Chih et al., 2019) confirm that biodiesel derived from soapnut oil complies with ASTM D6751 and EN 14214 standards, with acceptable ranges of viscosity, flash

point, cetane number, and energy content (39–41 MJ/kg). The high content of unsaturated fatty acids implies that oxidative stability may be a concern, but this can be addressed through antioxidants or blending with more saturated biodiesel sources (Fadda et al., 2022).

2.1.7.19. Cerbera odollam, commonly known as Sea Mango

Cerbera odollam, commonly known as Sea Mango or Suicide Tree, is a coastal evergreen species belonging to the Apocynaceae family(Gaillard et al., 2004).It is native to India and Southeast Asiaand typically grows in coastal marshes, estuaries, and mangrove margins. The plant produces fruit containing a single large seed rich in non-edible oil, and is widely recognized for its toxicity due to the presence of cerberin, a potent cardiac glycoside. Because of this toxicity, the oil is unsuitable for food but ideal for biodiesel applications, avoiding competition with edible oils(Kumar et al., 2020**)**.

The seeds of *C. odollam* yield about 40–50% oil by weight, which contains a significant proportion of oleic acid (35–45%), linoleic acid (25–30%), and saturated fatty acids like palmitic (15–20%) and stearic acid (5–10%)(Kansedo et al., 2009; Kumar & Sharma, 2011).These properties support favorable biodiesel characteristics, such as good lubricity, energy content, and combustion behavior. However, due to its high free fatty acid (FFA) content (often >5%), *C. odollam* oil typically requires acid esterification followed by base-catalyzed transesterification for efficient biodiesel production.

Research studies (Rizki et al., 2018) show that biodiesel produced from *Cerbera odollam* oil meets major standards such as ASTM D6751 and EN 14214, with acceptable ranges for kinematic viscosity, flash point, density, and cetane number. However, like many biodiesels with high unsaturation, the oxidative stability may be limited, requiring the use of antioxidants for long-term storage. Its cold flow properties are moderate and may be acceptable in tropical and subtropical climates (Rosli et al., 2023).

2.7.2. Fatty Acid Composition Profile of Various Feedstock

The fatty acid composition of a biodiesel feedstock is a crucial factor influencing the efficiency of biodiesel production(Moser, 2009).This composition largely depends on the plant species and the environmental conditions under which they grow. Fatty acids in most biodiesel feed stock are typically aliphatic compounds featuring a carboxyl group at the end of a straight hydrocarbon chain. The most prevalent types are C16 and C18 fatty acids(De Carvalho & Caramujo, 2018). However, certain feed stocks may also contain notable amounts of other fatty acids beyond the common C16 and C18 types (Knothe et al., 2010). Table 2.5 presents the fatty acid profiles of various feed stocks deemed suitable for biodiesel production.

Table 2. 5 The chemical structures of common fatty acids

Fatty acid	Structure	Systematic name	Chemical structure
Arachidic	(20:0)	Eicosanoic	$CH_3(CH_2)_{18}COOH$
Behenic	(22:0)	Docosanoic	$CH_3(CH_2)_{20}COOH$
Erucic	(22:1)	cis-13-Docosenoic	$CH_3(CH_2)_7CH=CH(CH_2)_{11}COOH$
Lauric	(12:0)	Dodecanoic	$CH_3(CH_2)_{10}COOH$
Lignoceric	(24:0)	Tetracosanoic	$CH_3(CH_2)_{22}COOH$
Linoleic	(18:2)	cis-9-cis-12-Octadecadienoic	$CH_3(CH_2)_4CH=CHCH_2CH=CH(CH_2)_7COOH$
Linolenic	(18:3)	cis-9-cis-12,	$CH_3CH_2CH=CHCH_2CH=CHCH_2CH=CH(CH_2)_7COOH$
Myristic	(14:0)	Tetradecanoic	$CH_3(CH_2)_{12}COOH$
Oleic	(18:1)	cis-9-Octadecenoic	$CH_3(CH_2)_7CH=CH(CH_2)_7COOH$
Palmitic	(16:0)	Hexadecanoic	$CH_3(CH_2)_{14}COOH$
Stearic	(18:0)	Octadecanoic	$CH_3(CH_2)_{16}COOH$

2.8. Classification of Biofuels

Transportation-grade biofuels can be produced from a diverse range of biological resources through various production technologies and methods(De Carvalho & Caramujo, 2018). These biofuels are generally classified into different generations, depending on the feedstock type and the production process used.

2.8.1. First-Generation Biofuels

These biofuel production technologies commonly use feed stocks such as sugars, starches, vegetable oils, and animal fats. Fuels like biodiesel, ethanol, and bio-methane produced through anaerobic digestion and upgraded to meet natural gas standards for transport use and are categorized as first-generation biofuels (Arshad et al., 2018)

2.8.2. Second-Generation Biofuels

These biofuel generations often refer to a broad spectrum of liquid fuels made using novel, inedible feed stocks and a number of intricate, cutting-edge techniques and technologies (Asase et al., 2024). For instance, the lignocellulose components of various biomass feed stocks can be converted into biofuels using a range of techniques and technologies that are at various stages of development and commercialization. Bioethanol is made from these components. They either split the biomass into lignin, cellulose, and hemicellulose components or pre-treat it using biochemical or thermochemical techniques (Gundekari et al., 2020).

Using enzymes and microorganisms to hydrolyze sugars prior to fermentation in order to make ethanol, methanol, butanol, and other biofuels or using the chemical hydrolysis of cellulose followed by fermentation are the two natural ways that biochemical production occurs(Fatma et al., 2018) .

Pyrolysis and gasification technologies are employed in the thermochemical process for generating biofuels. Fast pyrolysis can be used to create bio-oil, which can then be refined into biofuels. Gasification techniques can be used to create syngas, which can then be refined into LPG standards for use as car fuel or transformed into biofuel by chemical catalysts or biological processes. (Hirani et al., 2018).

2.8.3. Third-Generation Biofuels

These biofuel production technologies also include the use of algae and the extraction of hydrogen gas from biomass feed stocks (Jain & Sirisha, 2015). Algae-based biodiesel production is typically classified into two categories: microalgae and macroalgae (Suganya et al., 2016). Microalgae are photosynthetic microorganisms capable of producing lipids that can be converted into various biofuels, including biodiesel. In contrast, macroalgae are larger organisms such as seaweeds and can be cultivated and processed into biomethane or bioethanol through anaerobic digestion or fermentation, respectively (Rajkumar et al., 2014).

2.8.4. Fourth-Generation Biofuels

Fourth-generation biofuels represent an advanced class of biofuels derived from non-food feed stocks such as algae, waste biomass, and other inedible organic materials (Morone et al., 2023). Unlike first-, second-, and third-generation biofuels, which are often sourced from food crops or dedicated energy crops, fourth-generation biofuels do not compete with food production or contribute to deforestation. Produced from waste and non-arable sources, they offer a lower carbon footprint and are considered more environmentally sustainable. Additionally, these biofuels have the potential to be produced in larger quantities without the need for freshwater or arable land, enhancing their long-term viability (Paravantis, 2022).

2.9. Ethiopia and Biofuel

In Ethiopia, large-scale investments in biofuels have a recent history, with the first large-scale biofuel feedstock production being established in 2006 by the UK-based biofuel company Sun Biofuels. Since 2006, Ethiopia has become a major destination for Foreign Direct Investment (FDI) in biofuels in Africa (Weissleder, 2009). Although most biofuel investments have not yet been implemented, in 2011, the amount of capital that biofuel companies committed to investing in biofuels represented up to 50% of the FDI flow at the national level (Bossio et al., 2012). Within four years, interest in investing in biofuels increased significantly, so by 2010, approximately 83 companies had been granted licenses to invest in biofuels (Ethiopian Biofuels Directorate, 2010). According to the land deals matrix released in April 2012 by the International Land Coalition

(Fadda et al.), approximately 1,360,670 hectares of land in Ethiopia were reported to be leased for biofuel projects, out of which more than 700,000 hectares were leased for jatropha projects (Keeley et al., 2014).

Global Energy Ethiopia Ltd. also began building a bio-diesel factory in southern Ethiopia, which was intended to produce 40,000 tons of crude oil annually (Benti et al., 2023). When the company's project began, the planned production capacity was 250 tons of fuel per day from Castor beans and Jatropha, which easily grew in SNNP State. The company had four components: the processing factory, which spans 15 hectares; the modern farm, covering 30,000 hectares; purchasing seeds from farmers; and the introduction of community farming.

Global Energy Ethiopia Ltd. is an extension of Global Energy Pacific Ltd, based in Nevada, USA, and was registered with a capital of 222 million birr to engage in farming and processing oil seeds and extraction of bio-fuel (Besha et al., 2020).

Global Energy Ethiopia Ltd.'s mission was to commercialize innovative technologies that harness energy from waste and renewable sources, contributing to a cleaner environment. It also intends to use the most efficient and environmentally friendly of all currently available alternative fuel technologies, each originally developed and patented by scientists (Gielen et al., 2019)

To support the development of the biofuel sector in the country, the Ethiopian government has made two main policy amendments. First 2009, the government introduced an ethanol blending policy that mandates a 5% ethanol blend with 95% gasoline. The blending mandate was increased to 10% in early 2011, and a plan is in place to further increase it to 25% by 2014. Secondly, the government has made numerous amendments to its agricultural development and taxation policies to attract investments in large-scale agricultural projects, including those related to biofuels. Desalegn Rahmato, head of the Ethiopian Forum for Social Studies, described this as an "open door policy" that provides numerous incentives to attract investors to biofuels and other agricultural projects (Rahmato, 2011)

2.10. Oil Extraction Method

The extraction of oil from plant materials is a critical step in the production of biodiesel, influencing both the quantity and quality of the final product. Various oil-bearing feedstocks such as *Jatropha curcas*, *Azadirachta indica*, *Thevetia peruviana*, and *Madhuca indica* require efficient, cost-effective, and environmentally sound extraction techniques. The main oil extraction methods

used are mechanical pressing, solvent extraction, and emerging technologies like supercritical fluid extraction, ultrasound-assisted extraction, and enzymatic extraction (Pragya et al., 2013).

2.10.1. Mechanical extraction

Mechanical pressing is the most conventional method for oil extraction. It typically involves either a manual ram press or an engine-driven screw press. Engine-driven screw presses are more efficient, extracting approximately 68–80% of the available oil, while manual ram presses yield around 60–65% (Table 2.11). This variability is largely due to the number of extraction cycles that seeds undergo in the expeller (Achten et al., 2008; Mahanta & Shrivastava, 2011). However, oil obtained through mechanical pressing often requires further processing, such as filtration and degumming. A notable limitation of conventional presses is their seed-specific design, which can lead to reduced yields when used with other types of seeds. Table 2.6 presents the calculated oil yields and associated treatment steps for the mechanical extraction method. Studies have shown that pre-treatment methods—such as cooking—can significantly enhance oil recovery, boosting screw press yields to about 89% after a single pass and up to 91% with a dual pass (Achten et al., 2008; Mahanta & Shrivastava, 2011)

Table 2. 6 Calculated oil yields (% of contained oil) of mechanical extraction methods Keneni, Y.G., & Marchetti, J.M. (2017).

Feedstock	Screw Press Yield (% of oil content)	Ram Press Yield (% of oil content)	Oil Content (% by weight)
Jatropha Carcus	75–80%	60–65%	27–40%
Sunflower	80–85%	60–65%	35–45%
Soybean	65–75%	55–60%	18–20%
Rapeseed	80–85%	60–65%	40–45%
Castor	70–75%	55–60%	36%

2.10.2. Solvent extraction (chemical extraction)

Solvent extraction, also known as leaching, is a method that involves extracting a specific component from a solid using a liquid solvent (Wilson et al., 2014). The efficiency of this process is influenced by several factors, including particle size, solvent type, temperature, and agitation(Rajha et al., 2014). Smaller particle sizes are preferred, as they increase the surface area for interaction between the solid and liquid phases. An ideal solvent should be highly selective, with low viscosity to ensure efficient circulation. Temperature also plays a critical role; as it increases, the solubility of the target compound generally improves, thereby enhancing extraction efficiency. Agitation further boosts the process by increasing eddy diffusion, which facilitates faster mass transfer from the solid particles to the solvent. Solvent extraction becomes economically viable only for large-scale operations, typically producing more than 50 tons of

biodiesel per day. Common techniques under this method include hot water extraction, Soxhlet extraction, and ultra-sonication (Achten et al., 2008; Mahanta & Shrivastava, 2011)

2.10.3. Enzymatic oil extraction

Enzymatic oil extraction has gained attention as an effective and eco-friendly approach for extracting oil from crushed seeds using specific enzymes. One of its key benefits is that it does not release volatile organic compounds, making it environmentally sustainable. However, its major drawback is the extended processing time (Mahanta & Shrivastava, 2011).

Table 2.7 presents a comparison of various chemical and enzymatic extraction methods in terms of reaction temperature, pH, processing time, and oil yield. Among these, chemical extraction using n-hexane has been found to provide the highest oil yield, which is why it remains the most widely used method (Bhuiya et al., 2020). Nonetheless, this method tends to be more time-consuming and poses significant environmental concerns. The use of n-hexane contributes to wastewater generation, higher energy consumption, elevated emissions of volatile organic compounds, and health hazards due to its toxic and flammable nature.

In contrast, aqueous enzymatic extraction offers a safer and more sustainable alternative by minimizing these environmental and health risks. When using this method, alkaline protease has shown improved oil recovery performance. Additionally, incorporating ultra-sonication as a pre-treatment step has proven beneficial in enhancing the efficiency of aqueous oil extraction **(**Achten et al., 2008; Mahanta & Shrivastava, 2011).

Table 2. 7 Reported oil yields for different chemical and enzymatic extraction

Feedstock	Method	Yield (%)	Enzymes Used	Reaction Time	pH Range	Reference
Jatropha curcas	(Hexane)	85–90	–	1–2 hrs	Neutral	Keneni & Marchetti (2017)
	Enzymatic(Naeem et al.)	70–75	Cellulase,Protease	8–12 hrs	4.5–6.0	Keneni & Marchetti (2017)
Castor	Chemical (Hexane)	85–90	–	2 hrs	Neutral	Biodiesel Tech Review (2023)
	Enzymatic(Naeem et al.)	65–70	Pectinase	12–16 hrs	4.5–5.5	Biodiesel Tech Review (2023)
Rapeseed	(Hexane)	85–93	–	1.5–2 hrs	Neutral	Xu et al. (2019)
	Enzymatic(Naeem et al.)	72–80	Protease,Cellulase	10–14hr	4.8–5.8	Xu et al. (2019)

methods of Jatropha Carcus,Castor and Rapeseed

2.11. Vegetable oil Processing and refining

Vegetable oil processing involves extracting and refining oils from various plant-based sources such as fruits, seeds, and nuts(Ghouila et al., 2019),(Krist, 2020). These raw oils typically contain

impurities like free fatty acids, phospholipids, sterols, water, and odorants even refined oils may retain small traces of these(Mahesar et al., 2014).

Preparation of raw materials includes husking, cleaning, crushing, and conditioning. Oil extraction methods include mechanical pressing (for seeds and nuts), boiling (for fruits), or solvent extraction using hexane(Srivastav & Karunanithi, 2024). After extraction, the oil is separated by skimming, filtering, or evaporating the solvent using a rotary evaporator. Residual solids are dried and utilized for by-products like fire briquettes or biogas production(Parliment, 2020).

Crude oil refining involves stages such as degumming (removal of phospholipids and heavy metals), neutralization (with NaOH to remove free fatty acids and phosphatides), bleaching (to reduce color and remove residual metals), and decolorization. Caustic soda reacts with impurities but may also cause partial hydrolysis of triglycerides into soap(Demirbaş & Kara, 2006).

A key step in purification is physical refining, where free fatty acids are removed via steam stripping under vacuum at 5250 K and 2–3 mm Hg pressure (Gharby, 2022). High-quality crude oil is essential for efficient refining and to ensure a high-quality end product.

2.12. Direct use of vegetable oils in diesel propulsion

The potential of plant oils competing with petroleum was first proposed in the early 1980s (Ajala et al., 2015). Vegetable oils offer several advantages including portability, widespread availability, and renewability. They possess a high heat content, approximately 88% that of conventional diesel (D2) fuel, and contain a significant amount of oxygen, which can enhance combustion efficiency. Additionally, vegetable oils have lower sulfur and aromatic content, making them a cleaner-burning fuel option (Negm et al., 2017). Their biodegradability further adds to their environmental benefits, making them a promising alternative to diesel propulsion (Dimirbas, 2003).

Perfect combustion requires the presence of a stoichiometric amount of oxygen. However, this amount is often insufficient for complete combustion, as conventional fuels are not oxygenated(Mishra, 2007). The structural oxygen of the fuel enhances combustion efficiency by improving oxygen mixing during combustion. Hence, vegetable oils, which contain higher oxygen content, exhibit greater combustion efficiency and a higher cetane number compared to petroleum based fuel (Demirbas, 2008b).

The disadvantages of vegetable oils as diesel fuel include their corrosive nature, higher viscosity, lower volatility, and the reactivity of unsaturated hydrocarbon chains. These issues become more pronounced after prolonged engine operation, particularly in direct injection engines, which can lead to performance and durability concerns (Negm et al., 2017).

2.13. Challenges and potential solutions of using plant oils

The direct application of vegetable oils or their blends in diesel engines, whether direct or indirect injection, has largely been deemed impractical (Agarwal et al., 2017). This is primarily due to several challenges, including their high viscosity, low volatility, the presence of acids, free fatty acids, and moisture(Agnihotri et al., 2022). Additionally, vegetable oils are prone to gum formation caused by oxidation and polymerization during storage and combustion. Other operational issues include difficulty in cold starting, engine misfires, delayed ignition, incomplete combustion, carbon deposits near the nozzle orifice, ring sticking, injector fouling, and thickening of the lubricating oil (Hassan & Kalam, 2013).These challenges are generally classified into short-term and long-term engine performance issues. Table 2.8 outlines these problems along with their likely causes and possible solutions.

Table 2. 8 Problems, cause and potential solutions for using straight vegetable oil

Problem	Probable cause	Potential solution
Short-term		
Cold weather starting	High viscosity, low cetane number and high flash point of vegetable oils	Preheat fuel prior to injection.
Plugging and gumming of filters, lines and injectors	Natural gums (phosphatides) in vegetable oil. Other ash.	Refine the oil partially to remove gums.
Engine knocking	Low cetane numbers. Improper injection timing.	• Adjust injection timing. • Use higher compression engines. • Preheat fuel prior to injection. Chemically alter fuel to an ester.
Long term		
Cooking of injector on piston and engine head	• High viscosity of vegetable oil. • Incomplete combustion of fuel. • Poor combustion at part loads with vegetable oils.	• Heat fuel prior to injection. • Switch engine to diesel fuel when operation at part loads. • Chemically alter the vegetable oil to an ester.
Carbon deposits on piston and head of engine	• High viscosity of vegetable oil. • Incomplete combustion of fuel. • Poor combustion at part load with vegetable oils.	• Heat fuel prior to injection. • Switch engine to diesel fuel when operation at part loads. • Chemically alter the vegetable oil to an ester.
Excessive engine wear	• High viscosity of vegetable oil, incomplete combustion of fuel. Poor combustion at part loads with vegetable oils. Possibly free fatty acids in vegetable oil. Dilution of engine lubricating oil due to blow-by of vegetable oil.	• Heat fuel prior to injection. • Switch engine to diesel fuel when operation at part loads. • Chemically alter the vegetable oil to an ester. • Increase motor oil changes. • Motor oil additives to inhibit oxidation.
Failure of engine lubricating oil due to polymerization	• Collection of polyunsaturated vegetable oil blow-by in crankcase to the point where polymerization occurs.	• Heat fuel prior to injection. • Switch engine to diesel fuel when operation at part loads. • Chemically alter the vegetable oil to an ester. • Motor oil additives to inhibit oxidation.

2.14. Biodiesel production technologies

Worldwide, numerous initiatives are focused on enhancing the properties of vegetable oil to make them comparable to diesel fuel. A significant challenge is viscosity, which hinders the use of pure vegetable oils in conventional diesel engines. This issue can be addressed through four methods: pyrolysis, dilution with hydrocarbon blending, micro-emulsion, and transesterification (A. Demirbas, 2009; S. P. Singh & D. Singh, 2010). (Lin Lin et al., 2011) conducted a comparison of various biodiesel production technologies, as illustrated in Table2.9

Table 2. 9 Comparison of main biodiesel production technologies (L. Lin et al., 2011)

Technologies	Advantage	Disadvantage
Dilution (direct blending or micro-emulsion)	• Simple process	• High viscosity • Bad volatility • Bad stability
Pyrolysis	• Simple process No-polluting	• High temperature is required • Equipment is expensive • Low purity
Transesterification	• Fuel properties is closer to diesel • High conversion Efficiency • Low cost • It is suitable for industrialized production	• Low free fatty acid and water content are required (for base catalyst) • Pollutants will be produced because products must be neutralized and washed • Accompanied by side reactions • Difficult reaction products separation
Supercritical methanol	• No catalyst • Short reaction Time • High conversion • Good adaptability	• High temperature and pressure are required • Equipment cost is high • High energy consumption

2.14.1. Pyrolysis (thermal cracking)

Pyrolysis refers to the thermal breakdown of organic substances in the absence of oxygen, typically carried out with the aid of a catalyst (Al-Salem et al., 2017). This process can be applied to a range of feedstocks, including vegetable oils, animal fats, natural fatty acids, and methyl esters of fatty acids. Researchers have extensively explored the pyrolysis of triglycerides to generate diesel-engine-compatible fuels, along with byproducts such as carboxylic acids, aromatic compounds, and minor quantities of gases(Maher & Bressler, 2007).

The liquid fraction obtained from the thermal decomposition of vegetable oils bears similarities to conventional diesel fuel(Krutof & Hawboldt, 2016). Compared to diesel, the pyrolysis oil generally exhibits lower viscosity, flash point, and pour point, while maintaining comparable calorific values. However, its cetane number tends to be lower than that of diesel. While the pyrolyzed oil meets acceptable standards for sulfur content, moisture levels, copper corrosion, and

sediment formation, it falls short in terms of ash content, carbon residue, and pour point(Kaisan et al., 2020).

Despite these drawbacks, pyrolysis is considered an efficient, straightforward, and environmentally friendly method that produces minimal waste(S. P. Singh & D. Singh, 2010). Based on processing conditions, pyrolysis can be categorized into three main types: conventional, fast, and flash pyrolysis, as outlined in Table 2.11 (Demirbas & Arin, 2002). The typical ranges for key operating parameters in pyrolysis are detailed in Table 2.10.

Table 2. 10 The range of the main operating parameters for pyrolysis processes

Parameter	Fast pyrolysis	Flash pyrolysis	Conventional pyrolysis
Pyrolysis temperature (k)	850-1250	1050-1300	550-950
Heating rate (k/s)	10-200	>1000	0.1-1
Particle size (mm)	< 1	< 0.2	5-50
Heating time (Santos et al.)	0.5-10	< 0.5	450-550

2.14.2. Dilution

To improve engine performance and reduce the high viscosity of vegetable oils, they are often blended with diesel rather than used directly, avoiding the need for chemical processing (Corsini et al., 2015). Using 100% vegetable oil is generally impractical, while blending 20–25% vegetable oil with diesel has shown better engine compatibility(S. Singh & D. Singh, 2010).

Various vegetable oils such as sunflower, coconut, palm, soybean, jatropha, and pongamia have been tested in blends with diesel. For example, a 25% sunflower oil and 75% diesel blend exceeded ASTM viscosity limits (4.88 cSt at 313 K), making it unsuitable for long-term use in direct-injection engines (Ziejewski et al., 1986). However, a similar blend with high oleic sunflower oil passed the 200-hour EMA test, indicating potential for short-term use.

In general, both straight vegetable oils and their blends pose challenges for diesel engines, especially due to injector clogging and carbon buildup(Demirbaş, 2003). Adding solvents or forming microemulsions helps reduce these issues. Ethanol, for instance, not only lowers viscosity but also enhances brake thermal efficiency and power output while reducing specific fuel consumption, thanks to its lower boiling point which improves combustion(Bilgin et al., 2002)

2.14.3. Micro-emulsion.

A micro-emulsion is a thermodynamically stable mixture of two immiscible liquids (usually oil and water or biodiesel and diesel) stabilized by surfactants and sometimes co-surfactants(Attwood, 2014). In biodiesel fuel technology, micro-emulsions are used to improve fuel properties such as

viscosity, cold flow, and combustion efficiency without chemically altering the fuel(Burguera & Burguera, 2012).

By forming micro-emulsions, biodiesel or vegetable oils can be blended with water or lighter hydrocarbons at the molecular level, resulting in(Bora, 2015):

- Reduced viscosity and improved atomization during fuel injection.
- Better cold flow properties, minimizing problems like gelling in low temperatures.
- Enhanced combustion efficiency leading to lower emissions of pollutants like CO and particulate matter.

Micro-emulsion fuels can allow the use of straight vegetable oils (SVOs) or high-viscosity biodiesel blends in engines designed for diesel without major modifications(Sanli et al., 2022). Surfactant type and concentration, temperature, and the ratio of components are critical factors in micro-emulsion stability and performance(Sanli et al., 2022).

2.14.4. Transesterification Process

Plant oils contain impurities such as free fatty acids, phospholipids, water, and sterols, making them unsuitable for direct use as fuel(Krist, 2020).To address this, a chemical process called transesterification is used to convert the oils into biodiesel a cleaner, renewable alternative to conventional diesel (Farouk et al., 2024).Biodiesel consists of fatty acid methyl esters (FAME) produced by reacting triglycerides from vegetable oils or animal fats with methanol. This process, known as transesterification or alcoholysis, replaces one alcohol group with another and significantly reduces the oil's viscosity (Frohlich et al., 2000)

Transesterification involves a sequence of reversible reactions converting triglycerides into diglycerides, monoglycerides, and finally glycerol, releasing one ester molecule at each step. Though reversible, the reaction favors biodiesel and glycerol formation(Diaconis & Freedman, 1986; Freedman et al., 1986).Catalysts such as alkaline, acidic, enzymatic, or heterogeneous can be used to accelerate the process(Demirbas, 2008a).

2.14.5. The mechanism and kinetics

The alkali-catalyzed transesterification mechanism occurs in three steps (Tiwari & Garg, 2016). First, the methoxide ion attacks the carbonyl carbon of the triglyceride, forming a tetrahedral intermediate. Next, this intermediate reacts with methanol, regenerating the methoxide ion. Finally, the intermediate rearranges to produce a fatty acid ester and a diglyceride. Catalysts like NaOH, KOH, or K_2CO_3 react with alcohol to form the active alkoxide species (Vijay Kumar et al., 2019). However, any water present can lead to unwanted soap formation during the process (Chanakaewsomboon et al., 2020).The mechanism is illustrated in Figure 2.12.

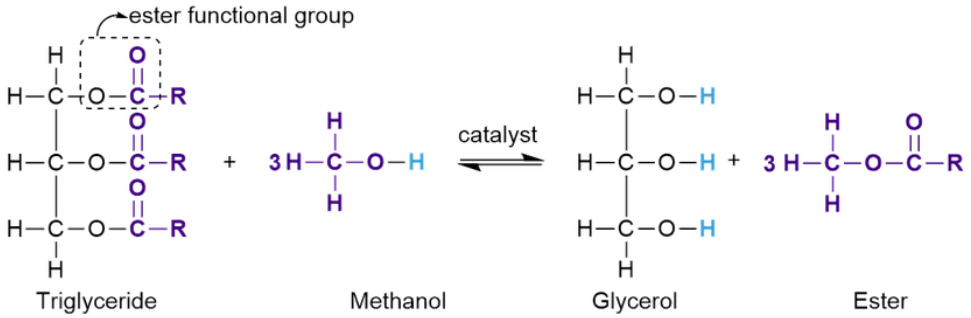

Figure 2. 11 The transesterification of triglycerides with alcohol

2.14.6. The effects of moisture and free fatty acids

For effective alkali-catalyzed transesterification, the feedstock must be nearly free of water and have a low acid value. According to (Foidl et al., 1996) the acid value should be below 1, and the materials should be anhydrous (Ayoub & Abdullah, 2012). Excess free fatty acids require more NaOH for neutralization, while water promotes soap formation, reducing catalyst efficiency and complicating glycerol separation. Therefore, water content should be below 0.3%, and free fatty acids should be under 0.5% (Ma & Hanna, 1999).

(Freedman, 1984)) found that failing to meet these standards significantly reduced ester yield. Sodium-based catalysts also lose effectiveness when exposed to moisture or CO_2. In studies on beef tallow, optimal transesterification was achieved when water content remained below 0.06% and free fatty acids below 0.5% (Hanna, 1989) and (Laurens et al., 2012) emphasized that water content had a greater negative impact on the reaction than free fatty acids.

2.14.7. The effect of molar ratio

The alcohol-to-triglyceride molar ratio is a key factor influencing ester yield in transesterification (Tobar & Núñez, 2018). The ideal stoichiometric ratio is 3:1 (alcohol to glyceride), producing three esters and one glycerol molecule. However, the actual ratio depends on the catalyst used. Acid-catalyzed reactions may require up to 30:1 (e.g., BuOH to soybean oil), while alkali-catalyzed processes typically need only 6:1 for similar yields (Mathes, 2000).

Practically, methanol-to-oil ratios range from 3.3:1 to 5.25:1, with 4.8:1 yielding up to 97–98% esters, depending on oil quality. A three-step process can reduce this to 3.3:1. Excess methanol beyond 1.75 equivalents can hinder glycerol separation, raising costs(Tiwari et al., 2006).

Higher molar ratios generally speed up ester conversion (Soriano Jr et al., 2009). For example, a 6:1 ethanol-to-peanut oil ratio released more glycerol than a 3:1 ratio(Feuge & Gros, 1949).For rapeseed oil, 6:1 methanol-to-oil with 1% NaOH or KOH gave optimal results (Tariq et al., 2012).

Oils with high free fatty acid content may require ratios as high as 15:1 under acid catalysis (Hayyan et al., 2011).

2.14.8. The effect of catalyst

The catalyst plays a crucial role in the transesterification process by accelerating the reaction between oil and alcohol to produce biodiesel. Commonly used catalysts are alkaline types such as sodium hydroxide (Tormos et al.) or potassium hydroxide (KOH) (Canakci & Van Gerpen, 2001), which are effective for oils with low free fatty acid (FFA) content (Dorado et al., 2004). These catalysts increase the reaction rate and yield under mild temperature and pressure conditions. However, if the oil contains high FFAs, alkaline catalysts can lead to soap formation, reducing biodiesel yield and complicating separation. In such cases, acid catalysts like sulfuric acid (H_2SO_4) are used (Encinar et al., 2011).in a pre-treatment step to esterify FFAs into biodiesel-friendly compounds (Mamtani et al., 2021). The concentration of the catalyst is also important and too little results in incomplete conversion, while too much can promote soap formation and increase processing difficulty. Therefore, selecting the right type and amount of catalyst based on the feedstock quality is essential for efficient biodiesel production.

2.14.8. The effect of reaction temperature

Transesterification temperature varies with oil type. For example, castor oil methanolysis to methyl ricinoleate is most effective at 20–35°C with a 6:1–12:1 methanol-to-oil ratio and 0.005–0.35% NaOH catalyst (Ahmad et al., 2013).In soybean oil transesterification with methanol (6:1) and 1% NaOH, ester yields after 0.1 hours were 94% at 60°C, 87% at 45°C, and 64% at 32°C (Freedman et al., 1986). After 1 hour, yields at 60°C and 45°C were similar, with a slight drop at 32°C, showing that higher temperatures accelerate reaction rates and improve initial ester yields (Ali & Hanna, 1994).

2.15. Biodiesel Standard Requirement

Plant oils are not considered biodiesel in their natural state. However, they must undergo a transesterification reaction to convert them into biodiesel that meets the quality of ASTM D6751 and EN 14214 standards. The physicochemical standards for biodiesel are specified according to ASTM D6751 and EN 14214, as presented in Table 2.11.

Table 2. 11 Biodiesel standard requirements(Bringas, 2004; Carrero & Pérez, 2012).

Parameter	ASTM D6751	EN 14214	Description
Ester Content	-	≥ 96.5%	Represents the proportion of fatty acid methyl esters in the fuel. (EN 14214 requires a minimum to ensure proper fuel quality.)
Kinematic Viscosity (40°C)	1.9–6.0 mm^2/s	3.5–5.0 mm^2/s	A measure of the fuel's resistance to flow. Lower viscosity can aid in atomization, while too high a value may affect fuel injection and combustion.
Cetane Number	≥ 47	≥ 51	Indicates the combustion quality of diesel fuel during compression ignition. A higher cetane number generally reflects better ignition quality.
Flash Point	≥ 93°C	≥ 130°C	The minimum temperature at which the fuel produces enough vapor to ignite. A higher flash point enhances safety during storage and handling.
Acid Number	≤0.5mg KOH/g	≤0.5mg KOH/g	Measures the free fatty acid content; a low value is critical to prevent engine corrosion and maintain fuel stability.
Density	Not explicitly defined	860–900 kg/m^3(at 15°C)	Density affects the energy content per unit volume. EN 14214 specifies a range to ensure consistent energy delivery in engines.
Iodine Value	≤120g I_2/100g	(Not specified)	Indicates the degree of unsaturation of the biodiesel; a lower value usually correlates with better oxidative stability and lower polymerization tendencies.
Pour Point	Not specified	Report	The minimum temperature at which the fuel remains fluid. In practice, this is determined by testing but no fixed limit is set in the biodiesel standards.
Cloud point	Not specified	Report	The temperature at which wax crystals first become visible, affecting low-temperature operability.
Ash Content	<0.01–0.02%	Not specified	Represents the residue remaining after complete combustion; low values are desirable to minimize deposit formation in engines.
Water and Sediment	Maximum 0.05% mass	Maximum 0.05% mass	The allowable amount of water and insoluble particles in the fuel; strict limits ensure reliable engine performance and long-term stability.
Glycerin Content	≤0.02% w/w	Not specified	Residual glycerin levels are controlled to ensure proper combustion and avoid engine deposits.
Total glycerin	≤0.25% w/w	Not specified	Residual glycerin levels are controlled to ensure proper combustion and avoid engine deposits.

2.16. Engine Performance

The effectiveness of an engine's performance is a measure of how successfully the stored chemical energy in the fuel is converted into practical mechanical work (Descombes et al., 2003). Key indicators of engine performance include power, torque, mean effective pressure, and specific fuel consumption (Burke & Brace, 2010). These output parameters are predominantly shaped by design factors such as cylinder displacement, compression ratio, bore-to-stroke ratio, connecting rod-to-crank radius ratio, swept volume, clearance volume, and combustion chamber design (Splitter et al., 2012). Additionally, operational factors like injection timing, injection volume, injection pressure, air intake temperature, and air mass flow rate play a significant role in influencing engine performance (Agarwal et al., 2013). The quality of the fuel utilized also impacts engine performance efficiency (Zaharin et al., 2017).

2.16.1. Engine Design Parameters

The ongoing stringent regulations governing vehicle exhaust emissions and the global push for reduced fuel consumption necessitate a constant improvement in engine thermal efficiency (Johnson & Joshi, 2018). Critical aspects for improving overall engine efficiency include fundamental engine geometrical configurations, such as cylinder displacement, bore, stroke, bore-to-stroke ratio, connecting rod to crank radius ratio, and combustion chamber geometry (Johnson & Joshi, 2018). These parameters play a crucial role in meeting the challenges posed by current emission regulations and the global imperative to enhance fuel efficiency (Ni et al., 2020).

2.16.2. Engine operating parameters

The following engine operating parameters are factors that predominantly affecting the engine performance characteristics.

2.16.2.1. Fuel quality

It is well known that petroleum diesel is a significant contributor to air pollution, having a detrimental impact on human health and overall greenhouse gas emissions. Biodiesel offers several advantages over petroleum diesel (Ajala et al., 2015). It possesses some environmentally friendly properties, including being non-toxic, biodegradable, and safer to breathe. It is a clean-burning and stable fuel (Aljaafari et al., 2022). Biodiesel properties are largely influenced by the feedstock used for its production (Demirbas, 2010).Properties of biodiesel, such as oxygen content, cetane number, viscosity, density, and heat value, are greatly dependent on the sources of biodiesel (Demirbas, 2010). Engine performance and emissions depend on the properties of biodiesel (Zaharin et al., 2017). Biodiesel is a highly oxygenated fuel that can improve combustion efficiency and reduce unburnt hydrocarbons (HCs), carbon dioxide (CO_2), carbon monoxide (CO), Sulphur dioxides (SO_2), nitrogen oxide (NOx), and polycyclic aromatic HC emissions(A Demirbas, 2009). The popularity of biodiesel as a renewable alternative to petroleum diesel is growing rapidly due to increased environmental awareness and rising diesel prices. The advancement of biodiesel fuels in various countries is primarily motivated by the urgent need to lower greenhouse gas emissions, a critical global concern. Additionally, the limited availability of petroleum diesel further promotes the worldwide development and production of (Suhara et al., 2024).

Rudolf Diesel (1858–1913), who developed the first engine, first used vegetable oil to run an engine (Knothe, 2010). However, vegetable oils create adverse effects on engine components, which may be due to their different volatility and molecular structure from diesel fuel as well as high viscosity compared with diesel fuel (Ramadhas et al., 2004). Currently, this problem is being

eliminated by applying different chemical processes, such as transesterification, supercritical, catalyst-free process, etc., on vegetable oils to convert them into biodiesel (Mathews, 2008).

Petroleum fuel properties such as hydrocarbon composition, cetane number, volatility, viscosity, and density are interdependent. Lower fuel density often means more paraffinic hydrocarbons, leading to higher cetane numbers, greater volatility, and lower viscosity, with multiple factors influencing emissions (Lack et al., 2011).. A higher cetane number improves cold starts and reduces HC and NOx emissions by shortening ignition delay(Jiaqiang et al., 2019). However, increased volatility can cause overmixing and faster evaporation, raising NOx and HC emissions (Yousefi & Birouk, 2017). Higher sulfur content also increases particulate emissions by forming more sulfates (Yang et al., 2016).

2.17. Variables that influence combustion and emission

The combustion process and emission characteristics of diesel engines are influenced by both engine design and operating variables (Diaz et al., 2019). Engine design variables include factors such as compression ratio, combustion chamber type, and design, as well as injection system parameters like injection pressure, timing, nozzle hole configuration, and nozzle sac volume (Köten & Parlakyiğit, 2018). On the other hand, operating variables encompass aspects such as exhaust gas recirculation (Mondal et al.), engine speed, engine load, and fuel quality. Together, these factors play a crucial role in determining the efficiency of combustion and the levels of emissions produced by diesel engines (Agarwal et al., 2011)

2.17.1. Compression Ratio

In diesel engines, the minimum usable compression ratio is primarily determined by the engine's ability to start reliably in cold conditions(Roberts et al., 2014).

For direct injection high-speed engines, a compression ratio of 16 to 17.5:1 is used (Milojević et al., 2022). The turbocharged heavy-duty engines employ a compression ratio (CR) in the range of 13 to 14:1. Cold-starting requirements prevent further reduction in the compression ratio (Giakoumis & Giakoumis, 2017). A higher compression ratio shortens the ignition delay, reducing fuel–air overmixing and lowering HC emissions. It also raises combustion temperatures, promoting better oxidation of unburned hydrocarbons (Porpatham et al., 2012). In contrast, a lower compression ratio increases ignition delay, leading to more fuel burning in the premixed phase, which raises peak pressures and NOx emissions. However, excessively long delays can shift combustion into the expansion stroke, lowering pressure, temperature, NOx emissions, and fuel efficiency (Palash et al., 2013). Low compression ratios also cause poor cold-start performance and white smoke due to unburned fuel. While high compression ratios raise

combustion temperature and soot formation, they also enhance soot oxidation. Therefore, an optimal compression ratio is essential to balance NOx and particulate emissions (Al-Dawody & Bhatti, 2013).

2.17.2. Direct Injection versus Indirect Injection Engines

Indirect Injection (IDI) engines, once common in small high-speed applications, are now being phased out due to poor fuel efficiency, especially with the rise of high-speed direct injection (HSDI) engines (Pundir, 2008).In IDI engines, fuel burns in two stages: a rich mixture combusts in the pre-chamber, then partially burned gases enter the main chamber, where excess air and high turbulence complete combustion as a lean mixture (Rao et al., 2015); (Zhou et al., 2019).

2.17.3. Fuel Injection Timing and Injection Pressure

Fuel injection timing in compression ignition (CI) engines affects NOx emissions similarly to spark timing in spark ignition (SI) engines (Wooldridge et al., 2023). Retarding injection timing significantly reduces NOx but increases smoke, and in naturally aspirated engines, may also raise HC emissions (Buyukkaya & Cerit, 2008). Higher injection pressure tends to increase NOx and HC emissions while reducing smoke and particulate matter (Ramegouda & Joseph) (Belgiorno et al., 2018).

2.18. Metal Based Nano Particles Additives in Diesel-Biodiesel Blends

Studies have shown that adding metal oxide nanoparticles to biodiesel improves combustion and reduces NOx emissions due to enhanced evaporation, shorter ignition delay, and catalytic effects (Sambandam et al., 2023) (Ghanati et al., 2024)found that AgO nanoparticles in biodiesel improved fuel properties and reduced NOx by 4.6%. Similarly, (Kishore Pandian et al., 2017) reported a 6.7% NOx reduction with titanium oxide. . (Yuvarajan & Ramanan, 2016) observed notable decreases in CO, HC, and NOx using ferrofluid. (Appavu et al., 2019) and Anbarasu et al. (2016) demonstrated that cerium and aluminum oxide additives lowered emissions, including NOx, CO, HC, and smoke, by up to 4.2%.

2.19. Basic Engine lubricating oil parameters

Lubricating oil is essential for minimizing friction, cooling components, and preventing wear in engines and machinery (Totten, 2017). The quality of lubricating oil is essential for the longevity and efficiency of mechanical components (Raghuvanshi et al., 2024). Lubricating oil quality is assessed through indicators such as viscosity, viscosity index, TAN, TBN, oxidation stability, flash and fire points, pour and cloud points, water content, and contamination levels.

Viscosity measures the oil's resistance to flow and is crucial for effective lubrication. The viscosity index determines how viscosity changes with temperature, ensuring stability under varying conditions (Khalafvandi et al., 2022). Oxidation stability prevents the formation of sludge and deposits, which can damage machinery (Li et al., 2021). The flash and fire points indicate the temperature at which the oil ignites, ensuring safety in high-temperature operations (Huang et al., 2021). Water content and contamination levels, including dirt and metal particles, impact performance and longevity. Regular oil analysis helps detect degradation, contamination, and depletion of essential additives (Mujahid & Dickert, 2012)

2.19.1. Viscosity

Viscosity, the resistance of oil to flow and shear, is one of its most important physical properties, significantly impacting engine wear and fuel efficiency (Martini et al., 2018). The most common measurement is kinematic viscosity, typically reported at 40 °C and 100 °C in centistokes (cSt), though the SI unit is mm^2/s (Azman et al., 2020). It indicates how easily oil flows to different engine components under the influence of gravity. Over time, contaminants such as fuel, water, and combustion by-products can lower oil viscosity, affecting its performance (Zhang et al., 2021).Viscosity plays a key role in reducing friction; higher viscosity supports heavier loads at bearings, while lower viscosity improves oil flow during cold starts and reduces drag (Ting & Chen, 2011). However, excessive viscosity can lead to increased power loss and fuel consumption. For this reason, an optimal viscosity is selected to balance load-carrying capacity and energy efficiency. Accurate measurements are commonly obtained using capillary viscometers in temperature-controlled environments (Zhao et al., 2016).

2.19.2.Viscosity index (VI)

The viscosity index (VI) is a dimensionless number used to compare how different oils' viscosities change with temperature (Khalafvandi et al., 2022). It's calculated by measuring kinematic viscosity at 40 °C and 100 °C and referencing an empirical scale (Braga et al., 2014; Kalaoja, 2020). The scale is based on two crude oils: Pennsylvania crude (VI = 100) and Texas Gulf crude (VI = 0) (Parker, KITTIWAKE)(Akeredolu, 2014). A higher VI means viscosity is less affected by temperature changes(Bashir et al., 2022). Calculation details are provided in ASTM 2270 or IP 226 standards. Although VI is helpful for comparing base oils, its arbitrary reference points are limited temperature range (40–100 °C) restrict its accuracy(Verdier et al., 2009). Extrapolating beyond this range can be misleading due to effects like wax crystallization at low temperatures(Sirota, 2025). VI also indicates the degree of aromatic removal during refining.

Comparisons are only meaningful for oils from the same feedstock, so care must be taken when using VI to assess base oil quality (Sarkar et al., 2023).

2.19.3.Total acid number

The Total Acid Number (TAN) is an important quality parameter that measures the acidic components in biodiesel, expressed as the amount of potassium hydroxide (KOH) in milligrams required to neutralize the acids in one gram of fuel (Park et al., 2017). A high TAN indicates the presence of free fatty acids (FFAs), oxidation products, or contaminants, which can lead to fuel instability, corrosion of engine components, injector fouling, and deposit formation. International biodiesel standards, such as ASTM D6751 and EN 14214, typically limit TAN to 0.5 mg KOH/g or lower to ensure fuel quality and engine safety(Bazina & He, 2018). Elevated TAN values often result from poor storage conditions, prolonged exposure to air and moisture, or the use of low-quality feedstock with high FFA content(Maina, 2021). Monitoring and controlling TAN is thus critical for maintaining biodiesel durability and performance.

2.19.4.Ash content

The term "sulfated ash" refers to the number of metallic elements in engine oils, which are primarily derived from the detergent and anti-wear additive chemistry of the engine oil (Howard, 2014). These additive packages contain multiple components, including metals such as calcium, magnesium, and zinc (Murphy, 2001). Because a 100 percent seal between the piston rings can never be achieved, a certain amount of engine oil will enter the combustion burn (Wu et al., 2014). As the engine oil enters the combustion chamber and burns, its residue forms an ash-like material (Lakshminarayanan & Nayak, 2011). This ash-like material contributes to deposits in the crown land above the piston ring as well as to deposits in the ring grooves(Venderbosch & Prins, 2010). These deposits can lead to rubbing wear on the cylinder liner and cause the piston rings to normal operation (Lakshminarayanan & Nayak, 2011). As the cylinder liner-to-ring interface is compromised, high oil consumption can occur. In addition to these deposits, inorganic compounds from the lubricating oil's additives can become oxidized during combustion and generate metal oxide particles (Ahmed & Nassar, 2011). These particles can be carried downstream with the exhaust and collected on the diesel particulate filter. These ash particles cannot be removed by filter regeneration because they are not combustible. As the ash particles accumulate, they cause filter blockage, which increases backpressure on the engine, leading to increased fuel consumption and reduced power. Ash particle buildup also necessitates more frequent cleaning of the particulate filters by mechanical means such as compressed air or water-pulse methods.

Engine oil's sulfated ash content also directly relates to engine oil's acid neutralization capabilities (Benti et al.), because most of engine oil's BN comes from the metal-containing detergent additives (Watson, 2010). Generally, the higher an engine oil's BN, the higher its ash content and the greater its ability to prevent acidic corrosion in the engine(Baskov et al., 2020). Fortunately, with the mandated use of ultra-low sulfur diesel fuel in on-highway applications, corrosion from fuel

2.19.5.Carbon Residue

Engine lubricant carbon residue refers to the carbon deposits that remain after engine oil breaks down due to high temperatures, oxidation, and contamination (Boadu et al., 2019). Over time, these residues accumulate in critical engine components such as pistons, valves, and bearings, leading to sludge formation, reduced lubrication efficiency, and increased wear (Monieta, 2020). Carbon build-up can also restrict oil flow, raise operating temperatures, and decrease engine performance. Poor-quality lubricants, extended oil change intervals, and high engine loads accelerate residue formation (Roberts et al., 2014). Regular oil changes with high-quality, detergent-rich lubricants help minimize carbon deposits, ensuring optimal engine efficiency and longevity(Van Rensselar, 2020).

2.20. Engine Friction Wear and Lubricity

This section covers engine friction, wear, and lubricity, and also explains the lubrication circuit and oil flow path within the engine. Additionally, it illustrates the two common lubrication conditions involved in oil film formation.

2.20.1. Engine friction

Engine friction refers to the resistance that occurs when different components inside an engine move against each other or interact with lubricants (Kragelsky & Alisin, 2016). This resistance is generated by parts such as pistons, bearings, camshafts, and crankshafts as they operate. While some friction is necessary for the engine to function properly, excessive friction can lead to energy loss, reduced efficiency, and increased wear on components. Controlling friction is a key aspect of engine design and maintenance to enhance performance and longevity (Wong & Tung, 2016).

If engine friction becomes too high, it can lead to problems such as overheating, loss of power, and increased fuel consumption (Wang et al., 2021). Over time, this wear and tear can lead to costly repairs and reduced reliability ((Holmberg et al., 2014). To prevent such issues, regular maintenance, such as changing the oil, inspecting engine components, and using the manufacturer's recommended lubricants, is crucial for keeping friction at manageable levels and ensuring smooth engine operation (Mobley, 2011).

With continuous advancements in automotive technology, efforts are being made to further reduce engine friction for improved efficiency and performance (Tung & McMillan, 2004). Hybrid and electric power trains are helping to minimize reliance on internal combustion engines, thereby reducing friction-related energy losses (Abebe et al., 2024). In conventional engines, new developments such as nanotechnology-based lubricants, advanced surface coatings, and improved thermal management systems are driving progress in friction reduction, making modern engines more efficient, durable, and environmentally friendly (Chen et al., 2020).

2.19.2. Engine wear

Engine wear occurs due to a combination of mechanical, thermal, and chemical factors that gradually degrade engine components over time (Lakshminarayanan & Nayak, 2011). One of the primary causes is friction, which arises when moving parts, such as pistons, bearings, and crankshafts, rub against each other. Without proper lubrication, metal-to-metal contact increases, leading to excessive wear. Heat also plays a significant role, as engines operate at high temperatures, causing components to expand and contract. Repeated thermal cycling can weaken materials, resulting in cracks, warping, or overall deterioration (Zhu et al., 2023). Corrosion further accelerates wear, as moisture, combustion by-products, and acidic residues from fuel break down metal surfaces (Su et al., 2023). Additionally, contaminants such as dirt, dust, and metal particles can enter the engine through inadequate filtration, leading to abrasive wear that grinds away critical components (Dziubak & Dziubak, 2022). Poor-quality fuel and degraded lubricants can also contribute to chemical damage, weakening engine parts over time. Finally, improper driving habits, such as frequent cold starts, rapid acceleration, and overloading, put excessive strain on the engine, accelerating the wear process (Morris, 2015). Together, these factors contribute to the gradual decline of engine performance, efficiency, and longevity.

2.19.3. Engine lubrication

Engine lubrication is a crucial process that reduces friction, minimizes wear, and ensures smooth engine operation(Zhang, 2010). The of engine oil to create a thin protective film between moving parts, preventing direct metal-to-metal contact. Proper lubrication helps dissipate heat, reduce corrosion, and keep the engine clean by carrying away contaminants (Wong & Tung, 2016). Without adequate lubrication, engines would experience excessive friction, overheating, and premature failure (Totten, 2017).

A well-functioning lubrication system ensures efficient engine performance and extends the life of engine components such as pistons, crankshafts, camshafts, and bearings (Lei et al., 2024). Engine oils are specially formulated with additives that enhance viscosity, prevent oxidation, and

provide anti-wear protection. Regular oil changes and maintenance are essential to ensure the lubrication system functions optimally, preventing damage and costly repairs (Trotsenko et al., 2022).

2.19.3.1. Boundary Lubrication

Boundary lubrication occurs when a very thin layer of lubricant is present between two surfaces, but it is not thick enough to separate (Zhang, 2006) them. This type of lubrication happens in situations where high loads, low speeds, or frequent start-stop operations prevent the formation of a full lubricant film (Zhang & Meng, 2015).

In boundary lubrication, the oil molecules form a protective layer that adheres to the metal surfaces, reducing direct contact and minimizing wear(Jacobson & Hogmark, 2009). Special additives, such as anti-wear (AW) and extreme pressure (EP) additives, are included in lubricating oils to enhance boundary lubrication (Hsu & Gates, 2005). These additives chemically react with metal surfaces to create a protective film that prevents excessive wear and damage. Characteristics of hydrodynamic lubrication include (Matveevsky & Buyanovsky, 1986):

- In conditions of high pressure and low speed.
- The lubricant film is very thin, and surfaces may partially touch.
- Relies on chemical additives to reduce wear.
- Common in engine startup, braking, and gear systems.

2.19.3.2. Hydrodynamic Lubrication

This type of lubrication takes place when a thick lubricant film fully separates two moving surfaces, effectively preventing metal-to-metal contact. It typically occurs under high-speed and low-load conditions, where component motion enables the formation of a stable oil film (Stephan et al., 2023).

As moving parts slide against each other, they generate a pressure difference that draws oil into the space between them, creating a continuous lubricating layer. This effect is especially important in components such as crankshaft bearings, where smooth and efficient motion is essential for engine performance (Hamel et al., 2023).

Key features of hydrodynamic lubrication (Spurk & Aksel, 2019**)**:

- Develops at high speeds under moderate loading.
- A continuous and thick oil film completely separates the surfaces.
- Friction is greatly reduced, enhancing overall efficiency.
- Commonly found in engine bearings, journal bearings, and rotating shafts.

The path followed by lubricating oil within the engine, along with the two types of oil film formation, is shown in Figures 2.13 and 2.14, respectively.

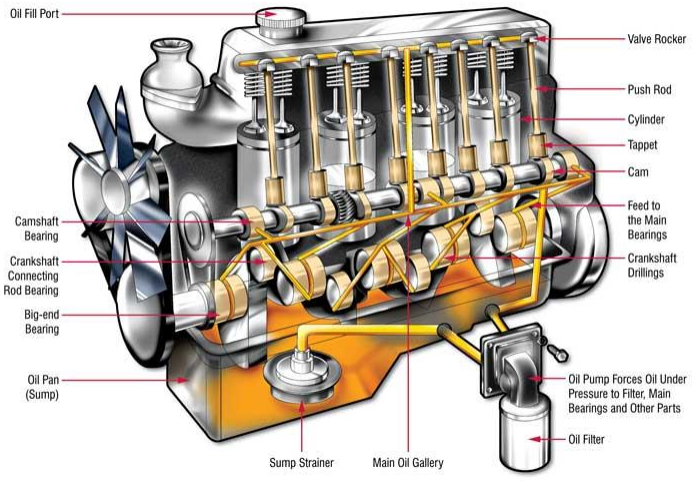

Figure 2. 12 Lubrication Circuit and Flow Path of Oil in Engine

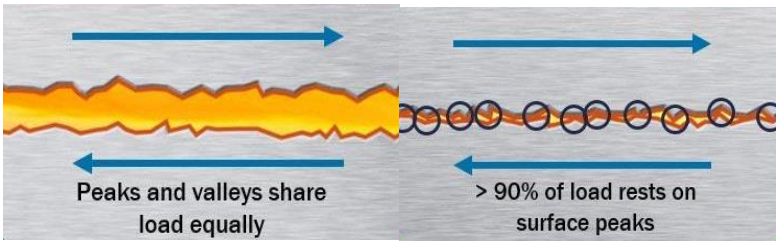

a) Hydrodynamic lubrication b) Boundary lubrication

Figure 2. 13 The two typical lubricating condition of oil film formation

2.20. Contamination of lubricant

Contamination of engine lubricating oil by diesel fuel is a serious issue that can significantly impact engine performance, lubrication efficiency, and component longevity (Ragupathi & Mani, 2021). Diesel fuel can enter the lubrication system through several mechanisms, including fuel injector leaks, excessive idling, incomplete combustion, or worn piston rings (Vasilakos, 2017). When diesel fuel mixes with engine oil, it alters its viscosity, reduces its lubrication properties, and accelerates wear and damage to critical engine components(Macian et al., 2016).

The primary consequences of diesel fuel contamination is the dilution of engine oil(Tormos et al., 2019). Since diesel fuel has a much lower viscosity than engine oil, its presence reduces the oil's ability to protect the friction of moving parts. This leads to increased metal-to-metal contact, resulting in higher friction, accelerated wear, and potential engine failure. Additionally, reduced oil viscosity can cause oil pressure to drop, leading to inadequate lubrication of bearings, camshafts, and other vital components(Wolak et al., 2018).

Another major issue associated with diesel fuel contamination is the loss of essential additives in the engine oil. Modern lubricants contain detergents, dispersants, anti-wear agents, and oxidation inhibitors that help protect the engine and maintain oil stability(Aldajah et al., 2007). However, when diluted with diesel fuel, these additives become less effective, leading to increased sludge formation, varnish deposits, and reduced oil film strength. This can result in premature wear of engine components, poor sealing performance, and potential overheating due to increased friction (Chybowski et al., 2023).

Furthermore, contamination of lubricating oil by diesel fuel can contribute to excessive carbon buildup and soot formation within the engine. Diesel fuel contamination disrupts the combustion process, resulting in incomplete fuel combustion and the formation of excessive carbon deposits on pistons, valves, and cylinder walls. These deposits can lead to increased engine knock, reduced fuel efficiency, and clogged oil passages, further aggravating lubrication problems(Kurre et al., 2017).

Preventing diesel fuel contamination in engine oil requires proper maintenance and early detection of potential leaks. Regular oil analysis can help identify fuel dilution levels, allowing corrective actions to be taken before severe engine damage occurs(Kurre et al., 2017). Using high-quality fuel, ensuring proper injector function, and avoiding prolonged idling can also help minimize the risk of contamination. Routine oil changes and adhering to the manufacturer's recommended service intervals are crucial for maintaining optimal lubrication and preventing the adverse effects of diesel fuel contamination(Lacey et al., 2012). The flow path of blow-by gas leaks is illustrated in Figure 2.15 below.

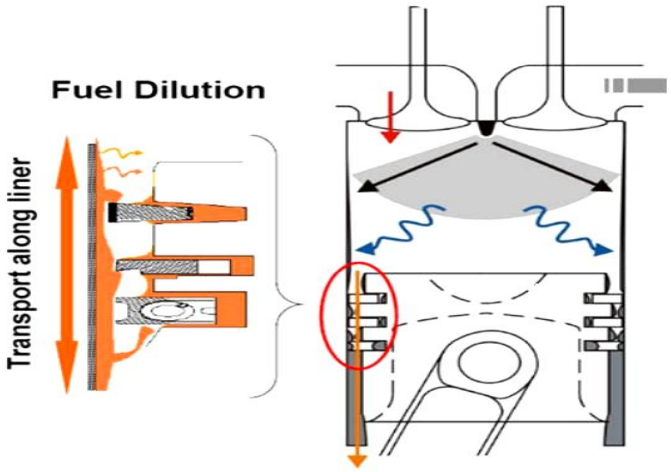

Figure 2. 14 Basic path of the blow by of partially burn fuel

2.20.1. Engine Oil Dilution When Using Biodiesel

Engine oil dilution by biodiesel occurs when unburned biodiesel fuel enters the crankcase and mixes with the lubricating oil. This dilution can negatively impact engine performance, lubrication efficiency, and overall longevity (Shanta, 2011). The primary cause of this issue is incomplete combustion, which allows fuel to bypass the piston rings and accumulate in the oil sump. Several factors contribute to this process, including fuel injection timing, cold starts, and post-injection strategies used in modern diesel engines (da S. Bezerra et al., 2021).

A major cause of engine oil dilution by biodiesel is the use of post-injection during diesel particulate filter (DPF) regeneration(Chen et al., 2014). In many modern diesel engines, extra fuel is injected late in the combustion cycle to raise exhaust temperatures and burn off soot in the DP (Luo et al., 2023). However, some of this unburned biodiesel can bypass the piston rings and enter the crankcase, mixing with the engine oil. Due to biodiesel's higher boiling point compared to petroleum diesel, it evaporates more slowly, leading to gradual accumulation in the lubricating oil(Luo et al., 2023).

Biodiesel requires higher temperatures for complete combustion, and it may not burn efficiently in cold conditions(Tompkins & Jacobs, 2013). When the engine does not reach an optimal operating temperature, unburned biodiesel is more likely to condense on cylinder walls and seep into the crankcase. Similarly, frequent short trips prevent the engine oil from reaching temperatures high enough to vaporize and remove small amounts of fuel contamination (Imtenan et al., 2014).

Additionally, fuel injector issues can lead to excessive oil dilution. Faulty or leaking fuel injectors may introduce excess biodiesel into the combustion chamber, increasing the chances of unburned fuel washing down the cylinder walls into the sump(Hu et al., 2015). Worn piston rings and cylinder liners can further worsen this issue by reducing the engine's ability to create a tight seal, allowing more fuel to pass through (Tormos et al., 2019).

Regular maintenance is essential to minimize oil dilution by biodiesel (Abd Manaf et al., 2019). Ensuring proper fuel injector function, avoiding excessive idling, and using high-quality biodiesel blends can help reduce the risk. Additionally, following recommended oil change intervals and using engine oils formulated for biodiesel compatibility can help maintain proper lubrication and engine performance (Thornton et al., 2009).

Some degree of engine oil dilution from diesel fuel is normal in all engines. However, when biodiesel or biodiesel blends are used, the dilution rate and its impacts can differ significantly from those of conventional diesel (S. Lahane & K. Subramanian, 2015). According to the study by (Tilli et al., 2018), there are three main reasons for increased oil dilution with biodiesel:

a) Biodiesel, being an ester-based fluid, exhibits stronger solvency and penetration than hydro carbon-based diesel, making it more likely to infiltrate and mix with engine oil.

b) Modern diesel engines equipped with diesel particulate filters (DPFs) often use post-injection strategies to raise exhaust temperatures and enable soot burn-off. This process can lead to increased amounts of unburned biodiesel entering the crankcase.

c) Biodiesel has a distillation temperature approximately 100 °C higher than that of diesel fuel, reducing its volatility. As a result, it evaporates more slowly and tends to accumulate in the engine oil over time, contributing to long-term dilution.

2.20.2. Problems Associated with Engine oil Dilution by Diesel Engine Fuel

Engine oil dilution by diesel fuel is a significant issue that can lead to mechanical problems, reduced lubrication efficiency, and long-term engine damage(Wolak et al., 2018). When diesel fuel mixes with engine oil, it alters the oil's physical and chemical properties, reducing its ability to protect moving components (Wattrus, 2013). The severity of the impact depends on the extent of dilution and the duration for which the contaminated oil remains in the engine. Below are some of the key problems associated with engine oil dilution by diesel fuel.

2.20.3. Reduced Oil Viscosity and Lubrication Efficiency

One of the primary issues with fuel dilution is the reduction in oil viscosity(Yu et al., 2023). Diesel fuel has a much lower viscosity than engine oil. When it contaminates the oil, it thins the lubricant, making it less effective at forming a protective film between moving parts. This increased friction leads to accelerated wear of critical components, such as pistons, bearings, and camshafts, ultimately shortening the engine's lifespan (Zhang et al., 2021).

2.20.4. Increased Engine Wear and Component Damage

Proper lubrication is essential for reducing friction and preventing metal-to-metal contact. Diluted oil loses its ability to provide sufficient lubrication, leading to excessive wear on engine parts (MAcián et al., 2020). Components such as cylinder walls, piston rings, and crankshaft bearings are particularly vulnerable to increased wear, which can cause performance issues and, in severe cases, lead to engine failure (Dziubak & Dziubak, 2022).

2.20.5. Decreased Oil Pressure

Since fuel contamination reduces oil viscosity, it also affects the engine's ability to maintain proper oil pressure(Green & Lewis, 2008). Lower viscosity oil flows more quickly, potentially causing oil pressure to drop below the recommended levels. Insufficient oil pressure can lead to inadequate

lubrication, especially in high-speed or high-load conditions, increasing the risk of engine damage (Nikolakopoulos et al., 2018).

2.20.6. Increased Sludge and Deposit Formation

Fuel dilution can cause the breakdown of oil additives, forming sludge, varnish, and carbon deposits inside the engine(Wattrus, 2013). These contaminants can clog oil passages, restrict lubrication flow, and reduce engine efficiency. Additionally, excessive sludge build-up can cause sticking of critical components, such as piston rings and hydraulic lifters, leading to reduced performance and higher maintenance costs (Kouame et al., 2015).

2.20.7. Higher Oil Consumption and Blow-by Gases

When engine oil is diluted with diesel fuel, it is more likely to be burned off during combustion, increasing oil consumption (Hasannuddin et al., 2016). This can result in more frequent oil top-ups and higher maintenance costs. Additionally, fuel-contaminated oil can increase blow-by gases, including unburned fuel and oil vapors, which escape past the piston rings into the crankcase. These gases contribute to further oil degradation and increased emissions (Mitchell et al., 2017).

2.20.8. Poor Engine Performance and Reduced Efficiency

An engine operating with diluted oil may experience reduced efficiency due to increased internal friction and improper combustion(Hasannuddin et al., 2016). The thinning of oil reduces its ability to properly seal the gaps between the piston rings and cylinder walls, leading to compression loss and decreased power output. Additionally, incomplete combustion caused by fuel dilution can result in poor fuel economy and higher emissions (Devlin, 2018).

2.20.9. Potential for Engine Overheating

The role of lubricating oil is crucial in dissipating heat from engine components (Ali & Xianjun, 2020). When oil is diluted with diesel fuel, its ability to transfer heat is compromised, resulting in localized overheating of engine parts(Abou-Ziyan, 2004). Excessive heat can cause the warping of engine components, accelerate oil oxidation, and increase thermal stress on vital parts, ultimately reducing engine longevity (Ali et al., 2016).

Therefore, engine oil dilution by diesel fuel presents a serious risk to engine performance, longevity, and efficiency. Reduced oil viscosity, increased wear, sludge formation, lower oil pressure, and overheating are among the key problems associated with this issue(da Silva et al., 2012). Regular maintenance, timely oil changes, proper fuel injection system checks, and oil quality monitoring are essential to mitigate these risks. Identifying and addressing the root causes of fuel dilution early can help prevent severe engine damage and ensure optimal performance.

2.21. Engine endurance test

Engine endurance measurement is critical to assessing an engine's durability and performance over extended periods(Piancastelli, 2012). Various methods with their specific standard procedures are employed to evaluate how engines withstand prolonged operational stresses in various regulatory documents and industry standards (Kumar & Chauhan, 2015)

2.21.1. Federal Aviation Administration (Rosli et al.) Regulations

It specifies that each engine must undergo an endurance test totaling at least 150 hours of operation (Atwood, 2010). The test consists of a series of runs designed to evaluate the engine's durability under various conditions. The regulation mandates that the prescribed 6-hour test sequence be conducted 25 times to complete 150 hours. Additionally, it provides guidance on the test objectives and methodologies for engine endurance testing (This, 1911). It emphasizes demonstrating an accelerated durability test of the engine to ensure a minimum level of operability and durability throughout the engine's assigned ratings and operating limitations.

2.21.2. Environmental Protection Agency (EPA) Regulations

For engines subject to emission standards, the EPA's 40 CFR Part 1065 outlines standardized testing procedures (Bougher et al., 2010). These procedures ensure that engines meet environmental requirements and include specifications for equipment, calibration, and test protocols. Engines are subjected to controlled environments to study their behavior under varying conditions, including changes in temperature and altitude. This helps in understanding how environmental factors impact engine performance and endurance.

2.21.3. Industry Standards:

The engine endurance test methods and procedures are outlined in the following section, according to ISO standards, Indian standards, and European standards.

2.21.4. The ISO Engine Endurance Test Standard

The International Organization for Standardization (Benti et al.) has developed a series of guidelines to assess the performance, durability, and lifespan of internal combustion engines across different operational conditions. ISO standards like ISO 15550:2016 and ISO 2534:2020 focus primarily on performance testing, such as power output and fuel consumption, while also laying the foundation for endurance testing through baseline measurements. ISO 3046-1:2002 specifies testing methods for industrial reciprocating engines, including endurance tests for power generation and heavy machinery, with durations ranging from a few hours to 500 hours. Meanwhile, ISO 8178 addresses off-road engine exhaust emissions, incorporating endurance tests up to 500 hours to replicate real-world conditions.

These endurance tests typically involve running engines under full load, partial load, and idle conditions while assessing performance over extended periods to ensure long-term reliability and efficiency. Engines are tested under varied thermal and environmental conditions to simulate real-world stress, with critical components monitored for wear and degradation. These tests also confirm that engines meet emission standards, fuel efficiency requirements, and maintain consistent performance over prolonged use. Industries such as automotive, industrial, and marine rely on these tests to verify engine reliability in harsh conditions, including high temperatures, heavy loads, and extended operation.

The 100-hour endurance test under the ISO 8178 standard offers a thorough evaluation of an engine's ability to perform reliably over long periods. By simulating different load conditions (full load, partial load, idle), it assesses durability, fuel efficiency, and compliance with emission standards, ensuring the engine can withstand real-world conditions without significant performance degradation or component failure. And the procedures for the 100-Hour Endurance Test under ISO 8178 are as follows(Broman, 2012):

1. **Preparation for the Test**:
   - Engine Setup: The engine is mounted on a dynamometer (test bench) that simulates real-world operational loads. All necessary instrumentation is in place to measure parameters such as fuel consumption, exhaust emissions, engine speed, and load.
   - Fuel and Lubricants: The engine is fueled with the appropriate fuel (e.g., diesel, biodiesel) and lubricants, as specified by the manufacturer. The fuel must meet relevant standards (EN 590 for diesel or ISO 14214 for biodiesel).
   - Test Conditions: Ambient conditions (temperature, humidity, atmospheric pressure) are carefully controlled and monitored to maintain consistency throughout the test.
2. **Start-Up and Initial Measurements**:
   - Engine Warm-Up: The engine is started and allowed to reach normal operating temperatures (approximately 15-30 minutes, depending on the engine size). During this period, baseline measurements for emissions and fuel consumption are recorded.
   - Baseline Data: Key parameters such as idle fuel consumption, emissions levels (NOx, CO2, particulate matter), and engine power output are recorded for future comparison.
3. **Test Cycles and Duration**: The 100-hour test consists of several cycles simulating various operating conditions:
   - Full Load Operation (typically 25% of test time): The engine operates at its maximum rated power output, simulating high-load scenarios such as heavy machinery under full capacity.

- Partial Load Operation (typically 50% of test time): The engine runs at varying loads to mimic typical operating conditions such as transportation or medium-load machinery use.
- Idle Operation (typically 15-25% of test time): The engine runs at idle speed, simulating stop-and-go traffic, idle periods in construction or agriculture, or rest phases between active works.

The test cycles vary in terms of full load, partial load, and idle operation, with the total test duration being 100 hours.

2.21.5. Indian engine endurance test standards

The Indian Standard for Engine Endurance Testing, primarily outlined in IS 10000-9:1980, offers a comprehensive method for evaluating the durability and performance of internal combustion engines over extended use. According to this standard, engines must undergo a test lasting 512 hours, divided into 32 cycles of 16 hours each. During these cycles, the engine is subjected to varying load conditions, including full load, partial load, and idling, to simulate real-world operational scenarios. The test also includes running the engine at different speeds and under diverse environmental conditions, assessing its overall reliability, performance, and fuel efficiency over time. The main goals of the test are to evaluate engine wear, fuel consumption, oil consumption, and emission levels during prolonged use, ensuring that the engine can endure long-term operation without significant performance degradation. This standard is specifically tailored to the diverse operating conditions found in India, making it essential for verifying engine durability in the country's unique climate and road environments. The IS 10000 (Part IX) - 1980 Section II standard also includes procedures for a 100-hour endurance test, which is a critical procedure for evaluating engine reliability, performance, and durability. The following outlines the steps for conducting 100-Hour Engine Endurance Test Procedure (IS 10000 - 1980 Section II)(Raj et al., 2009):

1. **Test Duration and Cycles**:
   - The total duration of the test is 100 hours, divided into multiple cycles where the engine is subjected to different load and speed conditions.
   - Each cycle includes periods of full load, partial load, and idle operation, simulating typical real-world usage over an extended period.

2. **Cycle Breakdown**:
   - **Full Load Cycle**: The engine operates at its maximum rated load for a designated portion of the test, simulating high-stress conditions and testing the engine's performance under maximum power demand.

- **Partial Load Cycle**: The engine is run under partial load conditions for another segment of the test, ensuring that it remains efficient under less demanding conditions.
- **Idle Cycle**: Periods of idle operation simulate stop-and-go driving, such as in traffic or when a vehicle is stationary.
- **Speed Variation**: The engine's speed is varied throughout the test to replicate the speed fluctuations typical in normal vehicle operation, including acceleration and deceleration.

The following outlines the steps for conducting 100-Hour Engine Endurance Test Procedure (IS 10000 - 1980 Section II): is essential for assessing engine reliability, performance, and durability. It simulates long-term operational stresses to ensure the engine performs as expected under real-world conditions while maintaining fuel efficiency, controlling emissions, and avoiding excessive wear(Prahladbhai & Brahmbhatt, 2023).

2.21.6. European engine endurance test standards

European engine endurance test standards primarily aim to ensure that engines remain durable and perform reliably under extended operational conditions (Giakoumis, 2017). A key set of regulations is the EURO 6, which governs emissions and performance for passenger vehicles (Giakoumis, 2016). These regulations require engines to undergo endurance tests that replicate real-world driving scenarios, such as city, highway, and idling cycles. These tests evaluate the engine's ability to maintain fuel efficiency, minimize emissions, and sustain performance over long periods. Moreover, the EURO 6 standards also set durability criteria for components like exhaust after-treatment systems, ensuring their continued effectiveness throughout the engine's lifespan.

For aviation engines, the EASA CS-E 740 regulation mandates a minimum of 150 hours of endurance testing. These tests involve cycles with varying power settings and operational conditions to simulate long-duration flight. Additionally, European standards like ISO 15550 and ISO 2534 are commonly used across Europe to assess the performance and durability of internal combustion engines. These standards focus on testing engines under continuous stress, fluctuating thermal conditions, and extended use, ensuring consistent performance, fuel efficiency, and emissions control. The overall goal of these European standards is to guarantee that engines in the European market can operate efficiently, reliably, and in compliance with environmental regulations throughout their service life.

The European engine endurance test standards for a 100-hour test are governed by various European Union regulations and standards aimed at evaluating engine durability, emissions, and performance. These tests simulate real-world operating conditions to confirm that engines meet strict performance and environmental criteria over long durations.

While there isn't a specific "100-hour endurance test" standard, many engines, especially those used in automotive, off-road, and marine applications, are tested for 100 hours or more, depending on the engine type and regulatory requirements. Below is a general outline of the procedures(Giakoumis, 2017):

a) Preparation:

- The engine is installed on the test rig following manufacturer specifications.
- Fuel, lubricants, and cooling fluids are checked and filled in accordance with the engine's specifications.
- A monitoring system is set up to record performance metrics, including speed, load, temperature, and fuel consumption.

b) Test Conditions:

- The engine is run under various load and speed conditions, including idle, full load, and partial load, simulating real-world operational use.
- Predefined testing conditions replicate the engine's typical usage over an extended period.

c) Monitoring:

- Key parameters, such as exhaust emissions, engine temperatures, and vibrations, are continuously monitored throughout the test.
- Periodic maintenance tasks, such as oil changes or filter replacements, are carried out at designated intervals to mimic real-life usage.

d) Test Duration:

- The test runs for 100 continuous hours, though in some cases, it may be split into smaller blocks (50-hour blocks with breaks).
- The engine's performance is assessed based on its ability to endure wear and maintain operational standards during the test.5. Evaluation:
- After the 100-hour test, the engine is thoroughly inspected for signs of wear, damage, or performance degradation.
- The test results are analyzed to ensure the engine meets European standards for durability, emissions, and efficiency.

2.22. Engine vibration

Engine vibration analysis is an essential aspect of engine endurance testing. It helps assess the structural integrity, reliability, and durability of engine components under prolonged operational conditions(De Donno, 2023). Excessive vibrations can lead to fatigue failure, misalignment, and premature wear of engine parts. By monitoring vibration levels during an endurance test, engineers

can identify potential failure points, optimize engine design, and ensure compliance with performance standards(Greuter & Zima, 2012).

Engine vibration analysis under steady and dynamic conditions plays a significant role in enhancing engine performance, reliability, and longevity(Boysal & Rahnejat, 1997; Tienhaara, 2004). Understanding fundamental equations and analytical methods allows engineers to diagnose vibration sources effectively and implement mitigation strategies. Further research in this area focuses on advanced signal processing techniques and machine learning applications for real-time vibration monitoring and fault diagnosis.

2.22.1. Primary vibration

The primary vibration, often referred to as the base or fundamental vibration, is the predominant oscillatory motion associated directly with the engine's rotational speed(Mahdisoozani et al., 2019). This type of vibration is a natural consequence of the repetitive movement of the engine's rotating components, such as the crankshaft, flywheel, pistons, connecting rods, and other associated parts(Schmitz & Smith, 2012). As the engine operates, the crankshaft undergoes rotational motion to convert linear piston movement into usable torque. This motion, while smooth in theory, inherently causes periodic forces and moments that generate vibrations. These vibrations are cyclic, following a predictable pattern that is synchronized with the engine's rotational speed(Tschöke et al., 2021). For instance, an engine running at 3000 revolutions per minute (RPM) will exhibit primary vibrations with a frequency corresponding to this speed. The primary vibration is influenced by several factors, including the design and balance of the rotating components, the engine's firing order, and the distribution of forces during combustion. When these forces are unevenly distributed or if the rotating parts are imbalanced, the intensity of the primary vibration can increase, potentially leading to mechanical wear, noise, and reduced efficiency. In automotive and mechanical engineering, managing primary vibrations is critical to ensuring smooth operation and prolonging the lifespan of the engine and connected systems(Hoag & Dondlinger, 2015). Techniques such as dynamic balancing of rotating parts, the use of vibration dampers, and optimizing the engine's mounting system are commonly employed to minimize the adverse effects of primary vibrations. Additionally, engineers analyse these vibrations during the design phase using tools such as finite element analysis (FEA) and vibration modelling to predict and mitigate potential issues. According to (Bishop et al., 2011),the mathematical expression for primary vibration is:

$$a_{primary}(t) = A_1 sin(2\pi f_1 t + \emptyset_1) \qquad \text{(Eqn. 1)}$$

Where; A_1 is the peak value of acceleration, representing the strength of the vibration. Larger A_1 values indicate more severe oscillations. f_1 is The fundamental frequency, calculated as f1=RPM/60, representing the number of oscillations per second. For instance, an engine running at 3000 RPM produces a fundamental frequency of 50 Hz. ϕ_1\phi is the phase angle, which indicates the starting point of the wave relative to time zero. The primary vibration is the most prominent component in the vibration signal, forming the basis for further analysis. It is often used to evaluate the engine's mechanical health, as excessive amplitude or irregular frequency could indicate issues such as misalignment, imbalanced components, or faulty bearings.

2.22.2. Secondary Vibration

Secondary vibrations arise due to the inherent complexities of an engine's mechanical and operational dynamics(Ewins, 2010). These vibrations are not directly linked to the primary rotational motion but are a result of factors such as imbalances in the moving parts, resonance effects, and minor imperfections in the manufacturing or assembly processes(Benaroya et al., 2017). While they may appear less significant than primary vibrations, secondary vibrations can still impact the overall performance, durability, and noise levels of the engine system. These vibrations are characterized as harmonics of the fundamental frequency f_1, which is the frequency of the primary vibration directly tied to the engine's rotational speed. Harmonics are integer multiples of this fundamental frequency(Marín & Rhea, 2010). For instance: The second harmonic occurs at $2f_1$, meaning it oscillates at twice the frequency of the primary vibration. The third harmonic occurs at $3f_1$, oscillating three times faster than the fundamental frequency. Higher-order harmonics, such as the fourth ($4f_1$) and fifth ($5f_1$) harmonics, continue to follow this pattern. The presence of these harmonics is due to non-linearity and asymmetries within the engine system(Ji, 2014). These could include variations in the mass or geometry of rotating components, uneven combustion forces, or misalignment of the crankshaft and connecting rods. Manufacturing tolerances, wear and tear, and external factors such as load variations and environmental conditions can further amplify secondary vibrations. Secondary vibrations are particularly significant when they coincide with the natural frequencies of the engine or its components, a condition known as resonance. Resonance amplifies the vibration amplitudes and can lead to severe mechanical stress, increased noise, and potential failure if not addressed. Engineers actively work to identify and mitigate secondary vibrations during the design and testing phases. This involves the use of advanced computational modeling, including harmonic analysis and modal testing, to predict the behavior of these vibrations. Solutions to control secondary vibrations include precision balancing of components, optimized engine designs, damping materials, and tuning engine mounts to isolate

vibrations. Additionally, modern systems may incorporate active vibration control mechanisms to dynamically counteract the effects of secondary harmonics, ensuring smoother and more reliable engine operation.

According to(Bishop et al., 2011) the equation for secondary vibration is:

$$a_{secondary}(t) = A_2 sin(2\pi n f_1 t + \emptyset_2) \quad \text{(Eqn. 2)}$$

Where, A_2: The amplitude of the harmonic, typically smaller than A_1but still significant: The harmonic order, an integer (n=2, 3, 4…). Higher-order harmonics are less pronounced but can still impact vibration behavior. ϕ_2 is the phase angle for the harmonic, affecting the relative timing of the harmonic waveform. Secondary vibrations provide insights into specific issues within the engine. For instance: Second Harmonic (n=2) is may indicate shaft misalignment or crankshaft imbalances. Higher-Order Harmonics (n>2): Often associated with resonance, nonlinearities, or structural vibrations. Analyzing secondary vibrations is essential in understanding the overall vibration spectrum and diagnosing issues that cannot be detected from the primary vibration alone.

2.23. Summary and Research Gap

Several researchers have examined the combustion, emissions, performance, and tribological behavior of compression ignition (CI) engines fueled with biodiesel, biodiesel-diesel blends, and biodiesel-diesel-alcohol mixtures, both with and without additives. However, after careful review process of biodiesel production and engine performance test of the selected articles of shown in the Tables 1.1 and 1.2 below, variability in the physio-chemical properties of biodiesel derived from different feed stocks and negligence of the total glycine content removed from the esterification reaction is observed which causes a major challenge especially on the ash content and carbon deposited formation. For example, the viscosity, fatty acid composition, carbon chain length, and oxygen content vary significantly between oils such as castor and Jatropha Carcus, affecting fuel atomization, spray pattern, and ultimately combustion and engine performance.

Despite this, many experimental studies lack critical data on total and free glycerin content, which is essential for evaluating fuel quality. Glycerin residues can lead to carbon deposits in the combustion chamber and gum formation in the fuel system. Additionally, the causes and characteristics of particulate matter emissions, as well as the roles of viscosity, glycerin content, and volatility, are not well documented.

Although there is growing interest in using metal oxide nanoparticles like aluminum oxide (Al_2O_3) to enhance the performance and emissions profile of biodiesel-diesel blends, comprehensive research on this topic remains limited. Specifically, there is insufficient clarity on the optimal

concentration of Al_2O_3 that balances combustion efficiency, emissions reduction, fuel stability, and engine wear.

Most existing studies emphasize performance and emissions, while overlooking essential tribological aspects such as lubricity, friction reduction, and wear resistance. The lack of standardized experimental procedures, nanoparticle dispersion methods, and blend ratios further complicates cross-study comparisons.

Therefore, there is a clear research gap in understanding the combined effects of biodiesel-diesel blends and Al_2O_3 nanoparticles on both engine performance and long-term durability. Systematic studies are needed to investigate the performance, combustion, and tribological behavior of these nano-enhanced fuels to support the development of efficient, reliable, and sustainable engine operation.

Table 2. 12 Comparison of total glycerol removal and transesterification method

N0	Authors & year	Catalyst	Methaoxilate oil ratio	(T^0C)	Time (min)	Optimization method	Maximum ester	Total glycerine
1	Jain et al. (2012)	Homogeneous NaOH	11:1	55	110	RSM (CCD)	98.3	0.12
2	Otieno et al.(2022)	Heterogeneous NaOH (zeolite Na–X)	10:1	70	300	Taguchi L_{16} design	93.94	–
3	Zarei et al.(2014)	Enzyme (immobilized *R. oryzae* lipase)	5:1	40	1020	RSM (CCD) + ANN	87.1	–
4	Goyal et al(2012)	Homogeneous NaOH	6:1	60	40	RSM	98.6	–
5	Singh et al.(2012)	Homogeneous NaOH	6:1	60	30	Empirical	87	10
6	Kumar et al.(2012)	Homogeneous NaOH	6:1	60	40	Empirical	98.6	–
7	Sharma et al.(2012)	Homogeneous NaOH	25% v/v	55–60	5–6	Empirical	76	–

Table 2. 13 Summary review of literature

No	Author & year	Title	Findings	Future work	References
1	Chauhan et al.(2012)	A study on the performance and emission of a diesel engine fueled with Jatropha biodiesel oil and its blends	A significant reduction of CO,UHC and smoke	Prediction of best blend at different engine operating parameters	Energy37(12)616-622
2	J. Sadhik Basha • R. B. Anand	The influence of nano additive blended biodiesel fuels on the working characteristics of a diesel engine	Peak pressure and heat release rate reduced with NPs. The brake thermal efficiency and BSFC with Nps blended are improved	Use multi-cylinder engines; evaluate lubricant degradation and engine wear.	J Braz. Soc. Mech. Sci. Eng. (2013) 35:257–264 DOI 10.1007/s40430-013-0023-0
3	H.K. Rashedul et al(2014)	The effect of additives on properties, performance and emission of biodiesel fuelled compression ignition engine	Improved combustion and emission profile; indications of wear reduction.	If a deposit is formed on the valve surface, the ratio and flow of air will alter and fuel does not completely burn.	Energy Conversion and Management Volume 88, December 2014, Pages 348-364
4	[Singh*, 4.(6): June, 2015]	Performance, combustion and emission characteristics of Compression ignition engine using nano-fuel: a review	performance improvements with nano-additives	Tribological and wear testing, long-duration tests, and real-world field validation.	International journal of engineering sciences & research Technology
5	Aalam et al. (2015)	Experimental investigations on a CRDI system assisted diesel engine fuelled with aluminium oxide nanoparticles blended biodiesel	Al_2O_3 nanoparticles improved combustion characteristics and reduced emissions.	Effects of different nanoparticle sizes and concentrations on engine performance, modified injection strategies	Alexanderia Engineering Journal,54(3),351-358
6	Prabu (2016)	Engine Characteristic Studies by Application of Antioxidants and Nanoparticles as Additives in Biodiesel Diesel Blends	Increased BTE; reduced CO and HC emissions significantly	Explore different engine loads and nanoparticle types; investigate post-combustion wear patterns	Journal of Energy Resources Technology AUGUST 2018, Vol. 140 / 082203-1
7	Ashish Dewangan et al (2019)	Effect of metal oxide nanoparticles and engine parameters on the performance of a diesel engine: A review	Better combustion and lower CO and HC; marginal NO_x increase	To examining nanoparticle dispersion stability, engine wear effects, and lubricant interaction	IJRASET,5,358-372
8	Chen et al. (2018)	Combustion and Emission Characteristics of Diesel Engine Fueled with Diesel/Biodiesel/Aluminum Oxide Nanoparticles	Improved combustion and emissions; NO_x marginally increased	Emphasize exhaust after-treatment compatibility, fuel stability, and impact on injector wear.	Energy conversion management 171,461-477
9	El-Seesy et al. (2018)	Performance, combustion, and emission characteristics of a diesel engine fueled	graphene oxide nanoparticles improved combustion and reduced emissions	Investigate the long-term effects of nanoparticle additives on engine wear and durability	Energy conversion and management 166,674-686

		with Jatropha methyl ester and graphene oxide additives			
10	Soudagar et al. (2018)	The potential of nanoparticle additives in biodiesel:- A fundamental outset	All the oxygenated additives increased the cetane number and reduced the ignition delay period.	Deeper investigation into nanoparticle-lubricant interaction and long-term engine integrity	https://doi.org/10.1063/5.0003775
11	Abul Kalam Hossain * and Abdul Hussain(2019)	Impact of Nanoadditives on the Performance and Combustion Characteristics of Neat Jatropha Biodiesel	Increased BTE; significant emission reduction with nanoparticle use.	To test other nanoparticles. and investigate long-term engine wear and combustion chamber deposits	MDPI Energies,
12	Prabu (2018)	Effect of Al_2O_3 nano-additives on the performance and emission characteristics of jatropha and pongamia methyl esters in compression ignition engine	Al_2O_3 nanoparticles enhanced brake thermal efficiency and reduced CO and HC emissions.	Explore the optimal concentration of nanoparticles for balancing performance and emissions. Effect of nanoparticles in the environment.	Energies 12(5),921
13	Manjunath et al. (2019)	Influence of the aluminium oxide (Al_2O_3) nanoparticle additive with biodiesel on modified diesel engine performance	Addition of Al_2O_3 nanoparticles to biodiesel blends enhanced engine performance and reduced emissions	Conduct long-term assessment of the engine components and lubricating oil	International Journal of Ambient Energy
14	(Mukul Tomar & Naveen Kumar (2019))	Influence of Nano additives on the performanceand emission characteristics of a CI engine fuelled with diesel, biodiesel, and blends – a review	Al_2O_3 improves BTE and reduces emissions; results vary with blend ratio.	Tapping unburned particles Stability of nanoparticles	Tailor and Francis Energy journal
15	Jaikumar et al. (2021)	Experimental studies on the performance and emission parameters of a direct injection diesel engine fueled with nanoparticle-dispersed biodiesel blend	Nanoparticle dispersion in biodiesel blends led to improved combustion efficiency and lower emissions.	Investigate the stability of nanoparticle dispersions over extended periods and their effects on engine wear.	International Journal of Thermophysics (2021) 42:91 https://doi.org/10.1007/s10765-021-02842-9

Table 2. 14 Sumary of esterification

Summary of Esterification								
N0	Authors & year	Catalyst	Methaoxilate oil ratio	Temperature (T^0C)	Time (min)	Optimization method	Maximum ester	Total glycerine
1	Jain et al. (2012)	Homogeneous NaOH	11:1	55	110	RSM (CCD)	98.3	0.12
2	Otieno et al. (2022)	Heterogeneous NaOH (zeolite Na–X)	10:1	70	300	Taguchi L_{16} design	93.94	–
3	Zarei et al. (2014)	Enzyme (immobilized *R. oryzae* lipase)	5:1	40	1020	RSM (CCD) + ANN	87.1	–
4	Goyal et al. (2012)	Homogeneous NaOH	6:1	60	40	RSM	98.6	–
5	Singh et al. (2012)	Homogeneous NaOH	6:1	60	30	Empirical	87	10
6	Kumar et al. (2012)	Homogeneous NaOH	6:1	60	40	Empirical	98.6	–
7	Sharma et al. (2012)	Homogeneous NaOH	25% v/v	55–60	5–6	Empirical	76	–

CHAPTER THREE

MATERIALS AND METHODS

This chapter outlines the research plan, methodology, selected feedstock, test fuel preparation procedures, and fuel additives used. It also provides an overview of the experimental process.

3.1. Materials and reagents

The research conducted required the use of specific equipment, materials, and reagents, which included the Gunt Model CT110 engine test stand, exhaust gas analyzer, two identical Robin DY-23 direct injection mono-cylinder diesel Engines, Expert II vibration tester, tachometer, screw press, Soxhlet apparatus, Jatropha curcas seeds, n-hexane, sulfuric acid, methanol, sodium hydroxide, aluminum oxide nanoparticles (Al_2O_3 NPs), and Cetyl-Trimethyl-Ammonium Bromide (CTAB) extra pure, AR, 99%. The equipment, laboratory ware, and chemicals are depicted in Table 3.1

Table 3. 1 Specification of equipment, laboratory ware, and chemicals

SN	Item	Specification
A	**Equipment**	
1	Screw oil pressing machine	Model 6YL68 Henan VIC Machinery Co., Ltd., China, specifications: capacity of 40 kg/h, power rating of 5.5 kW
2	Engine test stand	Gunt Model CT110, air-cooled, naturally aspirated 7.5 kW
3	Exhaust gas analyzer	Model, FD-600M-5GAS, USA
4	Diesel engine	Robin DY-23 2D, Japan
5	Vibration tester	Model, VIBXpert II Germany
6	Tachometer	Monarch PT99 Digital Non-Contact Optical Tachometer - made in the USA
7	Smoke or soot?? tester	Oakland RT-6000 Opacity Meter
B	**Laboratory equipment and glassware**	
1	Bath ultrasonicator	
2	Digital balance	
3	Hot plate with a magnetic stirrer	
4	Soxhlet extraction apparatus	Fisher Chemical, USA
5	Thermometers	ASTU Chemistry laboratory, Range 0-100^{0}C

6	Beakers	250-1000 mL
7	Graduated cylinders	100- 1000 mL
8	Burettes	ASTU Chemistry laboratory, Range250ml -1000ml
C	**Raw materials and chemicals**	
1	Jatropha carcus seeds	Purchased from local farmers (Bati-Amhara region)
2	Sodium hydroxide pellets	Fisher Chemical, Certified ACS, ≥ 97.0 %
3	n-Hexane	Fisher Chemical, HPLC Grade, 95% min
4	Methanol	Fisher Chemical, ≥ 99.8%
5	Sulfuric acid	Fisher Chemical, Certified ACS, 95.0 to 98.0 % (w/w)
6	Cetyltrimethylammonium bromide (CTAB)	Sigma-Aldrich, Extra pure, AR,99%
7	Aluminum oxide nanoparticles	Sigma-Aldrich, particle size 30-60nm
8	Diesel no 2	From filling gas station recommended by Ethiopian Petroleum Enterprise
9	SAE-30W lubricating oil	From filling gas station recommended by Ethiopian Petroleum Enterprise

3.1.1. Screw Oil Pressing Machine

The seeds of Jatropha curcas were pressed using a screw oil press machine illustrated in Figure 3.1 to obtain seed oil.

Figure 3. 1 Screw oil pressing machine

3.1.2. Soxhlet Apparatus

The Soxhlet extractor, initially designed for extracting lipids from solid materials, is vital laboratory equipment. It finds utility in cases where the desired compound exhibits limited solubility in a solvent and the impurity remains insoluble. When the desired compound has substantial solubility in a solvent, a straightforward filtration process can effectively separate

the compound from the insoluble substance. The Soxhlet extractor's design (Figure 3.2) addresses the complexities of extracting compounds with restricted solubility, making it an invaluable tool in laboratory processes.

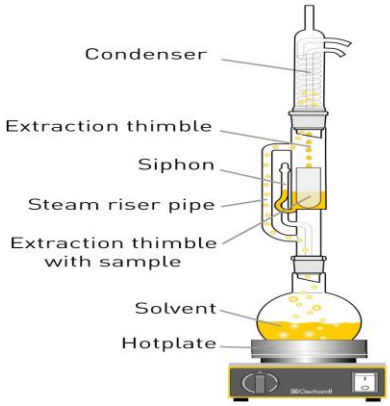

Figure 3. 2 Soxhlet apparatus

3.1.3. Sodium Hydroxide

In the biodiesel esterification process, the methoxide catalyst is formed by reacting methanol with a base ,like sodium hydroxide (Tormos et al.) pilates as shown in the figure3.3 below.

Figure 3.3 Sodium hydroxide Pilates

In the reaction, NaOH dissociates into sodium ions (Na+) and hydroxyl ions (OH-). The OH- ions then abstract hydrogen ions (H^+) from methanol (CH_3OH) to form water, leaving CH_3O- ions, which are then available for the esterification reaction(Kocián et al., 2022). Keeping CH_3OH as dry as possible is crucial to prevent the formation of unwanted byproducts. Excess water increases the risk of undesired side reactions with free fatty acids, leading to soap formation(Ahmed Elgharbawy, 2021). Excess methanol is essential to ensure a complete response. Once the catalyst is added, triglycerides react with three moles of methanol. The three carbons attached to hydrogen react with OH- ions, forming glycerin. Simultaneously,

the CH_3 groups react with free fatty acids, producing fatty acid methyl ester(Sahani et al., 2020), as illustrated in Figure 3.4.

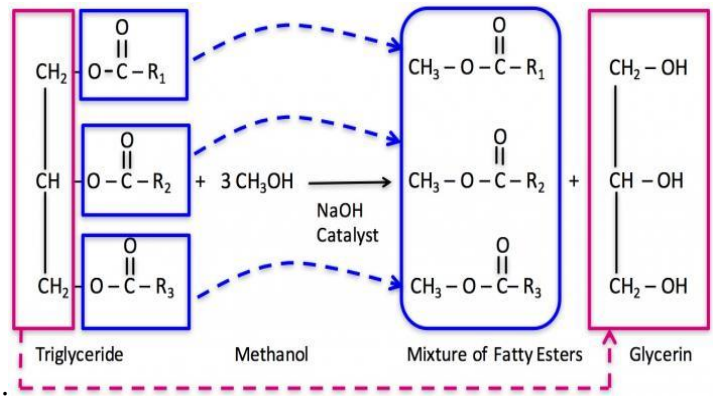

Figure 3. 4 Scheme of the transesterification reaction

3.1.4. Aluminum Oxide Nanoparticles

Aluminum oxide or alumina nanoparticles (Al_2O_3 NPs) exhibit a spherical morphology resembling a white pilates as shown in the Figure 3.5 below. The NPs, which possess high surface area, thermal stability, conductivity, mechanical strength, stiffness, inertness to most acids and alkalis, high adsorption capacity, wear resistance, electrical insulation, and non-toxicity, have potential applications in various industrial fields.

Incorporating Al_2O_3 nanoparticles (NPs) improves diesel engine performance and reduces emissions in diesel-biodiesel blends. Adding the NPs to the diesel–biodiesel blends substantially increases torque, brake power, cylinder pressure, temperature, and heat release rate. The Al_2O_3 NPs utilized in this study were procured from Sigma Aldrich and characterized by particle sizes ranging from 30 to 60 nanometers (nm).

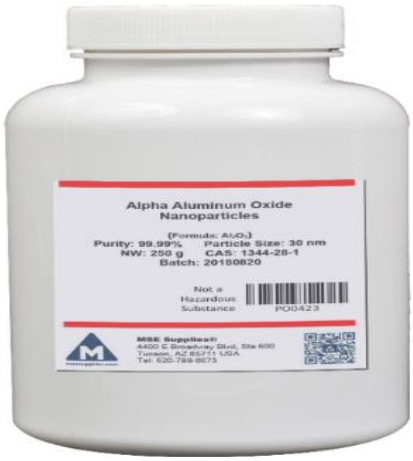

Figure 3. 5 Scheme of the transesterification reaction

3.1.5. Surfactant

The fundamental role of the cationic surfactant Cetyltrimethylammonium bromide (CTAB) is to modify the surface of NPs (Peetla & Labhasetwar, 2009). Its purpose is to create a coating on the NP surface, maintain colloidal stability, and prevent agglomeration (Anna et al., 2020). Introducing the surfactant and using ultrasonication at a specified surfactant-to-nanoparticle catalyst ratio facilitate the dispersion of nanoparticle catalysts(Abitbol et al., 2014). This process is crucial for achieving a homogeneous NP suspension and even distribution in the fuel medium. The surfactant (CMAB) is shown in Figure 3.6 below.

Figure 3. 6 Cetyl-trimethyl-ammonium bromide

3.1.6. Bath Ultra-sonicator

In diesel-biodiesel blends incorporating NPs, ultrasonicators ensure good NP dispersion (Elkelawy et al., 2023). The ultrasonicator is shown in Figure 3.7. The 2-liter capacity water bath sonicator employed for the experiments operated at a maximum temperature of 100°C and a 60-90 kHz frequency.

Figure 3. 7 Bath ultra-Sonicator

3.1.7. Zeta potential meter

When particles or droplets are suspended in a liquid, they create an electrical double layer comprising ions from the liquid. This occurs due to the surface charge carried by the particles, which attracts ions from the surrounding medium. As the particles move within the liquid, the electrical double layer moves along with them along a slipping plane. The electric potential at this slipping plane is referred to as the zeta potential. Zeta potential, typically measured in millivolts, falls within the range of -200mV to +200mV. Researchers classify the degree of stability of a Nano fluid dispersion based on the zeta potential voltage reading as shown in the Figure 3.8 below.

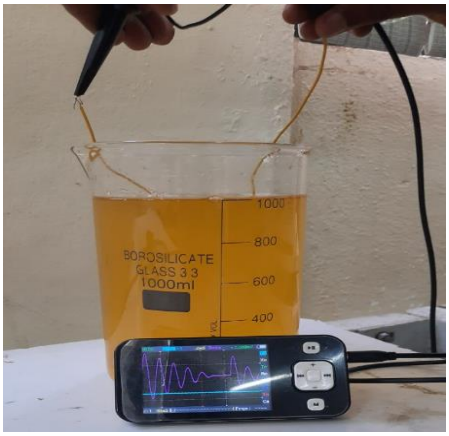

Figure 3. 8 Zeta potential meter

The stability of nanoparticle dispersion at different Zeta potential voltage reading is outlined in the table 3.2 below.

Table 3. 2 Stability of Nano fluids (Verma et al., 2017)

Zeta potential(Mv)	Degree of stability
0	Slight to no stability
±15	Less stability with light settling
±30	Moderate stability
±45	Decent stability with possible settling
±60	Excellent stability with lesser possible of settling

3.1.8. Engine Test Stand

The experiment was conducted in Jima University Institute of Technology and a Gunt engine test stand (Gunt CT110, G.U.N.T. Gerätebau GmbH, Germany), was utilized as shown in Figure 3.9, to investigate the effects of different blends of diesel and biodiesel blend fuels on key performance indicators for small diesel engines. The stand setup comprised three primary

components: the CT 110, the engine mount and control unit; a universal drive and brake unit (dynamometer) acting as the load unit; and a four-stroke diesel engine, the CT 100.22. The test stand performed essential functions, including engine mounting, fuel supply, and recording and displaying measured data. The CT 100.22 engine, employed for performance and emission studies, was an air-cooled, single-cylinder, 4-stroke diesel engine. The engine specification is depicted in Table 3.3. A flywheel with fan blades facilitated engine cooling, and an asynchronous motor within the CT 110 served as the starter motor. The engine had a temperature sensor for measuring exhaust gas temperature, connected to the CT 110 for electrical shutdown and fuel supply. The lower section of the mobile frame accommodated the fuel tanks, an air intake vessel, and a fuel consumption measuring tube. Speed and torque adjustments were made on the test stand and displayed accordingly.

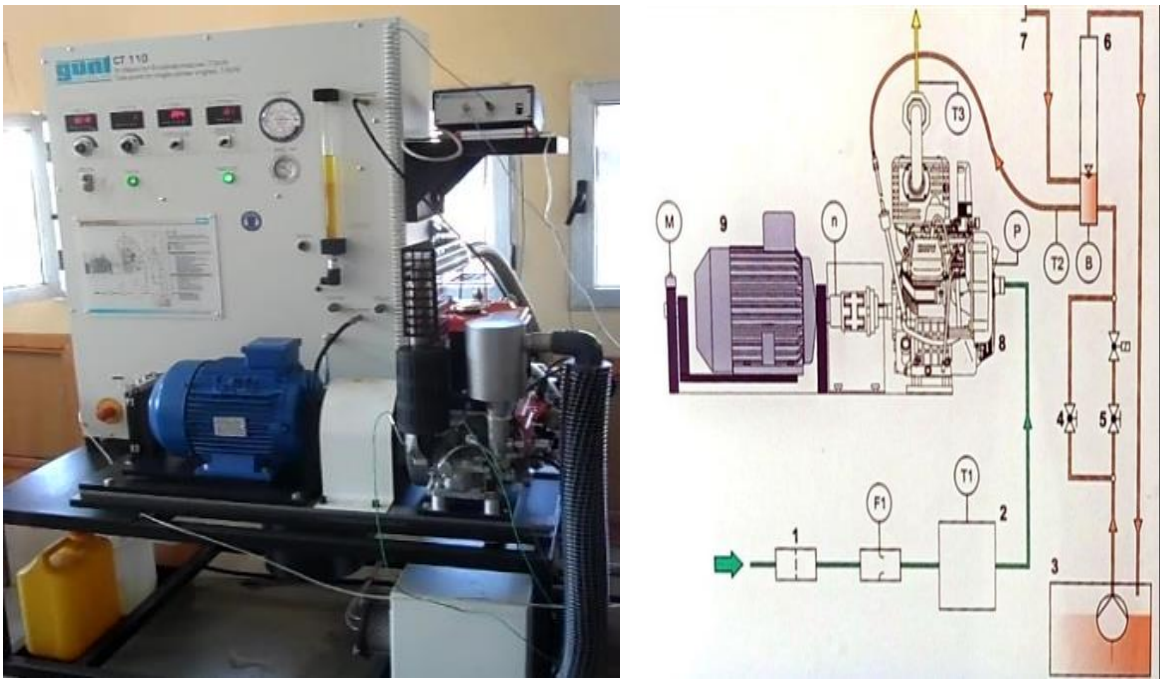

B = fuel consumption M= Torque 1=Air filter

2 = Settling tank 3 = Fuel tank 4 = Drain

F1 = Air flow rate P = intake pressure N = Speed

T1 = Intake temperature 5 = filling valve 6 = Fuel measuring tube

7 = fuel line T2 = fuel TOC T3 = Exhaust T0

Figure 3. 9 Engine test stand

Table 3. 3 Specification of CT 100.22 engine

SN	Parameter	Specification
1	Company	Hatz
2	Type	1B30-2
3	Output power at 3500rpm	5.5kW
4	Compression ratio	22: 1
5	Bore	80 mm
6	Stroke	69 mm
7	Stop solenoid	12V
8	Method of loading	Electrical load
9	Method of cooling	Air-cooled
10	Type of ignition	Compression ignition
11	Rod length	114.5mm
12	Crank length	34.5 mm

3.1.9. Exhaust Gas Analyzer

An additional component for the engine test stand was the exhaust gas analyzer. This device measured exhaust gas composition, including CO, HC, NOx, and O_2, and the engine's excess air factor, lambda (λ). The device's menu display operated, calibrated and showcased the measured data (Figure 3.10).

Figure 3. 10 Exhaust gas analyzer

3.1.10. Soot Tester

Although small and often overlooked, soot particles pose a significant environmental hazard because they contribute to emissions (Tang et al., 2024). Flue gas losses from vehicles and heating systems are a pressing concern, highlighting the need to follow performance indicators to minimize environmental contamination (Nyakuma et al., 2023). Some portable instruments

designed for soot measurement also assess the degree of blackening. These instruments can be conveniently taken to various operational locations for immediate on-site analysis, crucial in diesel engine testing to minimize emissions effectively. As shown in Figure 3.11, this study utilized a soot tester, Model Oakland RT-6000, to measure the soot opacity.

Figure 3. 11 Soot tester

3.1.11. Robin DY-23 -2D Diesel Engines

Due to its innovative features, the Robin DY23-2D diesel engine, was selected for endurance and tribology testing. The engine specification is depicted in Table 3.4. One notable attribute was its newly developed micro-fuel injection pump, which ensured superior combustion efficiency and reduced fuel consumption. The engine featured a light recoil and centrifugal decompressor, facilitating effortless starting. Its advantage was also the auxiliary fuel inlet, which was designed to enable easy starting in cold weather conditions. Furthermore, the engine featured a lightweight design for its reciprocating parts and incorporated a balancer shaft to promote smooth operation and minimize vibration. During the engine endurance test, which involved the operational engine running on baseline diesel and biodiesel-diesel blends, ensuring that both engines operated at identical speeds was imperative. A digital tachometer was employed to achieve this synchronization. This device is shown in Figure 3.12.below.

Figure 3. 12 Robin DY-23 -2D Diesel Engines and Tacho-meter

Table 3. 4 Robin DY23-2D diesel engine specification

SN	Model	DY23-2D
1.	Type	Air-cooled.4-cycle, overhead valve, single vertical cylinder, diesel engine
2.	Bore	70
3.	Stroke	60 mm
4.	Displacement	230 cc
5.	Compression ratio	21
6	Output HP/rpm	4.8/3600
7	Torque kg-m/rpm	1.07/2200
8	Rotation	Counter-clockwise
9	Fuel	Automotive diesel fuel
10	Fuel tank capacity	3.2 litres
11	Combustion system	Direct injection type
12	Starting system	Recoil starter
13	Dry weight	29 kg
14	Dimension L x W x H	329 x 357 x 402 mm

3.1.12. Vibration tester

Elevated machine vibrations are undesirable as they can adversely affect parts, subjecting them to strain and compromising operational safety (Živković et al., 2024). The primary reason for such vibrations is often imbalances, resulting in premature wear of machine components (Linhares et al., 2024).

Vibration testing was conducted using a VIBXPERT II tester from PRUFTECHNIC, Germany, as shown in Figure 3.13, to promptly and reliably identify imbalances and vibrations.

Figure 3. 13 Vibration tester

3.1.13. Engine disassembly and measuring devices

The tools that were used for disassembly and measuring the physical wear of the vital engine components are shown on Figure 3.14 below

Figure 3. 14Assembly and measuring tools

3.2. Methodology

The approach employed in this study primarily involved experimentation, coupled with subsequent statistical analysis of the data, encompassing the following phases:

- Biodiesel Production: This encompassed both the extraction and transesterification processes.
- Physicochemical characterization: Fuel's physicochemical properties were examined.
- Evaluation of biodiesel-diesel blends: Testing of these blends, both with and without the addition of Al_2O_3 NPs, was performed in a Gunt Model CT110 engine test stand equipped with a data logger and exhaust gas analyzer to assess the emission, combustion, and performance characteristics of the fuels.
- Endurance test and tribological analysis: An endurance test and a tribological analysis of physical wear and oil properties were conducted.

Figures 3.15. and, 3.16 Illustrates the pictorial abstract and the overall conceptual framework of the research method respectively.

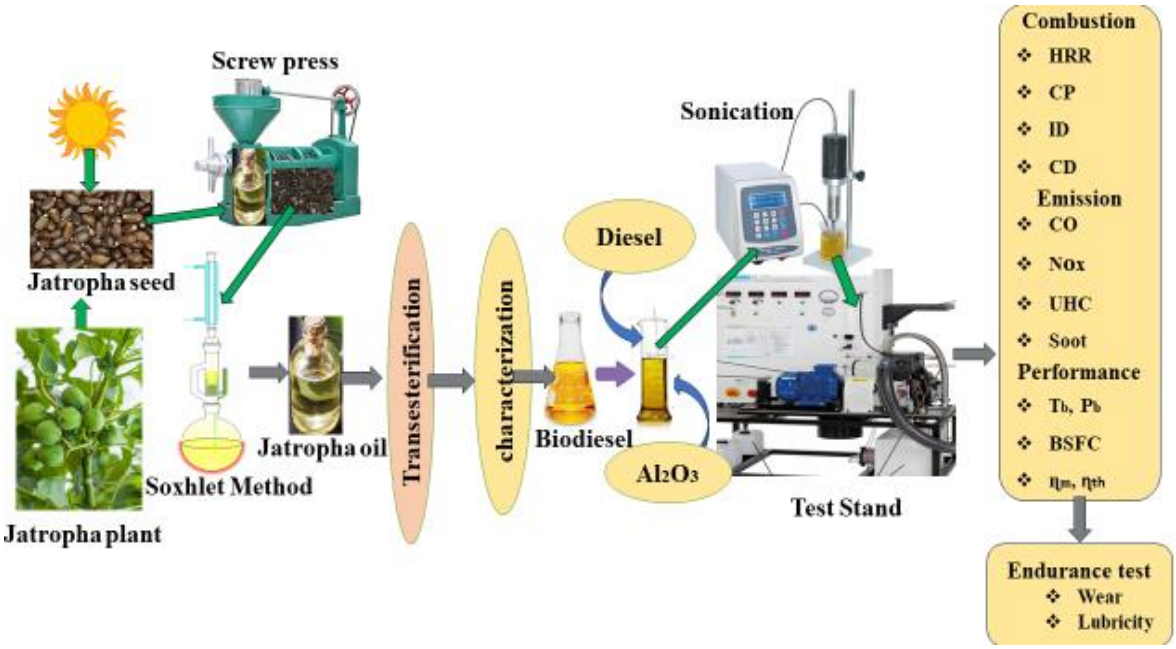

Figure 3. 15 Graphical abstract

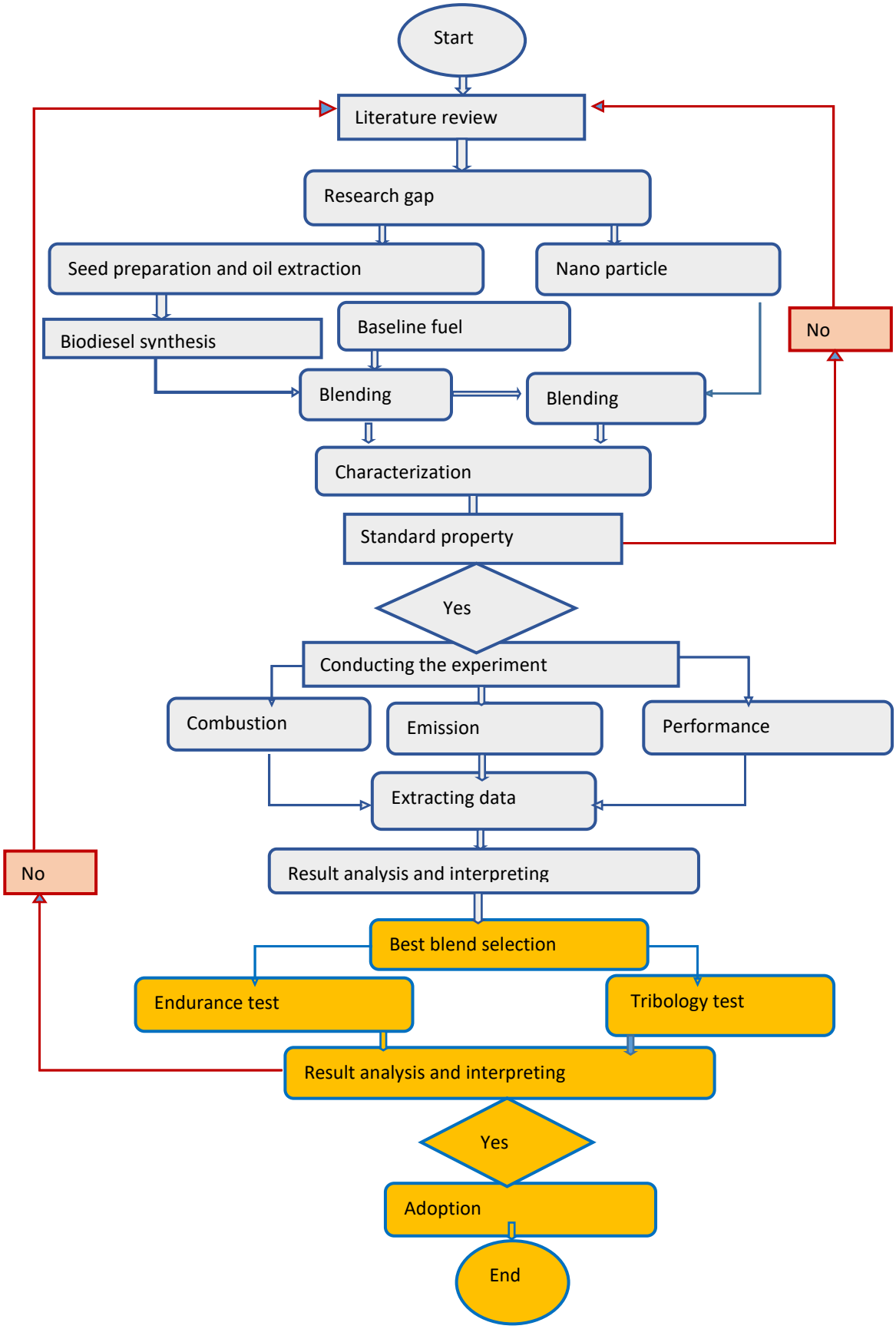

Figure 3. 16 Conceptual framework

3.2.1 Preparation for Biodiesel Production

Prior to biodiesel production, seed preparation and drying are essential to remove impurities and lower the moisture content of the feedstock. This step helps stabilize the transesterification process and minimizes the risk of saponification.

3.2.1.1. Seed Preparation

Seed preparation involves several steps: first, cleaning the samples to remove impurities; then drying them to a constant weight to reduce moisture content below 10%; and finally grinding them to weaken or break the cell walls, making it easier to release the vegetable oil during extraction(Lim et al., 2015).

Figure 3. 17 Dried Jatropha Seeds and weighed

3.2.1.2. Extraction and Determination of Oil Content

Two methods were used for the extraction process. The first method was solvent extraction, in which ten kilograms (kg) of dried Jatropha seeds were crushed and soaked in hexane. The mixture was stirred continuously for 24 hours and then allowed to settle for 24 hours. The filtered oil solution was fractionally distilled using a Rota vapor, and 2,200 mL of crude oil was collected and filtered. This crude oil was tried for esterification by taking a 100 ml sample of the oil to optimize the reaction temperature and time, which was achieved after six trials.

A pressing machine compressed 27 kg of Jatropha seeds to produce 9.18 L of crude oil. The crude oil, which contained some impurities, was mixed with hexane and allowed to settle for 24 hours. The Rota vapor separated the oil from the solvent, and 10.6 L of crude Jatropha oil was collected.

The procedure of this process is indicated further below

3.2.1.3. Oil extraction

- Jatropha seeds were mechanically crushed.
- The crushed seeds were soaked in hexane and stirred for 24 hours, allowed to settle stirred,and stored in plastic containers, as shown in Figure 3.18.

Figure 3. 18 Mechanically crushed and soaked Jatropha seeds with hexane

The settled oil solution was filtered using Whatman filter paper, Grade 41, and poured into glass beakers, as shown in Figure 3.19.

Figure 3. 19 Filtered solution of crude oil and hexane

- The oil solution was filtered again using Whatman filter paper Grade 41 into a round bottom flask, as shown in Figure 3.20.

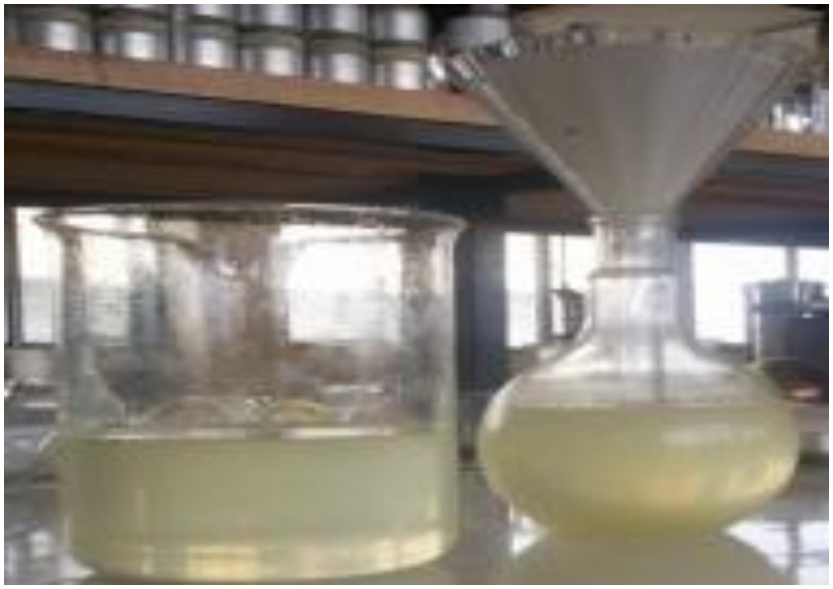

Figure 3. 20 Filtration of crude oil by using Whatman paper Grade 41

- The oil and hexane mixture was separated using a rotary evaporator (Rotavapor) to recover the n-hexane solvent, as illustrated in Figure 3.21.

Figure 3. 21 Hexane recovery

- Water trace removal was done by adding sodium sulfate (Na_2SO_4), after which the oil was allowed to settle for about eight hours and then filtered by Whatman filter paper Grade 41, as shown in Figure 3.22.

Figure 3. 22 Water removal by addition of sodium sulfate

- The crude Jatropha oil was collected into a separating vessel and boiled for one hour at a temperature of 120 °C in an air oven to eliminate water traces during washing, as shown in Figure 3.23.

Figure 3. 23 Water-free crude Jatropha oil

3.2.2. Transesterification of Oil

The effectiveness and outcome of biodiesel production are intricately linked to various pivotal factors, including the reaction temperature, reaction time, catalyst concentration, catalyst-to-oil ratio, and stirring speed. To methodically scrutinize and optimize these variables, an initial step involved creating a design of experiments. In this investigation, a central composite

design was employed, providing a comprehensive and systematic exploration of the esterification process prior to its actual implementation. The independent parameters were established to achieve the maximum yield and quality of biodiesel production, and a reduced number of experimental runs was generated, as depicted in Table 3.5.

Table 3. 5 Design of experiment for transesterification

		Factor 1	Factor 2	Factor 3	Factor 4	Response 1	Response 2
Std	Run	A:Temperature	B:Time	C:Catalyst concentration	D:Catalyst to oil ratio	Biodiesel	Glycerin
		C	min	g/l			
16	1	80	30	25	0.33		
13	2	50	20	25	0.33		
1	3	50	20	15	0.166		
25	4	65	25	20	0.248		
8	5	80	30	25	0.166		
5	6	50	20	25	0.166		
7	7	50	30	25	0.166		
21	8	65	25	10	0.248		
19	9	65	15	20	0.248		
2	10	80	20	15	0.166		
26	11	65	25	20	0.248		
14	12	80	20	25	0.33		
17	13	35	25	20	0.248		
20	14	65	35	20	0.248		
24	15	65	25	20	0.412		
10	16	80	20	15	0.33		
18	17	95	25	20	0.248		
9	18	50	20	15	0.33		
12	19	80	30	15	0.33		
4	20	80	30	15	0.166		
22	21	65	25	30	0.248		
15	22	50	30	25	0.33		
11	23	50	30	15	0.33		
23	24	65	25	20	0.084		
3	25	50	30	15	0.166		
6	26	80	20	25	0.166		
27	27	65	25	20	0.248		

Twenty-seven samples of biodiesel were meticulously prepared based on the experimental design outlined in the table, adhering to the input parameters assigned for the experiment, which spanned from 1 to 27. Moreover, the transesterification process was executed randomly, following the prescribed standard sequence stipulated by the central composite design methodology employed in the experiment. The oil samples used in the experiment are shown in Figure 3.24.

Figure 3. 24 Samples of biodiesel

Transesterification Procedure

- The potassium hydroxide pellets were measured and dissolved in methanol according to the experimental design specified in the table for each sample.
- The solution was thoroughly stirred while heating on a hot plate with a magnetic stirrer, gradually raising the temperature from 40°C to 60°C as shown in Figure 3.25.
- The catalyst was introduced to the oil via reflux, with the temperature carefully monitored based on the experiment's design for each oil sample

Figure 3. 25 Temperature control

- Once the oil completed the designated boiling time as per the experimental design, it was transferred into a separating vessel.
- Glycerin was separated after 24 hours of settling time, as shown in Figure 3.26.

Figure 3. 26 Separation of glycerin

- Glycerin were separated and collected into a glass container by opening the separating vessel's valve
- Any residual oil was collected using a pipette to recover waste oil, as shown in Figure 3.27.

Figure 3. 27 Waste oil recovery

Finally, biodiesel was collected for further processing, as shown in Figure 3.28. This procedure was repeated for all the oil samples as designated by the experimental design.

Figure 3. 28 Pure biodiesel

Washing procedure

- The biodiesel was poured into a decanter and suspended on a stand, as illustrated in Figure 3.29.

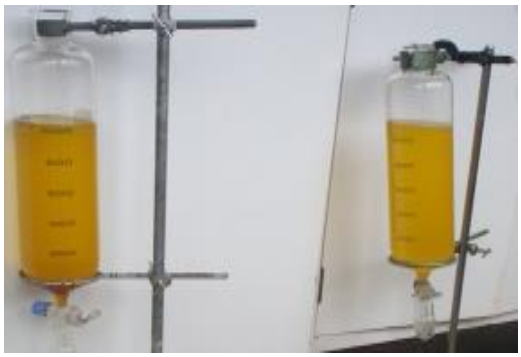

Figure 3. 29 Preparing the biodiesel for washing Figure

- Water was boiled to 50^0C
- Using the spray gun, water was slowly sprayed into the oil, as illustrated in Figure 3.30.

Figure 3. 30 Washing the biodiesel by spray method

- The oil was left to hang in a decanter for 24 hours.
- Soap water and were separated by opening the valve, as shown in Figure 3.31.

Figure 3. 31 Separation of soap and the biodiesel

- This procedure is repeated three times to get the biodiesel free from soap and glycerin.
- The collected biodiesel was heated in a furnace at 120 °C for one hour to remove any residual water left from the washing process through evaporation.
- Finally, Biodiesel was collected as shown in Figure 3.32.

Figure 3. 32 Biodiesel, glycerin, and soap

3.3. Fourier Transform Infrared Spectroscopy

To conclusively ascertain the transesterification of the oil into biodiesel, a Fourier Transform Infrared (FTIR) spectrometer was used to determine the purity of the biodiesel in the wavenumber range of 500 - 4000 cm^{-1}. The formation of biodiesel was monitored by the ester C=O group stretching at a wavenumber of 1742 cm^{-1} (Lamichhane et al., 2020).

3.4. Engine Performance Test

The efficiency of converting stored potential energy into fuel reflects the engine's performance. The performance attributes of a reciprocating engine are predominantly determined by factors such as engine design geometry, operational parameters, and the quality

of the fuel employed. Figure 3.33 illustrates the fundamental engine geometry, and Equations 3-8 further elucidate the parameters **(Khurmi, R. S., & Gupta, J. K., 2005)**

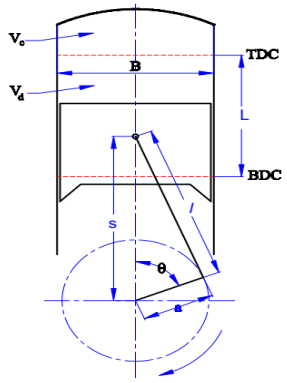

Figure 3. 33 Engine geometry

The following parameters define the basic geometry of a reciprocating engine. The relative location of the piston with respect to the crank axis at any crank angle,S(θ), is given by Eqn. 3:

$$S(\theta) = acos\theta + (l^2 - a^2 sin\theta)^{1/2} \quad \text{(Eqn. 3)}$$

Where "l" is connecting rod length, and "a" is crank radius

The instantaneous surface area of the thermodynamics system, A(θ), is given by Eqn. 4:

$$A(\theta) = A_{ch} + A_p + A_{wall}(\theta) \quad \text{(Eqn. 4)}$$

WhereA_{ch}, A_p andA_{wall} are the area of the cylinder head, the area of the piston head, and the area of the cylinder wall, respectively.

The cylinder volume when the piston is at TDC (S = l + a) is defined as the clearance volume, V_C. The cylinder volume at any crank angle (θ), is given by Eqn.5:

$$V(\theta) = A_{ch} + \frac{\pi d^2}{4}(l + a - s(\theta)) \quad \text{(Eqn.5)}$$

Where$V(\theta)$, A_{ch}, $l, a\ and\ s$ are instantaneous cylinder volume, area of the cylinder head, connecting rod length, and crank radius piston displacement, respectively.

The maximum displacement, or swept volume, $V_d = \frac{\pi B^2}{4}\ l$

Where 'B' and $'l'$ are bore and connecting rod, respectively.

And the compression ratio, $r = \frac{V_c + V_d}{V_d}$ (Eqn. 6)

Where $V_c$and V_d are clearance volume and swept volume, respectively.

Cylinder bore-to-stroke ratio:

$$R_{BS} = \frac{Bore}{stroke\ Length} = \frac{B}{2a} \quad \text{(Eqn.7)}$$

RBS = 0.8 – 1.2 for small and medium-sized engines, decreasing to about 0.5 for large, low-speed compression ignition engines. However, for most engines, B~L (square engine)

Kinematic Rod Ratio

$$R_R = \frac{Connecting\ rod\ length}{Crank\ Radius} = \frac{l}{a} \quad \text{(Eqn.8)}$$

$R_{R=}$ 3-4 for small and medium size engines

$R_{R=}$5-9 for large low-speed compression ignition engines

In engine designs, *l* and *a* are related by *l=2a*

3.4.1. Experimental Setup

In this study, fuel samples were evaluated using the Gunt CT110 test setup, as shown in Figure 3.5. The system consisted of a CT110 engine mount, a dynamometer, and a CT110.22 mono-cylinder, naturally aspirated diesel engine (see Table 3.2). The engine was started by an asynchronous motor and equipped with an exhaust gas temperature sensor. The engine mount served to record and display test data via the dashboard. The mobile frame included the fuel tank, air intake vessel, and fuel flow meter. The performance and emission measurements were conducted at 80% load across engine speeds ranging from 1600 to 3000 rpm. A data acquisition system displayed combustion and performance results on a PC, while an exhaust gas analyzer measured HC, CO, NOx, and soot opacity emissions at each speed.

Engine Performance test procedure

- The fuel system of the test engine was cleaned and flashed by diesel fuel.
- The baseline diesel No 2 operated the test engine until it reached the operating temperature of the engine.
- The test engine was set at 80% load.
- The baseline fuel's combustion, emission, and performance were tested from the speed range 1800 to 3000 rpm at intervals of 100, and data was collected.
- After the baseline diesel fuel, the B5 biodiesel-diesel blend was measured similarly and recorded data.
- Before proceeding to the following sample test, the test engine was operated by diesel fuel until the diesel biodiesel flashed from the fuel system.
- The remaining biodiesel-diesel samples were tested similarly to the procedure above.

3.4.2. Method of Performance Test

The power available at the engine shaft is referred to as brake power, typically derived from the engine's torque measurements when driving against the brake. The brake utilizes

mechanical friction, with a band acting on the flywheel. An electrical dynamometer loads the engine, dissipating power through a resistor network. The engine's torque is quantified through the electrical output of a linear potentiometer, which measures the displacement of a spring that counteracts the force exerted by the dynamometer casing as it rotates with the engine. Consequently, brake power and brake torque are interconnected as described by Equation 19, and were simultaneously recorded on the dashboard and retrieved from the data acquisition system for all fuel sample types (B0, B5, B10, B20, and B40), both with and without Al_2O_3 nano-additives.

Brake power is the sound power output from the engine, available at the crankshaft.

$$P_b = \omega \times T_b \quad \text{(Eqn.9)}$$

Where

ω =angular velocity of crankshaft = $\frac{2\pi N}{60}\ rad/sec$

N = RPM

T_b = Brake torque in N-m

Therefore, $P_b = \frac{2\pi N T_b}{60000}\ [kW]$ (Heywood, 1988)

P_m, the brake mean effective pressure, is the average pressure of the engine cycle. Alternatively, it can be written as: -

$$P_m = \frac{brake\ work\ done/cycle}{Swept\ volume}\ [N/m^2] \quad \text{(Cengel et al., 2019)} \quad \text{(Eqn. 10)}$$

Work done/cycle / = Brake work done/sec × sec/cycle

$$= P_b \times 1000 \times \frac{1}{n/60} \quad \text{(Eqn. 11)}$$

$$Swept\ Volume\ (Vh) = L \times A \times K \quad \text{(Eqn. 12)}$$

Where L = stroke length in, m;

A = $\frac{\pi}{4}B^2$ = Bore area in m^2;

B = Bore diameter in, m;

K = number of cylinders

n = number of cycles per minute =N/2 for four-stroke cycle engine and N for two stroke cycle engine

Therefore, $P_m = \frac{P_b \times 60 \times 1000}{LANK}\ N/m^2$ (Cengel et al., 2019) (Eqn.13)

The friction torque of the test engine was measured from each motor speed when the test engine was operated with the dynamometer acting as a motor. Therefore, the friction torque at each motor RPM is tabulated and the indicated power was calculated from the relation: -

$$P_f = \frac{2\pi N T_f}{60000} kW \qquad \text{(Heywood, 1988)} \qquad \text{(Eqn. 14)}$$

The combustion engine, standard in all its parts, is braked on a test rig at operating temperature and with a fully activated injection pump using a braking device. "Full load" is the stress that an engine's combustion can overcome without a speed reduction. In this case, the most significant possible quantity of fuel is made available. The values determined over the entire speed range under various loads serve as the basis for the progression of torque, output, and specific fuel consumption curves.

Reduced Output Power

The power data obtained should be referenced to standard conditions, which include a geodetic height above sea level, an air pressure of 1013 hPa, and an air temperature of 20°C, as specified by DIN 70200.

$$P_{red} = \sqrt{\frac{T_{amb}+273^0K}{293^0C}} \times \frac{1.013bar}{P_{amb}} \times P \qquad \text{(Eqn. 15)}$$

The formula provides the reduced output power Pred. Here, the ambient temperature in °C must be used for T_{amb} and the current ambient pressure in the bar forP_{abm}.

The reduced output power can be greater than the output power values determined.

Measurement of Specific Fuel Consumption

Fuel consumption over a specified period was measured by volume. The test engine is equipped with a rotameter connected to the fuel tank. During the test, fuel consumption was recorded using a stopwatch. The consumption rate was calculated by dividing the volume of fuel consumed by the time taken to measure that volume.

Total fuel consumption

Total fuel consumption (TFC) is the amount of fuel consumed by the engine over a specific time period. It is defined by Equation 13 and is usually measured in kilograms per hour (kg/h).

$$TFC = \frac{x}{t} \times 3.6 \times S.g[\frac{kg}{h}] \qquad \text{(Stone, 1999)} \qquad \text{(Eqn.16)}$$

Where x =fuel consumed in cc,

t = time in seconds,

S.g = specific gravity of the fuel. Specific fuel consumption is a valuable criterion for evaluating the economic efficiency of power production.

Brake-specific Fuel Consumption

Brake-specific fuel consumption refers to the fuel consumed per unit of time for each unit of brake power output, as described in Equation (17).

$$BSFC = \frac{TFC(mass/time)}{Brake\ power}\ [kg/kWh] \text{ (Stone, 1999)} \quad \text{(Eqn. 17)}$$

Efficiency

The efficiency of internal comustion engines is characterized by the ratio of the work done to the energy supplied to the engine. Brake thermal, mechanical, and volumetric efficiency are the most referenced efficiencies in engine performance tests.

Thermal Efficiency

The efficiency, known as brake thermal efficiency, is the ratio of brake power (Pb) or indicated power (Pi) to the heat energy of the fuel supplied during the same time interval. This efficiency is represented by Equation 18.

$$\eta_{bth} = \frac{P_b}{m_f \times cv} \times 100\% \quad \text{(Eqn.18)}$$

Where m_f = mass flow rate of fuel (kg/s)

C_v = calorific value of fuel in kJ/kg

Equation 16 provides the indicated thermal efficiency of the engine, calculated based on its indicated power.

$$\eta_{ITH} = \frac{P_I}{m_f} \times 100\% \quad \text{(Pulkrabek, 2004)} \quad \text{(Eqn. 19)}$$

Where η_{ITH} indicates thermal efficiency, P_I is the stated power, m_f is the mass flow rate of fuel, and cv is the calorific value of the fuel.

Mechanical Efficiency

Mechanical efficiency depends on the engine's design, piston and rotary speeds, cooling conditions, methods and quality of lubrication, and the accuracy of manufacturing, fitting, and aligning various engine parts when assembling the engine.

$$\eta_m = \frac{Brake\ power}{Indicated\ power} \times 100\% \text{ (Pulkrabek, 2004)} \quad \text{(Eqn.20)}$$

Volumetric Efficiency

The power output of an engine depends on the amount of charge that can be induced into the cylinder. In practice, the engine does not induce a complete cylinder of air on each stroke, and it is convenient to define the volumetric efficiency by Equation 21and its derivatives (Heywood, 1988).

$$\eta_v = \frac{Mass\ of\ air\ consumed/time}{Mass\ of\ air\ that\ fills\ the\ swept\ volum@P_a} \times 100\% \quad \text{(Equ.21)}$$

Where η_v is volumetric efficiency and P_{atm} is air pressure.

The engine has a swept volume of 582 cm^3. Equation 21 gives the mass flow of air required to fill this volume in unit time.

$$m_a = \rho_{a \times 58210^{-6} \frac{N}{2\times 60} = 4.8510^{-6} \rho_a \times N} \quad \text{(Eqn. 22)}$$

The volumetric efficiency is therefore given by Equation 23

$$\eta_v = \frac{m_a N}{4.85\times 10^{-6} \times \rho_a \times N} \quad \text{(Eqn. 23)}$$

Where m_a is the air consumption in kg/s and N is engine rpm.

In practice, since the value of m_a is minimal, it is usual to redefine m_a in terms of kg/h given by Equation 23.

$$\eta_{v=} \frac{Mass\ of\ air/h}{0.0175\times \rho_a \times N} \times 100\% \quad \text{(Eqn.24)}$$

ρ_a is the density of air @27^0C taken from a standard table = 1.162kg/m^3

Combustion

The combustion characteristics within an internal combustion engine are primarily shaped by factors such as fuel quality, engine geometry, combustion chamber design, and operating parameters. These elements collectively influence crucial aspects, such as engine cylinder pressure, heat release rate, and emission outputs. The engine combustion analysis determined the net heat release rate by integrating the pressure crank angle diagram derived from the engine dynamometer's data acquisition system. This integration was performed using the equation provided below. Subsequently, the heat release rate was plotted against the crank angle, and the results of different fuel samples were compared.

$$HRR = \frac{\gamma}{\gamma - 1} P \frac{dv}{d\theta} + \frac{1}{\gamma - 1} V \frac{dp}{d\theta} \quad \text{(Eriksson \& Sivertsson, 2015)} \quad \text{(Eqn. 25)}$$

Where γ is the ratio of specific heat capacities, **P** is in-cylinder pressure, **V** is cylinder volume, and $\boldsymbol{\theta}$ is the crank angle.

The heat release diagram provides information about the ignition delay and combustion duration. Combustion initiates when the heat release rate shifts to a positive value, typically near the end of the compression stroke. In contrast, combustion completion is characterized by the heat release rate decreasing to zero during the expansion stroke.

3.5. Emission Test

Fuel samples of biodiesel-diesel blends, both with and without Al_2O_3 nanoparticles (NPs), were assessed for their emission characteristics using the Gunt model CT110 engine dynamometer. An exhaust gas analyzer quantified the emission species in the exhaust. The tested fuels included B0, B5, B10, B20, and B40, each evaluated with and without a 100 ppm dose of Al_2O_3 NPs, under an 80% load and within a speed range of 1600 to 3000 rpm. Emissions measured included carbon monoxide (CO), unburned hydrocarbons (UHC), and nitrogen oxides (NOx). Additionally, the soot opacity of the engine exhaust was determined using a Blue-MS 101 opacity meter. A comparative evaluation of the emissions were followed.

3.6. Uncertainty Analysis

The highest mean percentage uncertainty ($\bar{U}max$) in engine exhaust emissions and combustion performance measurements is attributed to the accuracy of the measuring instruments, as presented in Table 3.6.

Table 3. 6 Accuracy and uncertainties

Measured parameters	Instrument	Measuring range	Accuracy%	$\bar{U}_{max}$ (%)
NO_x	Kane AUTO plus gas analyzer	0–5000 ppm	± 12 PPM	17.5
CO	CT159.02 Exhaust gas analyzer	0–10 % vol	± 0.06% Vol.	8.7
HC		0–2500 ppm	± 3 ppm	6.2
Speed	CT 100.10	0–5000 rpm	±12rpm	0.51
BrakePower	CT 100.10		±0.1	2.87

3.7. Endurance Test

Following combustion, emission and performance assessments of biodiesel-diesel blends, both with and without Al_2O_3 NPs, were conducted using the Gunt model CT110-Engine test stand. The optimal blend, B20 with a 100 ppm NP dose, was selected for the endurance test to assess its compatibility with the engine hardware and lubricating oil characteristics. Two identical Robin DY23-2D single-cylinder engines were chosen for a comprehensive comparison due to their specific features.

For comparative analysis, the study utilized diesel No. 2 and a biodiesel-diesel blend (B20) containing 100 ppm Al2O3 nanoparticles. The engines underwent a rigorous 100-hour operation, following the Indian Standard endurance test (IS: 10000 (Part IX)-1980, Section

II). During the testing period, close monitoring was implemented to identify and promptly address maintenance requirements.

Endurance Test Procedure

The endurance test was conducted according to the procedure outlined in IS: 10000 (Part IX)-1980, Section II.

- The test was conducted for a total running time of 100 hours, with each running period lasting 10 hours.
- Each running period comprises five cycles lasting two hours, following the sequence below: a) 50 minutes at 75% of full load and maximum speed. b) 45 minutes at full load corresponding to the maximum torque. c) 5 minutes at idle. d) 20 minutes at full load and maximum speed.
- Utilize the recommended lubricating oil throughout the test.
- The engine speed readings must not fall by more than 5% of the initial reading for more than two consecutive readings at any point during the test.
- Before commencing the next cycle, the engine must reach a temperature of 5^0C above room temperature.
- A maximum of two interruptions is allowed to address any faults or maladjustments.
- If the engine requires minor attention and a stoppage is needed, the running time will not be counted.
- In a significant breakdown, the entire test must be repeated.
- Conduct periodic checks on the oil, ensuring it conforms to the manufacturer's specification

3.8. Vibration Measurement

Vibration tests were conducted to assess the engines' reliability using the Expert II Vibration tester on both engines. Vibration measurements were taken at three points using a tri-axis accelerometer, as indicated on the engine block, as shown in Figure 3.34.

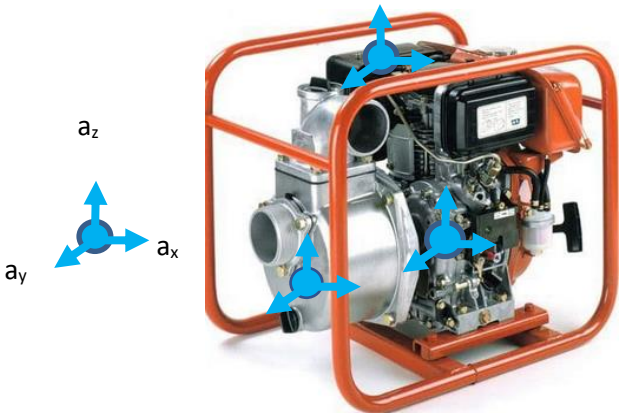

Figure 3. 34 Points of vibration measurement

Vibration data for the engine were evaluated as root mean square (RMS) values of the test engine on the x (longitudinal), y (lateral), and z (vertical) axes.

$$a_w = \sqrt{\frac{1}{T}\int_0^T a_W^2(t)dt} \qquad \text{(Eqn. 26)}$$

Where a_w (m/s^2) represents the weighted acceleration and T represents measurement time.

A combination of vertical (a_x), lateral (a_y), and longitudinal (a_z) weighted accelerations were calculated for evaluation of the resultant vibration acceleration using Equation

$$a_{total} = \sqrt{a_x^2 + a_y^2 + a_z^2} \qquad \text{(Eqn. 27)}$$

The vibration measurements were carried out without loading the engine to ensure minimal vibrations. During the experiments, the engines were operated from 1800 to 3000 rpm, and the analysis aimed to compare their susceptibility to failure. Additionally, the lubricants' physio-chemical properties were systematically measured at intervals of 25, 50, 75, and 100 operating hours.

The net resultant vibration of the two test engines was compared with the vibration acceleration limit of the severity standard.

As part of the comprehensive evaluation, the two identical engines were disassembled to examine carbon deposits at vital engine components, allowing for a detailed comparison. Finally, physical wear measurements of essential engine components were taken and subjected to a comparative analysis. This methodical approach comprehensively understood the engines' performance and durability under the specified experimental conditions.

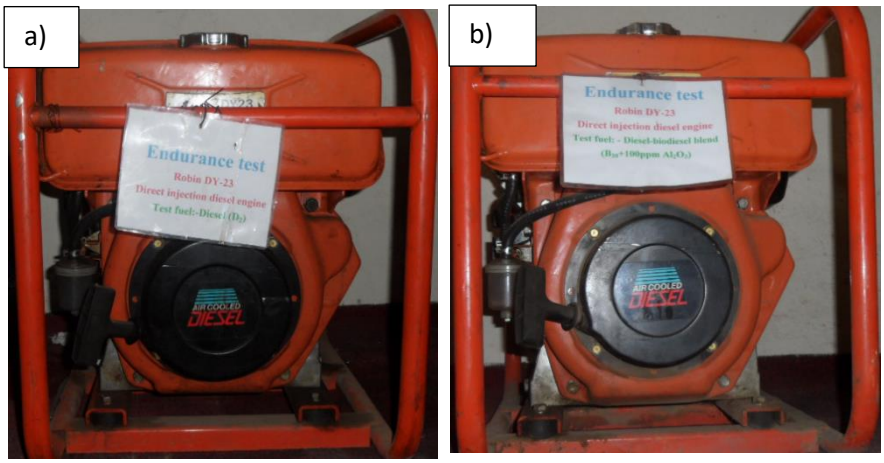

Figure 3. 35 a) diesel b) B20+Al_20_3 100ppm fueled

Soot Particle Size Measurement Procedure

The morphological characteristics of soot collected from the test engines were analyzed using a Transmission Electron Microscope (FEI, Tecnai G2 12 Twin TEM 120 kV) to determine the carbonaceous structure and particulate size distribution. This TEM can perform high-contrast cryogenic microscopy. The particulate-laden quartz filters were cut into pieces, and then these particulates were suspended in benzene. Soot particles detached from the filter paper and got transferred into benzene. The benzene drops with particulates were then deposited on the TEM copper grids (300 mesh), and the solvent (benzene) was allowed to evaporate, leaving the particulates deposited on the grid for TEM analysis (Aher et al., 2017).

3.9. Engine Disassembly and Measurement of Carbon Deposited

After the engines are disassembled, the carbon deposits on main engine components, such as the piston head, cylinder head, injector tips, piston side, exhaust and intake ports, and intake and exhaust valves, were measured and quantified for both engines operating on diesel and biodiesel-diesel blends with Al_2O_3 nanoparticles. The amount of carbon deposited on these components was measured in grams using the following procedure.

- After disassembling the engine, the components were dried, and their weight was measured using a digital gram measuring device.
- After the measured weight was recorded, the components were carefully cleaned to remove the carbon deposits from the components.
- They were again weighed,
- The difference in weight was taken as the amount of carbon deposits on the components.

3.9.1. Physical Wear Measurements

Prolonged engine operation leads to wear of various moving parts(Wong & Tung, 2017). The two engines were operated under identical conditions with similar loading cycles. The only difference was the use of different fuels, which allowed for a direct comparison of each fuel's effect on engine hardware life. The dimensions of the main working parts were checked and recorded according to IS: 10000 (Part V) (Preparation for Tests and Measurements for Wear). The wear of critical components was documented in a preformatted document prepared in accordance with Indian Standards (IS) and compared with the manufacturer's declarations. Prior to measurement, all engine parts were thoroughly cleaned to remove dirt, oil, and carbon deposits. The working area was also kept clean and organized to facilitate efficient performance. Measurements were conducted in the ASTU workshop using a logical, step-by-step procedure aligned with ISO standards to ensure accurate wear assessment.

The main engine parts included in comparison wear measurements are:

- Piston
- piston rings
- Cylinder bore
- Connecting rod
- Connecting Rod (Gudgeon Pin, Pin Bore, and Small End Bush)
- Inlet and exhaust valve
- Valve spring and
- Rocker arm.

3.9.2. Measurement of the Cylinder Bore

The cylinder and crankcase of DY23 engines are made from a single-piece aluminum die-casting. The cylinder liner, crafted from special cast iron, is integrated into the aluminum casting. The following outlines the procedure and equipment used for measuring the cylinder bore.

To measure the engine's cylinder bore, a bore gauge and micrometer were employed. An extension rod, measuring between 60-75 mm, was selected for obtaining readings. The gauge was calibrated to zero by measuring across the indicator with an outside micrometer, set to the specified bore size of 70 mm, and adjusting the dial face until the needle aligned with zero. The gauge was then inserted into the bore at depths of 1, 2, and 3 mm in both the X and Y directions, following the standard measurement procedure, as illustrated in Figure 30. The gauge was rocked back and forth until the lowest reading was obtained, which occurred when

the gauge was square to the bore and the indicator needle reversed direction. The measurement points are indicated in Figure 3.36.

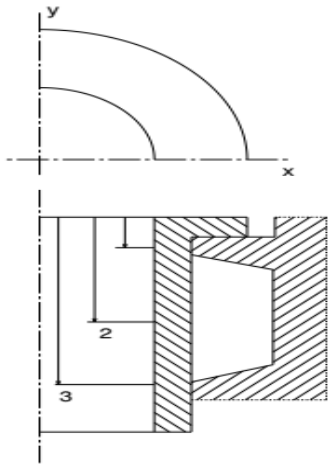

Figure 3. 36 Measurement of cylinder bore (IS standard)

3.9.3. Measurement of Connecting Rod Bearing Bore

The connecting rod is constructed from a forged aluminum alloy, designed to withstand high combustion pressures and tensions during heavy loads and high-speed operation. Kelmet bearings are used as large end bearings, while the connecting rod material itself functions as a small end bearing. The following describes the measurement procedure for the connecting rod and the equipment used. To measure the connecting rod bearing bore, a telescopic gauge and micrometer were employed. The measurement process began by selecting the appropriate size of the telescopic gauge, which is a "transfer-type" measuring instrument that is not calibrated. It records a distance that is then transferred to a micrometer. For the measurement, a 30-35 mm telescopic gauge was inserted into the two ends of the connecting rod, labeled "C" and "D." Measurements were taken at the center position "l" and at points "m" and "n," which are 40° apart, as illustrated in Figure 3.37, following the IS standard for connecting rod bearing bore measurements. After aligning the gauge handle with the centerline of the bearing bore, the handle was locked, and the gauge was removed to measure and record the setting with a micrometer. The measurement points are as indicated in the figure 3.37 below.

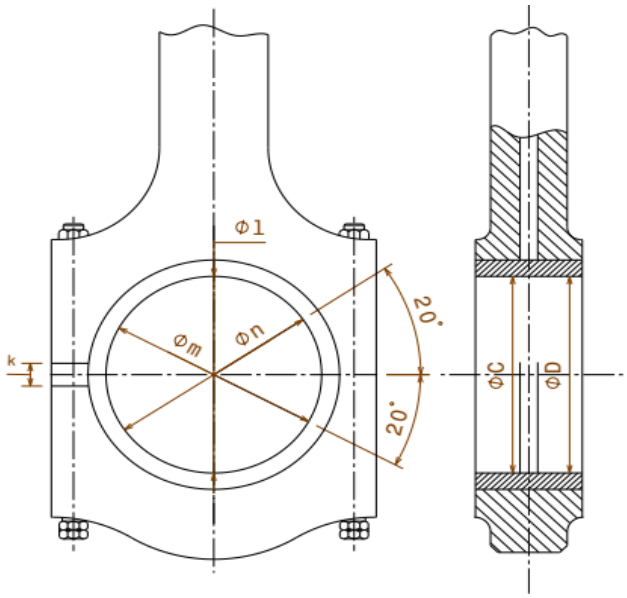

Figure 3. 37 Measurement of connecting rod bearing (IS standard)

3.9.4. Measurement of the Gudgeon Pin, Pin Bore, and Small End Bushing

The steps followed were consistent with those outlined in Section 3.9.3. However, the positions and measurement locations vary, as illustrated in Figure 3.38. Measurements were taken on the gudgeon pin bore or the piston at point's a1 and a2 in both the "X" and "Y" directions, and on the gudgeon pin or piston pin diameter at point's b1, b2, and b3 in the same directions. Additionally, measurements were made on the small end bush at points C1 and C2 in the "X" and "Y" directions. The telescopic gauge and micrometer used had ranges of 15 to 20 (units?) and 0 to 25 millimeters, respectively.

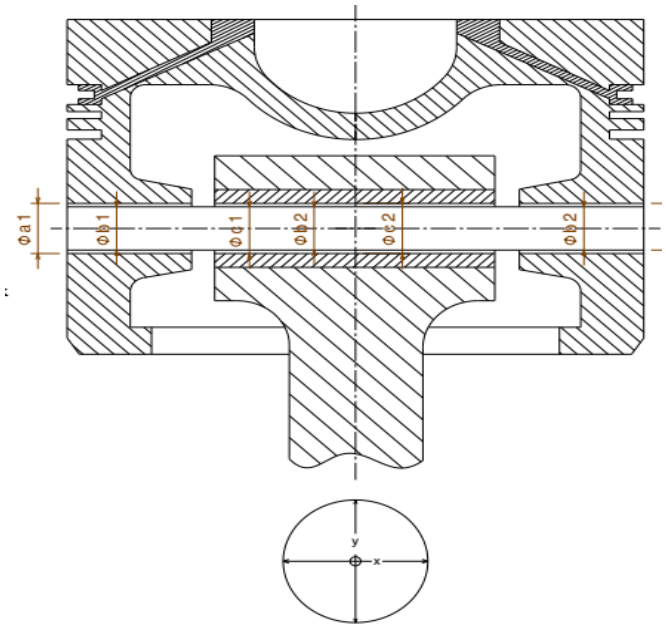

Figure 3.38 Connecting rod Gudgeon pin, pin bore, and small end bush (IS standard)

3.9.5. Measurement of Piston Wear

The piston is constructed from aluminum alloy casting and features three grooves for piston rings. At the top of the piston, a combustion chamber is designed for the mixing and ignition of injected fuel and air. The piston profile is optimized to reduce noise during operation. Details regarding the measurement procedures for the piston and the measuring equipment are provided.

To assess piston wear, measurements were taken at points a, b, and c in both the X and Y directions, as illustrated in Figure 3.39. A precise micrometer with a range of 50 to 75 millimeters was employed for these measurements. The dimensions were recorded by positioning and rotating the thimble of the micrometer until the two faces made contact with the piston at the specified points.

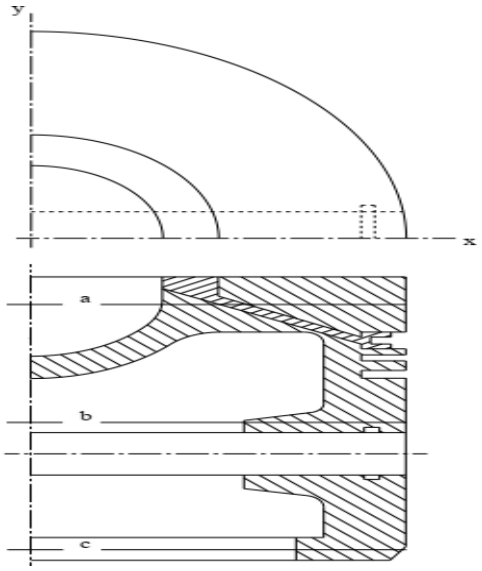

Figure 3. 39 Measurement of piston (IS standard)

3.9.6. Measurement of Piston Ring Wear

The piston rings are crafted from a special type of cast iron. The top ring features a barrel face profile, while the second ring has a tapered design with an undercut. The oil ring combines cutter rings and an expander, which effectively seals gas and minimizes oil consumption. The measurement procedure for the piston and the measuring equipment is outlined. A micrometer, feeler gauge, and Vernier caliper were utilized to assess piston ring wear. Four types of measurements were conducted on the piston rings, as illustrated in Figure 3.40. The first two measurements, radial wall thickness (a1) and axial width (h1), were taken using a micrometer with a 0-25 mm range. The remaining two measurements, closed gap (s1) and piston ring end gap, were obtained using a Vernier caliper and feeler gauge, respectively. To

read a Vernier dial caliper, add the value on the blade to the value on the dial. For the feeler gauge, measure the gap by adjusting the thickness of the steel pieces until the gauge of the correct size fits snugly into the ring gap.

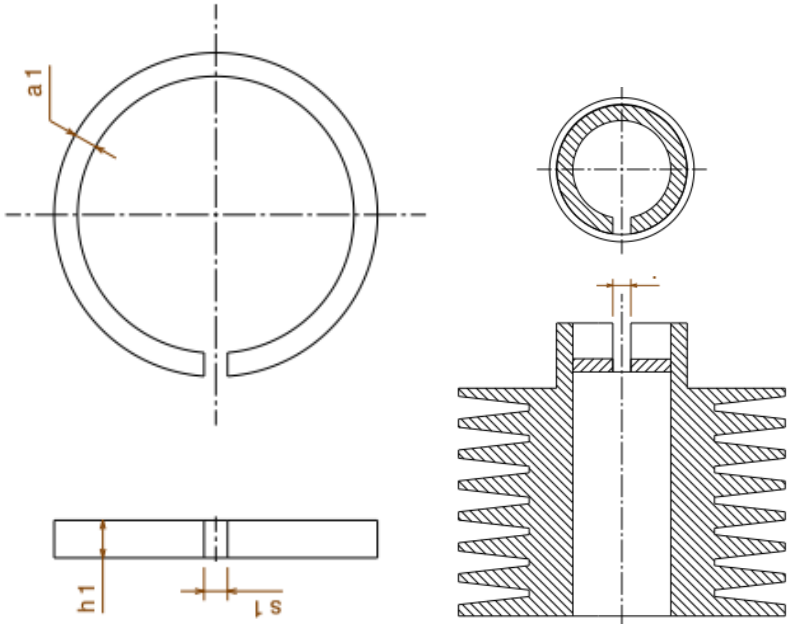

Figure 3. 40 Measurement of piston rings (IS standard)

3.9.7. Measurement of Inlet and Exhaust Valve

The valves are constructed from a forged heat-resistant alloy. To enhance durability, Stellite is fused to the head of the exhaust valve. The procedure for measuring the valves and the measuring equipment is outlined. A micrometer and a vernier caliper were utilized for the measurements. The steps for using this measuring equipment are consistent with the procedure described in the piston wear section. The valve length was measured using a vernier caliper with a range of less than 200 mm, while the stem diameter was measured with a micrometer ranging from 0 to 25 mm. The measuring positions are illustrated in Figure 3.41 below.

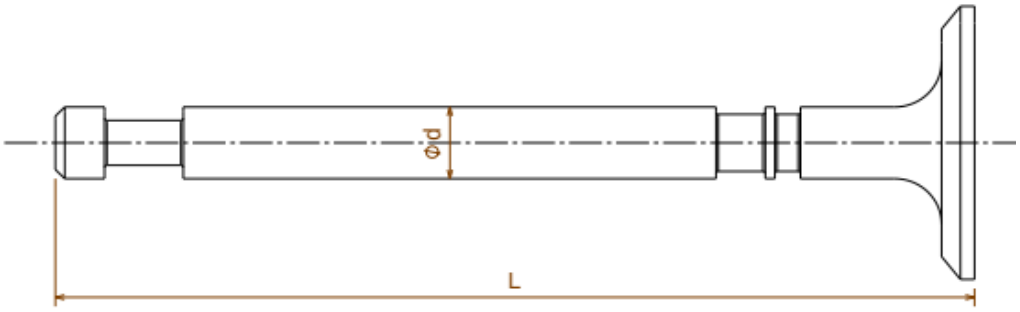

Figure 3. 41 Measurement of piston rings (IS standard)

3.9.8. Measurement of the Rocker Arm

Rocker arms are constructed from forged steel and are entirely sintered. Each rocker arm features a screw at its end for adjusting valve clearance. They are lubricated by oil mist from the crankcase's breathing air. To measure the rocker arms, a telescope gauge and a micrometer were utilized. The measurement points are illustrated in Figure 3.42 below. The steps for using the measuring equipment follow the same procedure outlined in the section on piston wear.

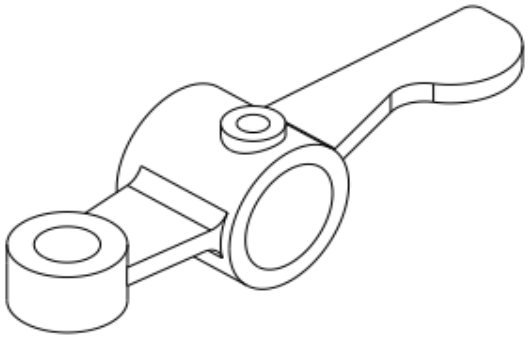

Figure 3. 42 Measurement of rocker arm (IS standard)

CHAPTER FOUR

RESULT AND DISCUSSION

4.1. Introduction

This study encompassed a range of activities, starting from the extraction of oil from Jatropha Physio-chemical properties of biodiesel. Moreover, it included testing the performance and emission characteristics of biodiesel-diesel blends. Specifically, the study examined blends containing 100ppm of Al_2O_3 nano additive alongside the Table 4.1 dose without nano additive in a diesel engine. The blend showing optimal results, labeled as B20, underwent an endurance test using two identical Robin DY-23D mono cylinder diesel engines. One engine operated on the baseline diesel no-2, while the other utilized the B20 biodiesel-diesel blend with 100ppm aluminum oxide nano additive. The study primarily focused on investigating the impact of the Al2O3 nano additive on engine combustion, emissions, performance, endurance, and its tribological effect on engine hardware.

Recent research has suggested that nanoparticles could offer a novel approach to improve engine efficiency when used as diesel additives. Prior investigations, which focused on a single diesel engine and a diesel-biodiesel blend derived from Jatropha carcus methyl ester, noted a gap in research in this domain. Consequently, it is essential to assess Jatropha diesel-biodiesel blends containing 100ppm Al_2O_3 nanoparticles to address emission reduction and enhance engine performance.

The goals of this investigation encompass reducing emissions, employing eco-friendly biodiesel-diesel blends sourced from Jatropha oil, and establishing the best operational parameters for diesel engines. The ensuing sections of this study will explore the outcomes obtained from all the conducted experiments.

4.2. Oil Extraction from Jatropha Carcus Seeds

In this research project, Jatropha curcas seeds sourced from local farmers were utilized as the primary material for biodiesel synthesis. The extraction process involved a pilot test solvent method to ascertain the oil content of the seeds. Initially, the seeds were crushed and soaked for a duration of forty-eight hours, with frequent stirring. Subsequently, the solution was left to settle for an additional twenty-four hours, followed by filtration using filter paper to separate it from the residue. The mixture of oil and solvent was then separated using a Rota-Vapor. For large-scale oil production, a mechanical screw press in conjunction with the Soxhelt method was employed. The oil extraction process yielded 22% (v/w) using the solvent method and

34.5% (v/w) with a combination of the screw press and Soxhelt method. The yield of the original oil was calculated using the equation provided below.

$$(\%yield) = \frac{Volume\ of\ oil\ in\ litre\ (l)}{Mass\ of\ seed\ (kg)} \times 100\% \quad \text{(Equ.28)}$$

4.3. Determination of percentage of free fatty acid

Prior to advancing to the transesterification phase, it is essential to assess the percentage of free fatty acids to ascertain if esterification treatment, involving acid treatment, is necessary. This step is crucial because oils with free fatty acid levels exceeding 1% necessitate esterification to prevent saponification, which can decrease biodiesel yield. The relationship between the percentage of free fatty acids and the acid value of the oil is determined by the equations 28 and 29 provided below.

$$Acid\ Value\ \frac{NaOH\ solution\ in(ml)\times N\times 40}{Mass\ of\ the\ oil} \times 100\% \quad \text{(Eqn. 29)}$$

Where=Normality of *NaOH* (i.e., 0.5)

$$\%FFA = \frac{Acid\ number}{2} \quad \text{(Eqn.30)}$$

The parent oil initially had an acid value of 4.6 mg KOH/g, posing a risk of saponification. To reduce this, esterification was carried out using sulfuric acid (H_2SO_4) and analytical-grade methanol at a 6:1 alcohol-to-oil molar ratio, with 1% sulfuric acid by volume. The reaction was conducted on a hotplate at 65 °C and 600 rpm for one hour. As a result, the acid value

4.4. Transesterification and optimization of biodiesel yield

In order to achieve an optimized biodiesel yield, the Central Composite design of experiments, implemented through the Response Surface Method software package, was utilized. This approach generated twenty-seven experimental runs. Consequently, twenty-seven oil samples were prepared as shown in the Figure 4.1 and the experiment was conducted as to the input parameters set on the Table 4.1.

Figure 4. 1 Oil samples

In the transesterification process, the methyl ester and glycerin were separated using a decanter after a settling period of twenty-four hours. The methyl ester then underwent three wash cycles to remove any residual soap. To eliminate moisture from the biodiesel, a furnace set to 120°C was employed. The yields of both biodiesel and glycerin were measured, and the optimal operating conditions that produced the highest biodiesel yield were identified, as shown in Table 4.1.

Table4. 1 Optimization of the esterification reaction

		Factor 1	Factor 2	Factor 3	Factor 4	Response 1	Response 2
Std	Run	A:Temperature (^{0}c)	B:Time (min)	C:Catalicst Concentration(g/l)	D:Catalyist to oil ratio	Biodiesel (%)	Glycerine (%)
16	1	80	30	25	0.33	71	7
13	2	50	20	25	0.33	64	5.5
1	3	50	20	15	0.166	46	4
25	4	65	25	20	0.248	98	17
8	5	80	30	25	0.166	75	8
5	6	50	20	25	0.166	55	5
7	7	50	30	25	0.166	66	6
21	8	65	25	10	0.248	67	5
19	9	65	15	20	0.248	70	8
2	10	80	20	15	0.166	64	5
26	11	65	25	20	0.248	98	17
14	12	80	20	25	0.33	70	6
17	13	35	25	20	0.248	10	0
20	14	65	35	20	0.248	84	8
24	15	65	25	20	0.412	78.8	9
10	16	80	20	15	0.33	62	6
18	17	95	25	20	0.248	22	0
9	18	50	20	15	0.33	57	5
12	19	80	30	15	0.33	67	5
4	20	80	30	15	0.166	70	6
22	21	65	25	30	0.248	87	8
15	22	50	30	25	0.33	65	5
11	23	50	30	15	0.33	60	4
23	24	65	25	20	0.084	88	9
3	25	50	30	15	0.166	63	5
6	26	80	20	25	0.166	70	8
27	27	65	25	20	0.248	98	17

The results indicated that the highest biodiesel yield was achieved under the conditions illustrated in Figure 4.2 below: a reaction temperature of 65°C, a reaction time of 25 minutes, a catalyst concentration of 20 g/l, a parent oil to catalyst ratio of 1:4, and a stirring speed of 600 rpm. The yield of Jatropha methyl ester was 97.89% by volume, while the yield of glycine was 17.75% by volume of the crude oil transesterified during the transesterification process.

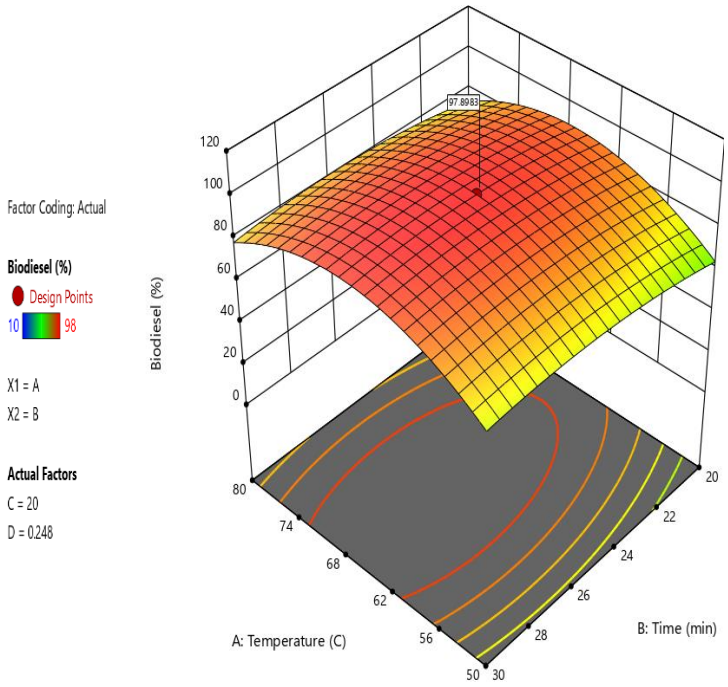

Figure 4. 2 Maximum biodiesel yield based on temperature and time

The multiple interaction plot of the input parameters are shown on the Figure 4.3 below.

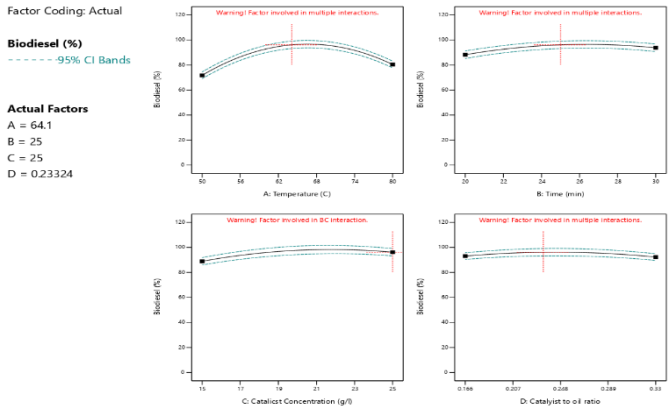

Figure 4. 3 Multiple interaction plot of the input parameters

Finally, a Fourier Transform Infrared (FTIR) test was conducted to confirm the presence of methyl ester in the oil after transesterification, as shown in Figure 4.4. The FTIR results indicated that the conversion of the parent oil to methyl ester was monitored by the C=O ester stretch at a wavelength of 1742 cm^{-1}. This strong ester peak confirms the formation of biodiesel(Lamichhane et al., 2020).

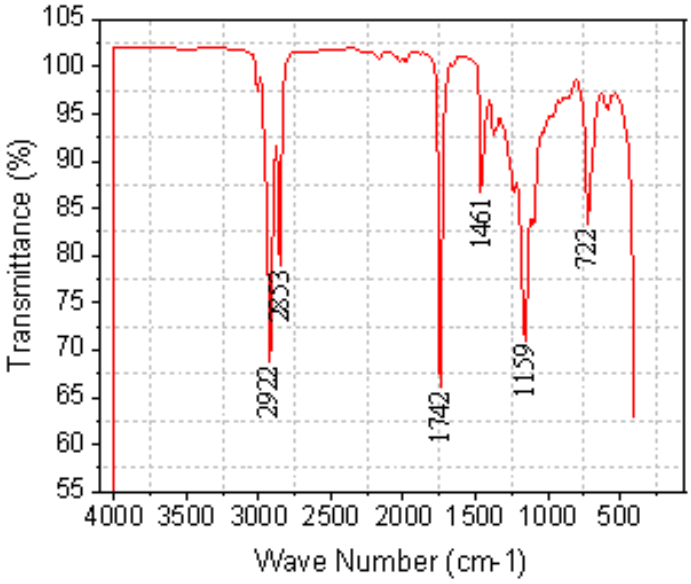

Figure 4. 4 Fourier Transform infrared test (FTIR)

4.5. Fatty Acid Profile Jatropha Carcus Biodiesel

The fatty acid analysis of Jatropha oil methyl ester was performed using a Varian 3800 model gas chromatograph (GC) with a flame ionization detector (FID). Additionally, a Varian CP-3800 GC, equipped with a DB-5 column and an FID detector, was utilized for this analysis, as detailed in Table 4.2. The free fatty acid composition of Jatropha curcas oil was also assessed using a Varian 450 GC, as indicated in the table below.

Table4. 2 Fatty acid profile of Jatropha Carcus

Oil seeds	Palmitic acid (C16:0)	Stearic acid (C18:0)	Oleic acid (C18:1)	Linoleic acid (C18:2)	Linolenic acid (C18:3)
Jatropha oil	6.1	3.9	52.8	33.6	3.3

4.6. Characterization of fuel samples

After the transesterification of the biodiesel was completed, it was blended with No. 2 diesel in the ratios of B0, B5, B10, B20, and B40. The physicochemical properties of these blends were characterized and measured according to the ASTM D6751-07B test standard, as shown in Table 4.3. All oil samples met the criteria for biodiesel, as their physicochemical properties fell within the limits set by the ASTM standards for diesel engine fuel. The cetane number or index was calculated using the ASTM D 796 standard equation.

Cetane Index = 454.74 -1641.416D + 774.74D2 – 0.554B +97.803(Kanyane et al.)2 (Eqn. 31)

Where, D = Density at 15^0C, g/ml

The physio-chemical properties of the diesel fuel (B0) and biodiesel diesel blends are shown in the table 4.3 shown below.

Table4. 3 Physiochemical properties of biodiesel blends

NO	PROPERTY	TESTS ASTM	LIMIT 6751-07B	TEST RESULT				
				B40	B20	B1O	B5	B0
1.	Density@15^{0}C, kg/m^3	D1298	Report	869	855.6	861.6	849.6	847.4
2.	Density@20^{0}C, kg/m^3	D1298	Report	855	852.2	858.2	846.2	844
3	Flashpoint (PMCC)	D93	100M	78.8	76.8	74.8	72.8	71.8
4.	Cu-Strip-corrosion	D130	Max3	1a	1a	1a	1a	1a
5.	Cloud point, ^{0}C	D2500	Report	0	- 1	-1	- 1	0
6.	Pour point, ^{0}C	D97	Repot	< - 8	< - 8	< - 8	< - 8	< - 8
7.	viscosity (mm^2/s)	D445	1.9__ 6	3.828	3.5116	3.2865	3.2013	3.1637
8.	Cetain Index	D976	Min47.0	51.34	51.127	47.56	50.46	52.905
9	ASTM colour	D1500	Max =3	1<x<1.5	1<x<1.5	1<x<1.5	1<x<1.5	1
10	Water& segment, %V	D2709	Max0.03	<0.025	<0.025	<0.025	<0.025	<0.025
11	Acidity, mg KOH/g	D974	0.5	0.113	0.0534	0.0327	0.02136	0.0106
12	Ash content, mass%	D482	Max0.01	0.006	0.0006	0.0006	0.0006	0.0001
13	Calorific value, MJ/kg	__	Report	41.99	44.45	44.77	45.21	46.51

4.7. Optimization of Nanoparticle Dose for Engine Performance (pilot test)

Prior to conducting full emission and performance tests on diesel-biodiesel blends enhanced with aluminium oxide nanoparticles, a pilot study was carried out to determine the optimal nanoparticle dose. The goal was to identify the concentration that minimized emissions of carbon monoxide (CO), unburned hydrocarbons (HC), and nitrogen oxides (NOx), which are key indicators of efficient combustion and for engine performance. The diesel–biodiesel blends tested included B5, B10, B20, and B40, with pure diesel (B0) serving as the reference fuel.

A full factorial design of experiment was employed as, involving two factors at four levels each as shown in the table 4.4 below, and the results were analyzed using ANOVA statistical methods to identify the most effective combination. Literature review indicated that most studies utilized nanoparticle doses around 50 to 60 ppm, though some explored concentrations exceeding 120 ppm. To ensure a comprehensive evaluation, we conducted the pilot test at the engine's rated speed of 2400 rpm where maximum torque and power are typically achieved using nanoparticle doses of 60 ppm, 80 ppm, 100 ppm, and 120 ppm.

Table4. 4 Experimental design

Factors	Levels			
	1	2	3	4
Blend ratio	B5	B10	B20	B40
Nps dose(ppm)	60	80	100	120

The results demonstrated a consistent reduction in emissions as the nanoparticle dose increased up to 100 ppm. Beyond this point, at 120 ppm, emissions stabilized and showed no further improvement compared to the 100 ppm dose. Based on these findings, a nanoparticle concentration of 100 ppm was selected as the optimal dose for subsequent experiments. The design of experiment and the measured results are as shown in the table 4.5 below.

Table4. 5 Pilot test emission results of measurement

Test No.	Blends	Nps dose (ppm)	NOx (ppm)	UHC (ppm)	CO (%V)
1	B5	60	155	85	0.27
2	B5	80	108	81	0.27
3	B5	100	86	88	0.29
4	B5	120	88	87	0.3
5	B10	60	136	124	0.29
6	B10	80	105	103	0.28
7	B10	100	85	87	0.26
8	B10	120	85	88	0.26
9	B20	60	86	78	0.26
10	B20	80	74	75	0.25
11	B20	100	66	73	0.23
12	B20	120	67	74	0.24
13	B40	60	115	69	0.37
14	B40	80	93	62	0.36
15	B40	100	71	60	0.32
16	B40	120	72	61	0.33

4.7.1. Two-way ANOVA analysis

Two-Way ANOVA was performed without replication as each combination has one measurement. Accordingly, the response emission were computed by determining the sum of squares (SS), degree of freedom, F-value and P-value as it is indicated on the table 4.6 below.

Table4. 6 Two-way ANOVA analysis

Response	source	Sum of squares (SS)	df	F-value	P-value
NOx	Blends	3106.0	3	11.07	0.0022
	Nps dose	5539.0	3	19.74	0.0003
	Residue	842.0	9		
UHC	Blends	3033.19	3	14.71	0.0008
	Nps dose	371.19	3	1.80	0.2171
	Residue	618.56	9		
CO	Blends	0.0214	3	26.51	0.0001
	Nps dose	0.0011	3	1.39	0.3072
	Residue	0.0024	9		

From the ANOVA result, both Blends and Nps dose have statistically significant effects on NOx emissions as the p-values is less than 0.05 which is at (F (11.07), P=0.0022). And the Nps dose showed a stronger influence than blends based on the higher (F (19.74), P= 0.0003). The response UHC, is significantly affected by the blend ratio as indicated from the table at (F (14.71), P= 0.0008) and the Nps dose doesn't have significant effect because at F (1.80), P=0.2171 which is greater than 0.05. Similarly blends also significantly affect CO emissions, but Nps dose does not as F (26.51), P=0.0001 and F (1.39), P=0.3072 respectively. Therefore the influences of the factors of blend ratio and NPs dose are summarized on the table 4.7 below.

Table4. 7 Emission influencing factors

Response	Significant Factor(s)	Dominant Influence
NOx	Blends, Nps dose	Nps dose (higher F-value)
UHC	Blends only	Blends
CO	Blends only	Blends

The interaction plots for NOx, UHC, and CO are indicated in the Figure 4 below

- NOx showed a clear decreasing trend with increasing Nps dose, especially for lower blend
- UHC varies more with blend type than with Nps dose.

- CO remains fairly stable across Nps doses but differs noticeably by blend

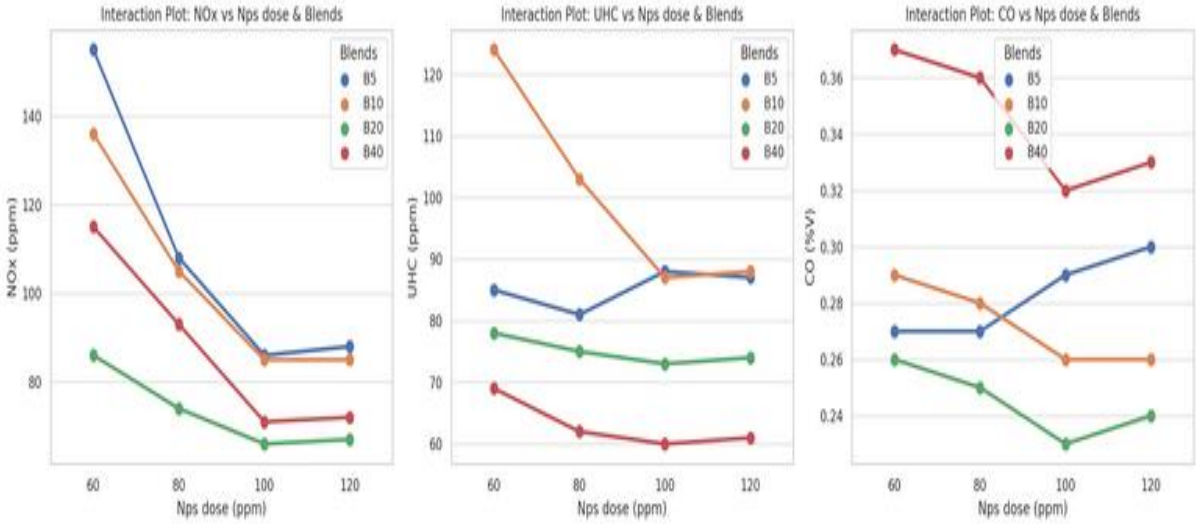

Figure 4. 5 Interaction plot for CO, UHC, and NOx

4.7.2. Response optimization of CO, UHC and NOx

The graph illustrates the outcomes of a multi-response optimization process that uses composite desirability to determine the best combination of two input variables Blends and Dosage for minimizing emissions of CO (Carbon Monoxide), HC (Hydrocarbons), and NOx (Nitrogen Oxides). The optimal configuration identified consists of a Blend value of approximately 24.2 and a Dosage of 100 ppm. This combination yields a composite desirability score of 0.8861, signifying a well-balanced and effective reduction across all three targeted emissions.

Among the individual responses, NOx exhibits the highest optimization, achieving a perfect desirability score of 1.0000. This suggests that under the given settings, NOx emissions are reduced to their minimum possible value. CO emissions also show a strong performance, with a desirability of 0.87818. Although HC emissions are slightly less optimized, their desirability score of 0.79225 still indicates an acceptable level of emission control.

Desirability plots indicated in Figure 4.6 demonstrate that the chosen input settings align closely with the minimum points on each emission curve. The red lines in the plots, representing current settings, visually confirm this optimal positioning. These results collectively validate the chosen settings as a robust solution for simultaneously reducing CO, HC, and NOx emissions.

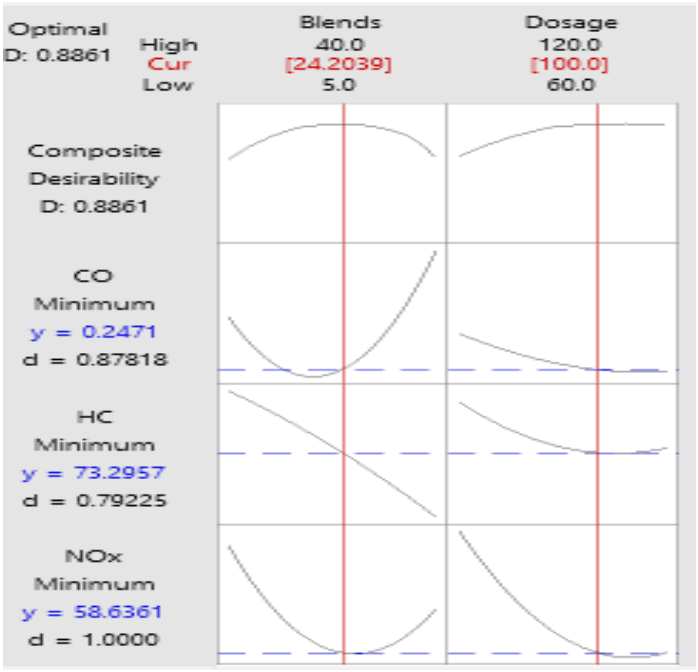

Figure 4. 6 Desirability plots for CO,UHC and NOx

In the analysis of emissions data based on nanoparticle doses and fuel blends, the 100 ppm nanoparticle dose emerges as the most effective in minimizing emissions. Across all three emission types NOx, UHC (Unburned Hydrocarbons), and CO the 100 ppm dose consistently delivers the lowest recorded values as shown in the surface plot indicated in Figure 4.7 below. For instance, the B20 blend at 100 ppm results in the lowest NOx (66 ppm) and CO (0.23%) emissions. Meanwhile, the B40 blend at the same dose produces the lowest UHC emissions, recorded at 60 ppm.

These findings reinforce that a 100 ppm nanoparticle dose is optimal for emission control. It offers a significant and consistent reduction across multiple emission types, making it the preferred setting for achieving cleaner combustion in this experimental context.

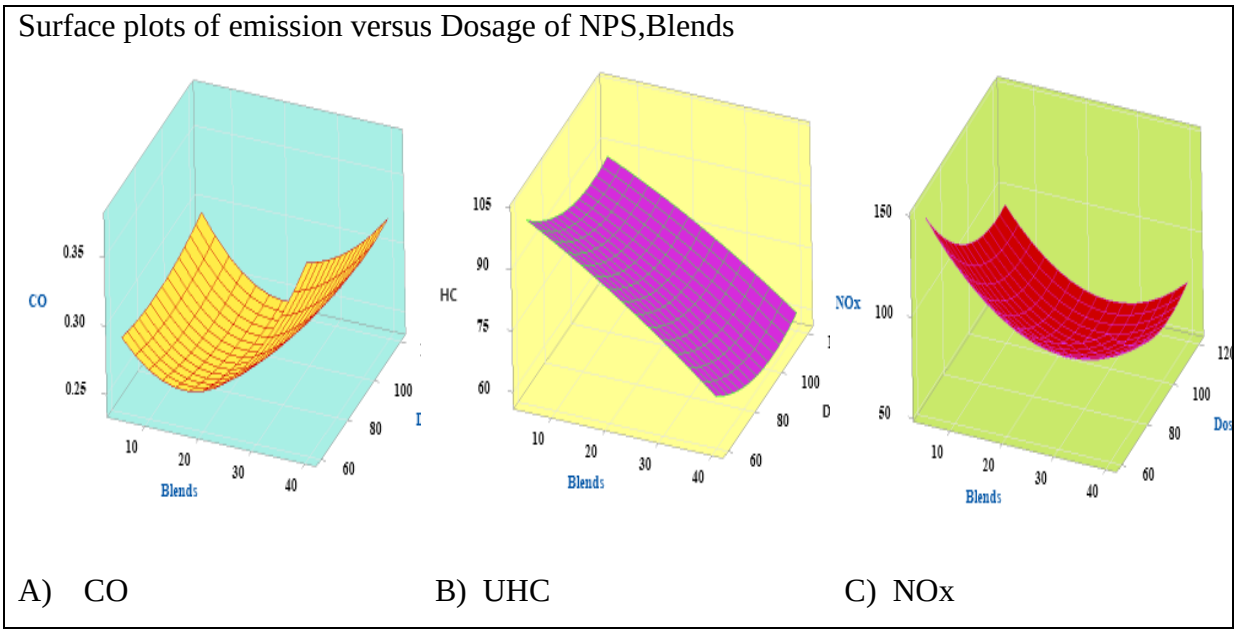

Figure 4. 7 Surface plots of emission versus Dose of NPs

4.8. Inclusion of Aluminum oxide nanoparticles (Al_2O_3)

The Nano additive used for the biodiesel-diesel mix was Al_2O_3, sized between 30-50 nm and commercially sourced from Sigma Aldrich, USA. To ensure proper dispersion of the nanoparticles, ultra-sonication was performed for 45 minutes at a frequency of 60-90 kHz during their incorporation. Additionally, Cetyl Methyl Ammonium Bromide (CTAB), an ultra-pure surfactant with 99% purity, was used to reduce the surface tension of the base fluid and stabilize the nanoparticles. The fuel samples prepared were B0, B5, B10, B20, and B40, each containing Al_2O_3 at a dosage of 100 ppm. This dosage was chosen based on pilot tests conducted with doses of 60, 80, 100, and 120 ppm, which showed only a slight reduction in UHC and NOx as the dosage increased, with stability observed at 100 ppm. Thus, the 100 ppm dosage was selected for this experimental research.

4.9. Combustion analysis

This section discusses the key characteristics that define the behavior of the fuel being analyzed. These parameters include in-cylinder pressure, heat release rate, ignition delay, and combustion duration.

4.9.1. Engine cylinder pressure

Figure 4.8a and b display the engine cylinder pressure results for biodiesel-diesel blends, both with and without the additive Al_2O_3 Nps

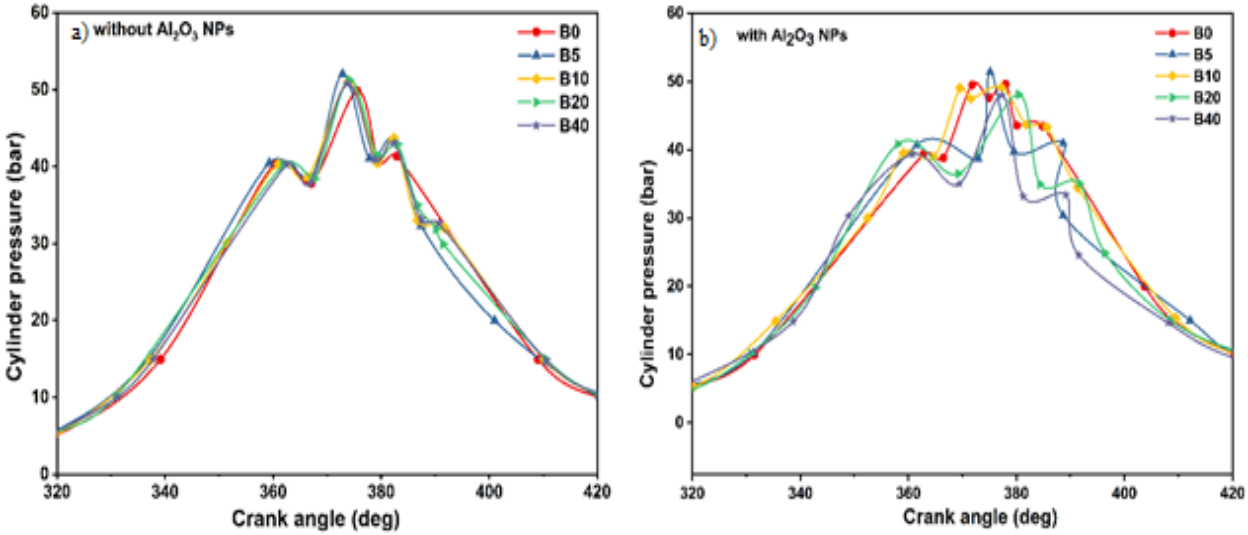

Figure 4. 8 Cylinder pressure vs. CA with and without Al_2O_3 Nps

The maximum cylinder pressure in a diesel engine's combustion is influenced by the premixed burning phase. Additionally, the ignition delay interval and the duration of air-fuel mixture formation play key roles in controlling premixed combustion.(Disassa et al., 2023; Sakthivel et al., 2014). Engine cylinder pressure is primarily influenced by the type of fuel, the air-fuel ratio, and additives that enhance the combustion reaction, alongside the engine's design and operating parameters.(Lü et al., 2005; Ramegouda & Joseph, 2021). The maximum cylinder pressure was measured at the rated engine speed of 2400 rpm, where the test engine generates its peak power and torque. In the absence of the additional Al2O3 nanoparticles, the peak cylinder pressures for the blends B0, B5, B10, B20, and B40 were recorded as follows: 49.63 bar at 378 CA, 51.4 bar at 375 CA, 49.1 bar at 374 CA, 48.8 bar at 382 CA, and 48 bar at 377 CA, respectively. These results indicate that, except for B5, diesel fuel exhibits higher peak cylinder pressures compared to the other biodiesel-diesel blends. The decrease in peak cylinder pressure with increasing biodiesel content can be attributed to biodiesel's lower volatility and higher viscosity. Similar findings have been reported by other researchers.(Giakoumis, 2013; Qi et al., 2009; Sakthivel et al., 2014). The inclusion of Al_2O_3 nanoparticles resulted in the following peak cylinder pressures for the biodiesel-diesel blends: 49.85 bar at 375 CA for B0, 52 bar at 372.8 CA for B5, 50.5 bar at 369 CA for B10, 51.27 bar at 374 CA for B20, and 50.7 bar at 373 CA for B40. Compared to biodiesel-diesel blends without Al_2O_3 nanoparticles, the cylinder pressures increased with the addition of these nanoparticles, showing percentage increases of 0.44%, 1.16%, 2.85%, 5.06%, and 5.63% for blends B0, B5, B10, B20, and B40, respectively. Moreover, as the biodiesel blend ratio increased, the maximum cylinder pressure of the test engine also rose. This engine operated

on biodiesel-diesel blends that included Al_2O_3 nanoparticles, which contributed to the increased cylinder pressure due to the presence of oxygen atoms in both the Al_2O3 and the biodiesel. This enhancement accelerated the combustion reaction, reduced ignition delay, and improved overall combustion efficiency(Shaafi et al., 2015; Shaafi & Velraj, 2015). The challenges associated with higher biodiesel ratios in blends include a lower calorific value, which results in decreased cylinder pressure. Additionally, longer combustion durations are required for the larger molecules of ester oil to decompose into smaller fractions.

4.9.2. Heat release rate

Diesel engine combustion relies on the compression pressure within the engine cylinder, which raises the temperature of the air-fuel mixture to the point of self-ignition. For optimal combustion, it is essential that the air and fuel are thoroughly mixed within the combustion chamber. This proper mixing promotes an efficient combustion reaction.(Bibin et al., 2021). The combustion process was examined using the heat release rate (HRR), derived from readings of cylinder pressure and crank angle. The first law of thermodynamics and the equation of state were applied to calculate the heat release rate.(Heywood, 2018). The HRR was obtained from the equation after rearranging and simplification:

$$\frac{dQ}{d\theta} = \frac{\gamma}{\gamma-1} P \frac{dV}{d\theta} + \frac{1}{\gamma-1} V \frac{dP}{d\theta} \qquad \text{(Eqn. 32)}$$

Where γ is the ratio specific heat capacities, P is in-cylinder pressure, V is cylinder volume, θ is crank angle.

The Heat Release Rate (HRR) is also known as the net heat release rate (NHRR) due to factors such as heat transfer to the walls, airflow dynamics, and the effects of fuel injection. The total net heat released is determined by integrating Equation 1 over the crank angle. Figures 4.9a and 4.9b illustrate the variation in HRR for different fuel mixtures, both with and without aluminum oxide nanoparticle additives, from idle to maximum engine RPM. Without the Al_2O_3 nanoparticles, the maximum HRRs for the Jatropha curcas biodiesel-diesel blends—B0, B5, B10, B20, and B40—were recorded at 25@367CA, 27.04@371.9CA, 24.5@382CA, 25@369CA, and 26@369CA, respectively. In contrast, with the addition of Al2O3 nanoparticles, the highest HRRs for B0, B5, B10, B20, and B40 were 26.5@366CA, 27.8@366CA, 27.1@367CA, and 28.5@337CA, respectively. Notably, the NHRR for blend B10 was lower than that of all other biodiesel-diesel blends, as shown in Figure 4.6.

When comparing the NHRR of blends B0, B5, B10, B20, and B40 without Al_2O_3 nanoparticles to those with the additive, the NHRR increased by 6%, 2.8%, 12.6%, 8.4%, and 9.6%, respectively. One challenge associated with higher proportions of biodiesel in the blends is their lower calorific value, which results in a decreased heat release rate. Additionally, the combustion duration is prolonged as the larger molecules of ester oil take longer to decompose into smaller fractions.

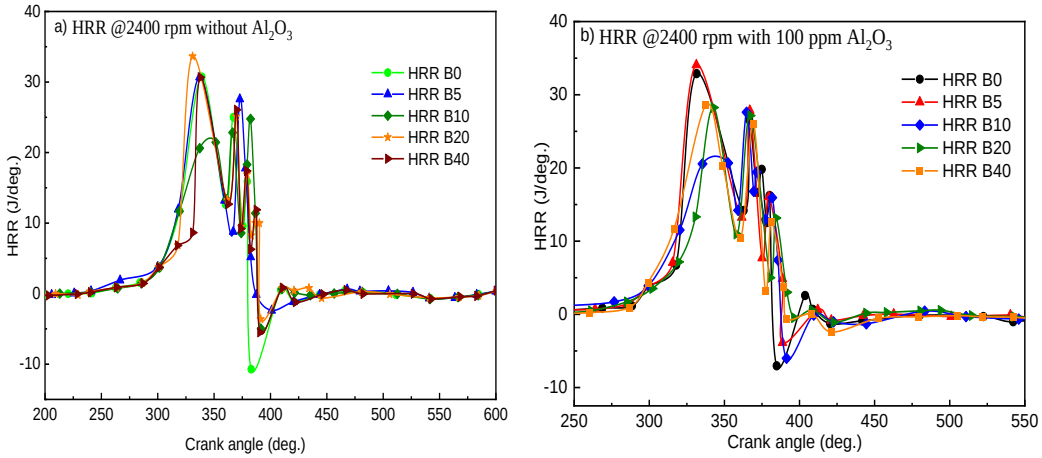

Figure 4. 9 HRR vs. with and without Al_2O_3 Nps

4.9.3. Ignition delay

The increase in viscosity, especially for petroleum-derived fuels, leads to poor atomization. The ignition delay period (IDP) is the time measured in crank angle between the start of fuel injection and the onset of fuel ignition.(Rajak et al., 2019; Singh & Verma, 2019). As the ignition delay lengthens, more fuel will be atomized, vaporized, and mixed with air, leading to an increase in both the amount of fuel burned and the heat generated during pre-combustion. Figure 4.10 illustrates the variation of ignition delay period (IDP) at the engine's rated speed, where the test engine achieves its maximum power and torque, for various blends (B0, B5, B10, B20, and B40) with and without the addition of Al2O3 nanoparticles. This results in slower mixing and a reduced cone angle, which contributes to a longer ignition delay. In contrast, the behavior of biodiesel and its blends exhibited opposing trends(El_Kassaby & Nemit_allah, 2013). The increased amount of fuel in the premixed combustion leads to a longer delay period, resulting in an acceptable rate of cylinder pressure rise that causes diesel knock. The ignition delay period (IDP) for biodiesel blends with 100-ppm aluminum oxide (Al2O3) nanoparticles was reduced by 30 degrees Celsius for all blends except for B5, which experienced a reduction of 20 degrees Celsius. Due to the lower cetane number of diesel, its

IDP was higher than that of all tested fuel blends, as shown in Figure 4.7. The addition of Al2O3 nanoparticles to the biodiesel-diesel blends significantly reduced the ignition delay period, increased the homogeneity of the fuel-air mixture, and enhanced the heat release rate of the blends(Sathiyamoorthi & Sankaranarayanan, 2017).

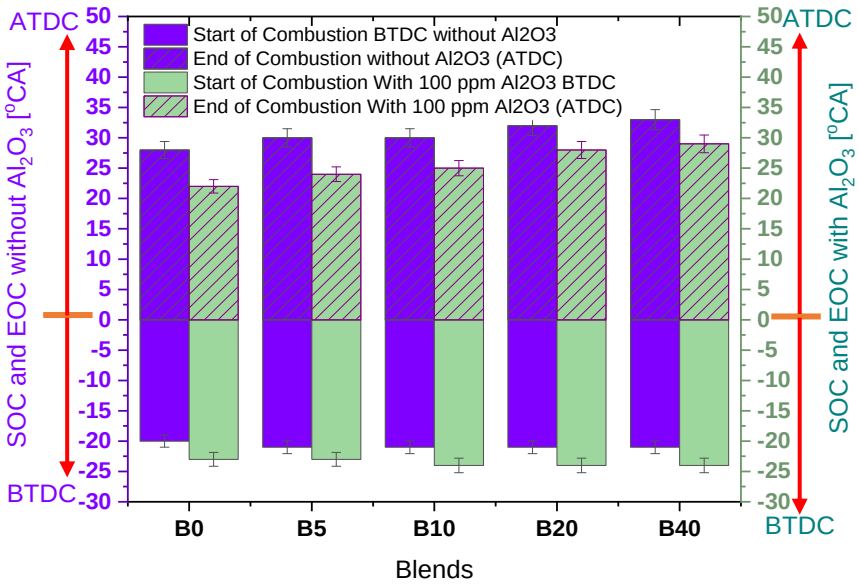

Figure 4. 10 Ignition delay

4.9.4. Combustion duration

The variation in combustion time for biodiesel-diesel mixes with and without Al_2O_3 nanoparticles is shown in Figure.4.11. The time it took for the fuel to completely burn is indicated by the term "combustion duration"(Selim, 2003). Without Al_2O_3 nanoparticles, the variation in combustion duration period in the degree of crank angle for the fuel samples was 48^0CA, 51^0CA, 51^0CA, 53^0CA, and 54^0CA, respectively, and it was 45^0CA, 47^0CA, 49^0CA, 52^0CA, and 53^0CA, respectively, for B_0, B_5, B_{10}, B_{20}, and B_{40} with Al_2O_3 nanoparticles. From the result of the experiment, diesel has less combustion duration for both with and without Al_2O_3 nanoparticles, whereas B_{40} has more combustion duration for both with and without Al_2O_3 nanoparticles. Moreover, the duration of combustion increased for all the fuel mixes as the biodiesel ratio increased. According to (S. Lahane & K. J. F. Subramanian, 2015; Li et al., 2017) the reason why the combustion duration is increased with higher percentage mix of biodiesel in the blend is because, during the injection of fuel at the higher cylinder temperature, the higher molecular weight esters break-down in to smaller fractions which

leads to lower volatility to commence early combustion and increases the combustion duration.

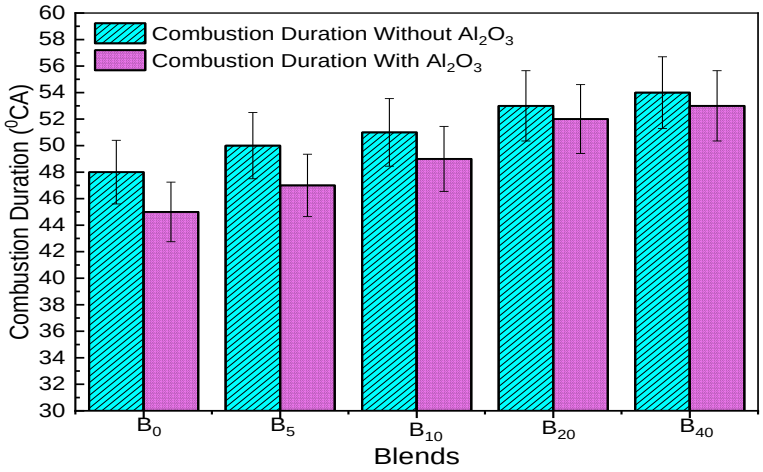

Figure 4. 11 Combustion Duration (^{0}CA) of all blends

4.10. Emission analysis

The emission species of the two fuel samples are measured and analyzed in these section

4.10.1. Carbon monoxide (CO)

The generation of CO in engine cylinders occurs when the flame front reaches cooler areas of the cylinder and piston surfaces. This temperature difference inhibits the formation of CO_2, leading to incomplete combustion(Lalvani et al., 2015). As illustrated in Figures 4.9a and 4.9b, the carbon monoxide (CO) emissions from biodiesel-diesel blends, both with and without Al_2O_3 nano additives, were generally lower than those from standard diesel fuel across the entire range from rated idle speed to maximum speed.

Figure 4.12a shows that CO emissions decrease across the engine speed range as the biodiesel ratio increases, with the exception of the B40 blend at speeds up to 2400 rpm. For all blends except B20, CO emissions decreased as engine speed increased from 2400 rpm to 3000 rpm. B20 consistently emitted less CO than both base diesel fuel and the other blends across all speed ranges, as demonstrated in Figures 4.12a and 4.12b. Additionally, Figure 4.12b indicates that the inclusion of Al_2O_3 nano additives further reduced CO emissions for all biodiesel-diesel blends at various engine speeds. The average percentage reductions in CO emissions were 31.6%, 32.9%, 29.5%, 30.0%, and 22.9% for B0, B5, B10, B20, and B40, respectively. These findings are consistent with several earlier studies(Gad et al., 2018; Ibrahim et al., 2014). The mechanism by which Al_2O_3 nanoparticles reduce CO emissions

during the combustion process in a diesel engine involves the oxidation of carbon monoxide into carbon dioxide by the oxygen atoms in the nanoparticles.

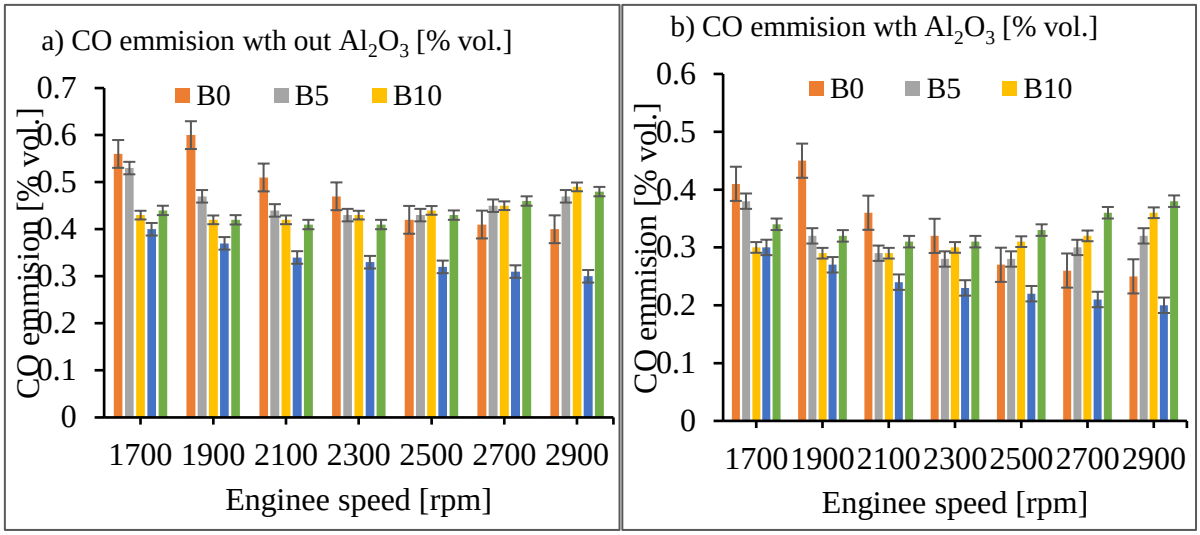

Figure 4. 12 CO a) without Al_2O_3, b) with Al_2O_3 Nps

4.10.2. Unburned hydrocarbons (UHC)

The relationship between engine speed and unburned hydrocarbon (UHC) emissions is illustrated in Figures 4.13a and 4.13b for engines with and without Al_2O_3 Nps. With the exception of B10 at the highest engine speed, HC concentrations decreased as the proportion of biodiesel increased. These findings align with earlier research conducted by(Ganapathy et al., 2011).Furthermore, HC emissions were reduced across all blend types, both with and without Al_2O_3 nano additions, and across all speed ranges. This reduction can be attributed to the higher cetane number, increased oxygen content, and the presence of Al_2O_3 in the biodiesel-diesel blends, which collectively minimize UHC formation in the engine cylinder (Agarwal et al., 2015; Shukla et al., 2017).The average percentage reductions in UHC emissions were 12.6%, 11.12%, 9.9%, 8.9%, and 8.1% for B0, B5, B10, B20, and B40, respectively. The mechanism by which Al_2O_3Nps reduce UHC emissions during combustion

in diesel engines involves the oxidation of hydrocarbons into water vapor and carbon dioxide by the oxygen atoms present in the Al_2O_3 nanoparticles.

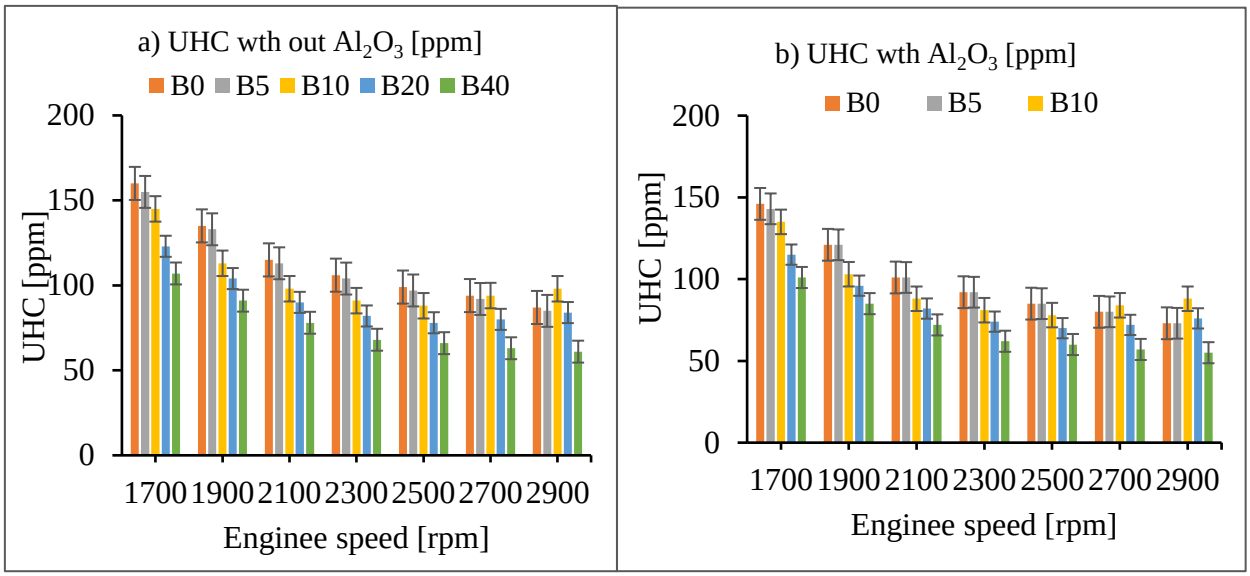

Figure 4. 13 UHC a) without Al_2O_3, b) with Al_2O_3 Nps

4.10.3. Nitrogen oxide emission (NO_X)

NOx generation is influenced by the combustion temperature, the concentrations of N_2 and O_2, and the duration of the reaction. Figures 4.14a and 4.14b illustrate the variation in NOx emissions with engine speed for biodiesel-diesel blends, both with and without Al_2O_3 nano additives. The highest NOx emissions occur at the rated speed of 2600 rpm, where maximum power and torque are achieved.

As engine speed increases, NOx emissions also rise. However, an increase in the biodiesel ratio within the blend leads to a decrease in NOx emissions for both types of blends, as demonstrated by Agarwal et al. (2015). Furthermore, the addition of Al_2O_3 nano additives resulted in reductions of NOx emissions by 19.7%, 15.9%, 14.0%, 7.6%, and 12.5% for B0, B5, B10, B20, and B40 blends, respectively.

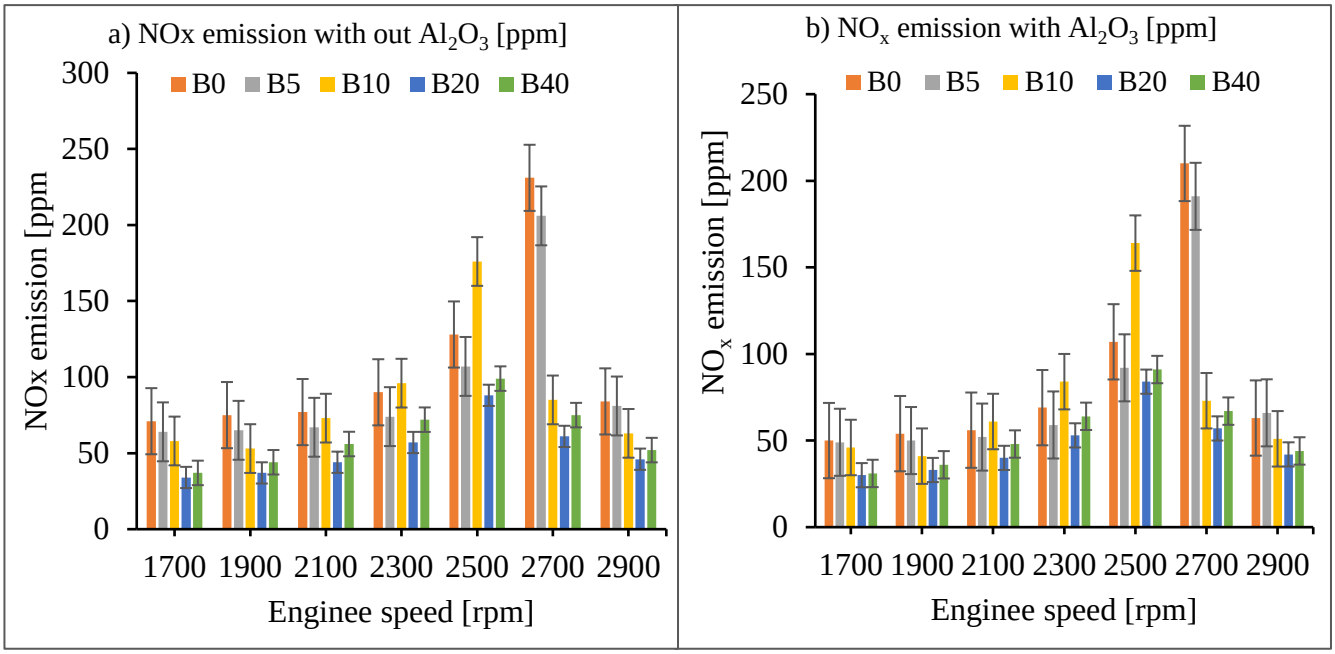

Figure 4. 14 NO_x a) without Al_2O_3, b) with Al_2O_3 Nps

4.10.4. Soot opacity

The ASTM D6216 standard defines soot opacity as a measurement of soot density, which compares the amount of light received by a sensor to the light blocked by particles in a vehicle's exhaust gas. Several factors contribute to incomplete fuel combustion and subsequent soot formation in compression ignition (CI) engines: inadequate fuel atomization due to increased viscosity, insufficient oxygen in the fuel, a shortage of air entering the engine, and lower in-cylinder temperatures (Dinkins & Jones). The soot opacity results from the experiment are presented in Figure 4.15a and 4.15b for biodiesel-diesel blends, both with and without the Al2O3 additive. The B20 blend, without the additive, exhibited less than 8% smoke opacity, the lowest observed at 2200 rpm. Notably, biodiesel-diesel blends consistently showed soot opacity of less than 10% between 2050 and 2550 rpm for both conditions—without and with the Al2O3 nano additive. Throughout all engine speeds, the fuel sample with the highest soot opacity was B0. However, the introduction of the Al2O3 nano additive to the biodiesel-diesel blends resulted in a significant average reduction in soot opacity by 8.4% across all blends within the tested engine operating speed range. This finding aligns with the study's overall conclusions(Wang et al., 2016).

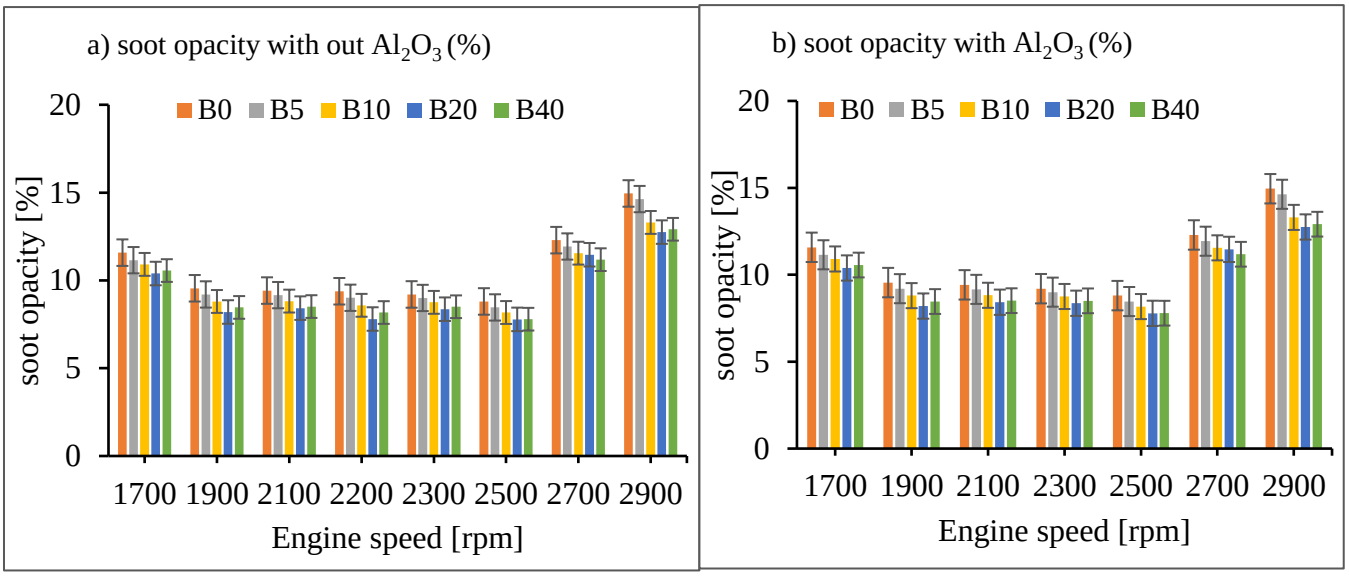

Figure 4. 15 Soot opacity a) without Al_2O_3, b) with Al_2O_3 Nps

4.11. Evaluation of engine performance

4.11.1. Brake power

When evaluating the brake power output of the test engine operated on diesel and biodiesel-diesel blends without Al2O3, the baseline diesel fuel produced the highest brake power. However, comparisons among the biodiesel-diesel blends revealed a significant increase in brake power as the percentage of biodiesel increased. Notably, the brake power of the B40 blend was 2.21% lower than that of the B20 blend. This finding aligns with results reported by other researchers(Ganapathy et al., 2011; Gebru, 2023). Under the same engine operating conditions that yield maximum power and torque, the brake power output of the baseline fuel was 3.3%, 1.78%, 0%, and 2.6% higher than those of B5, B10, B20, and B40, respectively. The slight decrease in power compared to the baseline fuel performance, as shown in Figure 4.16, can be attributed to the increased viscosity and lower calorific value of the alternative fuels. This finding is consistent with recent research (Carraretto et al., 2004; Tamrat et al., 2023). The inclusion of Al_2O_3 in the test engine resulted in an average increase in brake power output of 3.06%, 8.02%, 0.79%, 5.46%, and 4.55% for biodiesel blends B0, B5, B10, B20, and B40, respectively. Additionally, as the biodiesel blend ratio increased, the maximum power output shifted from 2400 rpm to 2700 rpm, as illustrated in Figures 4.16a and b. The

presence of Al_2O_3 Nps also contributed to a smoother power output across a wider operating speed range.

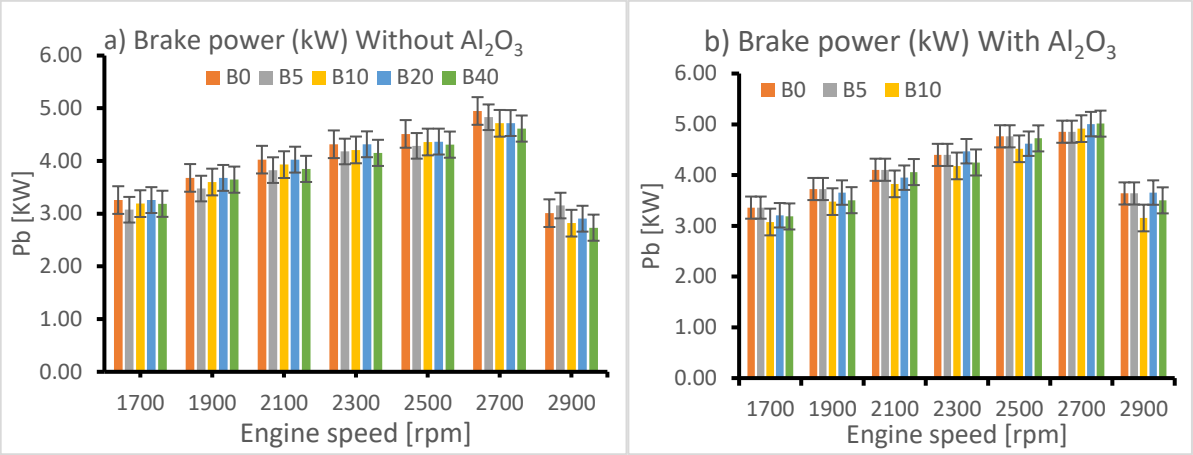

Figure 4. 16 Brake power vs. engine speed and blend ratio

4.11.2. Brake torque

This study presents the contour plot of torque for diesel-biodiesel blends with and without Al_2O_3 Nps, revealing similar patterns. However, the addition of Al_2O_3 nanoparticles significantly increased engine torque, particularly for the B20 blend, within the engine speed range of 2500 to 2800 rpm. The average brake torque output for the test engine with Al2O3 additives increased by 2.68%, 1.53%, 1.64%, 4.66%, and 4.34% for the blends B0, B5, B10, B20, and B40, respectively. Additionally, the maximum torque output shifted from the rated speed of 2400 rpm to 2200 rpm as the biodiesel proportion in the blend increased. As illustrated in Figure 4.17b, the inclusion of Al_2O_3 Nps resulted in a smooth torque output across a wide operational speed range.

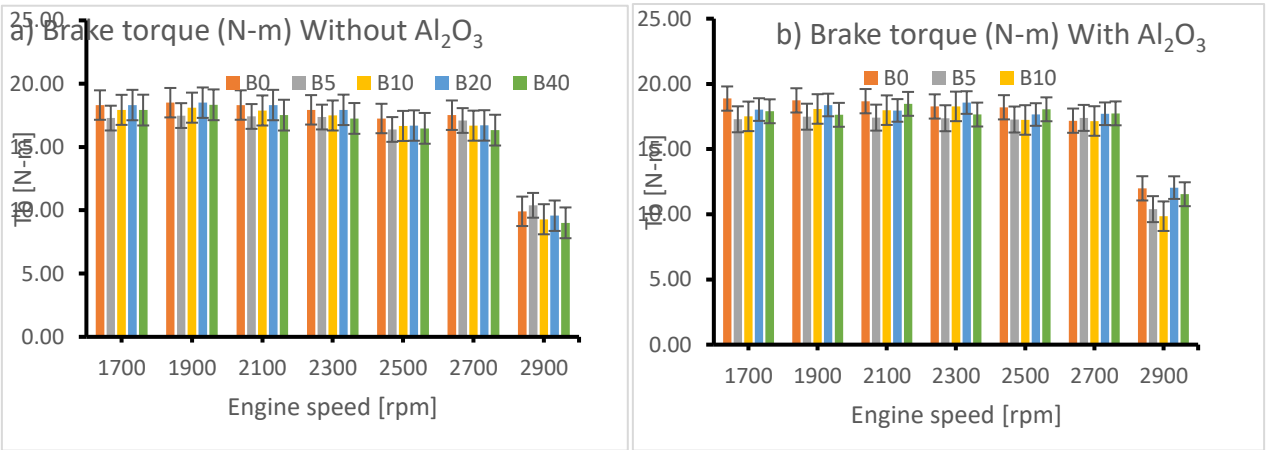

Figure 4. 17 Brake torque vs. engine speed and blend ratio

4.11.3. Brake-specific fuel consumption

Figures 4.18a and b illustrate the effect of brake-specific fuel consumption (BSFC) in relation to engine speed and biodiesel-diesel blends, both with and without Al_2O_3 Nps. This study found that BSFC for all blends, regardless of Al_2O_3 inclusion, was at a minimum within the engine's economic speed range of 2100 to 2800 RPM. Within this range, the BSFC for the biodiesel-diesel blends with Al_2O_3 showed reductions of 0.20%, 0.51%, 0.52%, 0.70%, and 0.90% for B0, B5, B10, B20, and B40, respectively. These findings align with previous research conducted by (Kalaimurugan et al., 2020) with a similar reported trends. Additionally, fuel consumption decreased as the biodiesel ratio in the blends increased, consistent with the findings of(Ganapathy et al., 2011).

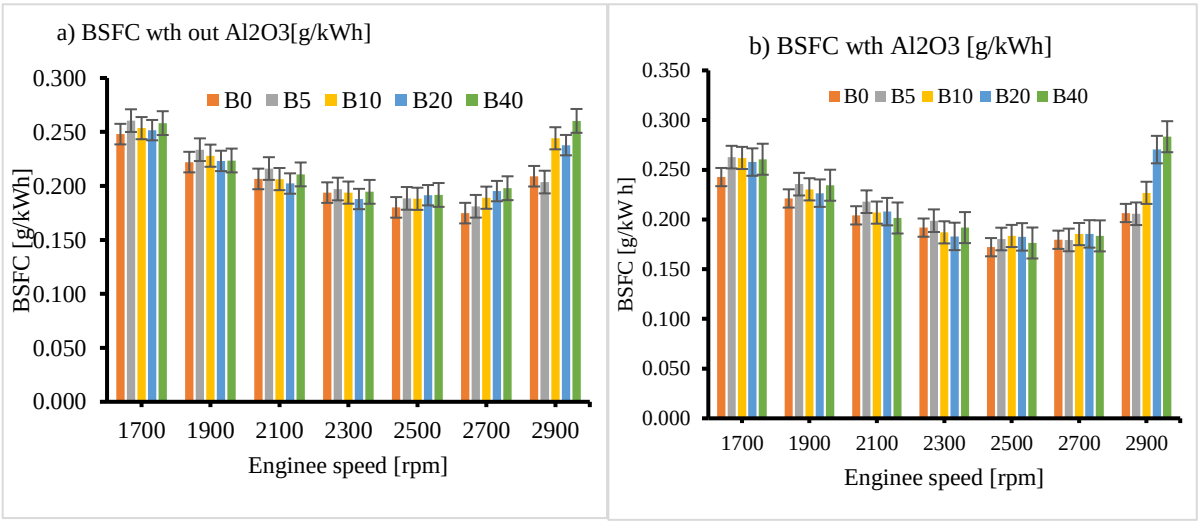

Figure 4. 18 BSFC vs. engine speed and blend ratio

4.11.4. Equivalence ratio

Figure 4.19a and b illustrate the impact of the equivalence ratio on engine speed for biodiesel-diesel blends, both with and without Al_2O_3 Nps. The study shows that the equivalence ratio decreases from the reference diesel fuel for both types of blends, ranging from 2500 to 2700 rpm. The plot indicates a reduction in the equivalence ratio as the biodiesel content increases, aligning with findings from previous studies by (Boldaji et al., 2011).Additionally, Figures 4.16a and 4.16b reveal that as engine speed rises, the equivalence ratio also increases for all blends. However, the equivalence ratio decreases as the percentage of biodiesel in the blends increased.

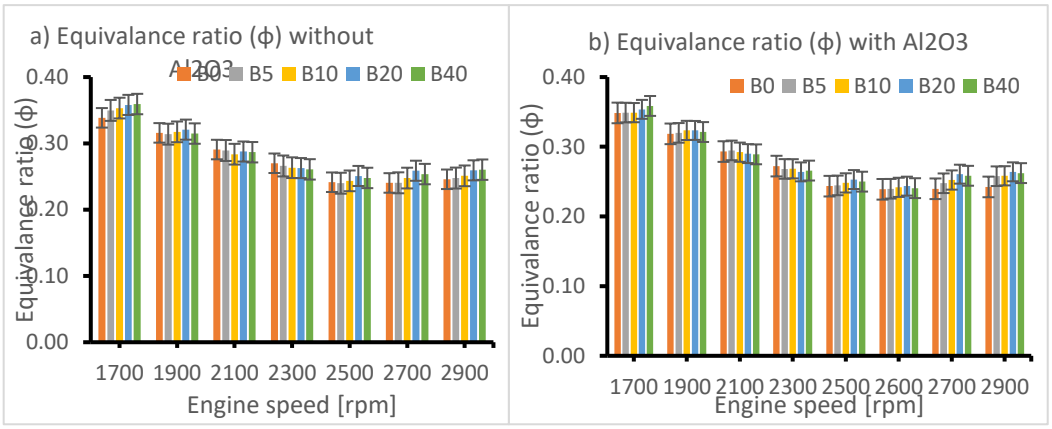

Figure 4. 19 Equivalence ratio vs. engine speed and blend ratio

4.11.5. Brake thermal efficiency (BTE)

For all the samples used with and without Al_2O_3 nanoparticles, the BTE of B_{20} and B_{40} were better in the entire engine operating range as shown in Fig.20a and b. However, B_{20} was with the greatest brake thermal efficiency at 2600 rpm for the blend without Al_2O_3 as shown in Figure.4.20a. Based on previous study, Jatropha biodiesel increases BTE when compared to diesel fuel (Ganapathy et al., 2011). The BTE decreased as the biodiesel ratio in the blends increased (Bibin et al., 2019; Bibin et al., 2020; Tamrat et al., 2023). However, this study demonstrated an increase in BTE with the addition of Al_2O_3 nanoparticles alongside the rising biodiesel ratio. The thermal efficiency of the biodiesel-diesel blends with Al_2O_3 showed improvements of 0.9%, 2.3%, 0.13%, 1.55%, and 1.43% for B0, B5, B10, B20, and B40, respectively, as indicated in Figures 4.20a and 4.20b.

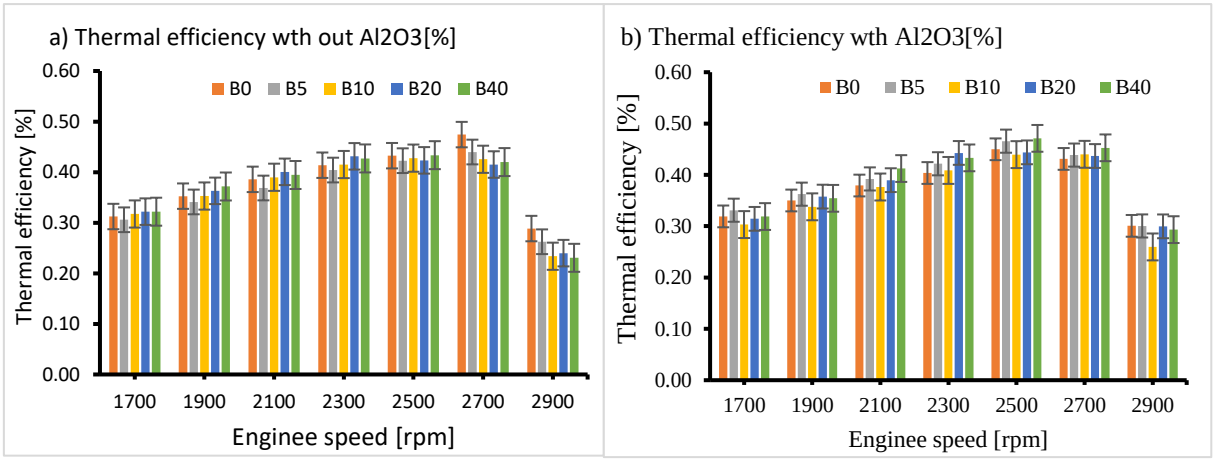

Figure 4. 20 Thermal efficiency vs. engine speed and blend ratio

4.11.6. Mechanical efficiency

As seen from Figure.4.21a and b the mechanical efficiency of B_{20} was better than all fuel samples used in the experiment at 2400 rpm. As engine speed increased, the mechanical efficiency decreased for both biodiesel-diesel blends with and without Al_2O_3 Nps. However, the mechanical efficiency of the biodiesel-diesel blends containing Al_2O_3 improved by 1%, 5.8%, 0.15%, 1.1%, and 0.48% for B0, B5, B10, B20, and B40, respectively, as shown in Figures 4.18a and 9b. The results indicate that incorporating Al_2O_3 Nps into biodiesel-diesel blends is beneficial for enhancing mechanical efficiency in high-speed and constant-speed engines.

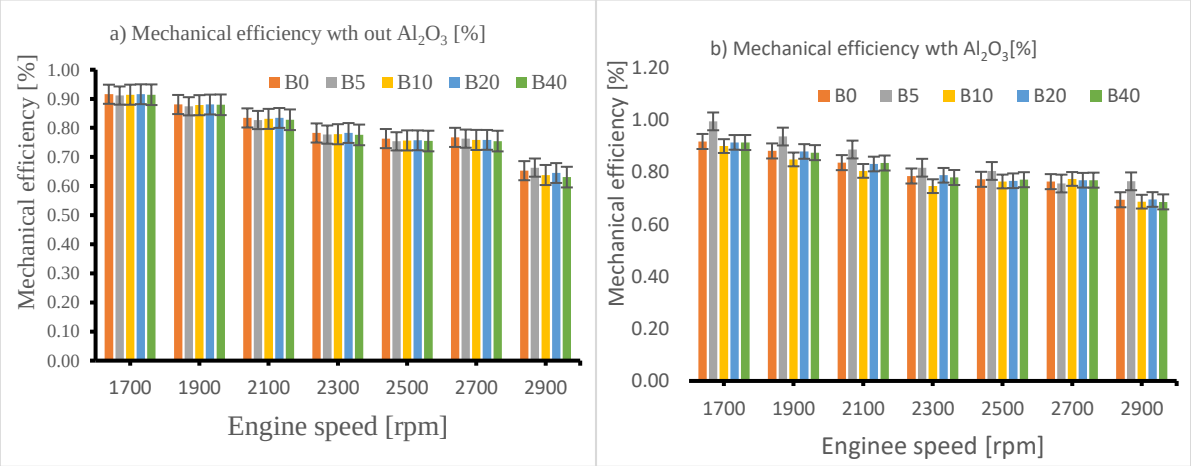

Figure 4. 21 Mechanical efficiency vs. engine speed and blend ratio

4.12. Engine endurance Test

The primary goal of the comparative short-term endurance test was to evaluate the wear characteristics of key engine components and any changes in lubricating properties. This test compared the performance of baseline diesel No. 2 fuel with a biodiesel-diesel blend (B20) that included Al_2O_3 Nps of 100 ppm. Following the Indian standard IS: 10000 Part IX, 1980 Section II, and the short-term endurance test lasted 100 hours. During this period, measurements were taken for vibration, lubricating oil properties, metallic traces in lubricants, and soot particle size, emphasizing a comparative analysis. After the test, both engines were disassembled to assess carbon deposits and physical wear, enabling a thorough evaluation of the compatibility of the test fuels.

This engine endurance test compares the performance of two identical engines under different fuel conditions. The key findings are:

The endurance test was conducted on two identical engines following the Indian Standard IS: 10000 (Part IX)-1980, Section II. The first engine, operated with the reference fuel (B0),

exhibited excessive vibration when running between 1800 rpm and 3000 rpm, requiring valve clearance adjustments at 75 hours and 100 hours. Additionally, the engine produced excessive noise, indicating possible combustion instability or mechanical stress. In contrast, the second test engine, a Robin DY-23-2D Diesel Engine running on B20 fuel with a 100 ppm dose of Al_2O_3 nanoparticles, demonstrated smooth operation throughout the test and completed the endurance run without requiring any maintenance. The improved performance of the B20 + Al_2O_3 engine suggests that the addition of nanoparticles enhanced combustion efficiency, reduced mechanical wear, and minimized vibrations, leading to better overall engine durability compared to the reference fuel engine.

4.12.1. Steady state Vibration analysis the two test fuels

The results, depicted in Figure 4.22, reveal the cumulative vibration acceleration for the tested fuels. It was observed that total vibration acceleration increased with engine speed for both fuel samples. Notably, the test fuel B20, enhanced with Al_2O_3 nanoparticles at a dosage of 100 ppm, exhibited the least vibration generation. Comparing the test fuels, B20 with 100-ppm Al_2O_3 nano additive displayed a noteworthy 12% reduction in total vibration acceleration relative to diesel no-2. Furthermore, when evaluating the vibration acceleration of both test fuels against the standard severity for internal combustion engines, they remained within acceptable limits.

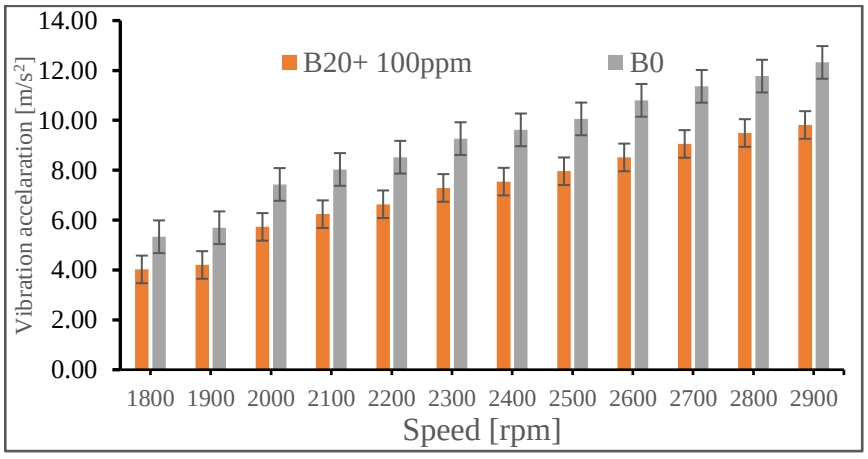

Figure 4. 22 Vibration acceleration

4.12.2. Dynamic Vibrational acceleration of engine operated by B0

The engine's dynamic vibration acceleration increases with engine speed as shown in Figure 4.23 below. At 1800 RPM, the maximum vibration acceleration (B0) is 17 m/s², and the RMS vibration acceleration is 4.61 m/s², reflecting a lower level of vibration at this speed. At 2400 RPM, the maximum vibration acceleration rises to 30.5 m/s², and the RMS value increases to

9.3 m/s², indicating that vibration levels are stronger at moderate speeds. The highest vibration acceleration occurs at 2900 RPM, where the maximum value reaches 37 m/s², and the RMS is 11.76 m/s², showing the substantial impact of higher speeds on vibration intensity. This pattern highlights the direct correlation between engine speed and vibration acceleration, which plays a crucial role in determining the engine's operational characteristics and lifespan.

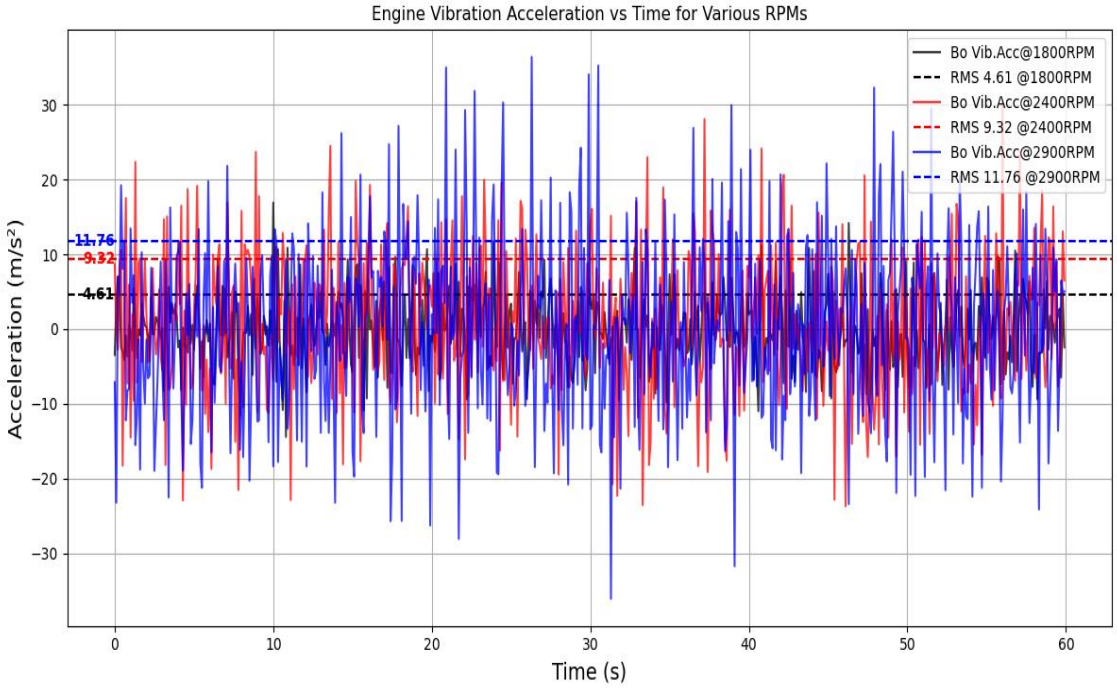

Figure 4. 23 Dynamic vibration acceleration for B0

4.12.3. Dynamic Vibrational acceleration of engine operated by B20 with 100ppm

The engine's maximum dynamic vibration acceleration, when operating on a diesel-biodiesel blend (B20+100ppm), increases as the speed rises as shown in Figure 4.24 below. At 1800 RPM, the maximum vibration acceleration (B0) is 15 m/s², and the RMS value is 3.97 m/s², reflecting lower vibration levels. At 2400 RPM, the maximum vibration acceleration increases to 22 m/s², with the RMS vibration acceleration at 7.75 m/s², showing a moderate increase in vibration intensity. At 2900 RPM, the vibration acceleration peaks at 30 m/s², accompanied by an RMS value of 9.54 m/s², indicating the highest vibration intensity at this speed. These results underscore the relationship between engine speed and vibration acceleration for engines powered by a diesel-biodiesel blend.

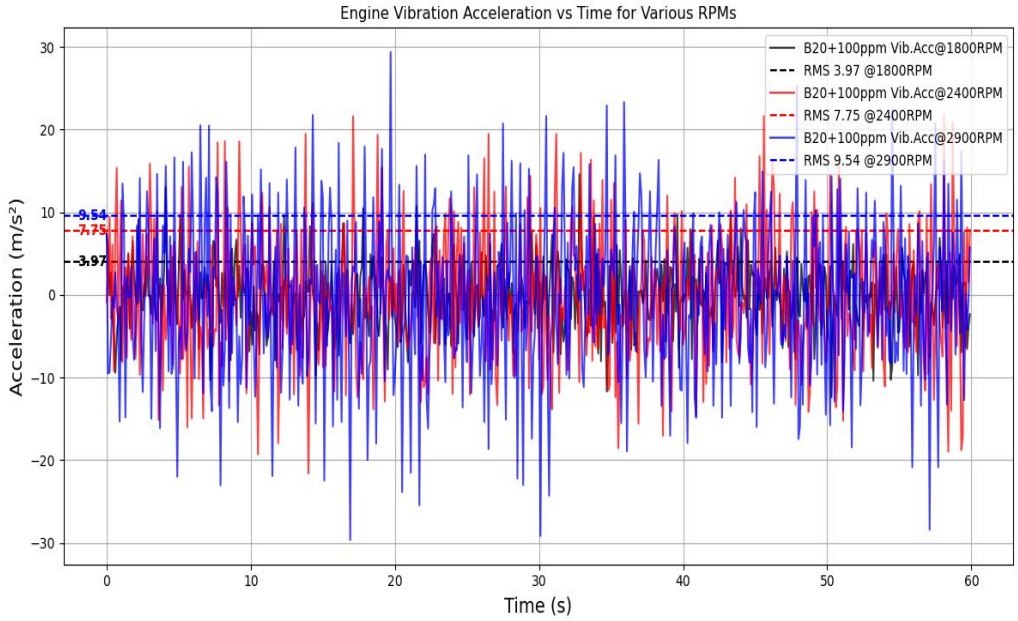

Figure 4. 24 Dynamic vibration acceleration for (B20+100ppm),

In contrast, the dynamic vibration acceleration increases with engine speed for both diesel and diesel-biodiesel blend engines. At 1800 RPM, the diesel engine's vibration acceleration (17 m/s²) is 13.33% higher than the biodiesel blend (15 m/s²). At 2400 RPM, diesel's acceleration (30.5 m/s²) surpasses the blend's (22 m/s²) by 38.64%. At 2900 RPM, diesel reaches 37 m/s², 23.33% higher than the biodiesel blend's 30 m/s². These results highlight that the diesel engine consistently produces higher vibration levels compared to the biodiesel blend at each speed.

4.13. Soot particle size (TEM)

The TEM pictures of the soot particles in the engine oils from the engines running on biodiesel and diesel, respectively, are displayed in Figures 4.25a and 4.25b. The shape of the morphological features vary according to the type of fuel, which affects combustion and the creation of pollutants. The images reveal that the size and distribution of the primary and secondary particles are two crucial factors. Typically, primary particles consist of 10^5–10^6 carbon atoms. The biodiesel soot comprises several primary particles of near-spherical shape with diameters varying from 20 to 40 nm (Figure. 4.25a). The microstructure of primary particles is turbostratic and consists of several concentric carbon layers around single or multiple nuclei. The engine combustion chamber's somewhat lower temperatures encouraged the formation of amorphous or turbostratic structures for the particulates, where the overlapping graphene fragments have none too little graphite crystal registry. Secondary particles encircle each primary particle, creating clusters of tiny, chain-like structures comprised of one-to-many particles. This could be because of collisions occurring inside the

combustion chamber, as the combustion proceeds, between particles and sub-particles (precursors). As a result, these particles and sub-particles fuse to form fractal chains and clusters (Calcote, 1981; Glassman, 1989; Palmer & Cullis, 1965). A greater quantity of organic carbon may prevent the particles from aggregating. The main soot particles form chains or clusters by tight or loose connections through thick joints or thin necks. The fact that soot particles lacked larger, bulky structures is a crucial characteristic. In addition, there may be more condensation and organic volatile adsorption/absorption due to lower combustion temperatures. The soot particles in the engine oil from the engine run on diesel appear agglomerated and lack chain structures (Figure. 4.25b). The primary particles, however, are of the same size distribution (20–40 nm size range) as the soot in the engine oil from the engine run on biodiesel. Within the agglomerates, the primary particles have distinct particle boundaries and are only slightly merged.

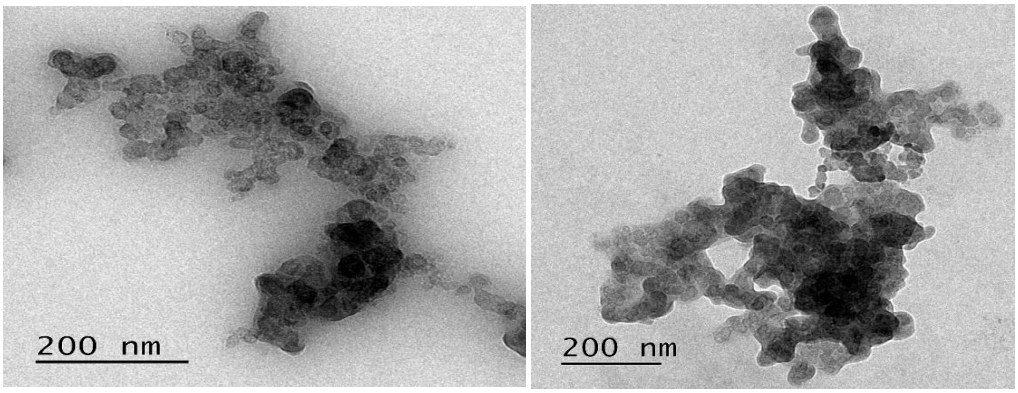

(a) (b)

(B20) Biodiesel diesel blend +100ppm Al_2O_3 Diesel no-2

Figure 4. 25 Soot particle size (TEM)

4.14. Lubricant properties

The performance characteristics of engine lubricating oil gradually degrade over time due to factors such as aging, exposure to mechanical and thermal loads, and contamination from external particles. In this research, SAE 30 grade oil was selected for use in both test engines. This lubricant was applied to engines running on conventional diesel as well as those fueled with a biodiesel-diesel (B20) blend containing Aluminum oxide (Al_2O_3) nanoparticles. The tribological behavior and changes in lubricant properties were assessed following the ASTM 6571 standard testing procedure. Measurements of lubricant properties were conducted after each operating cycle for both B0 and B20 with Al_2O_3 nanoparticles, and the results are presented in Tables 4.8 and 4.9, respectively.

Evaluating the impact of alternative fuels on lubricating oil properties is essential to determine their compatibility with existing engine systems. Several analyses were conducted on the lubricating oil to gauge its condition and, indirectly, the health of the engine. These evaluations serve as indirect indicators of how well a new fuel performs in engines without modifications. A comparative analysis was carried out to examine the behavior of engine oil when operating on conventional diesel and a biodiesel-diesel blend (B20) enhanced with 100 ppm of Al_2O_3 nanoparticles. The outcomes of these tests on the lubricant samples are detailed in Tables 4.8. and 4.9 below.

Table4. 8 Physio-chemical property of diesel operated used oil

NO	PROPERTY	TESTS ASTM	LIMIT 6751-07B	Test result for lubricant of diesel operated engine				
				Base oil	@25hr	@50hr	@75hr	@100hr
1.	Kinematic viscosity@40	D445	90-110cSt	112	102	95	94	86
	Kinematic viscosity@100		9.3-12.5cSt	12	11	10.25	9.8	9
2.	Density@15^0C, kg/m^3	D4052	0.88-0.89	893	892	891	890	891
	Density@20^0C, kg/m^3		870-890	890	888	889	888	887
3.	Flashpoint (PMCC)	D93	200-220^{0}C	210	218	224	218	205
4.	Viscosity index(VI)	D2270	~85-100	95.74	91.35	86.67	78.25	71.46
5.	Carbon residue %wt	D189	0.3-1.5	1.15	1.24	1.4	2.2	2.4
6.	Water& segment, %V	D4007	$\leq$0.05	0.84	0.93	1.06	1.42	1.85
7.	Ash content, mass%	D482	0.5-1.5	0.80	0.88	0.93	0.96	1.23
8.	TAN, mg KOH/g	D664	0.05-1.0	0.84	0.93	1.06	1.42	1.85

Table4. 9 Physio-chemical property of B20+Al_2O_3 operated engine used oil

NO	PROPERTY	TESTS ASTM	LIMIT 6751-07B	Test result for lubricant of B20+Al_2O_3 operated engine				
				Base oil	@25hr	@50hr	@75hr	@100hr
1.	Kinematic viscosity@40	D445	90-110cSt	112	106	100	96	94
	Kinematic viscosity@100		9.312.5cSt	12	11.4	10.8	10.3	9.6
2.	Density@15^0C, kg/m^3	D4052	880-890	893	892	894	898	900
	Density@20^0C, kg/m^3		887-890	890	891	892	896	896
3.	Flashpoint (PMCC)	D93	200-220^{0}c	210	222	227	221	216
4.	Viscosity index(VI)	D2270	~85-100	95.74	93.15	90.31	84.29	73.30
5.	Carbon residue	D189	0.3-1.5	1.15	1.26	1.6	2.25	2.46
6.	Water& segment, %V	D4007	<0.05	0.84	0.98	1.17	1.76	2.1
7.	Ash content, mass%	D482	0.5-1.5	0.80	0.85	0.88	0.91	1.12
8.	TAN, mg KOH/g	D664	0.05-1.0	0.84	0.98	1.17	1.76	2.1

4.14.1. Kinematic viscosity

Figures 4.26 and 4.27 present the viscosity data for lubricating oil at 40°C and 100°C for diesel-fueled engines and Biodiesel-diesel blend (B20) engines with 100-ppm Al_2O_3 Nps.

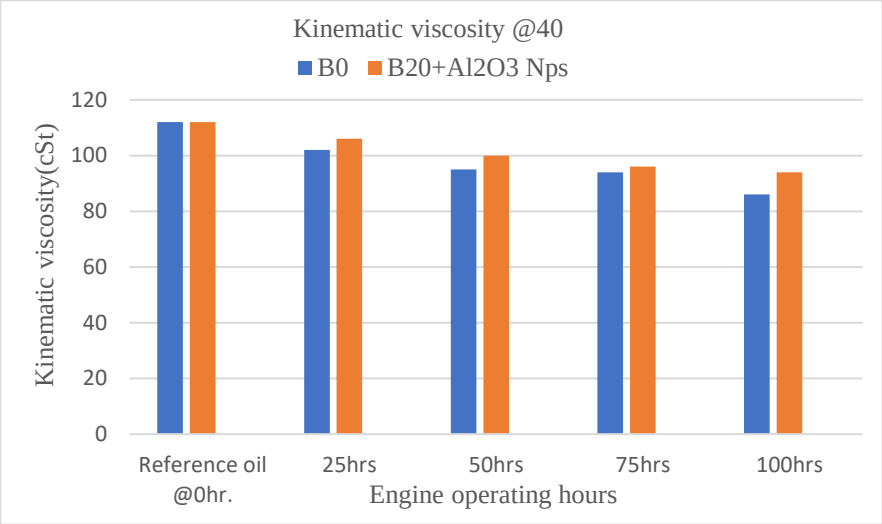

*F*igure 4. 26 Variation of Kinematic viscosity @ 40°C

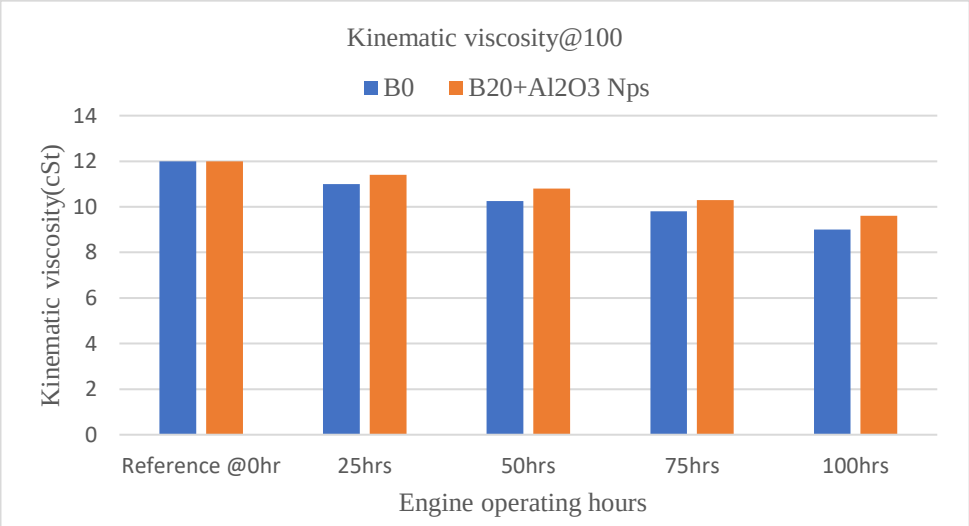

Figure 4. 27 Variation of Kinematic viscosity @ 100°C

Viscosity must remain within acceptable limits to ensure effective lubrication. Over time, it may increase due to oxidation, additive depletion, and contamination, or decrease because of fuel dilution, moisture, and mechanical shear. The dominant factor determines the overall change, which varies by engine system.

If oxidation and additive loss dominate, viscosity rises; if fuel dilution prevails, it drops. In this study, a greater viscosity reduction was observed in the diesel-fueled engine compared to the one using a B20 biodiesel-diesel blend with 100 ppm Al_2O_3. This is likely due to diesel's

lower viscosity and the biodiesel's larger triglyceride molecules, which enhance oil stability and help retain its lubricating properties longer

4.14.2. Viscosity Index

Viscosity index is an empirical number and indicates the effect of change in temperature on viscosity. It is calculated using the empirical equations of ASTM **D2270** formula, as shown in equations 32 and 35 for the kinematic viscosity less than 100 centistoke and greater than 100 centistoke receptively

$For\ \upsilon 100 \leq 100 cSt$

$$VI = \frac{L-U}{L-H} \times 100 \quad \text{(Eqn33)}$$

Where:

U = kinematic viscosity at 40°C (in centistokes, cSt)

L = reference viscosity at 40°C for a standard oil with the same ν100

H = reference viscosity at 40°C for another standard oil with the same ν100

To avoid using reference tables, the following simplified formula is commonly used:

$$VI = 100 + \frac{10^{(\log H - \log \nu 40)} - 1}{0.00715} \quad \text{(Eqn.34)}$$

Where:

$\nu 40$ = kinematic viscosity at $40°C\ (cSt)$

$$H = 0.168 \times (10^{(0.835 \times \log \nu 100 + 0.168)}) \quad \text{(Eqn.35)}$$

For $\nu 100 > 100\ cSt$:

$$VI = 10^{\left(\frac{\log H - \log \nu 40}{0.7 + 0.168 \log \nu 100}\right)} \quad \text{(Eqn.36)}$$

During an engine endurance test, the viscosity index (VI) decreases over time due to fuel dilution, oxidation, thermal degradation, shear-induced breakdown, and contaminant accumulation. As the engine operates for extended periods, unburned fuel leaks into the lubricant, reducing its viscosity, particularly at high temperatures. Continuous exposure to heat accelerates oxidation, leading to the formation of low-molecular-weight degradation products that thin the oil and lower its VI. Additionally, mechanical stress causes viscosity improvers in the lubricant to break down, making it less resistant to temperature variations. The accumulation of soot, wear metals, and acidic combustion by-products further alters the oil's composition, negatively impacting viscosity stability. In biodiesel-fueled engines, moisture absorption worsens oil degradation, contributing to a faster decline in VI. Overall, the combined effects of fuel contamination, oxidation, mechanical shear, and contaminant

build up progressively degrade the lubricant, reducing its ability to maintain viscosity over time. However, when the used oil of the engines operated by diesel (B0) and biodiesel-diesel blend (B2O) with the inclusion of 100 ppm of Al_2O_3 are compared, they showed similar trend of reduction of viscosity index (VI) but the engine that was fuelled by B20 with $Al_2O_3$was more stable at 50 hour and 75 hours endurance test. Figure 4.28 illustrates that the viscosity index of a Biodiesel-diesel blend (B20) with a 100-ppm Al_2O_3 Nps fueled engine continually increases compared to that of a diesel-fueled engine. A high viscosity index signifies minimal changes in viscosity with temperature, which provides better protection for engines operating under wide temperature variations. Additionally, it indicates good thermal stability and favorable low-temperature flow characteristics.

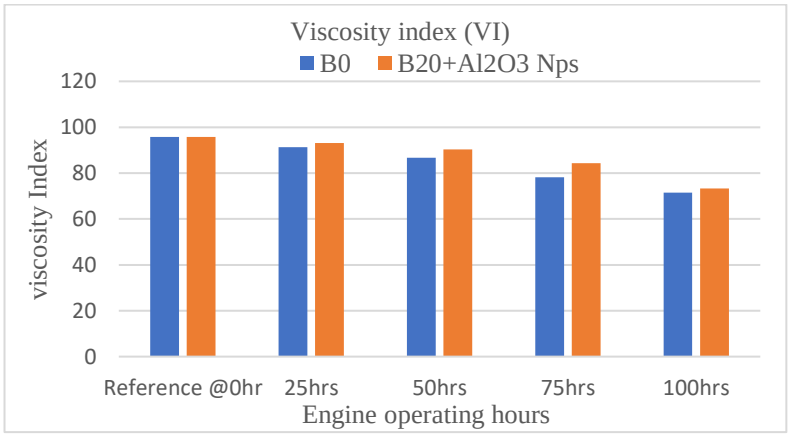

Figure 4. 28 Variation of viscosity index of lubricating oil

4.14.3. Density

Engine oil density can fluctuate due to oxidation, contamination, additive depletion, thermal breakdown, and mechanical stress. Regular oil analysis is essential for maintaining engine performance and longevity, while timely oil changes help keep density within optimal limits. When engines run on different fuels, variations in fuel composition and combustion behavior can influence oil density. In this study, lubricant density was compared for engines operating on B0 and B20 blended with 100 ppm Al_2O_3 nanoparticles. Results showed that, over time, oil density increased in the B20 with Al_2O_3-powered engine while it decreased in the diesel-fueled engine. Figures 4.29 and 4.30 illustrate the density variations and overall change during a 100-hour endurance test at 15°C and 20°C.

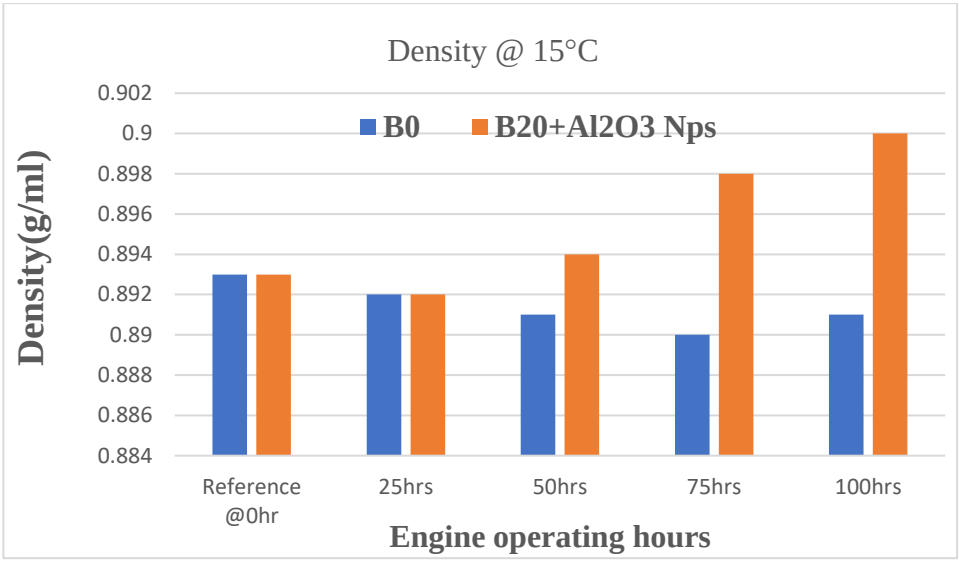

Figure 4. 29 Variation of density of lube oil @ 15°C

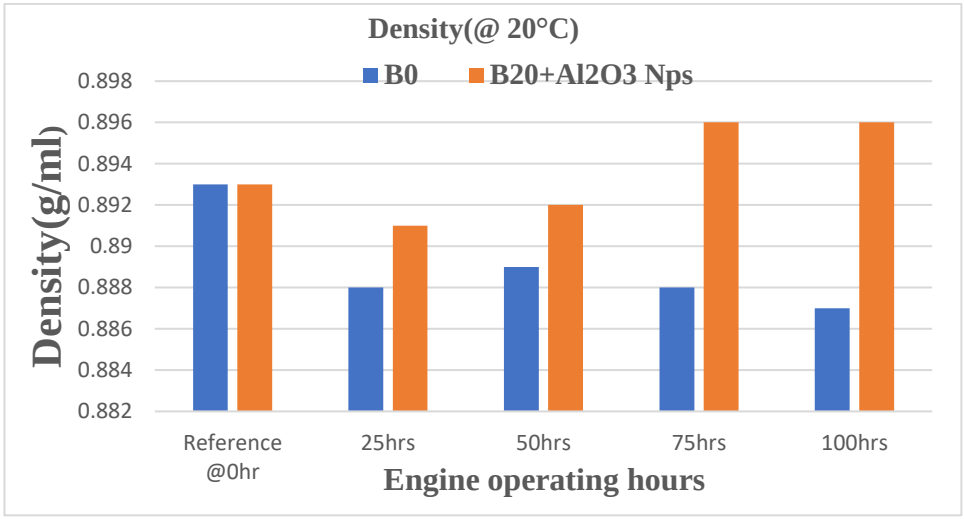

Figure 4. 30 Variation of density of lube oil @ 20°C

Figures 4.29 and 4.30 showed, the density of used lubricating oil in the B0-fueled engine decreased consistently at both 15°C and 20°C during the endurance test. This reduction, 0.34% at 15°C and 0.67% at 20°C, is attributed to diesel dilution, which lowers oil viscosity and thus density. In contrast, the engine running on the B20 biodiesel-diesel blend with 100 ppm Al_2O_3 nanoparticles exhibited an increase in oil density of 0.77% at 15°C and 5.6% at 20°C over 100 hours. This rise is linked to the presence of large triglyceride molecules in biodiesel, which contribute to higher viscosity and density. Additional factors include biodiesel dilution due to its higher molecular weight, its hygroscopic nature, and the oxidative behavior of Al_2O_3 nanoparticles, all of which promote increased oil density.

4.14.4. Flash Point

The data on flash point of lubricating oil for diesel and Biodiesel-diesel blend (B_{20}) with 100-ppm Al_2O_3 fuelled engines is presented in the figure 4.31.

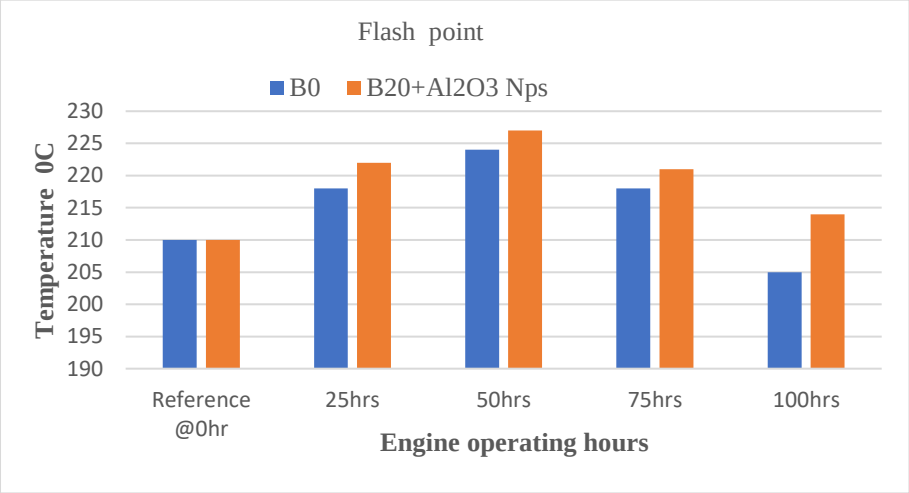

Figure 4. 31 Variation of Flash point of lube oil

During the endurance test, the flash point of used lubricating oil in both B0- and B20 with Al_2O_3 NPs fueled engines initially increased up to 50 hours, then declined by the 100-hour mark. This early rise was due to the evaporation of light volatiles and the formation of heavier, high-molecular-weight compounds through oxidation. Any initial fuel contamination from incomplete combustion also diminished, further raising the flash point.

After 50 hours, the flash point decreased as fuel dilution became more prominent—unburned fuel entered the lubricant, particularly under high load or with worn piston rings. The presence of fuel, with its lower boiling point, reduced the oil's flash point. Thermal degradation over time also produced lighter, low-flash-point compounds.

As shown in Figure 4.28, the flash point for B0 oil rose from 210°C to 224°C at 50 hours, then dropped to 205°C at 100 hours. For B20 with 100 ppm Al_2O_3, it increased to 227°C before falling to 214°C. This trend reflects the influence of fuel type and nanoparticle additives on the lubricant's thermal stability over prolonged use.

4.14.5. Carbon Residue

Figure 4.32 shows the variation in carbon residue of lubricating oil samples from engines fueled by mineral diesel and a B20 biodiesel-diesel blend with 100 ppm Al_2O_3. The results indicate a general increase in carbon residue over time, with the diesel-fueled engine showing a slightly higher carbon residue at 50 hours (Figure 4.29). This increase is a qualitative

indicator of oil polymerization, where non-combustible, high-molecular-weight compounds accumulate as carbon residue after combustion.

The rise in carbon residue negatively affects engine performance by forming deposits and sludge in critical components like piston rings, cylinder walls, and valves, leading to reduced efficiency and potential engine knock. As residue builds up, the oil thickens, impairing its lubrication abilities, increasing friction, and accelerating wear on engine parts. This not only shortens engine lifespan but also increases fuel consumption and reduces overall fuel efficiency. Furthermore, carbon buildup can obstruct heat dissipation, raising engine temperatures and the risk of overheating. Incomplete combustion due to carbon accumulation also leads to higher emissions, such as CO, unburned hydrocarbons, and particulate matter, which negatively affect environmental performance. Regular oil changes and engine maintenance are crucial to prevent these issues and maintain optimal engine performance.

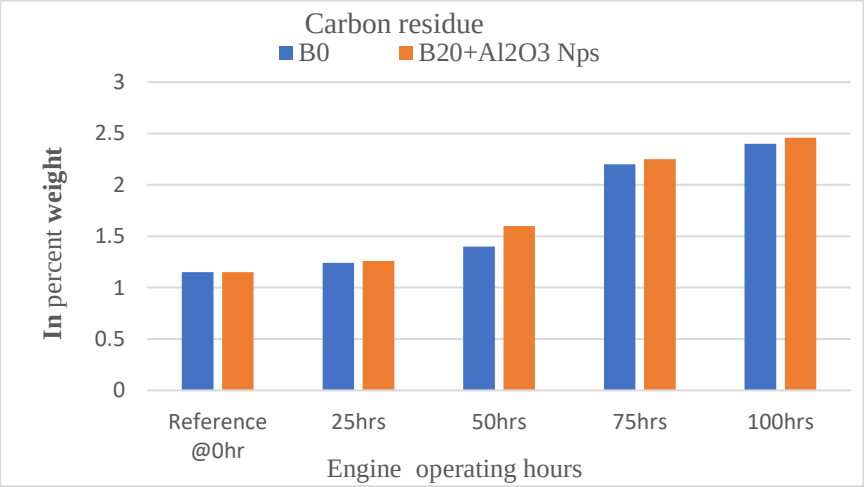

Figure 4. 32 Variation of Carbon residue lube oil

4.14.6. Water and Sediment

Water contamination in engine oil significantly affects oil quality, engine health, and component wear. Water content is influenced by factors such as oil composition, production methods, and operating conditions. It can enter engine oil through moisture absorption, condensation, leaks in heat exchangers, and combustion by-products seeping through worn engine rings. Oxidation, neutralization reactions, and even water entry during oil changes also contribute to water accumulation.

Water in engine oil triggers chemical reactions like hydrolysis, which degrades the base oil, additives, and contaminants. Combined with heat, oxygen, and metal surfaces, water accelerates oxidation, breaking down additives such as oxidation inhibitors and rust

preventatives, leading to sludge formation and reduced lubricant performance. High water content can also cause corrosion and operational inefficiencies.

As shown in Figure 4.33, the diesel engine maintained water and sediment content below 0.05% throughout the endurance test. However, for the B20 biodiesel-diesel blend with 100 ppm Al_2O_3, the water and sediment content rose to 0.3% after 25 hours. This increase may be linked to impurities like wax in the biodiesel blend, which enhances water retention and sediment accumulation.

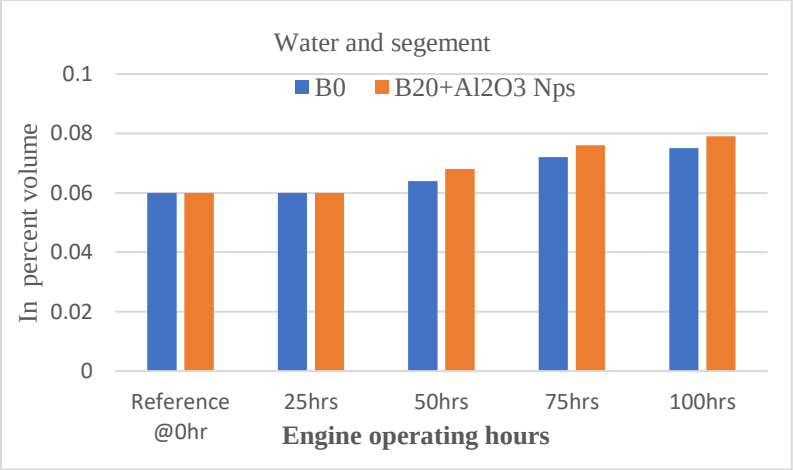

Figure 4. 33 Variation of Water and sediment lube oil

4.14.7. Ash Content

Figure 4.34 illustrates the difference of ash content of lubricant from engines operating on diesel and a biodiesel-diesel blend (B20) with 100-ppm Al_2O_3. The results show that after 50 hours of operation, the lubricating oil from the biodiesel-diesel blend (B20) with 100-ppm Al_2O_3 exhibits a higher ash content compared to the diesel-fueled engine, which maintains a lower ash content. Therefore, differences in ash content are likely due to variations in engine component wear. Physical wear measurements further confirm that the biodiesel-diesel blend (B20) with 100-ppm Al_2O_3 results in lower engine wear compared to the diesel-fueled engine, which may contribute to the observed differences in ash content.

The higher ash content in the biodiesel-diesel blend (B20) with 100-ppm Al_2O_3 suggests that the lubricant accumulates more combustion residues and additive by-products. However, since wear is lower in this engine, it indicates that the biodiesel-diesel blend, along with the nanoparticle additive, provides better lubrication and protection for engine components. This highlights the potential of biodiesel blends with nanoparticle additives in reducing engine

wear while maintaining effective lubrication, making them a viable alternative to conventional diesel fuel

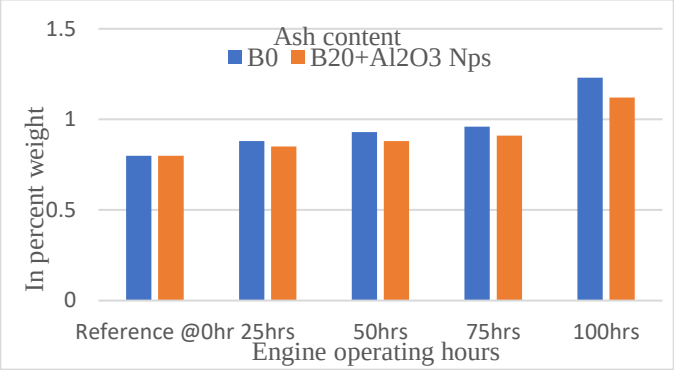

Figure 4. 34 Variation of Ash Content

4.14.8. Total Acid number

The Total Acid Number (TAN) is a key indicator of engine oil quality, as it reflects the levels of oxidation. In engine oil, oxygen and hydrocarbons can trigger chemical reactions that form carbonyl compounds which further oxidize to produce carboxylic acids, raising the TAN value.As engine oil ages and undergoes oxidation, the resulting products can polymerize into sludge, reducing oil efficiency and increasing wear. Figure 4.35 shows that TAN increases in both engines, with the diesel engine experiencing a 24% increase and the biodiesel-diesel blend (B20) with 100-ppm Al_2O_3 showing a 33% rise. The TAN of the biodiesel-diesel blend is higher than that of diesel fuel, primarily because the blend has a naturally higher TAN of 9.05 mg KOH/g. Additionally, the presence of oxidation by-products, including organic and inorganic compounds, metal salts, resins, and corrosive materials, further elevates the TAN.

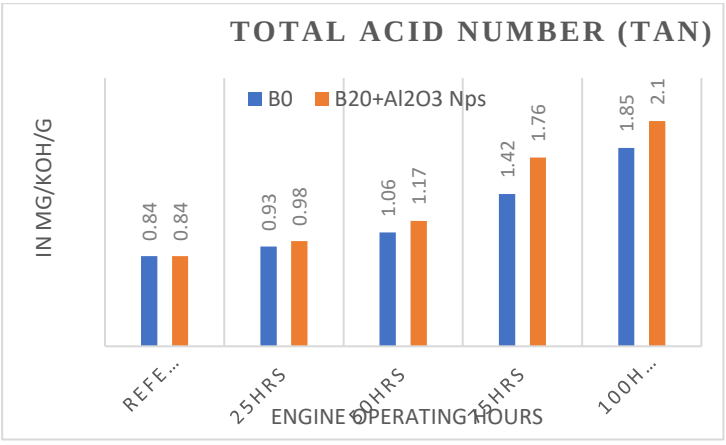

Figure 4. 35 Variation of Total acid number

4.15. Metallic traces in lubricants

Lubricating oil analysis was taken into consideration as a means of comparative assessment of the tribological impacts of the engines fuelled with B20 with Al_20_3 Nps and diesel No-2 on Robin DY23-2D diesel engines. This technique provided us with information on the internal workings of the engine and aided in the prompt identification of wear issues with its parts as well as lubricant degradation and contamination. During the engines' 100-hour endurance test, the oil was checked and tested four times every 25 hours of operation.

The goal of the lubricating oil analysis was to determine the amount of metals present in the lubricants such as zinc, lead, and magnesium after use in order to ensure their stability and proper operation. This makes it possible to determine the level of wear on components including copper, iron, aluminium, and chromium.

The new lubricating oil content of metallic traces served as a benchmark for this comparative analysis. Iron, copper, and chromium were not detected in any of the reference lubricating oil samples that were examined. Figure 4.33 displays the metallic traces found in the lubricating oil samples that were analysed. These samples were obtained from the engine crankcase every other twenty-five hours during the 100-hour endurance test during engine operating times of 25, 50, 75, and 100 hours. Numerous sliding components were examined in this investigation, and the lubricating oil under test had metallic residues in it. The following figures display the elements, including Fe, Al, Cu, Cr, Mg, and Pb, that were subjected to AAS analysis.

Magnesium: - The oil formulation had magnesium metallic traces that came from the additives. When the two test engines running on diesel fuel and diesel-biodiesel with the inclusion of Al_2O_3Nps were compared, the metallic traces in the lubricant decreased by 29% and 26%, respectively.

Lead: - Bearing wear and grease addition may be the cause of the concentration of lead metallic traces in the lubricating oil. Lead trace concentrations increased steadily and at a consistent rate for both test engines. While there was a 20% reduction in wear seen in the lubricant from the engine running on B_{20} with the addition of Al_2O_3Nps, there were 25% lead metallic traces in the engine running on diesel No-2

Copper: - Wear on bushings and bearings is the source of the copper in wear debris. According to the findings regarding copper concentration versus oil duration, copper grows at a constant rate in both test engines. The most crucial finding, therefore, was that lubricant from the engine fueled with B_{20} + Al_2O_3 showed 17.5% reduction in copper concentration, which translated into reduced wear.

Chrome. Because of wear on the cylinder liner, compression rings, gears, bearings, and crankshaft, lubricating oil contains chromium. According to the results of the chromium content as a function of oil usage, the engine fueled with the fuel sample B20 with Al_2O_3 Nps had the lowest percentage of metallic traces during the endurance test, at about 11.11%. This indicates that the diesel biodiesel with the nano component has worn the least.

Aluminum:- The piston is the engine component that contains aluminum most frequently. Pistons are almost always constructed of aluminum or one of its alloys. The metal can also be used to make bushes, thrust washers, and plain bearings. Additionally, aluminum may be contaminated. Aluminum may be present if grease is transferring into an oil-wet component because it is an added component of some greases. Therefore, all these possible sources of aluminum contributes metallic traces to the engine lubricating oil during operation. During the comparative investigation of the endurance test, the engine which was operated by the fuel B_{20} with the inclusion of Al_2O_3 Nps has shown a reduction of 25% from the engine fueled with diesel No-2 indicating superior lubricity.

Iron. Wear of the crankshaft, cylinder liner, piston, rings, valves, valve guides, gears, shafts, and bearings may be the cause of the iron in wear debris in the engine lubricating oil. The findings regarding the iron content in relation to operating hours showed a greater magnitude of change than the other metallic element traces in the lubricant. Iron metallic traces, however, are evidently increasing for both fuel samples at a steady rate throughout the engine endurance test. The most significant finding was that, thanks to the increased lubricating efficiency of biodiesel fuel, lubricants from B20 with the addition of Al_2O_3 Nps fuelled engines showed a smaller rise in iron content of almost 14% and, thus, less wear.

The figure 4.36 depict the periodic comparative analysis of metallic traces during the two oil samples' endurance test.

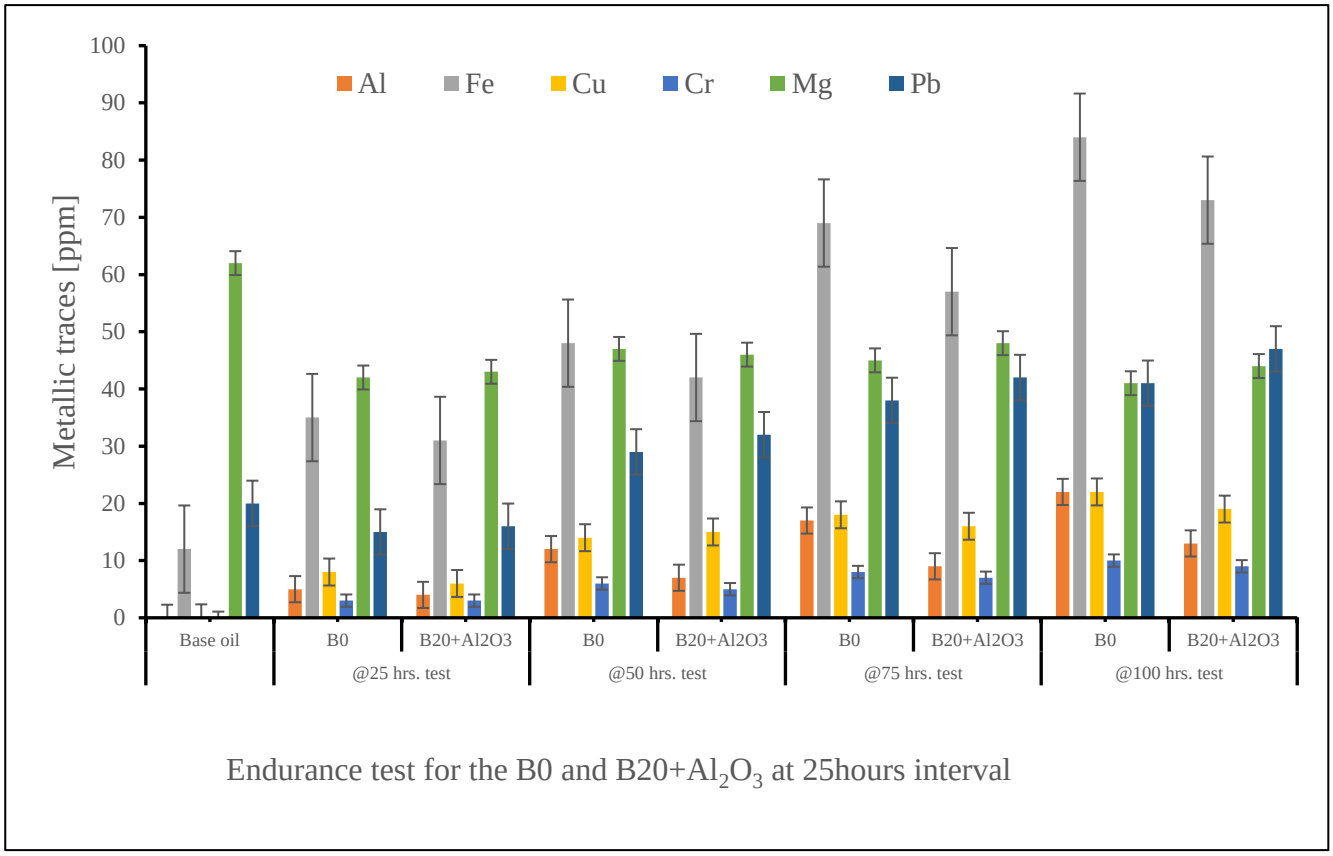

Endurance test for the B0 and B20+Al_2O_3 at 25hours interval

The periodic comparative investigation of metallic traces during the endurance test of the two oil samples are shown in the Table 4.10 and Figure 4.36.respectively.

Table4. 10 Metallic contents of lubricating oil [ppm] and the standard limit

*	ppm	@25 hrs. test		@50 hrs. test		@75 hrs. test		@100 hrs. test		Standard limit of metallic traces for diesel engine		
Element	Ref. oil	B0	$B_{20}+Al_2O_3$	B0	$B_{20}+Al_2O_3$	B0	$B_{20}+Al_2O_3$	B0	$B_{20}+Al_2O_3$	Normal	Abnormal	Critical
Al	0	5	4	12	7	17	9	22	13	< 20	20-30	>30
Fe	12	35	31	48	42	69	57	84	73	< 100	100-200	>200
Cu	0	8	6	14	15	18	16	22	19	<30	30-75	>75
Cr	0	3	3	6	5	8	7	10	9	<10	10-25	>25
Mg	62	42	43	47	46	45	48	41	44	< 20	20-30	>30
Pb	20	15	16	29	32	38	42	41	47	< 30	30-75	>75

Figure 4. 36 Metallic traces in lubricants

4.16. Engine disassembly and quantifying carbon deposited

As Carbon deposits reduce engine efficiency and durability this study compares deposits in two identical Robin DY-23 engines one using pure diesel (B0) and the other a biodiesel–diesel blend (B20) with Al_2O_3 nanoparticles. Key components analyzed include the piston crown, injector tips, and cylinder head. After disassembly as shown in Figure 4.37, deposits were mainly found in the clearance volume areas such as injector tips, piston crown, and valves as shown in Table 4.5.

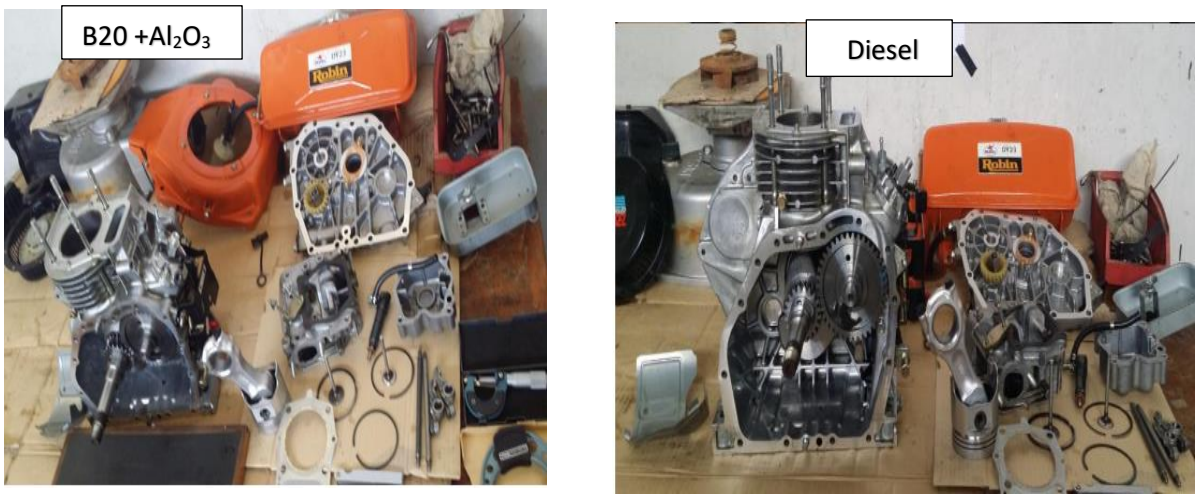

Figure 4. 37 Engine disassembly and quantifying carbon deposited

4.17. Carbon deposit formed on engine components

Results showed clear differences in carbon deposit formation between the two fuels. The diesel engine (B0) developed heavy deposits on the piston crown, injector tips, and cylinder head due to incomplete combustion, reducing efficiency and causing wear. In contrast, the B20 blend with 100 ppm Al_2O_3nanoparticles produced fewer deposits, as the oxygen in biodiesel improved combustion and heat dissipation. Measured deposits for B20 were 936 mg on the piston, 1040 mg on the cylinder head, and 483 mg on the injector tip, compared to 1155 mg, 1283 mg, and 282 mg respectively for B0. As shown in Figure 4.38 and Table 4.11, B0 produced about 21% more carbon deposits, while B20 with Al_2O_3 yielded cleaner combustion, higher efficiency, and lower soot emissions making it a more sustainable alternative despite slightly higher ash content.

Table4. 11 Comparison of Carbon deposit

Engine parts	Diesel fuelled engine	B20 withAl_2O_3 Nps fuelled engine
Cylinder head	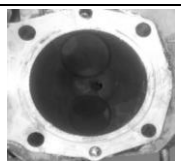	
Piston side		
Piston head	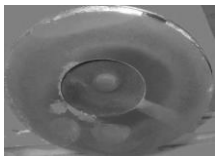	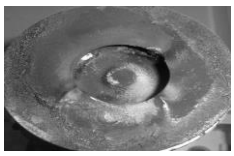
Exhaust port		
Intake port		
Exhaust valve		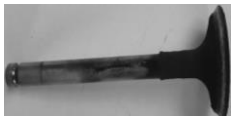
Intake valve	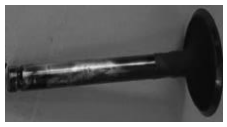	
Injector		

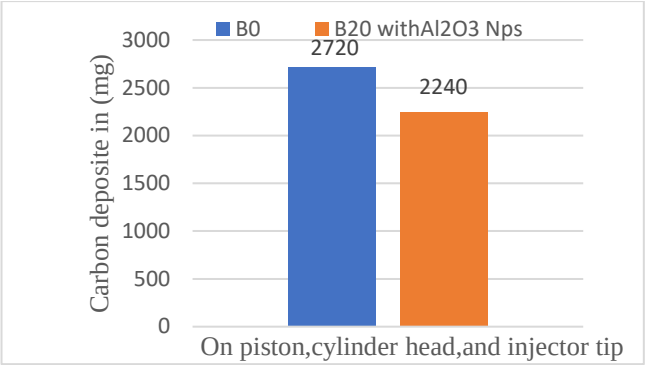

Figure 4. 38 Carbon deposits (B20) with 100-ppm Al_2O_3 and diesel

4.18. Engine Parts Wear Measurements after Endurance Test

Engine wear results from prolonged operation. This study compared two engines under identical conditions, differing only by fuel type, to assess the impact on component lifespan. Critical parts were cleaned and measured following IS: 10000 (Part V) standards. Wear was recorded for both standard diesel and a B20 biodiesel blend with 100 ppm Al_2O_3 NPs enabling a direct comparison of fuel effects on engine durability and material compatibility.

4.18.1. Measurement of wear on vital engine parts

Engine oil reduces friction and wear by forming a protective film on moving parts, preventing heat damage and extending engine life. A 100-hour endurance test on DY23-2D engines compared wear using B20 biodiesel with 100 ppm Al_2O_3 nanoparticles versus conventional diesel (B0) under identical conditions. Critical components including the cylinder bore, piston and rings, gudgeon pin, valves, connecting rod, bearings, and rocker arm were measured before and after testing. Wear, expressed relative to manufacturer limits as shown in Tables 4.12–4.18, highlights the comparative durability and performance of the two fuels.

4.18.2. Piston rings

Piston rings maintain compression, control oil consumption, and reduce friction. During extended operation, they experience high temperatures and continuous stress, leading to wear, increased blow-by, and reduced efficiency.

After a 100-hour endurance test, piston ring wear was measured using a micrometer and feeler gauge, focusing on ring thickness reduction, end-gap expansion, and surface wear (scoring, pitting, material degradation). Wear values were compared to manufacturer limits.

Engines running on B20 biodiesel with 100 ppm Al_2O_3 nanoparticles showed lower wear, indicating improved lubrication and reduced friction, while diesel-fueled engines experienced

greater wear. Table 4.12 summarizes the results, highlighting the effectiveness of nano-additive biodiesel blends in enhancing durability.

Table4. 12 Comparison of wear of piston ring

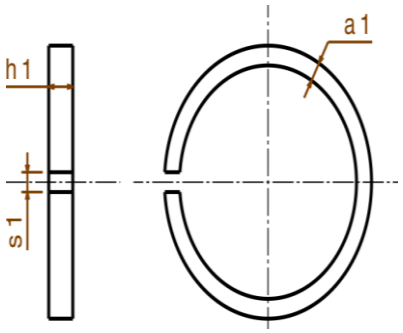

Piston Ring measurement (in mm)

a_1 = Radial thickness, s_1= Ring gap, h_1=Axial thickness

Engine	Ring No	Before Endurance Test			After Endurance Test		
		a_1	s_1	h_1	a_1	s_1	h_1
Diesel	1(top)	3	10	1.3	2.98	10.14	1.3
	2(mid)	3	13	1.5	3	13..08	1.5
	3(bottom)	2	8.5	3.5	2.98	8.05	3.5
B20+Al_2O_3Nps	1(top)	3	10	1.3	3	10.11	1.3
	2(mid)	3	13	1.5	3	13.04	1.5
	3(bottom)	2	8.5	3.5	2	8.5	3.5

Max.limit	1st ring S_1=10.7(0.7mm) a_1= 2.65(0.35mm)	2nd ring S_1= 13.6 (0.6 mm) a_1= 2.7(0.30 mm)	3rd ring S_1= 9 (0.5 mm) a_1= 2.5(0.5 mm)

4.18.3. Cylinder bore

The cylinder bore is vital for combustion efficiency and piston movement but wears over time due to friction, heat, and material degradation, reducing compression and efficiency. After a 100-hour test, bore wear was measured using a bore gauge, micrometer, and surface roughness tester at the top, middle, and bottom positions. Wear percentages were compared to manufacturer limits. Engines running on B20 biodiesel with 100 ppm Al_2O_3 nanoparticles showed lower wear than diesel-fueled engines, indicating improved lubrication and reduced friction. Detailed results are in Table 4.13

Table4. 13 Comparison of wear of cylinder between B_{20} biodiesel-diesel and diesel

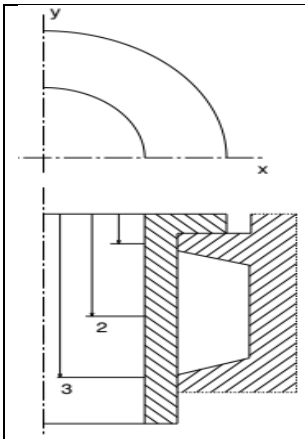

Before endurance test for diesel and B_{20}+Al_2O_3 (x-direction 'mm')			After endurance test					
			Diesel			B_{20}+Al_2O_3		
1	2	3	1	2	3	1	2	3
70.000	70.000	70.000	70.053	70.044	70.012	70.038	70.035	70.010
Diesel and B_{20}+Al_2O_3 Nps X-direction			Diesel			B_{20}+Al_2O_3 Nps		
1	2	3	1	2	3	1	2	3
70.00	70.00	70.00	70.046	70.042	70.008	70.038	70.032	70.006
Max. limit =70.25mm			Difference =70.25-70 = 0.25mm					

4.18.4. Piston skirt

The piston skirt stabilizes piston movement, reduces side forces, and ensures smooth engine operation but wears over time due to friction, heat, and lateral forces, causing higher friction and reduced efficiency. After a 100-hour test, skirt wear was measured using a micrometer and dial gauge, assessing diameter reduction, ovality, and taper. Engines running on B20 biodiesel with 100 ppm Al_2O_3 nanoparticles showed lower wear than diesel-fueled engines, indicating improved lubrication and reduced friction. Detailed results are in Table 4.14, highlighting the effectiveness of nano-additive biodiesel blends in enhancing durability

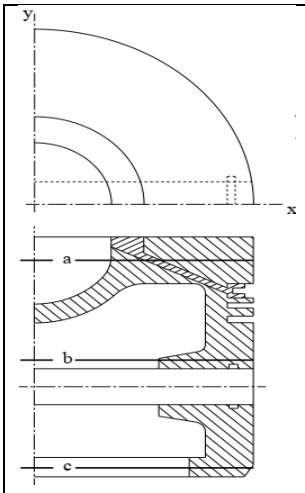

position	Before Endurance Test Diesel & B20+Al_2O_3		After Endurance Test			
			Diesel		B20+Al_2O_3	
a	69.98	69.98	69.94	69.93	69.96	69.94
b	69.98	69.98	69.95	69.94	69.97	69.95
Max limit = 69.87		69.98 -69.87 = 0.11% wear				

Table4. 14 Comparison of wear on Piston skirt

4.18.5. Valve train

The diesel engine valve train, comprising camshafts, rocker arms, pushrods, lifters, and valve springs, controls valve timing but is exposed to friction, high temperatures, and stress that cause wear. Endurance testing evaluates long-term wear patterns, material degradation, and reliability. In this study, engines fueled with B20 biodiesel + 100 ppm Al_2O_3 nanoparticles were compared to diesel engines, focusing on valves and rocker arms. Results are shown in Tables 4.15 and 4.16.

Table4. 15 Wear on valve

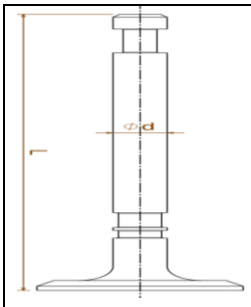	Dimensions			
	Measuring points	Valves	Before endurance test	After Endurance test	
				Diesel	$B20+Al_2O_3$
	Stem Diameter	IV	5.30	5.30	5.30
		EV	5.30	5.30	5.30
	Length ,l	IV	70.00	70.00	70.00
		EV	70.00	70.00	70.00
Steam diameter = 5.32		Limit = 5.25		Difference:-5.32-5.25=0.07 (100%)wear	

Table4. 16 Wear on rocker arm

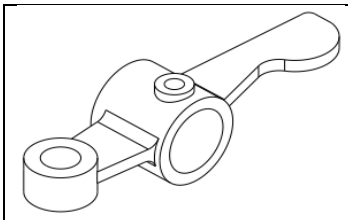	Rocker arm shaft diameter	Before test	After endurance test	
			Diesel	$B_{20}+Al_2O_3$
	Intake	12	12.02	12.01
	Exhaust	12	12.03	12.02
	Max Limit = 12.08		12.08 -12 = 0.08	

4.18.6. Connecting rod big end bore

The connecting rod transfers power from the piston to the crankshaft and is prone to wear from high loads, cyclic stress, and friction. After a 100-hour test, big-end bore wear was measured using micrometers, bore gauges, and dial indicators. Engines running on B20 biodiesel with 100 ppm Al_2O_3 nanoparticles showed lower wear than diesel engines, indicating improved lubrication and reduced friction. Detailed results are in Table 4.17, highlighting the durability benefits of nano-additive biodiesel blends.

Table4. 17 Wear on connecting rod big end bore

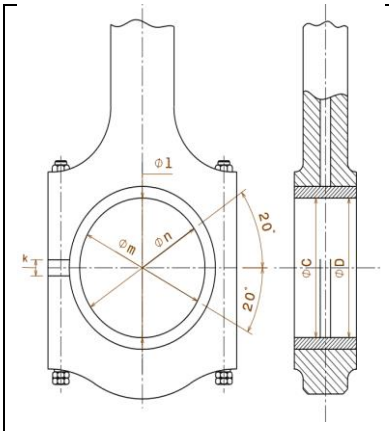	Axis of measurement		Measurements		
			Pre-endurance	After endurance	
			B0 and B20 with Al_2O_3 Nps	B0	B20with Al_2O_3 Nps
	C	l	33.06	33.09	33.08
		m	33.06	33.08	33.09
		n	33.06	33.08	33.07
	D	l	33.06	33.09	33.08
		m	33.06	33.08	33.08
		n	33.06	33.09	33.08
Maximum limit = 33.20, 33.20-33.06 =0.14 (100)%					

Table4. 18 Wear on Gudgeon pin bore

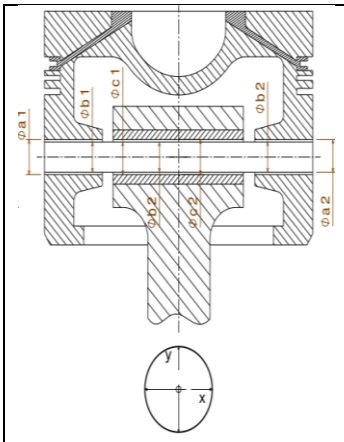

Dimensions											
Before Endurance Test diesel and B_{20}+Al_2O_3Nps											
Gudgeon pin bore			Gudgeon pin diameter			Clearance between		Small end		Between	
	a_1	a_2	b_1	b_2	b_3	a_1&b_1	a_2&b_3	c_1	c_2	b_2&c_1	b_2&c_2
Diesel	18.01	18.01	18	18	18	0.01	0.01	18.13	18.03	0.03	0.03
B20+Al_2O_3	18.01	18.01	18	18	18	0.01	0.01	18.13	18.03	0.03	0.03
Maximum limit a=0.029,b=0.02,&c=0.021						Maximum limit between a, b,& c a+b =0.049(100%) wear, b+c =0.041(100%)					

The observation of physical wear provided a basis for comparing the performance of engines fueled with B20 biodiesel with Al_2O_3 nanoparticles versus conventional diesel in terms of gudgeon pin bore and pin diameter, as shown in Table 4.14. The identical wear observed in the connecting rod bearing bore across both endurance tests can be explained by several factors. Consistent operating conditions including engine load, RPM, oil pressure, and temperature directly affect wear patterns. Additionally, an effective lubrication system maintains a stable oil film between the bearing and journal, minimizing friction and wear. The use of high-quality materials and surface treatments in the bearing bore further ensures uniform wear. Precision in manufacturing and assembly, particularly proper bearing clearances and surface finishes, also contributes to consistent results. Moreover, bearing wear typically stabilizes after the initial break-in phase, meaning subsequent wear is minimal. Finally, following identical endurance cycles with the same duration, speed variations, and stop-start sequences ensures similar wear characteristics across tests. These factors collectively account for the identical wear outcomes observed.

CHAPTER FIVE

CONCLUSIONS AND RECOMENDATION

This section elaborates on the physicochemical properties of the test fuel produced from Jatropha Curcas, focusing on biodiesel production and optimization, as well as its physicochemical characteristics, combustion and emissions, endurance, performance, and tribological properties. The current study investigated the effects of Al_2O_3 Nps on four fuel blends in a single-cylinder direct injection diesel engine. This was achieved by adjusting the blend ratio and engine speed, both with and without Al_2O_3, while maintaining a fixed compression ratio and operating at 80% load, using a dose level of 100 ppm. The findings and recommendations based on this study are presented below.

5.1. Conclusion Based on the production method

- The yield of parent oil was found to be 22% (v/w) using the solvent method and 33.3% (v/w) using a combination of mechanical pressing and the solvent method. The mechanical extraction method for biodiesel yielded more oil, making it both more economical and time-efficient.
- When the crude oil was converted into biodiesel, the resulting oil was found to be 97% pure biodiesel. Additionally, the volume of glycerin collected accounted for 18.75% of the crude oil that was esterified, hence this is a promising feature to supply to cosmetic industry to generate money for the coverage of production cost.
- The pressed residue from biodiesel extraction can be used as a cake break for baking purposes..
- The other alternative of using the residue of the biodiesel is, for fertilizer, because about 64% by weight is extracted and it can reduce importation of fertilizer
- Another alternative for using biodiesel residue is as a fertilizer. Approximately 64% by weight of the residue can be utilized, which could help reduce fertilizer imports.

5.2. Based on the physio-chemical properties

- The flash point of biodiesel is 173.8°C, significantly higher than that of conventional petro-diesel, which is 71.8°C. This higher flash point makes biodiesel safer in terms of fire hazards during storage and fuel handling.
- The cloud point, which is the lowest temperature at which biodiesel begins to form haze or wax crystals, is 7°C significantly higher than that of pure diesel, which has a

cloud point of 0°C. Therefore, biodiesel produced from *Jatropha curcas* should only be used in climates where temperatures remain above 7°C, unless the fuel system is modified or cold flow improvers are added to lower the freezing point.

- Biodiesel produced from Jatropha curcas is safer for storage and handling due to its higher density compared to petro-diesel. The densities are 0.8812 g/mL for biodiesel and 0.8440 g/mL for diesel, which contributes to lower volatility and reduced fire hazards.
- The initial boiling point of neat Jatropha curcas biodiesel is 298°C, significantly higher than that of diesel fuel, which is 176°C. This higher boiling point can hinder cold starting performance and may lead to increased fuel consumption during engine start-up. Additionally, at low engine speeds, an increase in unburned hydrocarbon emissions has been observed.
- This test evaluates the potential corrosiveness of fuel on copper, brass, and bronze components within the fuel system. Biodiesel and diesel fuels were rated [1b] and [1a], respectively. These ratings fall within the acceptable corrosion range ([1a–3a]) as per fuel standards for automotive, aviation, and marine applications, indicating that biodiesel's corrosive effect is comparable to that of diesel.
- The kinematic viscosity of Jatropha curcas biodiesel is 5.12 mm^2/s, while that of diesel fuel is 3.16 mm^2/s. Due to its higher viscosity and density, biodiesel tends to show slightly lower fuel consumption, though it may require proper injector calibration to ensure efficient combustion.
- The cetane index of biodiesel is 47.13, compared to 52.9 for diesel fuel. The lower cetane index suggests that biodiesel requires more advanced injection timing to achieve complete and efficient combustion.
- The color of Jatropha curcas biodiesel varies with the extraction method. Biodiesel produced via solvent extraction appears yellow, while that obtained through mechanical pressing exhibits a golden amber hue. These characteristic colors can help detect adulteration or contamination during storage or use.
- The biodiesel showed a water and sediment content of less than 0.025% by volume. Ash formation in biodiesel can result from water-soluble or oil-soluble metal compounds, as well as contaminants such as rust or dirt. However, the measured values indicate minimal risk of fouling or damage to fuel system components.

- The total acid number (TAN) of biodiesel and diesel fuel is 0.1686 mg KOH/g and 0.0106 mg KOH/g, respectively. While the acidity of biodiesel is higher, it remains within acceptable limits. This measurement reflects the potential oxidative degradation of biodiesel during use.
- The higher heating value (HHV) of Jatropha curcas biodiesel is 9,633.06 cal/g (40.26 kJ/g), while diesel fuel registers at 11,111.36 cal/g (46.44 kJ/g). This indicates that biodiesel has approximately 13.3% lower energy content compared to diesel, which may influence engine power output and fuel economy.

5.3. Based on emission and combustion

- Al_2O_3 nanoparticles significantly reduced carbon monoxide emissions across all biodiesel–diesel blends and engine speeds. Average reductions were 31.6% (B0), 32.9% (B5), 29.5% (B10), 30.0% (B20), and 22.9% (B40).
- Unburned hydrocarbon emissions decreased with increasing biodiesel content, except for B10 at maximum engine speed. This reduction is attributed to the higher cetane number and oxygen content of biodiesel, combined with the catalytic effect of Al_2O_3 nanoparticles. Average UHC reductions were 12.6% (B0), 11.12% (B5), 9.9% (B10), 8.9% (B20), and 8.1% (B40).
- Al_2O_3 additives led to notable reductions in nitrogen oxide emissions, with average decreases of 19.7% (B0), 15.9% (B5), 14.0% (B10), 7.6% (B20), and 12.5% (B40), likely due to improved combustion uniformity.
- The addition of Al_2O_3 nanoparticles resulted in an average reduction of 8.4% in soot opacity across all blends, indicating cleaner combustion.
- Al_2O_3 nanoparticles enhanced combustion by increasing the net heat release rate by 6% (B0), 2.8% (B5), 12.6% (B10), 8.4% (B20), and 9.6% (B40).
- : The high surface area of the nanoparticles contributed to reduced ignition delay. While diesel generally exhibited shorter combustion durations, B40 showed the longest. Combustion duration also increased progressively with higher biodiesel content.
- Al_2O_3 nanoparticles improve combustion efficiency, reduce emissions, and enhance the overall performance of biodiesel–diesel blends, making them a promising additive for cleaner diesel engine operation.

5.4. Based performance characteristics

- Increasing biodiesel content reduced peak cylinder pressure due to lower volatility and higher viscosity, but adding Al_2O_3 nanoparticles boosted pressure and improved engine performance by providing extra oxygen.
- Brake power slightly decreased with biodiesel blends because of lower calorific value and higher viscosity.
- Brake thermal efficiency improved with Al_2O_3 nanoparticles as biodiesel proportion increased.
- Mechanical efficiency increased overall with higher biodiesel content in the blends.

5.5. Based on the endurance characteristics

The engine that was operated by the reference fuel showed excessive noise and vibration at 75 hour and 100 hour endurance test and required valve clearance adjustment and maintenance. But the engine that was operated by B20 with Al_2O_3 Nps has passed through out the test cycle with smooth engine operation.

5.6. Based on the tribological properties

- Some scratches were observed on the cylinder, caused by carbon deposits on the piston rings and piston grooves in the diesel-fueled engine.
- The improved performance of the B20 with Al_2O_3 fueled engine suggests that the addition of nanoparticles reduced mechanical wear, and minimized vibrations, leading to better overall engine durability compared to the reference fuel operated engine.
- The engine endurance test revealed heavy carbon deposits on the top two compression rings of the diesel-fueled engine, while the third ring remained in good condition.
- Inlet and exhaust valves, as well as the ports, showed higher carbon buildup in the diesel engine compared to the B20 blend with Al_2O_3additive.
- Excessive carbon deposits were observed on the piston crown and cylinder head in the diesel engine, leading to reduced piston ring groove clearance. The injector tips also exhibited greater carbon accumulation in diesel engines.
- Cylinder scratches found in the diesel engine were attributed to carbon deposits on the piston rings and grooves.

5.7. Recommendation

- For optimal diesel engine performance, further studies should investigate how injection timing, compression ratio, and injection rate affect combustion, emissions, performance, and tribological behavior.
- Using Jatropha curcas biodiesel with alumina nanoparticles shows great promise as an alternative fuel; thus, producing alumina nanoparticle fuel sticks for distribution at gas stations is recommended.
- The biodiesel for the purpose of engine test should be Trans esterified by monitoring the parameters of esterification reaction which yields maximum yield of biodiesel and glycerin.
- The pressed residue during the extraction of the biodiesel can be used as a break cake for baking purpose.
- The other alternative of using the residue of the biodiesel is, for fertilizer, because about 64% by weight is extracted and it can reduce importation of fertilizer
- Finally, I recommend the Department of Mechanical and Vehicle Engineering of Adama University to Set–up a biodiesel Laboratory which is very important to make a research work on renewable energy sources like bioethanol ,biodiesel from cotton seed, biodiesel from jatropha ,and biodiesel from palm trees so that the undergraduate students, post graduate students and staff members can participate in energy research work activities

5.8. Future work

- To reduce elevated NO_x emissions, further research into modified injection strategies, such as multiple injection events, is recommended for optimizing diesel engine performance.
- Long-term engine endurance tests across various engine types and operating conditions are necessary to fully understand the effects of biodiesel–diesel blends.

REFERENCES

Abd Manaf, I. S., Embong, N. H., Khazaai, S. N. M., Rahim, M. H. A., Yusoff, M. M., Lee, K. T., & Maniam, G. P. (2019). A review for key challenges of the development of biodiesel industry. *Energy conversion and management*, *185*, 508-517.

Abd, S. O., & Mohamad, R. R. (2010). Antibacterial activity of Aleurites moluccana (Euphorbiaceae) against some clinical isolates. *Res J Biotechnol*, *5*(3), 25-30.

Abdul-Manan, A. F., Baharuddin, A., & Chang, L. W. (2014). A detailed survey of the palm and biodiesel industry landscape in Malaysia. *Energy*, *76*, 931-941.

Abebe, B. A., Çelebi, S., & Kılıç, R. (2024). A Review on Tribological Considerations in the Transition from IC Engines to Electric Vehicles. *International Journal of Automotive Science And Technology*, *8*(3), 369-380.

Abitbol, T., Marway, H., & Cranston, E. D. (2014). Surface modification of cellulose nanocrystals with cetyltrimethylammonium bromide. *Nordic Pulp & Paper Research Journal*, *29*(1), 46-57.

Abou-Ziyan, H. Z. (2004). Heat transfer characteristics of some oils used for engine cooling. *Energy conversion and management*, *45*(15-16), 2553-2569.

Achten, W. M. J., Verchot, L., Franken, Y. J., Mathijs, E., Singh, V. P., Aerts, R., & Muys, B. (2008). Jatropha bio-diesel production and use. *Biomass and Bioenergy*, *32*(12), 1063-1084. http://www.sciencedirect.com/science/article/B6V22-4SF9MSS-1/2/d1c24f817d1c574c54af1dd3c141a04e

Adhikari, M., Ghimire, L. P., Kim, Y., Aryal, P., & Khadka, S. B. (2020). Identification and analysis of barriers against electric vehicle use. *Sustainability*, *12*(12), 4850.

Agarwal, A. K., Gupta, J. G., & Dhar, A. (2017). Potential and challenges for large-scale application of biodiesel in automotive sector. *Progress in Energy and Combustion Science*, *61*, 113-149.

Agarwal, A. K., Gupta, T., Shukla, P. C., Dhar, A. J. E. C., & Management. (2015). Particulate emissions from biodiesel fuelled CI engines. *94*, 311-330.

Agarwal, A. K., Srivastava, D. K., Dhar, A., Maurya, R. K., Shukla, P. C., & Singh, A. P. (2013). Effect of fuel injection timing and pressure on combustion, emissions and performance characteristics of a single cylinder diesel engine. *Fuel*, *111*, 374-383.

Agarwal, D., Singh, S. K., & Agarwal, A. K. (2011). Effect of Exhaust Gas Recirculation (EGR) on performance, emissions, deposits and durability of a constant speed compression ignition engine. *Applied Energy*, *88*(8), 2900-2907.

Agnihotri, S., Yin, D.-M., Mahboubi, A., Sapmaz, T., Varjani, S., Qiao, W., Koseoglu-Imer, D. Y., & Taherzadeh, M. J. (2022). A glimpse of the world of volatile fatty acids production and application: a review. *Bioengineered*, *13*(1), 1249-1275.

Aher, Y. B., Jain, G. H., Patil, G. E., Savale, A. R., Ghotekar, S. K., Pore, D. M., Pansambal, S. S., & Deshmukh, K. K. (2017). Biosynthesis of copper oxide nanoparticles using leaves extract of Leucaena leucocephala L. and their promising upshot against diverse pathogens. *International Journal of Molecular and Clinical Microbiology*, *7*(1), 776-786.

Ahmad, A. L., Yasin, N. H. M., Derek, C. J. C., & Lim, J. K. (2011). Microalgae as a sustainable energy source for biodiesel production: A review. *Renewable and Sustainable Energy Reviews*, *15*(1), 584-593. http://www.sciencedirect.com/science/article/B6VMY-513DTNV-3/2/6ab2933b167bab06bedec92f3af50078

Ahmad, F. T., Asenstorfer, R. E., Soriano, I. R., & Mares, D. J. (2013). Effect of temperature on lutein esterification and lutein stability in wheat grain. *Journal of Cereal Science*, *58*(3), 408-413.

Ahmed Elgharbawy, A. (2021). Transesterification reaction conditions and low-quality feedstock treatment processes for biodiesel production-A review. *Journal of Petroleum and Mining Engineering*, *23*(1), 89-94.

Ahmed, N. S., & Nassar, A. M. (2011). Lubricating oil additives. *Tribology-lubricants and lubrication*, 249-268.

Ajala, O. E., Aberuagba, F., Odetoye, T. E., & Ajala, A. M. (2015). Biodiesel: sustainable energy replacement to petroleum-based diesel fuel–a review. *ChemBioEng Reviews*, *2*(3), 145-156.

Akbar, E., Yaakob, Z., Kamarudin, S. K., Ismail, M., & Salimon, J. (2009). Characteristic and composition of Jatropha curcas oil seed from Malaysia and its potential as biodiesel feedstock feedstock. *European journal of scientific research*, *29*(3), 396-403.

Akeredolu, B. (2014). *Rheological characterization of Alaska heavy oils*. Colorado School of Mines.

Al-Dawody, M. F., & Bhatti, S. (2013). Optimization strategies to reduce the biodiesel NOx effect in diesel engine with experimental verification. *Energy conversion and management*, *68*, 96-104.

Al-Salem, S., Antelava, A., Constantinou, A., Manos, G., & Dutta, A. (2017). A review on thermal and catalytic pyrolysis of plastic solid waste (PSW). *Journal of environmental management*, *197*, 177-198.

Aldajah, S., Ajayi, O., Fenske, G., & Goldblatt, I. (2007). Effect of exhaust gas recirculation (EGR) contamination of diesel engine oil on wear. *Wear*, *263*(1-6), 93-98.

Aleklett, K., Höök, M., Jakobsson, K., Lardelli, M., Snowden, S., & Söderbergh, B. (2010). The peak of the oil age–analyzing the world oil production reference scenario in world energy outlook 2008. *Energy policy*, *38*(3), 1398-1414.

Ali, M. K. A., & Xianjun, H. (2020). Improving the heat transfer capability and thermal stability of vehicle engine oils using Al2O3/TiO2 nanomaterials. *Powder technology*, *363*, 48-58.

Ali, M. K. A., Xianjun, H., Turkson, R. F., Peng, Z., & Chen, X. (2016). Enhancing the thermophysical properties and tribological behaviour of engine oils using nano-lubricant additives. *RSC Advances*, *6*(81), 77913-77924.

Ali, Y., & Hanna, M. (1994). Physical properties of tallow ester and diesel fuel blends. *Bioresource technology*, *47*(2), 131-134.

Aliyu, B., Agnew, B., & Douglas, S. (2010). Croton megalocarpus (Musine) seeds as a potential source of bio-diesel. *Biomass and Bioenergy*, *34*(10), 1495-1499.

Aljaafari, A., Fattah, I., Jahirul, M., Gu, Y., Mahlia, T., Islam, M. A., & Islam, M. S. (2022). Biodiesel emissions: a state-of-the-art review on health and environmental impacts. *Energies*, *15*(18), 6854.

Amare, D., Endeblhatu, A., & Muhabaw, A. (2015). Enhancing biomass energy efficiency in rural households of Ethiopia. *Journal of energy and Natural Resources*, *4*(2), 27-33.

Ambat, I., Srivastava, V., & Sillanpää, M. (2018). Recent advancement in biodiesel production methodologies using various feedstock: A review. *Renewable and Sustainable Energy Reviews*, *90*, 356-369.

Amigun, B., & Musango, J. K. (2011). An analysis of potential feedstock and location for biodiesel production in Southern Africa. *International Journal of Sustainable Energy*, *30*(sup1), S35-S58.

Aminzadegan, S., Shahriari, M., Mehranfar, F., & Abramović, B. (2022). Factors affecting the emission of pollutants in different types of transportation: A literature review. *Energy Reports*, *8*, 2508-2529.

Anna, K. K., Bogireddy, N. K. R., & Ramírez-Bon, R. (2020). Synthesis of cetyl trimethyl ammonium bromide (CTAB) capped copper oxide nanocubes for the remediation of organic pollutants using photocatalysis and catalysis. *Nanotechnology*, *32*(10), 105707.

Anuar, M. R., & Abdullah, A. Z. (2016). Challenges in biodiesel industry with regards to feedstock, environmental, social and sustainability issues: A critical review. *Renewable and Sustainable Energy Reviews*, *58*, 208-223.

Appavu, P., Madhavan, V. R., Venu, H., & Jayaraman, J. (2019). A novel alternative fuel mixture (diesel–biodiesel–pentanol) for the existing unmodified direct injection diesel engine: performance and emission characteristics. *Transactions of the Canadian Society for Mechanical Engineering*, *44*(1), 1-9.

ArifSyed, J. M., Thorpe, S., & Penney, K. (2010). Australian energy projections to 2029-30. *ABARE research report*, *10*.

Armaroli, N., & Balzani, V. (2007). The future of energy supply: challenges and opportunities. *Angewandte Chemie International Edition*, *46*(1-2), 52-66.

Arshad, M., Zia, M. A., Shah, F. A., & Ahmad, M. (2018). An overview of biofuel. *Perspectives on water usage for biofuels production: Aquatic contamination and climate change*, 1-37.

Asase, R. V., Okechukwu, Q. N., & Ivantsova, M. N. (2024). Biofuels: present and future. *Environment, Development and Sustainability*, 1-29.

Asfaw, Y. (2017). *Challenges of Supply Chain Management in the Petroleum Supplier Company. The Case of Total Ethiopia S. Co* Addis Ababa University].

Atabani, A., Badruddin, I. A., Mekhilef, S., & Silitonga, A. S. (2011). A review on global fuel economy standards, labels and technologies in the transportation sector. *Renewable and Sustainable Energy Reviews*, *15*(9), 4586-4610.

Atabani, A., Silitonga, A., Ong, H., Mahlia, T., Masjuki, H., Badruddin, I. A., & Fayaz, H. (2013). Non-edible vegetable oils: a critical evaluation of oil extraction, fatty acid compositions, biodiesel production, characteristics, engine performance and emissions production. *Renewable and Sustainable Energy Reviews*, *18*, 211-245.

Atabani, A. E., Irfan Anjum Badruddin., Mekhilef, S., & Silitonga, A. S. (2011). A review on global fuel economy standards, labels and technologies in the transportation sector. *Renewable and Sustainable Energy Reviews*, *15*(9), 4586-4610.

Atabani, A. E., Silitonga, A., Ong, H., Mahlia, T., Masjuki, H., Badruddin, I. A., & Fayaz, H. (2013). Non-edible vegetable oils: a critical evaluation of oil extraction, fatty acid compositions, biodiesel production, characteristics, engine performance and emissions production. *Renewable and Sustainable Energy Reviews*, *18*, 211-245.

Atabani, A. E., Silitonga, A. S., Badruddin, I. A., Mahlia, T., Masjuki, H., & Mekhilef, S. (2012). A comprehensive review on biodiesel as an alternative energy resource and its characteristics. *Renewable and Sustainable Energy Reviews*, *16*(4), 2070-2093.

Attwood, D. (2014). Microemulsions. In *Colloidal drug delivery systems* (pp. 43-84). CRC Press.

Atwood, D. (2010). *Full Scale Engine Endurance Test of Swift Enterprises UL102 Fuel*.

Ayoub, M., & Abdullah, A. Z. (2012). Critical review on the current scenario and significance of crude glycerol resulting from biodiesel industry towards more sustainable renewable energy industry. *Renewable and Sustainable Energy Reviews*, *16*(5), 2671-2686.

Azam, M. M., Waris, A., & Nahar, N. M. (2005). Prospects and potential of fatty acid methyl esters of some non-traditional seed oils for use as biodiesel in India. *Biomass and Bioenergy*, *29*(4), 293-302. http://www.sciencedirect.com/science/article/B6V22-4GJKTPH-1/2/1e020f7f0cb48ed843eabc59c585dfc1

Azhar, U., Yaseen, S., Arif, M., Babar, M., & Sagir, M. (2024). Emission of greenhouse gases from transportation. In *Advances and Technology Development in Greenhouse Gases: Emission, Capture and Conversion* (pp. 147-163). Elsevier.

Azman, A. S., Abu Bakar, N., & Zainal Abidin, S. (2020). Study of viscosity and flash point of bio-lubricants (engine oil) from unused and used palm oil. *International Innovation Competition (INNOCOM)*.

Bajan, B., Łukasiewicz, J., & Smutka, L. (2021). Similarity and competition of Polish agri-food export with the largest agricultural producers in the EU. Analysis of EU, US and China market. *Agris on-line Papers in Economics and Informatics*, *13*(1), 29-47.

Balat, M. (2007). An overview of biofuels and policies in the European Union. *Energy Sources, Part B*, *2*(2), 167-181.

Balat, M. (2010). Security of energy supply in Turkey: Challenges and solutions. *Energy conversion and management*, *51*(10), 1998-2011.

Balat, M. (2011). Potential alternatives to edible oils for biodiesel production - A review of current work. *Energy Conversion and Management*, *52*(2), 1479-1492. http://www.sciencedirect.com/science/article/B6V2P-51B8G17-5/2/f5325e668804e137169c1cf218b19cb4

Balat, M., & Balat, H. (2010). Progress in biodiesel processing. *Applied Energy*, *87*(6), 1815-1835. http://www.sciencedirect.com/science/article/B6V1T-4YD9XFT-1/2/a8667d774877ee1db5a03877096327ac

Bania, J. K., Nath, A. J., Das, A. K., & Sileshi, G. W. (2023). Integrating Moringa oleifera and Moringa stenopetala in Agroforestry for adaptation and mitigation of climate change in Asia and Africa. *Agroforestry for sustainable intensification of agriculture in Asia and Africa*, 719-737.

Barca, S. (2011). Energy, property, and the industrial revolution narrative. *Ecological Economics*, *70*(7), 1309-1315.

Bashir, A., Haddad, A. S., & Rafati, R. (2022). An experimental investigation of dynamic viscosity of foam at different temperatures. *Chemical Engineering Science*, *248*, 117262.

Baskov, V., Ignatov, A., & Polotnyanschikov, V. (2020). Assessing the influence of operating factors on the properties of engine oil and the environmental safety of internal combustion engine. *Transportation Research Procedia*, *50*, 37-43.

Bazina, N., & He, J. (2018). Analysis of fatty acid profiles of free fatty acids generated in deep-frying process. *Journal of food science and technology*, *55*(8), 3085-3092.

Belgiorno, G., Di Blasio, G., Shamun, S., Beatrice, C., Tunestål, P., & Tunér, M. (2018). Performance and emissions of diesel-gasoline-ethanol blends in a light duty compression ignition engine. *Fuel*, *217*, 78-90.

Benaroya, H., Nagurka, M., & Han, S. (2017). *Mechanical vibration: analysis, uncertainties, and control*. CRC Press.

Benti, N. E., Aneseyee, A. B., Geffe, C. A., Woldegiyorgis, T. A., Gurmesa, G. S., Bibiso, M., Asfaw, A. A., Milki, A. W., & Mekonnen, Y. S. (2023). Biodiesel production in Ethiopia: Current status and future prospects. *Scientific African*, *19*, e01531.

Benti, N. E., Gurmesa, G. S., Argaw, T., Aneseyee, A. B., Gunta, S., Kassahun, G. B., Aga, G. S., & Asfaw, A. A. (2021). The current status, challenges and prospects of using biomass energy in Ethiopia. *Biotechnology for Biofuels*, *14*, 1-24.

Bergmann, J., Tupinambá, D., Costa, O., Almeida, J., Barreto, C., & Quirino, B. (2013). Biodiesel production in Brazil and alternative biomass feedstocks. *Renewable and Sustainable Energy Reviews*, *21*, 411-420.

Besha, A. T., Tsehaye, M. T., Tiruye, G. A., Gebreyohannes, A. Y., Awoke, A., & Tufa, R. A. (2020). Deployable membrane-based energy technologies: The Ethiopian prospect. *Sustainability*, *12*(21), 8792.

Bessou, C., Ferchaud, F., Gabrielle, B., & Mary, B. (2011). Biofuels, greenhouse gases and climate change. *Sustainable Agriculture Volume 2*, 365-468.

Bhandari, N. (2018). Hike in prices of petrol and its impact on demand and supply. *International Journal for Advance Research and Development*, *3*(8), 33-37.

Bhuiya, M., Rasul, M., Khan, M., Ashwath, N., & Mofijur, M. (2020). Comparison of oil extraction between screw press and solvent (n-hexane) extraction technique from beauty leaf (Calophyllum inophyllum L.) feedstock. *Industrial crops and products*, *144*, 112024.

Bibin, C., Devan, P., Kumar, S. S., Gopinath, S., & Sheeja, R. (2021). Influence of palmitic and oleic acid mixtures on combustion evaluation of a diesel engine. *Materials Today: Proceedings*, *45*, 6638-6644.

Bibin, C., Kannan, P. S., Devan, P., & Rajesh, R. (2019). Performance and emission characteristics of a DI diesel engine using diestrol blends and diesel as fuel. *International Journal of Enterprise Network Management*, *10*(2), 91-108.

Bibin, C., Seeni, K. P., & Devan, P. (2020). Performance, emission and combustion characteristics of a direct injection diesel engine using blends of punnai oil biodiesel and diesel as fuel. *Thermal Science*, *24*(1A), 13.

Bilgin, A., Durgun, O., & Sahin, Z. (2002). The effects of diesel-ethanol blends on diesel engine performance. *Energy sources*, *24*(5), 431-440.

Bishop, R. E. D., Bishop, R., & Johnson, D. (2011). *The mechanics of vibration*. Cambridge University Press.

Bleviss, D. L. (2021). Transportation is critical to reducing greenhouse gas emissions in the United States. *Wiley Interdisciplinary Reviews: Energy and Environment*, *10*(2), e390.

Boadu, K., Joel, O., Essumang, D., & Evbuomwan, B. (2019). A review of methods for removal of contaminants in used lubricating oil. *Chemical Science International Journal*, *26*(4), 1-11.

Boke, M. T., Moges, S. A., & Dejen, Z. A. (2022). Optimizing renewable-based energy supply options for power generation in Ethiopia. *Plos one*, *17*(1), e0262595.

Boldaji, M. T., Ebrahimzadeh, R., Kheiralipour, K., & Borghei, A. M. (2011). Effect of some BED blends on the equivalence ratio, exhaust oxygen fraction and water and oil temperature of a diesel engine. *Biomass and bioenergy*, *35*(10), 4099-4106.

Bora, P. (2015). Formulation of micro-emulsion based hybrid biofuels from non-edible vegetable oil using non-ionic surface active agents.

Bose, R. (2022). Sterculia foetida-Eco-friendly, cost effective and rich sources of nutritious edible oil, animal food supplements as well as biofuel and to evaluate its antimicrobial and cytotoxic efficacy by comparing with other edible vegetable oils to validate its pharmaceutical application.

Bossio, M. R., Raimundi, M. J., & Correa, L. G. (2012). Programa de Entrenamiento en Habilidades Psicolgógicas en jugadoras de voleibol de alto rendimiento. *Cuadernos de psicología del deporte*, *12*(1).

Bougher, T., Khalek, I. A., Trevitz, S., & Akard, M. (2010). *Verification of a gaseous Portable Emissions Measurement System with a laboratory system using the Code of Federal Regulations Part 1065* (0148-7191).

Boysal, A., & Rahnejat, H. (1997). Torsional vibration analysis of a multi-body single cylinder internal combustion engine model. *Applied Mathematical Modelling*, *21*(8), 481-493.

Braga, J. W. B., dos Santos Junior, A. A., & Martins, I. S. (2014). Determination of viscosity index in lubricant oils by infrared spectroscopy and PLSR. *Fuel*, *120*, 171-178.

Bringas, J. E. (2004). *Hand Book of Comparative World Steel Standard s*.

British petroleum (BP). (2010). *BP Statistical Review of World Energy June 2010*. Retrieved 20th January from http://www.bp.com/productlanding.do?categoryId=6929&contentId=7044622

Broman, J. (2012). Development and demonstration of a low emissions four-stroke outboard marine engine utilizing Catalyst Technology. *SAE International Journal of Engines*, *5*(3), 1347-1360.

Burguera, J. L., & Burguera, M. (2012). Analytical applications of emulsions and microemulsions. *Talanta*, *96*, 11-20.

Burke, R., & Brace, C. (2010). *The effects of engine thermal conditions on performance, emissions and fuel consumption* (0148-7191).

Buyukkaya, E., & Cerit, M. (2008). Experimental study of NOx emissions and injection timing of a low heat rejection diesel engine. *International journal of thermal sciences*, *47*(8), 1096-1106.

Calcote, H. F. (1981). Mechanisms of soot nucleation in flames—A critical review. *Combustion and Flame*, *42*, 215-242.

Canakci, M., & Van Gerpen, J. (2001). Biodiesel production from oils and fats with high free fatty acids. *Transactions of the ASAE*, *44*(6), 1429.

Carraretto, C., Macor, A., Mirandola, A., Stoppato, A., & Tonon, S. (2004). Biodiesel as alternative fuel: Experimental analysis and energetic evaluations. *Energy*, *29*(12-15), 2195-2211.

Carrero, A., & Pérez, Á. (2012). Advances in biodiesel quality control, characterisation and standards development. In *Advances in biodiesel production* (pp. 91-130). Elsevier.

Castellanos, M. C., & Stevenson, P. R. (2011). Phenology, seed dispersal and difficulties in natural recruitment of the canopy tree Pachira quinata (Malvaceae). *Revista de Biología Tropical*, *59*(2), 921-933.

Cengel, Y., Boles, M., & Kanoğlu, M. (2019). Thermodynamics: an engineering approach, Nine Edition ed. In: McGraw-hill, New York.

Chakrabarty, S. (2021). Castor (Ricinus communis): An Underutilized Oil Crop in the. *Agroecosystems: Very Complex Environmental Systems*, 61.

Chanakaewsomboon, I., Tongurai, C., Photaworn, S., Kungsanant, S., & Nikhom, R. (2020). Investigation of saponification mechanisms in biodiesel production: Microscopic visualization of the effects of FFA, water and the amount of alkaline catalyst. *Journal of Environmental Chemical Engineering*, *8*(2), 103538.

Chang-Chih, C., Nien, C.-J., Chen, L.-G., Kuen-Yu, H., Wei-Jen, C., & Huang, H.-M. (2019). Effects of Sapindus mukorossi Seed Oil on Skin Wound Healing: In Vivo and in Vitro Testing. *International Journal of Molecular Sciences*, *20*(10).

Change, I. C. (2013). The physical science basis. *Contribution of working group I to the fifth assessment report of the intergovernmental panel on climate change*, *1535*, 2013.

Chapagain, S., Shrestha, S., Nakamura, T., Pandey, V., & Kazama, F. (2009). Arsenic occurrence in groundwater of Kathmandu Valley, Nepal. *Desalination and water treatment*, *4*(1-3), 248-254.

Charles, C., Gerasimchuk, I., Bridle, R., Moerenhout, T., Asmelash, E., & Laan, T. (2013). Biofuels—At what cost. *A review of costs and benefits of EU biofuel policies. Winnipeg, Manitoba, Canada: International Institute for Sustainable Development*.

Chatterjee, R., Mukherjee, S. K., Paul, B., & Chattopadhyaya, S. (2021). Comparative spectroscopic analysis, performance and emissions evaluation of Madhuca longifolia and Jatropha curcas produced biodiesel. *Environmental Science and Pollution Research*, *28*(44), 62444-62460.

Chen, H., He, J., Geng, L., Zhao, X., & Ma, J. (2019). Combustion and emission characteristics of a common rail diesel engine fueled with reformed diesel/palm oil/gasoline blend fuels. *International Journal of Green Energy*, *16*(14), 1165-1178.

Chen, H., He, J., & Hua, H. (2017). Investigation on combustion and emission performance of a common rail diesel engine fueled with diesel/biodiesel/polyoxymethylene dimethyl ethers blends. *Energy & Fuels*, *31*(11), 11710-11722.

Chen, P., Ibrahim, U., & Wang, J. (2014). Experimental investigation of diesel and biodiesel post injections during active diesel particulate filter regenerations. *Fuel*, *130*, 286-295.

Chen, R., Qin, Z., Han, J., Wang, M., Taheripour, F., Tyner, W., O'Connor, D., & Duffield, J. (2018). Life cycle energy and greenhouse gas emission effects of biodiesel in the United States with induced land use change impacts. *Bioresource technology*, *251*, 249-258.

Chen, Y., Jha, S., Raut, A., Zhang, W., & Liang, H. (2020). Performance characteristics of lubricants in electric and hybrid vehicles: a review of current and future needs. *Frontiers in Mechanical Engineering*, *6*, 571464.

Chisti, Y. (2007). Biodiesel from microalgae. *Biotechnology Advances*, *25*(3), 294-306. www.elsevier.com/locate/biotechadv

Chybowski, L., Kowalak, P., & Dąbrowski, P. (2023). Assessment of the Impact of Lubricating Oil Contamination by Biodiesel on Trunk Piston Engine Reliability. *Energies*, *16*(13), 5056.

Corsini, A., Marchegiani, A., Rispoli, F., Sciulli, F., & Venturini, P. (2015). Vegetable oils as fuels in diesel engine. Engine performance and emissions. *Energy Procedia*, *81*, 942-949.

da S. Bezerra, K., de O Zuppa Neto, T., Souza, C. L., Gomes, L. O., & Antoniosi Filho, N. R. (2021). Monitoring of lubricating oils used in diesel engine by biodiesel contamination from fuel dilution. *Lubrication Science*, *33*(8), 432-438.

da Silva, L. J., Alves, F. C., & de França, F. P. (2012). A review of the technological solutions for the treatment of oily sludges from petroleum refineries. *Waste Management & Research*, *30*(10), 1016-1030.

De Carvalho, C. C., & Caramujo, M. J. (2018). The various roles of fatty acids. *Molecules*, *23*(10), 2583.

De Donno, G. (2023). *Definition and Vibration Monitoring of the Endurance Test for an e-Axle* Politecnico di Torino].

Demirbas, A. (2008a). Comparison of transesterification methods for production of biodiesel from vegetable oils and fats. *Energy conversion and management*, *49*(1), 125-130.

Demirbas, A. (2008b). Heavy metal adsorption onto agro-based waste materials: a review. *Journal of hazardous materials*, *157*(2-3), 220-229.

Demirbas, A. (2009). Combustion efficiency impacts of biofuels. *Energy Sources, Part A: Recovery, Utilization, and Environmental Effects*, *31*(7), 602-609.

Demirbas, A. (2009). Progress and recent trends in biodiesel fuels. *Energy Conversion and Management*, *50*(1), 14-34. http://www.sciencedirect.com/science/article/B6V2P-4TP7H1N-1/2/5c9c1452cb34a9ce6f12403b4bd1a093

Demirbas, A. (2010). Use of algae as biofuel sources. *Energy conversion and management*, *51*(12), 2738-2749.
Demirbaş, A. (2003). Biodiesel fuels from vegetable oils via catalytic and non-catalytic supercritical alcohol transesterifications and other methods: a survey. *Energy conversion and management*, *44*(13), 2093-2109.
Demirbas, A., & Arin, G. (2002). An overview of biomass pyrolysis. *Energy sources*, *24*(5), 471-482.
Demirbaş, A., & Kara, H. (2006). New options for conversion of vegetable oils to alternative fuels. *Energy Sources, Part A*, *28*(7), 619-626.
Descombes, G., Maroteaux, F., & Feidt, M. (2003). Study of the interaction between mechanical energy and heat exchanges applied to IC engines. *Applied Thermal Engineering*, *23*(16), 2061-2078.
Devlin, M. T. (2018). Common properties of lubricants that affect vehicle fuel efficiency: A North American historical perspective. *Lubricants*, *6*(3), 68.
Dharmaraja, J., Nguyen, D. D., Shobana, S., Saratale, G. D., Arvindnarayan, S., Atabani, A., Chang, S. W., & Kumar, G. (2019). Engine performance, emission and bio characteristics of rice bran oil derived biodiesel blends. *Fuel*, *239*, 153-161.
Diaconis, P., & Freedman, D. (1986). On the consistency of Bayes estimates. *The Annals of Statistics*, 1-26.
Diaz, G. J. A., Montoya, J. P. G., Martinez, L. A. C., Olsen, D. B., & Navarro, A. S. (2019). Influence of engine operating conditions on combustion parameters in a spark ignited internal combustion engine fueled with blends of methane and hydrogen. *Energy conversion and management*, *181*, 414-424.
Dimirbas, A. (2003). Biodesel fuels from vegetable oils via catalytic and non-catalytic supercritical alcohol transesterification and other methods: a survey. *Energy conversion and management*, *44*(13), 2-093.
Dinkins, C., & Jones, C. J. M. S. U. E. M. P. n. M. A. (2013). Interpretation of soil test results for agriculture.
Disassa, H. D., Ancha, V. R., & Nallamothu, R. B. J. R. i. E. (2023). Experimental study of triple fuel physiognomies on LDRCCI diesel engine combustion. *20*, 101451.
Dorado, M. P., Ballesteros, E., Mittelbach, M., & López, F. J. (2004). Kinetic parameters affecting the alkali-catalyzed transesterification process of used olive oil. *Energy & Fuels*, *18*(5), 1457-1462.
Dunford, N. T. (2019). Chemistry of rice bran oil. In *Rice bran and rice bran oil* (pp. 1-18). Elsevier.
Dziubak, T., & Dziubak, S. D. (2022). A study on the effect of inlet air pollution on the engine component wear and operation. *Energies*, *15*(3), 1182.
Ebert, A., Olson, M., Bates, R., & Palada, M. (2019). Genetic resources, diversity and crop improvement. *The miracle tree: Moringa oleifera*.
El-Araby, R. (2024). Biofuel production: exploring renewable energy solutions for a greener future. *Biotechnology for Biofuels and Bioproducts*, *17*(1), 129.
El_Kassaby, M., & Nemit_allah, M. A. (2013). Studying the effect of compression ratio on an engine fueled with waste oil produced biodiesel/diesel fuel. *Alexandria Engineering Journal*, *52*(1), 1-11. https://doi.org/https://doi.org/10.1016/j.aej.2012.11.007
Elevitch, C. R., & Manner, H. I. (2006). Aleurites moluccana (kukui). *Traditional trees of Pacific Islands: their culture, environment and use Permanent Agriculture Resource, Holualoa*, *41*, 56.
Elkelawy, M., Mohamad, H. A. E., Abo-Samra, S., & Elshennawy, I. A.-E. (2023). Nanoparticles additives for diesel/biodiesel fuel blends as a performance and

emissions enhancer in the applications of direct injection diesel engines: A comparative review. *Journal of Engineering Research*, *7*(1), 112-121.
Encinar, J., Sánchez, N., Martínez, G., & García, L. (2011). Study of biodiesel production from animal fats with high free fatty acid content. *Bioresource technology*, *102*(23), 10907-10914.
Eriksson, L., & Sivertsson, M. (2015). Computing optimal heat release rates in combustion engines. *SAE International Journal of Engines*, *8*(3), 1069-1079.
Eryilmaz, T., Yesilyurt, M. K., Cesur, C., & Gokdogan, O. (2016). Biodiesel production potential from oil seeds in Turkey. *Renewable and Sustainable Energy Reviews*, *58*, 842-851.
Ewins, D. (2010). Control of vibration and resonance in aero engines and rotating machinery–An overview. *International journal of pressure vessels and piping*, *87*(9), 504-510.
Fadda, A., Sanna, D., Sakar, E. H., Gharby, S., Mulas, M., Medda, S., Yesilcubuk, N. S., Karaca, A. C., Gozukirmizi, C. K., & Lucarini, M. (2022). Innovative and sustainable technologies to enhance the oxidative stability of vegetable oils. *Sustainability*, *14*(2), 849.
Farouk, S. M., Tayeb, A. M., Abdel-Hamid, S. M., & Osman, R. M. (2024). Recent advances in transesterification for sustainable biodiesel production, challenges, and prospects: a comprehensive review. *Environmental Science and Pollution Research*, *31*(9), 12722-12747.
Fatma, S., Hameed, A., Noman, M., Ahmed, T., Shahid, M., Tariq, M., Sohail, I., & Tabassum, R. (2018). Lignocellulosic biomass: a sustainable bioenergy source for the future. *Protein and peptide letters*, *25*(2), 148-163.
Feuge, R., & Gros, A. T. (1949). Modification of vegetable oils. VII. Alkali catalyzed interesterification of peanut oil with ethanol. *Journal of the American oil chemists' society*, *26*(3), 97-102.
Firoz, S. (2017). A review: advantages and disadvantages of biodiesel. *International Research Journal of Engineering and Technology*, *4*(11), 530-533.
Foidl, N., Foidl, G., Sanchez, M., Mittelbach, M., & Hackel, S. (1996). Jatropha curcas L. as a source for the production of biofuel in Nicaragua. *Bioresource technology*, *58*(1), 77-82.
Freedman, B., Butterfield, R. O., & Pryde, E. H. (1986). Transesterification kinetics of soybean oil 1. *Journal of the American oil chemists' society*, *63*, 1375-1380.
Freedman, J. L. (1984). Effect of television violence on aggressiveness. *Psychological bulletin*, *96*(2), 227.
Frohlich, M., Michaelis, D., Strube, H. W., & Kruse, E. (2000). Acoustic voice analysis by means of the hoarseness diagram. *Journal of Speech, Language, and Hearing Research*, *43*(3), 706-720.
Gad, M., El-Araby, R., Abed, K., El-Ibiari, N., El Morsi, A., & El-Diwani, G. (2018). Performance and emissions characteristics of CI engine fueled with palm oil/palm oil methyl ester blended with diesel fuel. *Egyptian Journal of Petroleum*, *27*(2), 215-219.
Gaillard, Y., Krishnamoorthy, A., & Bevalot, F. (2004). Cerbera odollam: a 'suicide tree' and cause of death in the state of Kerala, India. *Journal of Ethnopharmacology 95*(2-3), 123-126.
Ganapathy, T., Gakkhar, R. P., & Murugesan, K. (2011). Influence of injection timing on performance, combustion and emission characteristics of Jatropha biodiesel engine. *Applied Energy*, *88*(12), 4376-4386. https://doi.org/https://doi.org/10.1016/j.apenergy.2011.05.016

Gashaw, A., & Teshita, A. (2014). Production of biodiesel from waste cooking oil and factors affecting its formation: A review. *International journal of renewable and sustainable energy*, *3*(5), 92-98.
Gebremariam, S. N., & Marchetti, J. M. (2018). Economics of biodiesel production. *Energy conversion and management*, *168*, 74-84.
Gebru, H. T. (2023). Investigation of the Performance and Emission Character Biodiesel-Diesel Blends in Direct Injection Diesel Engines. *10*(2), 60-73.
Ghadikolaei, M. A., Cheung, C. S., & Yung, K.-F. (2018). Study of combustion, performance and emissions of diesel engine fueled with diesel/biodiesel/alcohol blends having the same oxygen concentration. *Energy*, *157*, 258-269.
Ghanati, S. G., Doğan, B., & Yeşilyurt, M. K. (2024). The effects of the usage of silicon dioxide (SiO2) and titanium dioxide (TiO2) as nano-sized fuel additives on the engine characteristics in diesel engines: a review. *Biofuels*, *15*(2), 229-243.
Gharby, S. (2022). Refining vegetable oils: Chemical and physical refining. *The Scientific World Journal*, *2022*(1), 6627013.
Ghouila, Z., Sehailia, M., & Chemat, S. (2019). Vegetable oils and fats: Extraction, composition and applications. *Plant based "green chemistry 2.0" moving from evolutionary to revolutionary*, 339-375.
Giakoumis, E. G. (2013). A statistical investigation of biodiesel physical and chemical properties, and their correlation with the degree of unsaturation. *Renewable energy*, *50*, 858-878.
Giakoumis, E. G. (2016). Light-duty vehicles. In *Driving and Engine Cycles* (pp. 65-166). Springer.
Giakoumis, E. G. (2017). *Driving and engine cycles* (Vol. 1). Springer.
Giakoumis, E. G., & Giakoumis, E. G. (2017). Heavy-Duty Vehicles and Engines. *Driving and Engine Cycles*, 193-284.
Gielen, D., Boshell, F., Saygin, D., Bazilian, M. D., Wagner, N., & Gorini, R. (2019). The role of renewable energy in the global energy transformation. *Energy strategy reviews*, *24*, 38-50.
Glassman, I. (1989). Soot formation in combustion processes. Symposium (international) on combustion,
Graver, B., Zhang, K., & Rutherford, D. (2019). emissions from commercial aviation, 2018. *International Council on Clean Transportation*.
Green, D., & Lewis, R. (2008). The effects of soot-contaminated engine oil on wear and friction: a review. *Proceedings of the Institution of Mechanical Engineers, Part D: Journal of Automobile Engineering*, *222*(9), 1669-1689.
Greuter, E., & Zima, S. (2012). *Engine failure analysis*. Sae International.
Gui, M. M., Lee, K. T., & Bhatia, S. (2008). Feasibility of edible oil vs. non-edible oil vs. waste edible oil as biodiesel feedstock. *Energy*, *33*(11), 1646-1653. http://www.sciencedirect.com/science/article/B6V2S-4SYKKTH-2/2/4ac86a9326f66655c406ede735d3fed0
Gundekari, S., Mitra, J., & Varkolu, M. (2020). Classification, characterization, and properties of edible and non-edible biomass feedstocks. In *Advanced Functional Solid Catalysts for Biomass Valorization* (pp. 89-120). Elsevier.
Gunstone, F. D. (2011). Production and trade of vegetable oils. *Vegetable oils in food technology: composition, properties and uses*, *2*, 1-24.
Hamel, R., Lahmar, M., & Bou-Saïd, B. (2023). Elasto-hydrodynamic lubrication analysis of a porous misaligned crankshaft bearing operating with nanolubricants. *Mechanics & Industry*, *24*, 2.

Hanaki, K., & Portugal-Pereira, J. (2018). The effect of biofuel production on greenhouse gas emission reductions. *Biofuels and sustainability: holistic perspectives for policy-making*, 53-71.

Hanna, G. (1989). Proofs that prove and proofs that explain. *Proceedings of the international group for the psychology of mathematics education*, *2*, 45-51.

Hao, H., Geng, Y., Li, W., & Guo, B. (2015). Energy consumption and GHG emissions from China's freight transport sector: scenarios through 2050. *Energy policy*, *85*, 94-101.

Hasannuddin, A., Wira, J., Sarah, S., Aqma, W. W. S., Hadi, A. A., Hirofumi, N., Aizam, S., Aiman, M., Watanabe, S., & Ahmad, M. (2016). Performance, emissions and lubricant oil analysis of diesel engine running on emulsion fuel. *Energy conversion and management*, *117*, 548-557.

Hassan, M. H., & Kalam, M. A. (2013). An overview of biofuel as a renewable energy source: development and challenges. *Procedia engineering*, *56*, 39-53.

Hathurusingha, S., Ashwath, N., & Midmore, D. (2011). Provenance variations in seed-related characters and oil content of Calophyllum inophyllum L. in northern Australia and Sri Lanka. *New Forests*, *41*, 89-94.

Hayyan, A., Alam, M. Z., Mirghani, M. E., Kabbashi, N. A., Hakimi, N. I. N. M., Siran, Y. M., & Tahiruddin, S. (2011). Reduction of high content of free fatty acid in sludge palm oil via acid catalyst for biodiesel production. *Fuel Processing Technology*, *92*(5), 920-924.

Heywood, J. B. (1988). Combustion engine fundamentals. *1ª Edição. Estados Unidos*, *25*, 1117-1128.

Heywood, J. B. (2018). *Internal combustion engine fundamentals*. McGraw-Hill Education.

Hirani, A. H., Javed, N., Asif, M., Basu, S. K., & Kumar, A. (2018). A review on first-and second-generation biofuel productions. *Biofuels: greenhouse gas mitigation and global warming: next generation biofuels and role of biotechnology*, 141-154.

Ho, D. P., Ngo, H. H., & Guo, W. (2014). A mini review on renewable sources for biofuel. *Bioresource technology*, *169*, 742-749.

Hoag, K., & Dondlinger, B. (2015). *Vehicular engine design*. Springer.

Hoegh-Guldberg, O., Jacob, D., Taylor, M., Guillén Bolaños, T., Bindi, M., Brown, S., Camilloni, I. A., Diedhiou, A., Djalante, R., & Ebi, K. (2019). The human imperative of stabilizing global climate change at 1.5 C. *Science*, *365*(6459), eaaw6974.

Holechek, J. L., Geli, H. M., Sawalhah, M. N., & Valdez, R. (2022). A global assessment: can renewable energy replace fossil fuels by 2050? *Sustainability*, *14*(8), 4792.

Holmberg, K., Andersson, P., Nylund, N.-O., Mäkelä, K., & Erdemir, A. (2014). Global energy consumption due to friction in trucks and buses. *Tribology International*, *78*, 94-114.

Howard, K. (2014). Advanced engine oils to improve the performance of modern internal combustion engines. In *Alternative fuels and advanced vehicle technologies for improved environmental performance* (pp. 138-164). Elsevier.

Hsu, S. M., & Gates, R. S. (2005). Boundary lubricating films: formation and lubrication mechanism. *Tribology International*, *38*(3), 305-312.

Hu, T., Teng, H., Luo, X., & Chen, B. (2015). Impact of fuel injection on dilution of engine crankcase oil for turbocharged gasoline direct-injection engines. *SAE International Journal of Engines*, *8*(3), 1107-1116.

Huang, L., Wang, Y., Li, Z., Zhang, L., Yin, Y., Chen, C., & Ren, S. (2021). Experimental study on piloted ignition temperature and auto ignition temperature of heavy oils at high pressure. *Energy*, *229*, 120644.

Hussain, J., & Zhou, K. (2022). Globalization, industrialization, and urbanization in Belt and Road Initiative countries: implications for environmental sustainability and energy demand. *Environmental Science and Pollution Research*, *29*(53), 80549-80567.

Ibrahim, S., Abed, K., & Gad, M. (2014). Experimental Investigation of Diesel Engine Performance Burning Preheated Jatropha Oil. *World Applied Sciences Journal*, *31*(7), 1231-1236.

Imtenan, S., Varman, M., Masjuki, H., Kalam, M., Sajjad, H., Arbab, M., & Fattah, I. R. (2014). Impact of low temperature combustion attaining strategies on diesel engine emissions for diesel and biodiesels: A review. *Energy conversion and management*, *80*, 329-356.

Jacobson, S., & Hogmark, S. (2009). Surface modifications in tribological contacts. *Wear*, *266*(3-4), 370-378.

Jain, A., & Sirisha, V. (2015). Algal biodiesel: Third-generation biofuel. *Marine Bioenergy: Trends and Developments*, 423-457.

Jena, P. C., Raheman, H., Prasanna, G. V. K., & Machavaram, R. (2010). Biodiesel production from mixture of mahua and simarouba oils with high free fatty acids. *Biomass and Bioenergy*, *34*(8), 1108-1116. http://www.sciencedirect.com/science/article/B6V22-4YP6SCY-2/2/0f1aaecd1398d5271a0098b779c09f31

Ji, J. (2014). Secondary resonances of a quadratic nonlinear oscillator following two-to-one resonant Hopf bifurcations. *Nonlinear Dynamics*, *78*, 2161-2184.

Jiaqiang, E., Liu, G., Zhang, Z., Han, D., Chen, J., Wei, K., Gong, J., & Yin, Z. (2019). Effect analysis on cold starting performance enhancement of a diesel engine fueled with biodiesel fuel based on an improved thermodynamic model. *Applied Energy*, *243*, 321-335.

Johnson, T., & Joshi, A. (2018). Review of vehicle engine efficiency and emissions. *SAE International Journal of Engines*, *11*(6), 1307-1330.

Joshi, G., Pandey, J. K., Rana, S., & Rawat, D. S. (2017). Challenges and opportunities for the application of biofuel. *Renewable and Sustainable Energy Reviews*, *79*, 850-866.

Kaisan, M., Anafi, F., Nuszkowski, J., Kulla, D., & Umaru, S. (2020). Calorific value, flash point and cetane number of biodiesel from cotton, jatropha and neem binary and multi-blends with diesel. *Biofuels*.

Kalaimurugan, K., Karthikeyan, S., Periyasamy, M., & Mahendran, G. (2020). Experimental investigations on the performance characteristics of CI engine fuelled with cerium oxide nanoparticle added biodiesel-diesel blends. *Materials Today: Proceedings*, *33*, 2882-2885.

Kalaoja, J. (2020). *On-Line Oil Condition Monitoring for Marine Gearboxes: This thesis addresses the importance of oil condition monitoring in marine reduction gearboxes and compares the sensitivity and usage of three different sensors, each with its own working principle* University of Agder].

Kannahi, M., & Arulmozhi, R. (2013). Production of biodiesel from edible and non-edible oils using Rhizopus oryzae and Aspergillus niger. *Asian Journal of Plant Science and Research*, *3*(5), 60-64.

Kansedo, J., Lee, K. T., & Bhatia, S. (2009). Cerbera odollam (sea mango) oil as a promising non-edible feedstock for biodiesel production. *Fuel*, *88*(6), 1148-1150. http://www.sciencedirect.com/science/article/B6V3B-4V82J2M-1/2/a9c9afbc8cf3d2198830467df5d328bb

Kanyane, L. R., Popoola, A. P., Pityana, S., & Tlotleng, M. (2022). Heat-treatment effect on anti-corrosion behaviour and tribological properties of LENS in-situ synthesized

titanium aluminide. *International Journal of Lightweight Materials and Manufacture*, *5*(2), 153-161. https://doi.org/10.1016/j.ijlmm.2021.11.006
Karmakar, A., Karmakar, S., & Mukherjee, S. (2010). Properties of various plants and animals feedstocks for biodiesel production. *Bioresource Technology*, *101*(19), 7201-7210.
Karmee, S. K., & Chadha, A. (2005). Preparation of biodiesel from crude oil of Pongamia pinnata. *Bioresource technology*, *96*(13), 1425-1429.
Kaur, A., Roy, M., & Kundu, K. (2017). Transesterification process optimization for tung oil methyl ester (Aleurites fordii) and characterization of fuel as a substitute for diesel. *IJCS*, *5*(6), 632-638.
Kebede, L., Tulu, G. S., & Lisinge, R. T. (2022). Diesel-fueled public transport vehicles and air pollution in Addis Ababa, Ethiopia: Effects of vehicle size, age and kilometers travelled. *Atmospheric Environment: X*, *13*, 100144.
Keeley, J., Seide, W. M., Eid, A., & Kidewa, A. L. (2014). Large-scale land deals in Ethiopia. *International Institute for Environment and Development: London, UK*.
halafvandi, S. A., Pazokian, M. A., & Fathollahi, E. (2022). The investigation of viscometric properties of the most reputable types of viscosity index improvers in different lubricant base oils: API groups I, II, and III. *Lubricants*, *10*(1), 6.
khan, T. M. Y., Atabani, A. E., Badruddin, I. A., Badarudin, A., Khayoon, M. S., & Triwahyono, S. (2014). Recent scenario and technologies to utilize non-edible oils for biodiesel production. *Renewable and Sustainable Energy Reviews*, *37*, 840-851. https://doi.org/https://doi.org/10.1016/j.rser.2014.05.064
Khurmi, R. S., & Gupta, J. K. (2005). *A Textbook of Internal Combustion Engines*. Eurasia Publishing House (P) Ltd.
Khurana, S., & Bhatnagar, S. (2024). Non-Edible Oils as Biodiesel. *Oils and Fats as Raw Materials for Industry*, 267-284.
Kibazohi, O., & Sangwan, R. S. (2011). Vegetable oil production potential from Jatropha curcas, Croton megalocarpus, Aleurites moluccana, Moringa oleifera and Pachira glabra: Assessment of renewable energy resources for bio-energy production in Africa. *Biomass and Bioenergy*, *35*(3), 1352-1356. http://www.sciencedirect.com/science/article/B6V22-520CTNV-4/2/f51e74cb58724e5f1f8955c6fe81f87c
Kirschstein, T., & Meisel, F. (2015). GHG-emission models for assessing the eco-friendliness of road and rail freight transports. *Transportation Research Part B: Methodological*, *73*, 13-33.
Kishore Pandian, A., Munuswamy, D. B., Radhakrishana, S., Bathey Ramakrishnan, R. B., Nagappan, B., & Devarajan, Y. (2017). Influence of an oxygenated additive on emission of an engine fueled with neat biodiesel. *Petroleum Science*, *14*, 791-797.
Knothe, G. (2005). Dependence of biodiesel fuel properties on the structure of fatty acid alkyl esters. *Fuel Processing Technology*, *86*(10), 1059-1070.
Knothe, G. (2010). History of vegetable oil-based diesel fuels. In *The biodiesel handbook* (pp. 5-19). Elsevier.
Knothe, G., Cermak, S. C., & Evangelista, R. L. (2010). Biodiesel and renewable diesel: A comparison. *Progress in Energy and Combustion Science*, *36*(3), 364-373. http://www.sciencedirect.com/science/article/B6V3W-4Y0TDNV-1/2/31a164bcb4286f523b4358ba43b4c91c
Kocián, D., Hájek, M., Vávra, A., Frolich, K., & Kocik, J. (2022). The influence of residue sodium ions in mixed oxide on catalytic activity in transesterification of vegetable oil. *Molecular Catalysis*, *517*, 112017.

Koizumi, T. (2015). Biofuels and food security. *Renewable and Sustainable Energy Reviews*, *52*, 829-841.
Köten, H., & Parlakyiğit, A. S. (2018). Effects of the diesel engine parameters on the ignition delay. *Fuel*, *216*, 23-28.
Kouame, S. D. B., Vander Wal, R. L., & Perez, J. (2015). Deposit formation from lubricant degradation: a uniform layer deposition model. *Lubrication Science*, *27*(1), 1-13.
Kragelsky, I. V., & Alisin, V. V. e. (2016). *Friction wear lubrication: tribology handbook*. Elsevier.
Krist, S. (2020). Vegetable fats and oils.
Krutof, A., & Hawboldt, K. (2016). Blends of pyrolysis oil, petroleum, and other bio-based fuels: a review. *Renewable and Sustainable Energy Reviews*, *59*, 406-419.
Kumar, A., & Sharma, S. (2011). Potential non-edible oil resources as biodiesel feedstock: An Indian perspective. *Renewable and Sustainable Energy Reviews*, *15*(4), 1791-1800. http://www.sciencedirect.com/science/article/B6VMY-525GV5J-4/2/add9c93b7421fcfdb424e2ab8aab5890
Kumar, N., & Chauhan, S. R. (2015). Evaluation of endurance characteristics for a modified diesel engine runs on jatropha biodiesel. *Applied Energy*, *155*, 253-269.
Kumar, S., Thakur, A., Kumar, N., & Husein, M. M. (2020). A novel oil-in-water drilling mud formulated with extracts from Indian mango seed oil. *Petroleum Science*, *17*(1), 196-210.
Kurre, S. K., Garg, R., & Pandey, S. (2017). A review of biofuel generated contamination, engine oil degradation and engine wear. *Biofuels*, *8*(2), 273-280.
Lacerda, T. M., & Gandini, A. (2020). The cationic polymerization of tung oil and its fatty-acid methyl ester. *Industrial crops and products*, *157*, 112886.
Lacey, P., Gail, S., Kientz, J. M., Benoist, G., Downes, P., & Daveau, C. (2012). Fuel quality and diesel injector deposits. *SAE International Journal of Fuels and Lubricants*, *5*(3), 1187-1198.
Lack, D. A., Cappa, C. D., Langridge, J., Bahreini, R., Buffaloe, G., Brock, C., Cerully, K., Coffman, D., Hayden, K., & Holloway, J. (2011). Impact of fuel quality regulation and speed reductions on shipping emissions: implications for climate and air quality. *Environmental science & technology*, *45*(20), 9052-9060.
Lahane, S., & Subramanian, K. (2015). Effect of different percentages of biodiesel–diesel blends on injection, spray, combustion, performance, and emission characteristics of a diesel engine. *Fuel*, *139*, 537-545.
Lahane, S., & Subramanian, K. J. F. (2015). Effect of different percentages of biodiesel–diesel blends on injection, spray, combustion, performance, and emission characteristics of a diesel engine. *139*, 537-545.
Lakshmi, D. V., & Lakshmi, M. S. (2020). Integrated technological tools for effective blended learning. 2020 IEEE Bombay Section Signature Conference (IBSSC),
Lakshminarayanan, P., & Nayak, N. S. (2011). *Critical component wear in heavy duty engines*. John Wiley & Sons.
Lalvani, J. I. J., Parthasarathy, M., Dhinesh, B., & Annamalai, K. (2015). Experimental investigation of combustion, performance and emission characteristics of a modified piston. *Journal of Mechanical Science and Technology*, *29*, 4519-4525.
Lamichhane, G., Khadka, S., Adhikari, S., Koirala, N., & Poudyal, D. P. (2020). Biofuel production from waste cooking oils and its physicochemical properties in comparison to petrodiesel. *Nepal Journal of Biotechnology*, *8*(3), 87-94.
Laurens, L. M., Quinn, M., Van Wychen, S., Templeton, D. W., & Wolfrum, E. J. (2012). Accurate and reliable quantification of total microalgal fuel potential as fatty acid

methyl esters by in situ transesterification. *Analytical and bioanalytical chemistry*, *403*, 167-178.
Lei, B., Shen, N., Ji, D., Ouyang, R., Yang, L., Liu, Q., Gao, B., & Wang, Z. (2024). A Comprehensive Review of Key Technologies for Enhancing the Reliability of Aero-Engines. *IEEE Access*.
Li, B., Li, Y., Liu, H., Liu, F., Wang, Z., & Wang, J. J. A. E. (2017). Combustion and emission characteristics of diesel engine fueled with biodiesel/PODE blends. *206*, 425-431.
Li, X.-Y., & Tang, B.-J. (2017). Incorporating the transport sector into carbon emission trading scheme: an overview and outlook. *Natural Hazards*, *88*, 683-698.
Li, Y., Wang, S., Xu, T., Li, J., Zhang, Y., Xu, T., & Yang, J. (2021). Novel designs for the reliability and safety of supercritical water oxidation process for sludge treatment. *Process Safety and Environmental Protection*, *149*, 385-398.
Lim, B. Y., Shamsudin, R., Baharudin, B. H. T., & Yunus, R. (2015). A review of processing and machinery for Jatropha curcas L. fruits and seeds in biodiesel production: Harvesting, shelling, pretreatment and storage. *Renewable and Sustainable Energy Reviews*, *52*, 991-1002.
Lin, C.-Y., & Lu, C. (2021). Development perspectives of promising lignocellulose feedstocks for production of advanced generation biofuels: A review. *Renewable and Sustainable Energy Reviews*, *136*, 110445.
Lin, L., Cunshan, Z., Vittayapadung, S., Xiangqian, S., & Mingdong, D. (2011). Opportunities and challenges for biodiesel fuel. *Applied Energy*, *88*(4), 1020-1031.
Lin, L., Zhou, C., Saritporn, V., Shen, X., & Dong, M. (2011). Opportunities and challenges for biodiesel fuel. *Applied Energy*, *88*(4), 1020-1031. http://www.sciencedirect.com/science/article/B6V1T-51BWXXB-2/2/e3497034b154252119e399aa26608544
Linhares, T. B., da Silva Scari, A., & Vimieiro, C. B. S. (2024). Causes of failures in vibrating screens: A literature review. *Minerals Engineering*, *218*, 109027.
Lopez, D. C., & Neto, S. (2011). Potential Crops for Biodiesel Production in Brazil: A Review. *World Journal of Agricultural Sciences*, *7*(2), 206-217.
Lü, X.-c., Yang, J.-g., Zhang, W.-g., Huang, Z. J. E., & Fuels. (2005). Improving the combustion and emissions of direct injection compression ignition engines using oxygenated fuel additives combined with a cetane number improver. *19*(5), 1879-1888.
Luo, J., Zhang, H., Liu, Z., Zhang, Z., Pan, Y., Liang, X., Wu, S., Xu, H., Xu, S., & Jiang, C. (2023). A review of regeneration mechanism and methods for reducing soot emissions from diesel particulate filter in diesel engine. *Environmental Science and Pollution Research*, *30*(37), 86556-86597.
Luque, R., Herrero-Davila, L., Campelo, J. M., Clark, J. H., Hidalgo, J. M., Luna, D., Marinas, J. M., & Romero, A. A. (2008). Biofuels: a technological perspective. *Energy & Environmental Science*, *1*(5), 542-564.
Ma, F., & Hanna, M. A. (1999). Biodiesel production: a review. *Bioresource technology*, *70*(1), 1-15.
Ma, M., Li, X., Liang, H., Jiang, H., & Cui, H. (2023). Chemical constituents variation of seed oil of the Chinese tallow tree (Sapium sebiferum (L.) Roxb) at different harvesting time. *Industrial crops and products*, *202*, 117061.
MAcián, V., TorMos, B., Bastidas, S., & Pérez, T. (2020). Improved fleet operation and maintenance through the use of low viscosity engine oils: fuel economy and oil performance. *Eksploatacja i Niezawodność*, *22*(2).

Macian, V., Tormos, B., Ruiz, S., & Miro, G. (2016). Low viscosity engine oils: Study of wear effects and oil key parameters in a heavy duty engine fleet test. *Tribology International*, *94*, 240-248.

Mahanta, P., & Shrivastava, A. (2011). *Technology development of bio-diesel as an energy alternative.* Retrieved 12th March from http://www.newagepublishers.com/samplechapter/001305.pdf.

Mahdisoozani, H., Mohsenizadeh, M., Bahiraei, M., Kasaeian, A., Daneshvar, A., Goodarzi, M., & Safaei, M. R. (2019). Performance enhancement of internal combustion engines through vibration control: state of the art and challenges. *Applied Sciences*, *9*(3), 406.

Maher, K., & Bressler, D. (2007). Pyrolysis of triglyceride materials for the production of renewable fuels and chemicals. *Bioresource technology*, *98*(12), 2351-2368.

Mahesar, S., Sherazi, S., Khaskheli, A. R., & Kandhro, A. A. (2014). Analytical approaches for the assessment of free fatty acids in oils and fats. *Analytical Methods*, *6*(14), 4956-4963.

Maina, L. (2021). *Investigation of potential of a bifunctional catalyst for the simultaneous esterification and transesterification of high free fatty acid feedstock* Cape Peninsula University of Technology].

Malla, F. A., Bandh, S. A., Wani, S. A., Hoang, A. T., & Sofi, N. A. (2023). Biofuels: potential alternatives to fossil fuels. In *Biofuels in circular economy* (pp. 1-15). Springer.

Mamtani, K., Shahbaz, K., & Farid, M. M. (2021). Glycerolysis of free fatty acids: A review. *Renewable and Sustainable Energy Reviews*, *137*, 110501.

Marín, P. J., & Rhea, M. R. (2010). Effects of vibration training on muscle strength: a meta-analysis. *The Journal of Strength & Conditioning Research*, *24*(2), 548-556.

Marques, A. C., Fuinhas, J. A., & Pereira, D. A. (2018). Have fossil fuels been substituted by renewables? An empirical assessment for 10 European countries. *Energy policy*, *116*, 257-265.

Martini, A., Ramasamy, U. S., & Len, M. (2018). Review of viscosity modifier lubricant additives. *Tribology Letters*, *66*, 1-14.

Mas'ud, F., Mahendradatta, M., Laga, A., & Zainal, Z. (2017). Component, fatty acid and mineral composition of rice bran oil extracted by multistage with hexane and ethanol. *International Journal of Scientific & Technology Research*, *6*(11), 63-69.

Mathes, K. (2000). ASTM Committee D09—A History of Success. In *Electrical Insulating Materials: International Issues*. ASTM International.

Mathews, J. A. (2008). Carbon-negative biofuels. *Energy policy*, *36*(3), 940-945.

Matveevsky, R., & Buyanovsky, I. (1986). Principal characteristics of boundary lubrication. *ASLE transactions*, *30*(4), 526-530.

Md Ruhul, A. (2017). *Optimization of aphanamixis based biodiesel and its combustion characteristics/Md. Ruhul Amin* University of Malaya].

Mijić, A., Liović, I., Zdunić, Z., Marić, S., Marjanović-Jeromela, A., & Jankulovska, M. (2009). Quantitative analysis of oil yield and its components in sunflower (Helianthus annuus L.). *Romanian Agricultural Research*, *26*, 41-46.

Milojević, S., Savić, S., Marić, D., Stopka, O., Krstić, B., & Stojanović, B. (2022). Correlation between emission and combustion characteristics with the compression ratio and fuel injection timing in tribologically optimized diesel engine. *Tehnički vjesnik*, *29*(4), 1210-1219.

Mishra, D. (2007). *Fundamentals of combustion*. PHI Learning Pvt. Ltd.

Misra, R. D., & Murthy, M. S. (2011). Performance, emission and combustion evaluation of soapnut oil-diesel blends in a compression ignition engine. *Fuel*, *90*(7), 2514-2518.

http://www.sciencedirect.com/science/article/B6V3B-52D3W3B-3/2/651fd675a849c28607fb6edc100c9f38
Mitchell, B. J., Zare, A., Bodisco, T. A., Nabi, M. N., Hossain, F. M., Ristovski, Z. D., & Brown, R. J. (2017). Engine blow-by with oxygenated fuels: A comparative study into cold and hot start operation. *Energy*, *140*, 612-624.
Mitiku, B. (2020). The Need for Environmental pollution Tax in Ethiopia.
Mobley, R. K. (2011). *Maintenance fundamentals*. Elsevier.
Mondal, M. A. H., Bryan, E., Ringler, C., Mekonnen, D., & Rosegrant, M. (2018). Ethiopian energy status and demand scenarios: prospects to improve energy efficiency and mitigate GHG emissions. *Energy*, *149*, 161-172.
Monieta, J. (2020). *Impact of Using Residual Fuels on the Wear of Selected Elements of Self-Ignition Internal Combustion Engines* (0148-7191).
Morone, P., Cottoni, L., & Giudice, F. (2023). Biofuels: Technology, economics, and policy issues. In *Handbook of biofuels production* (pp. 55-92). Elsevier.
Morris, D. M. (2015). *The cold driver: Driving performance under thermal stress* Clemson University].
Moser, B. R. (2009). Biodiesel production, properties, and feedstocks. *In Vitro Cellular & Developmental Biology-Plant*, *45*, 229-266.
Mujahid, A., & Dickert, F. L. (2012). Monitoring automotive oil degradation: analytical tools and onboard sensing technologies. *Analytical and bioanalytical chemistry*, *404*, 1197-1209.
Murawski, A. (2017). α-Eleostearic Acid Extraction by Saponification of Tung Oil and Its Subsequent Polymerization.
Murphy, J. (2001). *Additives for plastics handbook*. Elsevier.
Naeem, M. M., Al-Sakkari, E. G., Boffito, D. C., Rene, E. R., Gadalla, M. A., & Ashour, F. H. (2023). Single-stage waste oil conversion into biodiesel via sonication over bio-based bifunctional catalyst: Optimization, preliminary techno-economic and environmental analysis. *Fuel*, *341*, 127587. https://doi.org/https://doi.org/10.1016/j.fuel.2023.127587
Negm, N. A., Abou Kana, M. T., Youssif, M. A., Mohamed, M. Y., Biresaw, G., & Mittal, K. (2017). Biofuels from Vegetable Oils as Alternative Fuels: Advantages and Disadvantages290. In *Surfactants in Tribology, Volume 5* (pp. 289-367). CRC Press.
Newman, P., Kenworthy, J., & Glazebrook, G. (2013). Peak car use and the rise of global rail: why this is happening and what it means for large and small cities. *Journal of Transportation Technologies*, *3*.
Ni, P., Wang, X., & Li, H. (2020). A review on regulations, current status, effects and reduction strategies of emissions for marine diesel engines. *Fuel*, *279*, 118477.
Nikolakopoulos, P. G., Mavroudis, S., & Zavos, A. (2018). Lubrication performance of engine commercial oils with different performance levels: The effect of engine synthetic oil aging on piston ring tribology under real engine conditions. *Lubricants*, *6*(4), 90.
No, S.-Y. (2011). Inedible vegetable oils and their derivatives for alternative diesel fuels in CI engines: A review. *Renewable and Sustainable Energy Reviews*, *15*(1), 131-149.
No, S. Y. (2011). Inedible vegetable oils and their derivatives for alternative diesel fuels in CI engines: A review. *Renewable and Sustainable Energy Reviews*, *15*(1), 131-149. http://www.sciencedirect.com/science/article/B6VMY-50TY2CM-3/2/4910f78106778b85f8bbbaf6a0c2bdb4
Nordin, I., Elofsson, K., & Jansson, T. (2024). Cost-effective reductions in greenhouse gas emissions: Reducing fuel consumption or replacing fossil fuels with biofuels. *Energy policy*, *190*, 114138.

Norouzi, N., Fani, M., & Ziarani, Z. K. (2020). The fall of oil Age: A scenario planning approach over the last peak oil of human history by 2040. *Journal of Petroleum Science and Engineering*, *188*, 106827.

Nyakuma, B. B., Mahyon, N. I., Chiong, M. S., Rajoo, S., Pesiridis, A., Wong, S. L., & Martinez-Botas, R. (2023). Recovery and utilisation of waste heat from flue/exhaust gases: a bibliometric analysis (2010–2022). *Environmental Science and Pollution Research*, *30*(39), 90522-90546.

O'Driscoll, R., Stettler, M. E., Molden, N., Oxley, T., & ApSimon, H. M. (2018). Real world CO2 and NOx emissions from 149 Euro 5 and 6 diesel, gasoline and hybrid passenger cars. *Science of the total environment*, *621*, 282-290.

Oliveira, L., & Da Silva, M. (2013). Comparative study of calorific value of rapeseed, soybean, jatropha curcas and crambe biodiesel. *Renewable Energy and Power Quality Journal*, *1*(1), 679-682.

Osawa, W. O. (2016). *Two-stage chemical and enzymatic strategies for the preparation of biodiesel from croton megalocarpus oil and evaluation of its engine performance and oxidation stability* University of Nairobi].

Outlook, B. E. (2016). BP Energy Outlook 2035, BP PLC. In.

Palash, S., Kalam, M., Masjuki, H., Masum, B., Fattah, I. R., & Mofijur, M. (2013). Impacts of biodiesel combustion on NOx emissions and their reduction approaches. *Renewable and Sustainable Energy Reviews*, *23*, 473-490.

Palmer, H. B., & Cullis, C. F. (1965). The formation of carbon from gases. *Chemistry and physics of carbon*, *1*, 265-325.

Panchal, T. M., Patel, A., Chauhan, D., Thomas, M., & Patel, J. V. (2017). A methodological review on bio-lubricants from vegetable oil based resources. *Renewable and Sustainable Energy Reviews*, *70*, 65-70.

Paravantis, J. A. (2022). Socioeconomic aspects of third-generation biofuels. In *3rd Generation Biofuels* (pp. 869-917). Elsevier.

Park, L. K., Liu, J., Yiacoumi, S., Borole, A. P., & Tsouris, C. (2017). Contribution of acidic components to the total acid number (TAN) of bio-oil. *Fuel*, *200*, 171-181.

Park, Y.-J., Choe, Y.-h., & Kim, B.-S. (2015). Bovine viral diarrhoea (BVD) virus antiviral activity of Korean Tung Tree (Aleurites fordii) extracts in vivo. *Indian Journal of Animal Research*, *49*(6), 823-826.

Parliment, T. H. (2020). Solvent extraction and distillation techniques. *Techniques for analyzing food aroma*, 1-26.

Patil-Gadhe, A., & Pokharkar, V. (2014). Montelukast-loaded nanostructured lipid carriers: part I oral bioavailability improvement. *European Journal of Pharmaceutics and Biopharmaceutics*, *88*(1), 160-168.

Peetla, C., & Labhasetwar, V. (2009). Effect of molecular structure of cationic surfactants on biophysical interactions of surfactant-modified nanoparticles with a model membrane and cellular uptake. *Langmuir*, *25*(4), 2369-2377.

PENFOLD, A., & SMITH-WHITE, S. (1941). STUDIES ON THE CULTIVATION OF THE TUNG OIL TREE. Journal and Proceedings of the Royal Society of New South Wales,

Perona, J. J. (2017). Biodiesel for the 21st century renewable energy economy. *Energy LJ*, *38*, 165.

Piancastelli, L. (2012). Method evaluating the durability of aircraft piston engines. *DOAJ: Directory of Open Access Journals-DOAJ*.

Pinzi, S., Garcia, I. L., Gimenez, F. J. L., Castro, M. D. L., Dorado, G., & Dorado, M. P. (2009). The Ideal Vegetable Oil-based Biodiesel Composition: A Review of Social, Economical and Technical Implications. *Energy & Fuels*, *23*(5), 2325-2341.

Porpatham, E., Ramesh, A., & Nagalingam, B. (2012). Effect of compression ratio on the performance and combustion of a biogas fuelled spark ignition engine. *Fuel*, *95*, 247-256.

Pradhan, D., Singh, R., Bendu, H., & Mund, R. (2016). Pyrolysis of Mahua seed (Madhuca indica)–Production of biofuel and its characterization. *Energy conversion and management*, *108*, 529-538.

Pragya, N., Pandey, K. K., & Sahoo, P. (2013). A review on harvesting, oil extraction and biofuels production technologies from microalgae. *Renewable and Sustainable Energy Reviews*, *24*, 159-171.

Prahladbhai, P. S., & Brahmbhatt, P. K. (2023). INFLUENCE OF BIO LUBRICANT ON TRIBOLOGICAL ASSESSMENT IN CI ENGINE FUELED WITH BIODIESEL BLEND.

Pulkrabek, W. W. (2004). Engineering fundamentals of the internal combustion engine. In.

Pundir, B. (2008). Fuel economy of indian passenger vehicles-status of technology and potential FE improvements. *Greenpeace India Society*.

Pydimalla, M., Husaini, S., Kadire, A., & Verma, R. K. (2023). Sustainable biodiesel: A comprehensive review on feedstock, production methods, applications, challenges and opportunities. *Materials Today: Proceedings*, *92*, 458-464.

Qi, D., Geng, L., Chen, H., Bian, Y. Z., Liu, J., & Ren, X. C. (2009). Combustion and performance evaluation of a diesel engine fueled with biodiesel produced from soybean crude oil. *Renewable energy*, *34*(12), 2706-2713.

Raboni, M., Viotti, P., & Capodaglio, A. G. (2015). A comprehensive analysis of the current and future role of biofuels for transport in the European Union (EU). *Revista ambiente & agua*, *10*(1), 9-21.

Raghuvanshi, N. S., Johari, A., Saxena, M., Gupta, A. K., Kumar, A., Kumar, A., Kumar, A., & Gupta, A. (2024). Eco-friendly lubricants. In *Performance Characterization of Lubricants* (pp. 70-96). CRC Press.

Ragit, S. S., Mohapatra, S. K., Kundu, K., & Gill, P. (2011). Optimization of neem methyl ester from transesterification process and fuel characterization as a diesel substitute. *Biomass and Bioenergy*, *35*(3), 1138-1144. http://www.sciencedirect.com/science/article/B6V22-51ST6RT-1/2/51f06a4a37752c97f1826a5ac6137199

Ragupathi, K., & Mani, I. (2021). Durability and lube oil contamination study on diesel engine fueled with various alternative fuels: A review. *Energy Sources, Part A: Recovery, Utilization, and Environmental Effects*, *43*(8), 932-943.

Rahmato, D. (2011). *Land to investors: Large-scale land transfers in Ethiopia*. African Books Collective.

Raj, G. S. S., Rabibunnisa, H., Faizul, A. H., Nandagopal, R., Venkataraman, S., Gunasekaran, G., & Venugopal, R. (2009). *Development of Engine Test Facility of Armoured Fighting Vehicles* (0148-7191).

Rajak, U., Nashine, P., & Verma, T. N. (2019). Effect of fuel injection pressure in a diesel engine using microalgae-diesel Emulsion. *International Journal of Engineering and Advanced Technology*, *8*(3), 263-271.

Rajha, H. N., El Darra, N., Hobaika, Z., Boussetta, N., Vorobiev, E., Maroun, R. G., & Louka, N. (2014). Extraction of total phenolic compounds, flavonoids, anthocyanins and tannins from grape byproducts by response surface methodology. Influence of solid-liquid ratio, particle size, time, temperature and solvent mixtures on the optimization process. *Food and Nutrition Sciences*, *2014*.

Rajkumar, R., Yaakob, Z., & Takriff, M. S. (2014). Potential of the Micro and Macro Algae for Biofuel Production: A Brief Review. *Bioresources*, *9*(1).

Ramadhas, A., Jayaraj, S., & Muraleedharan, C. (2004). Use of vegetable oils as IC engine fuels—a review. *Renewable energy*, *29*(5), 727-742.

Ramanjaneyulu, A., Chaitanya, T., Raghu Rami Reddy, P., Rajashekhar, M., Handa, A., Arunachalam, A., Suresh Ramanan, S., Giri Rao, L., Sreemannarayana, B., & Joseph, B. (2025). Monograph on "Pongamia"(Pongamia pinnata). *Professor Jayashankar Telangana Agricultural University (PJTAU), Rajendranagar, Hyderabad*, *500*(030), 1-86.

Ramegouda, R., & Joseph, A. A. J. I. J. o. R. E. D. (2021). Effect of compression ratio on performance and emission characteristics of dual spark plug ignition engine fueled with n-butanol as additive fuel. *10*(1), 37.

Ramos-Silva, A., Tavares-Carreón, F., Figueroa, M., De la Torre-Zavala, S., Gastelum-Arellanez, A., Rodríguez-García, A., Galán-Wong, L. J., & Avilés-Arnaut, H. (2017). Anticancer potential of Thevetia peruviana fruit methanolic extract. *BMC complementary and alternative medicine*, *17*(1), 241.

Rao, K. P., Rao, B. A., & Babu, V. R. (2015). Heat release rate and engine vibration correlation to investigate combustion propensity of an IDI engine run with biodiesel (MME) and methanol additive as an alternative to diesel fuel. *Biofuels*, *6*(1-2), 45-54.

Rashid, U., Anwar, F., Moser, B. R., & Knothe, G. (2008). Moringa oleifera oil: a possible source of biodiesel. *Bioresource technology*, *99*(17), 8175-8179.

Ravi, G., & Sastry, K. (2009). *Bio-diesel: biodegradable alternative fuel for diesel engines*. Readworthy.

Razon, L. F. (2009). *Review Alternative crops for biodiesel feedstock.* Retrieved 8th February from http://api.ning.com/files/jO49XV9mGACSwHXA2ylDuSraO61K0puIyFGiocX8pto_/Razon2009AlternativeCropsforBiodieselfeedstock.pdf

Resta, V. (2024). *Sustainable biofuel production from oleaginous crops in Kenya* Politecnico di Torino].

Rizki, A., Silitonga, A., Masjuki, H., & Mahlia, T. (2018). The potential biodiesel production from Cerbera odollam oil (Bintaro) in Aceh. MATEC web of Conferences,

Roberts, A., Brooks, R., & Shipway, P. (2014). Internal combustion engine cold-start efficiency: A review of the problem, causes and potential solutions. *Energy conversion and management*, *82*, 327-350.

Rodionova, M. V., Poudyal, R. S., Tiwari, I., Voloshin, R. A., Zharmukhamedov, S. K., Nam, H. G., Zayadan, B. K., Bruce, B. D., Hou, H. J., & Allakhverdiev, S. I. (2017). Biofuel production: challenges and opportunities. *International Journal of Hydrogen Energy*, *42*(12), 8450-8461.

Roick, C., Otun, K. O., Diankanua, N., & Joshua, G. (2021). Non-edible feedstock for biodiesel production. *Biodiesel Technology and Applications*, 285-309.

Rosli, N. R., Abdullah, I. S., Mohd Rosli, N. A., & Zulbakeriamerudin, N. N. (2023). Extraction and characterisation of Cerbera odollam seed oil as a potential plant-based corrosion inhibitor. *Malaysian Journal of Chemical Engineering and Technology (MJCET)*, *6*(2), 174-180.

Sahani, S., Upadhyay, S. N., & Sharma, Y. C. (2020). Critical review on production of glycerol carbonate from byproduct glycerol through transesterification. *Industrial & Engineering Chemistry Research*, *60*(1), 67-88.

Sahoo, P. K., Das, L. M., Babu, M. K. G., & Naik, S. N. (2007). Biodiesel development from high acid value polanga seed oil and performance evaluation in a CI engine. *Fuel*, *86*(3), 448-454. http://www.sciencedirect.com/science/article/B6V3B-4KTN8VK-3/2/a5a2e5235810d8db9e52abe22016a1b4

Sakthivel, G., Nagarajan, G., Ilangkumaran, M., & Gaikwad, A. B. (2014). Comparative analysis of performance, emission and combustion parameters of diesel engine fuelled with ethyl ester of fish oil and its diesel blends. *Fuel*, *132*, 116-124.

Sambandam, P., Raj, D. J., Krishnan, G., Balasubramaniam, S., Nagaraj, N., Mahalingam, A., & Ramaswamy, K. (2023). Effects of nanoadditives on the performance and emissions of rapeseed biodiesel in an insulated piston diesel engine. *Environmental Science and Pollution Research*, 1-13.

Sanford, E., & Kelly, M. W. (2011). Local adaptation in marine invertebrates. *Annual review of marine science*, *3*(1), 509-535.

Sanford, S. D., White, J. M., Shah, P. S., Wee, C., Valverde, M. A., & Meier, G. R. (2009). *Feedstock and Biodiesel Characteristics Report*. Renewable Energy Group, Inc. Retrieved 21th January from http://www.biodiesel.org/resources/reportsdatabase/reports/gen/20091117_GEN-398.pdf

Sanli, H., Alptekin, E., & Canakci, M. (2022). Using low viscosity micro-emulsification fuels composed of waste frying oil-diesel fuel-higher bio-alcohols in a turbocharged-CRDI diesel engine. *Fuel*, *308*, 121966.

Santos, W. A., Bonfim, G. B. R., Jesus, J. S., Fonseca, R. F. S., da Conceição, M. d. F. B., Sousa, L. S., Soares, S. A. R., Mendes, B. A., Anjos, J. P., & Dala-Paula, B. M. (2025). Influence of Jackfruit Wood Barrels and Chips During Aging on the Quality and Phenolic Compounds of Cachaça. *Foods*, *14*(10), 1812.

Sarangthem, I., Haldhar, S., Mishra, L., & Thakuria, D. (2023). The book of abstract: international conference on natural farming for revitalizing environment and resilient agriculture (NF-RERA, 2023). *Pub: College of Agriculture, CAU, Imphal*, *374*(3), 498-501.

Sarkar, S., Datta, D., Deepak, K., Mondal, B. K., & Das, B. (2023). Comprehensive investigation of various re-refining technologies of used lubricating oil: A review. *Journal of Material Cycles and Waste Management*, *25*(4), 1935-1965.

Sarwer, A., Hussain, M., Al-Muhtaseb, A. a. H., Inayat, A., Rafiq, S., Khurram, M. S., Ul-Haq, N., Shah, N. S., Alaud Din, A., & Ahmad, I. (2022). Suitability of Biofuels Production on Commercial Scale from Various Feedstocks: A Critical Review. *ChemBioEng Reviews*.

Sathiyamoorthi, R., & Sankaranarayanan, G. (2017). The effects of using ethanol as additive on the combustion and emissions of a direct injection diesel engine fuelled with neat lemongrass oil-diesel fuel blend. *Renewable energy*, *101*, 747-756.

Sawo, B. A. (2024). Prospects and Challenges of Renewable Energy in Ethiopia With Special Focus on Trends and Practices. *JIM: Jurnal Ilmiah Mahasiswa Pendidikan Sejarah*, *9*(2), 651-664.

Schmitz, T. L., & Smith, K. S. (2012). Mechanical vibrations. *Modeling and measurement*.

Selim, M. Y. (2003). A study of some combustion characterstics of dual fuel engine using EGR. *SAE transactions*, 1152-1160.

Selvakumar, M., & Alexis, S. (2016). Renewable fuel production technologies. *MEJSR*, *24*, 2502-2509.

Sen, S. (2020). 'Green'-ing Kolkata: Creating a Sustainable City–An Overview. *ing Kolkata: Creating a Sustainable City–An Overview (July 21, 2020). International Journal of Research and Analytical ReviewsMay*, *7*(2).

Setyadi, D. L., Ilminnafik, N., Sutjahjono, H., Kusumadewi, T. V., & Raka, R. (2020). Analysis of mixed premixed combustion characteristics of biodiesel candlenut oil (Aleurites Moluccana) with biodiesel fuel. AIP conference proceedings,

Shaafi, T., Sairam, K., Gopinath, A., Kumaresan, G., & Velraj, R. (2015). Effect of dispersion of various nanoadditives on the performance and emission characteristics of a CI engine fuelled with diesel, biodiesel and blends—A review. *Renewable and Sustainable Energy Reviews*, *49*, 563-573.

Shaafi, T., & Velraj, R. (2015). Influence of alumina nanoparticles, ethanol and isopropanol blend as additive with diesel–soybean biodiesel blend fuel: Combustion, engine performance and emissions. *Renewable energy*, *80*, 655-663.

Shaah, M. A. H., Hossain, M. S., Allafi, F. A. S., Alsaedi, A., Ismail, N., Ab Kadir, M. O., & Ahmad, M. I. (2021). A review on non-edible oil as a potential feedstock for biodiesel: physicochemical properties and production technologies. *RSC Advances*, *11*(40), 25018-25037.

Shanta, S. M. (2011). Investigations of the tribological effects of engine oil dilution by vegetable and animal fat feedstock biodiesel on selected surfaces.

Sharma, A. K., & Kumar, S. (2011). Effect of working capital management on firm profitability: Empirical evidence from India. *Global business review*, *12*(1), 159-173.

Sharma, Y. C., Singh, B. (2009). Development of biodiesel: Current scenario. *Renewable and Sustainable Energy Reviews*, *13*(6-7), 1646-1651. www.elsevier.com/locate/rser

Shukla, P. C., Gupta, T., Labhsetwar, N. K., & Agarwal, A. K. J. F. (2017). Trace metals and ions in particulates emitted by biodiesel fuelled engine. *188*, 603-609.

Silitonga, A., Atabani, A., Mahlia, T., Masjuki, H., Badruddin, I. A., & Mekhilef, S. (2011). A review on prospect of Jatropha curcas for biodiesel in Indonesia. *Renewable and Sustainable Energy Reviews*, *15*(8), 3733-3756.

Singh, D., Sharma, D., Soni, S., Sharma, S., Sharma, P. K., & Jhalani, A. (2020). A review on feedstocks, production processes, and yield for different generations of biodiesel. *Fuel*, *262*, 116553.

Singh, R., & Sharma, B. (2019). Morphological characteristics of Sapindus species. In *Biotechnological Advances, Phytochemical Analysis and Ethnomedical Implications of Sapindus species* (pp. 5-15). Springer.

Singh, S., & Singh, D. (2010). Biodiesel production through the use of different sources and characterization of oils and their esters as the substitute of diesel: a review. *Renewable and Sustainable Energy Reviews*, *14*(1), 200-216.

Singh, S. P., & Singh, D. (2010). Biodiesel production through the use of different sources and characterization of oils and their esters as the substitute of diesel: A review. *Renewable and Sustainable Energy Reviews*, *14*(1), 200-216. http://www.sciencedirect.com/science/article/B6VMY-4WXB2C1-1/2/1d997f156b08b291cb124c5b6ff9aa91

Singh, T. S., & Verma, T. N. (2019). Biodiesel production from Momordica Charantia (L.): Extraction and engine characteristics. *Energy*, *189*, 116198. https://doi.org/https://doi.org/10.1016/j.energy.2019.116198

Sirota, E. B. (2025). The Viscosity of Oils. *Energy & Fuels*, *39*(30), 14511-14533.

Soriano Jr, N. U., Venditti, R., & Argyropoulos, D. S. (2009). Biodiesel synthesis via homogeneous Lewis acid-catalyzed transesterification. *Fuel*, *88*(3), 560-565.

Splitter, D., Wissink, M., Kokjohn, S., & Reitz, R. D. (2012). *Effect of compression ratio and piston geometry on RCCI load limits and efficiency* (0148-7191).

Spurk, J. H., & Aksel, N. (2019). Hydrodynamic Lubrication. In *Fluid Mechanics* (pp. 251-283). Springer.

Srivastav, P. P., & Karunanithi, S. (2024). Emerging Methods for Oil Extraction from Food Processing Waste.

Stephan, S., Schmitt, S., Hasse, H., & Urbassek, H. M. (2023). Molecular dynamics simulation of the Stribeck curve: Boundary lubrication, mixed lubrication, and hydrodynamic lubrication on the atomistic level. *Friction*, *11*(12), 2342-2366.

Stone, R. (1999). *Introduction to internal combustion engines* (Vol. 3). Springer.

Su, X., Xu, G., Zhu, M., Zhang, Q., Cai, F., & Liu, M. (2023). Investigation on the interaction between corrosion and wear of U68CuCr rail steel with different corrosion periods. *Wear*, *516*, 204598.

Suardi, S., Suanggana, D., & Said, B. (2023). Biodiesel Potentials of Waste Cooking Oil (WCO): Production, Content of Fuel Properties, and Effects on Engine Performance. *Int. J. Mar. Eng. Innov. Res*, *8*(2), 213-221.

Suganya, T., Varman, M., Masjuki, H., & Renganathan, S. (2016). Macroalgae and microalgae as a potential source for commercial applications along with biofuels production: a biorefinery approach. *Renewable and Sustainable Energy Reviews*, *55*, 909-941.

Suhara, A., Karyadi, Herawan, S. G., Tirta, A., Idris, M., Roslan, M. F., Putra, N. R., Hananto, A. L., & Veza, I. (2024). Biodiesel sustainability: review of progress and challenges of biodiesel as sustainable biofuel. *Clean Technologies*, *6*(3), 886-906.

Susanto, D. F., Aparamarta, H. W., Widjaja, A., & Gunawan, S. (2017). Identification of phytochemical compounds in Calophyllum inophyllum leaves. *Asian Pacific Journal of Tropical Biomedicine*, *7*(9), 773-781.

Sutanto, S., Go, A. W., Ismadji, S., & Ju, Y.-H. (2020). Hydrolyzed rice bran as source of lipids and solid acid catalyst during in situ (trans) esterification. *Biofuels*, *11*(2), 221-227.

Syers, J. K., Wood, D., & Thongbai, P. (2007, 25th-27th May). The Proceedings of the International Technical Workshop on the “Feasibility of Non-edible Oil Seed Crops for Biofuel Production. Mae Fah Luang University, Chiang Rai, Thailand. .

Tamrat, S., Ramayya, V., Gopal, R., & Nallamothu, R. B. (2023). Study on the Effect of Dimethyl Ether and Diesel-Castor Biodiesel Blends on Emission and Combustion Characteristics. 100098.

Tang, R., Shang, J., Qiu, X., Gong, J., Xue, T., & Zhu, T. (2024). Origin, structural characteristics, and health effects of atmospheric soot particles: A review. *Current Pollution Reports*, *10*(3), 532-547.

Tang, Y., Li, X., Chen, P. X., Zhang, B., Hernandez, M., Zhang, H., Marcone, M. F., Liu, R., & Tsao, R. (2015). Characterisation of fatty acid, carotenoid, tocopherol/tocotrienol compositions and antioxidant activities in seeds of three Chenopodium quinoa Willd. genotypes. *Food chemistry*, *174*, 502-508.

Tariq, M., Ali, S., & Khalid, N. (2012). Activity of homogeneous and heterogeneous catalysts, spectroscopic and chromatographic characterization of biodiesel: A review. *Renewable and Sustainable Energy Reviews*, *16*(8), 6303-6316.

Tebe, U. C. K., Tangka, J. K., Djoukeng, H. G., Kamdem, B. M., & Folepe, E. A. (2024). Effects of extraction parameters on the yield of oils from non-edible seeds of Bauhinia variegata and Pachira glabra. *Heliyon*, *10*(9).

This, A. (1911). US Department of Transportation.

Thornton, M. J., Alleman, T. L., Luecke, J., & McCormick, R. L. (2009). Impacts of biodiesel fuel blends oil dilution on light-duty diesel engine operation. *SAE International Journal of Fuels and Lubricants*, *2*(1), 781-788.

Tienhaara, H. (2004). Guidelines to engine dynamics and vibration. *Wärtsilä Corporation*, 20-25.

Tilli, A., Hulkkonen, T., Kaario, O., Larmi, M., Sarjovaara, T., & Lehto, K. (2018). Biofuel blend late post-injection effects on oil dilution and diesel oxidation catalyst performance. *International Journal of Engine Research*, *19*(9), 941-951.
Ting, C.-C., & Chen, C.-C. (2011). Viscosity and working efficiency analysis of soybean oil based bio-lubricants. *Measurement*, *44*(8), 1337-1341.
Tiwari, P., & Garg, S. (2016). Study of reversible kinetic models for alkali-catalyzed Jatropha curcas transesterification. *Biomass Conversion and Biorefinery*, *6*, 61-70.
Tiwari, P., Kumar, R., & Garg, S. (2006). Transesterification: Modeling and Simulation of Batch Kinetics of Non-edible Vegetable Oils for Biodiesel Production. In: American Institute of Chemical Engineers.
Tobar, M., & Núñez, G. A. (2018). Supercritical transesterification of microalgae triglycerides for biodiesel production: Effect of alcohol type and co-solvent. *The Journal of Supercritical Fluids*, *137*, 50-56.
Tompkins, B. T., & Jacobs, T. J. (2013). Low-temperature combustion with biodiesel: Its enabling features in improving efficiency and emissions. *Energy & Fuels*, *27*(5), 2794-2803.
Torkashvand, M., Hasan-Zadeh, A., & Torkashvand, A. (2022). Mini review on importance, application, advantages and disadvantages of biofuels. *J. Mater. Environ. Sci*, *13*(6), 612-630.
Tormos, B., Novella, R., Gomez-Soriano, J., García-Barberá, A., Tsuji, N., Uehara, I., & Alonso, M. (2019). Study of the influence of emission control strategies on the soot content and fuel dilution in engine oil. *Tribology International*, *136*, 285-298.
Totten, G. E. (2017). *Friction, lubrication, and wear technology*. ASM international.
Trotsenko, O., Grigorov, A., Nazarov, V., & Nahliuk, M. (2022). Modern Trends in The Use of Additives in Fuel and Oil Materials (Overview). *Petroleum & Coal*, *64*(3).
Tschöke, H., Piacenti, V., Keppy, B., Singh, A. A., White, S. D., Kern, J., & van Gerpen, J. H. (2021). Piston Machines. *Springer Handbook of Mechanical Engineering*, 683-751.
Tung, S. C., & McMillan, M. L. (2004). Automotive tribology overview of current advances and challenges for the future. *Tribology International*, *37*(7), 517-536.
U.S Energy Information Administration. (2010). *International Energy Outlook 2010*. Retrieved 22nd February from http://www.eia.doe.gov/oiaf/ieo/pdf/0484%282010%29.pdf
Ubeda, L. C. C., Araújo, A. C., Barbalho, S. M., dos Santos Bueno, P. C., Guiguer, É. L., de Sousa, M. d. S. S., de Assis Dias, F., Modesto, A. L., Pinheiro, R. A., & Marutani, V. H. (2017). Effects of the seeds of Aleurites moluccana on the metabolic profile of Wistar rats. *The Pharma Innovation*, *6*(1, Part B), 98.
Van Rensselar, J. (2020). Engine oil analysis. *Tribology & Lubrication Technology*, *76*(9), 28-30.
Vasilakos, I. (2017). *Cavitation in the cylinder-liner and piston-ring interaction in internal combustion engines* City, University of London].
Vélez-Gavilán, J. (2023). Sterculia foetida (Java olive). *CABI Compend*, *51446*.
Venderbosch, R., & Prins, W. (2010). Fast pyrolysis technology development. *Biofuels, bioproducts and biorefining*, *4*(2), 178-208.
Venkanna, B. K., & Venkataramana, R. C. (2009). Biodiesel production and optimization from Calophyllum inophyllum linn oil (honne oil) - A three stage method. *Bioresource Technology*, *100*(21), 5122-5125.
Verdier, S., Coutinho, J. A., Silva, A. M., Alkilde, O. F., & Hansen, J. A. (2009). A critical approach to viscosity index. *Fuel*, *88*(11), 2199-2206.

Verma, S. K., Tiwari, A. K., & Chauhan, D. S. (2017). Experimental evaluation of flat plate solar collector using nanofluids. *Energy conversion and management*, *134*, 103-115.
Vijay Kumar, M., Veeresh Babu, A., & Ravi Kumar, P. (2019). Producing biodiesel from crude Mahua oil by two steps of transesterification process. *Australian Journal of Mechanical Engineering*, *17*(1), 2-7.
Wang, Q., & Jiang, R. (2020). Is carbon emission growth decoupled from economic growth in emerging countries? New insights from labor and investment effects. *Journal of Cleaner Production*, *248*, 119188.
Wang, Z., Lei, T., Yan, X., Chen, G., Xin, X., Yang, M., Guan, Q., He, X., & Gupta, A. K. (2019). Common characteristics of feedstock stage in life cycle assessments of agricultural residue-based biofuels. *Fuel*, *253*, 1256-1263.
Wang, Z., Li, L., Wang, J., & Reitz, R. D. (2016). Effect of biodiesel saturation on soot formation in diesel engines. *Fuel*, *175*, 240-248. https://doi.org/https://doi.org/10.1016/j.fuel.2016.02.048
Wang, Z., Shuai, S., Li, Z., & Yu, W. (2021). A review of energy loss reduction technologies for internal combustion engines to improve brake thermal efficiency. *Energies*, *14*(20), 6656.
Waseem, S., Imadi, S. R., Gul, A., & Ahmad, P. (2017). Oilseed crops: present scenario and future prospects. *Oilseed crops: yield and adaptations under environmental stress*, 1-18.
Watson, S. A. G. (2010). *Lubricant-derived ash: in-engine sources and opportunities for reduction* Massachusetts Institute of Technology].
Wattrus, M. (2013). Fuel property effects on oil dilution in diesel engines. *SAE International Journal of Fuels and Lubricants*, *6*(3), 794-806.
Weissleder, L. (2009). Foreign direct investment in the agricultural sector in Ethiopia. *Ecofair trade dialogue discussion papers*, *12*.
Wilson, A. M., Bailey, P. J., Tasker, P. A., Turkington, J. R., Grant, R. A., & Love, J. B. (2014). Solvent extraction: the coordination chemistry behind extractive metallurgy. *Chemical Society Reviews*, *43*(1), 123-134.
Wolak, A., Zając, G., & Żółty, M. (2018). Changes of properties of engine oils diluted with diesel oil under real operating conditions. *Combustion Engines*, *57*(2), 34-40.
Wong, V. W., & Tung, S. C. (2016). Overview of automotive engine friction and reduction trends–Effects of surface, material, and lubricant-additive technologies. *Friction*, *4*, 1-28.
Wong, V. W., & Tung, S. C. (2017). Friction, Lubrication, and Wear of Internal Combustion Engine Parts.
Wooldridge, M. S., Singh, R., Gutierrez, L. G., & Clancy, S. (2023). Survey of strategies to reduce cold-start particulate, CO, NOx, and hydrocarbon emissions from direct-injection spark-ignition engines. *International Journal of Engine Research*, *24*(2), 456-480.
Wu, D., Roskilly, A. P., & Yu, H. (2012). oil-fired micro-trigeneration prototype Croton megalocarpus.
Wu, X., Zhao, Q., Zhang, M., Li, W., Zhao, G., & Wang, X. (2014). Tribological properties of castor oil tris (diphenyl phosphate) as a high-performance antiwear additive in lubricating greases for steel/steel contacts at elevated temperature. *RSC Advances*, *4*(97), 54760-54768.
Yacob Gebreyohannes Hiben, Y. (2013). Long-term Bioethanol Shift and Transport Fuel Substitution in Ethiopia: Status, Prospects, and Implications. In.
Yalew, A. W., Nechifor, V., & Ferrari, E. (2023). *Implications of Russia's war against Ukraine for African economies: A CGE analysis for Ethiopia*.

Yang, B., Wang, L., Ning, L., & Zeng, K. (2016). Effects of pilot injection timing on the combustion noise and particle emissions of a diesel/natural gas dual-fuel engine at low load. *Applied Thermal Engineering*, *102*, 822-828.

Yang, L., Takase, M., Zhang, M., Zhao, T., & Wu, X. (2014). Potential non-edible oil feedstock for biodiesel production in Africa: a survey. *Renewable and Sustainable Energy Reviews*, *38*, 461-477.

Yang, M., Wu, Y., Jin, S., Hou, J., Mao, Y., Liu, W., Shen, Y., & Wu, L. (2015). Flower bud transcriptome analysis of Sapium sebiferum (Linn.) Roxb. and primary investigation of drought induced flowering: pathway construction and G-quadruplex prediction based on transcriptome. *Plos one*, *10*(3), e0118479.

Yin, X., Chen, W., Eom, J., Clarke, L. E., Kim, S. H., Patel, P. L., Yu, S., & Kyle, G. P. (2015). China's transportation energy consumption and CO2 emissions from a global perspective. *Energy policy*, *82*, 233-248.

You, Y.-D., Shie, J.-L., Chang, C.-Y., Huang, S.-H., Pai, C.-Y., Yu, Y.-H., & Chang, C. H. (2008). Economic cost analysis of biodiesel production: case in soybean oil. *Energy & Fuels*, *22*(1), 182-189.

Yousefi, A., & Birouk, M. (2017). Investigation of natural gas energy fraction and injection timing on the performance and emissions of a dual-fuel engine with pre-combustion chamber under low engine load. *Applied Energy*, *189*, 492-505.

Yu, T., Li, K., Wu, Q., Yao, P., Ke, J., Wang, B., & Wang, Y. (2023). Diesel engine emission aftertreatment device aging mechanism and durability assessment methods: A review. *Atmosphere*, *14*(2), 314.

Yuvarajan, D., & Ramanan, M. V. (2016). Effect of magnetite ferrofluid on the performance and emissions characteristics of diesel engine using methyl esters of mustard oil. *Arabian Journal for Science and Engineering*, *41*, 2023-2030.

Zaharin, M., Abdullah, N., Najafi, G., Sharudin, H., & Yusaf, T. (2017). Effects of physicochemical properties of biodiesel fuel blends with alcohol on diesel engine performance and exhaust emissions: A review. *Renewable and Sustainable Energy Reviews*, *79*, 475-493.

Zhang, J. (2010). *Nonlinear vibration in powertrain systems induced by friction couplings*. University of Technology Sydney (Australia).

Zhang, J., & Meng, Y. (2015). Boundary lubrication by adsorption film. *Friction*, *3*, 115-147.

Zhang, Y. (2006). Boundary lubrication—An important lubrication in the following time. *Journal of Molecular Liquids*, *128*(1-3), 56-59.

Zhang, Y., Ma, Z., Feng, Y., Diao, Z., & Liu, Z. (2021). The effects of ultra-low viscosity engine oil on mechanical efficiency and fuel economy. *Energies*, *14*(8), 2320.

Zhao, H., Memon, A., Gao, J., Taylor, S. D., Sieben, D., Ratulowski, J., Alboudwarej, H., Pappas, J., & Creek, J. (2016). Heavy oil viscosity measurements: Best practices and guidelines. *Energy & Fuels*, *30*(7), 5277-5290.

Zhao, T., Qian, C., Gao, Y., Chen, L., Zhu, M., Pan, Y., & Li, S. (2019). Germination inhibitors detected in Sapium sebiferum seeds. *Journal of Forestry Research*, *30*(6), 2305-2312.

Zhou, H., Zhao, H.-W., Huang, Y.-P., Wei, J.-H., & Peng, Y.-H. (2019). Effects of injection timing on combustion and emission performance of dual-fuel diesel engine under low to medium load conditions. *Energies*, *12*(12), 2349.

Zhu, S., Yuan, W., Cong, J., Guo, Q., Chi, B., & Yu, J. (2023). Analysis of regional wear failure of crankshaft pair of heavy duty engine. *Engineering Failure Analysis*, *154*, 107635.

Ziejewski, M., Goettler, H., & Pratt, G. (1986). *Comparative analysis of the long-term performance of a diesel engine on vegetable oil based alternate fuels* (0148-7191).
Ziolkowska, J. R. (2013). Evaluating sustainability of biofuels feedstocks: A multi-objective framework for supporting decision making. *Biomass and bioenergy*, *59*, 425-440.
Živković, V. B., Grković, V. R., & Kljajić, M. V. (2024). The instigating factors behind the occurrence of vibration in steam turbines: A review analysis. *Thermal Science*, *28*(6 Part A), 4451-4471.

Appendix

The percentage uncertainty of the measured parameters and derived parameters of the experimentation of the research work are shown in the tables below.

Appendix: Table 1: Percentage Uncertainty of indicated power

Measured parameters		Accuracy		Derived parameter	Equation	Equation of Uncertainty	Maximum uncertainty in %
N(rpm)	Ti(N-m)	N ± 30	Ti ± 0.01	(P) (kw)	$Pi = \frac{2\pi NTi}{60{,}000}$	$cTi\Delta N + cN\Delta Ti$	$\{\frac{\Delta N}{N} + \frac{\Delta Ti}{Ti}\}$*100%
1900	20.89						1.627
2100	21.60						1.475
2300	23.55						1.347
2500	23.00						1.243
2700	23.02						1.155
2900	17.31						1.092

Appendix: Table 2: Percentage Uncertainty of brake power

Measured parameters		Accuracy		Derived parameter	Equation	Equation of Uncertainty	Maximum uncertainty in %
N(rpm)	Tb(N-m)	N=30	Tb = 0.01	Pb (kw)	$Pb = \frac{2\pi NTb}{60{,}000}$	$cTb\Delta N + cN\Delta Tb$	$\{\frac{\Delta N}{N} + \frac{\Delta Tb}{Tb}\}$*100%
1900	18.38						1.633
2100	17.96						1.484
2300	18.57						1.358
2500	17.65						1.257
2700	17.71						1.168
2900	12.04						1.118

Appendix: Table 3: Percentage Uncertainty of friction power

Measured parameters		Accuracy		Derived parameter	Equation	Equation of Uncertainty	Maximum uncertainty in %
N(rpm)	Tf(N-m)	N =30	Tf=0.01	Pf (kw)	Pf= $\frac{2\pi NTf}{60{,}000}$	$cTf\Delta N + cN\Delta Tf$	$\{\frac{\Delta N}{N} + \frac{\Delta Tf}{Tf}\}$*100%
1900	0.500						3.579
2100	0.800						2.679
2300	1.200						2.138
2500	1.400						1.914
2700	1.500						1.778
2900	1.600						1.659

Appendix: Table 4: Percentage Uncertainty of total fuel consumption

Measured parameters			Accuracy		Derived parameter	Equation	Equation of Uncertainty	Maximum uncertainty in %
N(rpm)	X(cm^3)	t(sec.)	X=0.05	t=0.01	(TFC)	TFC=3.6*s,g* $\frac{x}{t}$	c $\frac{\Delta x}{t}$ + c $\frac{x\Delta t}{t^2}$	$\{\frac{\Delta x}{x} + \frac{\Delta t}{t}\}$*100%
1900	10	47.42						0.521
2100	10	36.76						0.527
2300	10	34.12						0.529
2500	10	29.52						0.534
2700	10	25.43						0.539
2900	10	23.42						0.543

Appendix Table5: Percentage Uncertainty of brake specific fuel consumption

Measured parameters				Accuracy				Derived parameter	Equation	Equation of Uncertainty	Maximum uncertainty in %
N(rpm)	Tb(N-m)	X(cm^3)	t(sec.)	N= 30	Tb= 0.01	X = 0.05	t= 0.01	(BFC)	$\frac{TFC}{Pb}=3.6*s.g*\frac{x}{t}*\frac{60,000}{2\pi NTb}$	$\left\{\frac{c}{\frac{cx}{\Delta x+\frac{cx}{t^2}\Delta t+\frac{cx}{tN^2Tb}\Delta N+\frac{cx}{tNTb^2}\Delta Tb}}\right\}$	$\{\frac{\Delta x}{x}+\frac{\Delta t}{t}+\frac{\Delta N}{N}+\frac{\Delta Tb}{Tb}\}*100\%$
1900	18.38	10	47.42								2.004
2100	17.96	10	36.76								0.583
2300	18.57	10	34.12								0.583
2500	17.65	10	29.52								1.791
2700	17.71	10	25.43								1.707
2900	12.04	10	23.42								1.660

Appendix Table 6: Percentage Uncertainty of brake thermal efficiency

Measured parameters			Accuracy			Derived parameter	Equation	Equation of Uncertainty	Maximum uncertainty in %
N(rpm)	Tb(N-m)	m_f (g/s)	N 30	T_b 0.01	m_f 0.008	(η_{BTH})	$\eta_{BTH}=\frac{Pb}{mf*Cv}$	$\Delta N+\Delta Tb+\Delta m_f$	$\{+\frac{\Delta N}{N}\frac{\Delta Tb}{Tb}+\frac{\Delta m_f}{m_f}\}*100\%$
1900	18.38	0.228							5.142
2100	17.96	0.226							5.024
2300	18.57	0.225							4.914
2500	17.65	0.232							4.705
2700	17.71	0.256							4.293
2900	12.04	0.273							4.048

Appendix Table7: Percentage Uncertainty of volumetric efficiency

Measured parameters		Accuracy		Derived parameter	Equation	Uncertainty	Maximum uncertainty in %
N(rpm)	ma (kg/h)	N 30	ma (kg/h)=0.08	ηv	$\eta v = \frac{ma}{4.85*10^{-6}\rho a * N}$	$\{\Delta ma + \Delta N\}$	$\{\frac{\Delta N}{N} + \frac{\Delta ma}{ma}\}$*100%
1900	10.239						2.360
2100	11.317						2.135
2300	12.394						1.950
2500	13.331						1.800
2700	14.244						1.673
2900	14.969						1.569

Appendix Table 8: Percentage Uncertainty of mechanical efficiency

Measured parameters			Accuracy		Derived parameter	Equation	Uncertainty	Maximum uncertainty in %
N(rpm)	Tb (N-m)	Ti (N-m)	Tb 0.01	Ti 0.01	(ηm)	$\eta m = \frac{Tb}{Ti}$	$\frac{\Delta Tb}{Ti} + \frac{Tb\Delta Ti}{Ti^2}$	$\{\frac{\Delta Tb}{Tb} + \frac{\Delta Ti}{Ti}\}$*100%
1900	18.38	20.89						0.102
2100	17.96	21.60						0.102
2300	18.57	23.55						0.096
2500	17.65	23.00						0.100
2700	17.71	23.02						0.100
2900	12.04	17.31						0.141

Measured parameters				accuracy			Derived parameter	Equation	Equation of Uncertainty	Maximum uncertainty in %
N(rpm)	ma (kg/h)	m_f (g/s)	Ti (N-m)	Ti ± 0.01	Ma (kg/h)	m_f 0.008	$(\frac{A}{F})$(kg/h)	$\frac{A}{F}=\frac{ma}{mf}$	$\frac{\Delta ma}{mf}+\frac{ma\Delta mf}{m_f{}^2}$	$\{\frac{\Delta N}{N}+\frac{\Delta Ti}{Ti}+\frac{\Delta m_f}{m_f}\}$*100%
1900	10.239	0.228	20.89							5.136
2100	11.317	0.226	21.60							5.015
2300	12.394	0.225	23.55							4.902
2500	13.331	0.232	23.00							4.692
2700	14.244	0.256	23.02							4.280
2900	14.969	0.273	17.31							4.023

Appendix Table 10: Percentage Uncertainty of combustion heat release rate

Blends	parameters		Accuracy		Equation	U_{max} (%)
	P(bar)	$V_{normalized}$	0.25	0.02	$\frac{dQ}{d\theta}=\frac{\gamma}{\gamma-1}P\frac{dv}{d\theta}+\frac{1}{\gamma-1}V\frac{dp}{d\theta}$	% error
B0	10.57	1	0.25	0.02		4.4%
B5	12.49	1	0.25	0.02		4.0%
B10	14.10	1	0.25	0.02	Equation of U_{max}	3.8%
B20	13.46	1	0.25	0.02	$U_{max}=\left(\frac{\Delta V}{V}+\frac{\Delta p}{P}\right)*100\%$	3.9%
B40	12.73	1	0.25	0.02		4.0%

Appendix Table11: Accuracy and percentage uncertainty for exhaust gas emission

Parameters	Instrument	Measurement range	Accuracy (%)	$\bar{U}_{max}$ (%)
NO_x	Kane AUTO plus gas analyzer	0 – 5000 ppm	± 12 ppm	17.5
CO	CT159.02 exhaust gas analyzer	0 – 10 % vol.	± 0.06% vol.	8.7
UHC		0 – 2500 ppm	± 3 ppm	6.2

Appendix Table12 Vibration evaluation standard for reciprocating machine

Vibration Evaluation Standard - Reciprocating machine

Vibration Severity Grade	Overall Vibration measurment measured on the machine Structure			Machine Class*						
	Displacement in um - micron (rms)	Velocity in mm/ sec (rms)	Acceleration meter/ sec (rms)	1	2	3	4	5	6	7
1.1	≤ 17.8	≤ 1.12	≤ 1.76	A	A	A	A	A	A	A
1.8	≤ 28.3	≤ 1.78	≤ 2.79							
2.8	≤ 44.8	≤ 2.82	≤ 4.42	B	B	B	B	B	B	B
4.5	≤ 71.0	≤ 4.46	≤ 7.01							
7.1	≤ 113	≤ 7.07	≤ 11.1	C	C	C	C	C	C	C
11	≤ 178	≤ 11.2	≤ 17.6	D	D	D	D	D	D	D
18	≤ 283	≤ 17.8	≤ 27.9							
28	≤ 448	≤ 28.2	≤ 44.2							
45	≤ 710	≤ 44.6	≤ 70.1							
71	≤ 1125	≤ 70.7	≤ 111							
112	≤ 1784	≤ 112	≤ 176							
180	≤ 1784	> 112	> 176							

Zone A: Vibration of newly Commissioned Machines;
Zone B: Machines considered acceptable for unrestricted long-term operation
Zone C: Machines considered unsatisfactory for long-term continuous operation
Zone D: Vibration values normally considered to be sufficient severity to cause damage to the machine

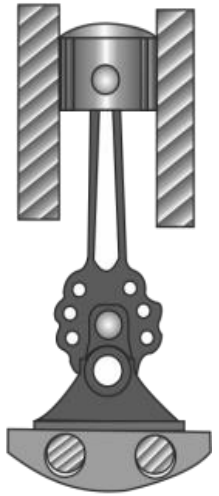

Appendix Table13 Scheme of Indian standard endurance test for IC Engines

UDC 621-43-018 : 620-169-1 (First Reprint JULY 1988) IS : 10000 (Part IX) - 1980

(Reaffirmed 2006)

Indian Standard

METHODS OF TESTS FOR INTERNAL COMBUSTION ENGINES

PART IX ENDURANCE TESTS

Internal Combustion Engines Sectional Committee, EDC 14; Methods of Test and Codes of Practice for Engines Subcommittee, EDC 14:3 [Ref : Doc : EDC 14 (3136)]

1. Scope — Specifies the method of conducting endurance tests on constant speed and variable speed internal combustion engines.

2. Section I — Endurance Tests for Constant Speed Engines — These tests shall be performed after the initial performance tests specified in IS : 10000 (Part VIII)-1980 'Methods of tests for internal combustion engines: Part VIII Performance tests'.

2.1 After completion of the initial performance test the engine shall be run for 32 cycles (each of 16 hours continuous running) at rated speed.

2.1.1 *Test cycle for IS Rating A*

Load (Percent of Rated Load)	*Running Time* (Hours)
100	4 (Including warm-up period of 0·5 h)
50	4
110	1
No load (Idling)	0·5
100	3
50	3·5

2.1.2 *Test cycle for IS Rating B*

Load (Percent of Rated Load)	*Running Time* (Hours)
100	4 (Including warm-up period of 0·5 h)
50	4
100	1
No load (Idling)	0·5
100	3
50	3·5

2.2 At the end of each 16 hours cycle, the engine shall be stopped and necessary servicing and minor adjustments may be carried out in accordance with the manufacturer's schedule.

2.3 Before starting the next cycle, the temperature of the engine sump oil shall have reached within 5 K of the room temperature.

2.4 The engine shall be topped up with engine oil, if required and the quantity consumed recorded. In case the duration of the endurance test is longer than the period of oil change recommended by the engine manufacturer, the oil shall be changed according to the manufacturer's recommended schedule. The amount of make up oil used during the tests shall be used to establish the lubricating oil consumption rate.

Adopted 31 December 1980 | © May 1981, BIS | Gr 2

BUREAU OF INDIAN STANDARDS
MANAK BHAVAN, 9 BAHADUR SHAH ZAFAR MARG

EXPLANATORY NOTE

The testing and performance of constant speed and variable speed internal combustion engines was earlier covered by the following Indian Standards:

i) IS : 1600-1960 'Code for type testing of constant speed internal combustion engines for general purposes'

ii) IS : 1601-1960 'Performance of constant speed internal combustion engines for general purposes'

iii) IS : 1602-1960 'Code for type testing of variable speed internal combustion engines for automotive purposes'

iv) IS : 1603-1960 'Performance of variable speed internal combustion engines for automotive purposes'

These standards were originally issued in the year 1960 and as a result of implementation of these standards by the manufacturers of engines and testing laboratories, as also the operation of ISI Certification Marking Scheme, these standards have now been extensively revised.

While IS : 1600 and IS : 1602 covered the codes for type testing of constant and variable speed engines respectively, the performance requirements of such engines were covered by IS : 1601 and IS : 1603 respectively. These standards are replaced by two sets of standards, one set covers the methods of testing of engines and the other covers the specification and performance requirements of both constant speed and variable speed engines.

The standard covering methods of tests for internal combustion engines is being published in the following 12 parts (each part covering a particular test method or information related to methods of tests):

i) IS : 10000 (Part I) Glossary of terms relating to test methods

ii) IS : 10000 (Part II) Standard reference conditions

iii) IS : 10000 (Part III) Measurements for testing, units and limits of accuracy

iv) IS : 10000 (Part IV) Declarations of power, efficiency, fuel consumption and lubricating oil consumption

v) IS : 10000 (Part V) Preparation for tests and measurements for wear

vi) IS : 10000 (Part VI) Recording of test results

vii) IS : 10000 (Part VII) Governing tests for constant speed engines and selection of engines for use with electrical generators

viii) IS : 10000 (Part VIII) Performance tests

ix) IS : 10000 (Part IX) Endurance tests

x) IS : 10000 (Part X) Tests for smoke levels, limits and corrections for smoke levels for variable speed engines

xi) IS : 10000 (Part XI) Information required with inquiry or order and information supplied by the manufacturer with the engine

xii) IS : 10000 (Part XII) Test certificates

This standard will be complementary to specifications for performance requirements of different types of engines covered by the following standards:

i) IS : 10001 Specification for performance requirements for constant speed compression ignition (diesel) engines for general purposes (up to 20 kW)

ii) IS : 10002 Specification for performance requirements for constant speed compression ignition (diesel) engines for general purposes (above 20 kW)

iii) IS : 10003 Specification for performance requirements for variable speed compression ignition (diesel) engines for automotive purposes

iv) IS : 10004 Specification for performance requirements for variable speed spark ignition engines for automotive purposes

Spark ignition engines for sprayers and similar applications have been covered by IS : 7347-1974 ' Specification for performance requirements of small size spark ignition engines for sprayers '.

Two stroke spark ignition engines for automotive applications which were earlier covered by IS : 1603 will be covered by a separate specification.

The revised methods of tests covered by IS : 10000 have been aligned with the current international practices in the field of I.C. engines. These parts are in general agreement with the following ISO standards — issued by the International Organization for Standardization:

a) ISO 3046/I-1975 Reciprocating internal combustion engines — Performance: Part I Standard reference conditions and declarations of power, fuel consumption and lubrication oil consumption

b) ISO 3046/II-1977 Reciprocating internal combustion engines — Performance: Part II Test methods

c) ISO 3046/III-1979 Reciprocating internal combustion engines — Performance: Part III Test measurements

d) ISO 2710-1978 Reciprocating internal combustion engines — Vocabulary

IS : 10000 (Part I to Part XII) and IS : 10001, IS : 10002, IS : 10003 and IS : 10004 collectively supersede IS : 1600, IS : 1601, IS : 1602 and IS : 1603.

hadish gebru

A Study of Performance on Compression Ignition Engine Fuelled by Biodiesel-Diesel Blends with the inclusion of Al203 ...

A Study of Performance on Compression Ignition Engine Fuelled by Biodiesel-Diesel Blends with the inclusion of Al203 Nanoparticles

thesis

Adama Science and Technology University

Document Details

Submission ID
trn:oid:::1:3384718192

Submission Date
Oct 24, 2025, 9:11 AM GMT

Download Date
Oct 24, 2025, 10:48 AM GMT

File Name
Ramesh.docx

File Size
55.6 MB

214 Pages

61,772 Words

354,239 Characters

turnitin Page 1 of 233 - Cover Page Submission ID trn:oid:::1:3384718192

Plagirism report

21% Overall Similarity

The combined total of all matches, including overlapping sources, for each database.

Filtered from the Report

- Bibliography

Exclusions

- 31 Excluded Matches

Match Groups

- 638 Not Cited or Quoted 15%
  Matches with neither in-text citation nor quotation marks
- 304 Missing Quotations 6%
  Matches that are still very similar to source material
- 9 Missing Citation 0%
  Matches that have quotation marks, but no in-text citation
- 0 Cited and Quoted 0%
  Matches with in-text citation present, but no quotation marks

Top Sources

12% Internet sources
15% Publications
7% Submitted works (Student Papers)

Integrity Flags

2 Integrity Flags for Review

- Replaced Characters
  319 suspect characters on 76 pages
  Letters are swapped with similar characters from another alphabet.
- Hidden Text
  19 suspect characters on 1 page
  Text is altered to blend into the white background of the document.

Our system's algorithms look deeply at a document for any inconsistencies that would set it apart from a normal submission. If we notice something strange, we flag it for you to review.

A Flag is not necessarily an indicator of a problem. However, we'd recommend you focus your attention there for further review.

Match Groups

- 638 Not Cited or Quoted 15%
  Matches with neither in-text citation nor quotation marks
- 304 Missing Quotations 6%
  Matches that are still very similar to source material
- 9 Missing Citation 0%
  Matches that have quotation marks, but no in-text citation
- 0 Cited and Quoted 0%
  Matches with in-text citation present, but no quotation marks

Top Sources

12% Internet sources
15% Publications
7% Submitted works (Student Papers)

Top Sources

The sources with the highest number of matches within the submission. Overlapping sources will not be displayed.

1	Internet	
etd.astu.edu.et		2%
2	Publication	
Hadish Teklehaimanot, Neeraj Gupta, Ramesh Babu Nallamothu. "The impact of ...		2%
3	Student papers	
Adama Science and Technology University		1%
4	Internet	
dspace.dtu.ac.in:8080		<1%
5	Student papers	
University of Malaya		<1%
6	Student papers	
Southern Illinois University		<1%
7	Publication	
M. Balat. "Modeling Vegetable Oil Viscosity", Energy Sources, Part A: Recovery, Ut...		<1%
8	Publication	
Samuel Tamrat, Venkata Ramayya Ancha, Rajendiran Gopal, Ramesh Babu Nalla...		<1%
9	Internet	
pdfs.semanticscholar.org		<1%
10	Internet	
ebin.pub		<1%

11	Internet	
ethesis.nitrkl.ac.in		<1%
12	Internet	
worldwidescience.org		<1%
13	Internet	
ejssd.astu.edu.et		<1%
14	Internet	
coek.info		<1%
15	Publication	
Geok, How Heoy. "Fuel Injection Parameters Study for Low Exhaust Emissions of ...		<1%
16	Internet	
everant.org		<1%
17	Publication	
Atabani, A.E.. "A comprehensive review on biodiesel as an alternative energy reso...		<1%
18	Publication	
Samuel Paul Raj, Pravin Raj Solomon, Baskar Thangaraj. "Biodiesel from Flowerin...		<1%
19	Internet	
studentsrepo.um.edu.my		<1%
20	Publication	
Mofijur, M., A.E. Atabani, H.H. Masjuki, M.A. Kalam, and B.M. Masum. "A study on ...		<1%
21	Publication	
Ashok Pandey. "Handbook of Plant-Based Biofuels", CRC Press, 2019		<1%
22	Internet	
autodocbox.com		<1%
23	Publication	
Ayhan Demirbas, Abdullah Bafail, Waqar Ahmad, Manzoor Sheikh. "Biodiesel pro...		<1%
24	Publication	
Samuel Tamrat, Venkata Ramayya Ancha, Rajendiran Gopal, Ramesh Babu Nalla...		<1%